

PHENOMENOLOGY OF PARTICLE PHYSICS

NIU FALL 2018 PHYS 686 LECTURE NOTES

STEPHEN P. MARTIN
Physics Department
Northern Illinois University
DeKalb IL 60115
spmartin@niu.edu

August 22, 2018

Contents

1	Introduction	4
1.1	Fundamental forces	4
1.2	Resonances, widths, and lifetimes	5
1.3	Leptons and quarks	6
1.4	Hadrons	7
1.5	Decays and branching ratios	12
2	Special Relativity and Lorentz Transformations	15
2.1	Lorentz transformations	15
2.2	Relativistic kinematics	18
2.3	Tensors and Lorentz invariant quantities	22
2.4	Maxwell's equations and electromagnetism	25
3	Relativistic Quantum Mechanics of Single Particles	28
3.1	Klein-Gordon and Dirac equations	28
3.2	Solutions of the Dirac equation	35
3.3	The Weyl equation	43
3.4	Majorana fermions	45
4	Field Theory and Lagrangians	46
4.1	The field concept and Lagrangian dynamics	46
4.2	Quantization of free scalar field theory	53
4.3	Quantization of free Dirac fermion field theory	58
4.4	Scalar field with ϕ^4 coupling	61
4.5	Scattering processes and cross-sections	67
4.6	Scalar field with ϕ^3 coupling	77
4.7	Feynman rules	84
5	Quantum Electro-Dynamics (QED)	92
5.1	QED Lagrangian and Feynman rules	92
5.2	Electron-positron scattering	100
5.2.1	$e^-e^+ \rightarrow \mu^-\mu^+$	100
5.2.2	$e^-e^+ \rightarrow f\bar{f}$	105
5.2.3	Helicities in $e^-e^+ \rightarrow \mu^-\mu^+$	110
5.2.4	Bhabha scattering ($e^-e^+ \rightarrow e^-e^+$)	118
5.3	Crossing symmetry	123
5.3.1	$e^-\mu^+ \rightarrow e^-\mu^+$ and $e^-\mu^- \rightarrow e^-\mu^-$	124
5.3.2	Møller scattering ($e^-e^- \rightarrow e^-e^-$)	126
5.4	Gauge invariance in Feynman diagrams	128
5.5	External photon scattering	130
5.5.1	Compton scattering ($\gamma e^- \rightarrow \gamma e^-$)	130
5.5.2	$e^+e^- \rightarrow \gamma\gamma$	138
6	Decay Processes	140
6.1	Decay rates and partial widths	140
6.2	Two-body decays	141
6.3	Scalar decays to fermion-antifermion pairs: Higgs decay	143
6.4	Three-body decays	147

7	Fermi Theory of Weak Interactions	150
7.1	Weak nuclear decays	150
7.2	Muon decay	152
7.3	Corrections to muon decay	162
7.4	Inverse muon decay ($e^- \nu_\mu \rightarrow \nu_e \mu^-$)	164
7.5	$e^- \bar{\nu}_e \rightarrow \mu^- \bar{\nu}_\mu$	167
7.6	Charged currents and π^\pm decay	168
7.7	Unitarity, renormalizability, and the W boson	175
8	Gauge theories	180
8.1	Groups and representations	180
8.2	The Yang-Mills Lagrangian and Feynman rules	191
9	Quantum Chromo-Dynamics (QCD)	198
9.1	QCD Lagrangian and Feynman rules	198
9.2	Scattering of quarks and gluons	200
9.2.1	Quark-quark scattering ($qq \rightarrow qq$)	200
9.2.2	Gluon-gluon scattering ($gg \rightarrow gg$)	203
9.3	Renormalization	204
9.4	Parton distribution functions and hadron-hadron scattering	215
9.5	Top-antitop production in $p\bar{p}$ and pp collisions	224
9.6	Kinematics in hadron-hadron scattering	228
9.7	Drell-Yan scattering ($\ell^+ \ell^-$ production in hadron collisions)	231
10	Spontaneous Symmetry Breaking	235
10.1	Global symmetry breaking	235
10.2	Local symmetry breaking and the Higgs mechanism	239
10.3	Goldstone's Theorem and the Higgs mechanism in general	242
11	The Standard Electroweak Model	245
11.1	$SU(2)_L \times U(1)_Y$ representations and Lagrangian	245
11.2	The Standard Model Higgs mechanism	250
11.3	Fermion masses and Cabibbo-Kobayashi-Maskawa mixing	255
11.4	Neutrino masses and the seesaw mechanism	264
11.5	The Higgs boson discovery	266
11.5.1	Higgs boson decays revisited	267
11.5.2	Higgs boson production at the LHC	271
11.5.3	The Higgs boson discovery	275
	Further Reading	278
	Appendices	279
	A.1 Natural units and conversions	279
	A.2 Dirac Spinor Formulas	280
	Index	281

1 Introduction

In this course, we will explore some of the tools necessary for attacking the fundamental questions of elementary particle physics. These questions include:

- What fundamental particles is everything made out of?
- How do the particles interact with each other?
- What principles underlie the answers to these questions?
- How can we use this information to predict and interpret the results of experiments?

The Standard Model of particle physics proposes some answers to these questions. Although it is highly doubtful that the Standard Model will survive intact beyond this decade, it is the benchmark against which future theories will be compared. Furthermore, it is highly likely that the new physics to be uncovered at the CERN Large Hadron Collider (LHC) can be described using the same set of tools.

This Introduction contains a brief outline of the known fundamental particle content of the Standard Model, for purposes of orientation. These and many other experimental results about elementary particles can be found in the *Review of Particle Properties*, hereafter known as the RPP, authored by the Particle Data Group, and in its pocket-sized abridged form, the *Particle Physics Booklet*. The current edition of the RPP was published as M. Tanabashi et al. (Particle Data Group), Phys. Rev. D **98**, 030001 (2018). It is updated and republished every even-numbered year. An always-up-to-date version is available on-line, at <http://pdg.lbl.gov>, and it is usually considered the definitive source for elementary particle physics data and analysis. Each result is referenced according to the experiments that provided it. Background theoretical material needed for interpreting the results is also included. Copies can be ordered for free from their website.

1.1 Fundamental forces

The known interaction forces in nature are the universal attraction of gravity, the electromagnetic force, the weak nuclear force, and the strong nuclear force. Among these, gravity is special and is governed by Einstein's theory of General Relativity. The other forces are gauge theories. The definition of gauge theories and their properties will be explored extensively throughout this book. Here let it suffice to say that a gauge force is one that is mediated by a spin-1 (vector) boson. The force-mediator gauge bosons that we know about in the Standard Model are listed in Table 1.1.

	Boson	Charge	Mass (GeV/ c^2)	Width (GeV/ c^2)	Lifetime (sec)	Force
photon	γ	0	0	0	∞	EM
	W^\pm	± 1	80.379 ± 0.012	2.085 ± 0.042	3.14×10^{-25}	weak
	Z^0	0	91.1876 ± 0.0021	2.4952 ± 0.0023	2.64×10^{-25}	weak
gluon	g	0	“0”			strong

Table 1.1: The fundamental vector bosons of the Standard Model.

The photon is the mediator of the electromagnetic force, while the W^\pm and Z^0 bosons mediate the weak nuclear force, which is seen primarily in decays and in neutrino interactions. The W^+ and W^- bosons are antiparticles of each other, so they have exactly the same mass and lifetime. The gluon has an exact 8-fold degeneracy due to a degree of freedom known as “color”. Color is the charge associated with the strong nuclear force. Particles that carry net color charges are always confined by the strong nuclear force, meaning that they can only exist in bound states. Therefore, no value is listed for the gluon lifetime, and the entry “0” for its mass is meant to indicate only that the classical wave equation for it has the same character as that of the photon. Although the fundamental spin-1 bosons are often called force carriers, that is not their only role, since they are particles in their own right.

1.2 Resonances, widths, and lifetimes

Table 1.1 also includes information about the width Γ of the W and Z particle resonances, measured in units of mass, GeV/ c^2 . In general, resonances can be described by a relativistic Breit-Wigner lineshape, which gives the probability for the kinematic mass reconstructed from the production and decay of the particle to have a particular value M , in the idealized limit of perfect detector resolution and an isolated state. For a particle of mass m , the probability is:

$$P(M) = \frac{f(M)}{(M^2 - m^2)^2 + m^2\Gamma(M)^2}, \quad (1.2.1)$$

where $f(M)$ and $\Gamma(M)$ are functions that usually vary slowly over the resonance region $M \approx m$, and thus can be treated as constants. The resonance width $\Gamma \equiv \Gamma(m)$ is equivalent to the mean lifetime, which appears in the next column of Table 1.1; they are related by

$$\tau \text{ (in seconds)} = (6.58212 \times 10^{-25})/[\Gamma \text{ (in GeV}/c^2)]. \quad (1.2.2)$$

The Review of Particle Properties (RPP), a publication of the Particle Data Group (pdg.lbl.gov), lists the mean lifetime τ for some particles, and the width Γ for others. Actually, the Standard Model of particle physics predicts the width of the W boson far more accurately than the

experimentally measured width indicated in Table 1.1. The predicted width, with uncertainties from input parameters, is $\Gamma_W = 2.091 \pm 0.002 \text{ GeV}/c^2$.

1.3 Leptons and quarks

The remaining known indivisible constituents of matter are spin-1/2 fermions, known as leptons (those without strong nuclear interactions) and quarks (those with strong nuclear interactions). All experimental tests are consistent with the proposition that these particles have no substructure. The leptons are listed in Table 1.2.

	Lepton	Charge	Mass (GeV/c^2)	Mean Lifetime (sec)
electron	e^-	-1	$5.109989461(31) \times 10^{-4}$	∞
	ν_e	0	$< 2 \times 10^{-9}$	
muon	μ^-	-1	$0.1056583745(24)$	$2.1969811(22) \times 10^{-6}$
	ν_μ	0	$< 1.9 \times 10^{-4}$	
tau	τ^-	-1	$1.77686(12)$	$2.903(5) \times 10^{-13}$
	ν_τ	0	< 0.018	

Table 1.2: The leptons of the Standard Model.

They consist of negatively charged electrons, muons, and taus, and weakly interacting neutrinos. There is now good evidence (from experiments that measure oscillations of neutrinos produced by the sun and in cosmic rays) that the neutrinos have non-zero masses, but their absolute values are not known except for upper bounds as shown. The quarks come in 6 types, known as “flavors”, listed in Table 1.3.

	Quark	Charge	Mass (GeV/c^2)
down	d	-1/3	4.4×10^{-3} to 5.2×10^{-3}
up	u	2/3	1.8×10^{-3} to 2.7×10^{-3}
strange	s	-1/3	0.092 to 0.104
charm	c	2/3	1.275 ± 0.025
bottom	b	-1/3	4.18 ± 0.03
top	t	2/3	173.1 ± 0.9

Table 1.3: The quarks of the Standard Model.

The fermions listed in Tables 1.2 and 1.3 are often considered as divided into families, or generations. The first family is e^-, ν_e, d, u , the second is μ^-, ν_μ, s, c , and the third is τ^-, ν_τ, b, t .

The masses of the fermions of a given charge increase with the family. The weak interactions mediated by W^\pm bosons can change quarks of one family into those of another, but it is an experimental fact that these family-changing reactions are highly suppressed. All of the fermions listed above also have corresponding antiparticles, with the opposite charge and color, but the same mass and spin. The antileptons are positively charged e^+, μ^+, τ^+ and antineutrinos $\bar{\nu}_e, \bar{\nu}_\mu, \bar{\nu}_\tau$. For each quark, there is an antiquark ($\bar{d}, \bar{u}, \bar{s}, \bar{c}, \bar{b}, \bar{t}$) with the same mass but the opposite charge. Antiquarks carry anticolor (anti-red, anti-blue, or anti-green).

The masses of the five lightest quarks (d, u, s, c, b) are somewhat uncertain, and even the definition of the mass of a quark is subject to technical difficulties and ambiguities. This is related to the fact that quarks exist only in colorless bound states, called hadrons, due to the confining nature of the strong force. A colorless bound state can be formed either from three quarks (a baryon), or from three antiquarks (an anti-baryon), or from a quark with a given color and an antiquark with the corresponding anti-color (a meson). All baryons are fermions with half-integer spin, and all mesons are bosons with integer spin. The quark mass values shown in Table 1.3 correspond to particular technical definitions of quark mass used by the RPP[†], but other definitions give quite different values. The lifetimes of the d, u, s, c, b quarks are also fuzzy, and are best described in terms of the hadrons in which they live. In contrast, the top quark mass is relatively well-known, with an uncertainty under a percent. This is because the top-quark mean lifetime (about 4.6×10^{-25} seconds) is so short that it decays before it can form hadronic bound states (which take roughly 3×10^{-24} seconds to form). Therefore it behaves like a free particle during its short life, and so its mass and width can be defined in a way that is not subject to large ambiguities. Each of these quarks has an exact 3-fold degeneracy, associated with the color that is the source charge for the strong force. The colors are often represented by the labels red, green, and blue, but these are just arbitrary labels; there is no experiment that could tell a red quark from a green quark, even in principle.

There is also a Higgs boson, with spin 0 and charge 0. It was discovered in 2012, and its mass has been measured to be 125.18 ± 0.16 GeV. Some extensions of the Standard Model predict that this Higgs boson is not fundamental and is a composite state of other particles. However, the data collected to date are consistent with the Higgs boson being another elementary particle.

1.4 Hadrons

As remarked above, quarks and antiquarks are always found as part of colorless bound states. The most common are the nucleons (the proton and the neutron), the baryons that make up most of the directly visible mass in the universe. They and other similar baryons with total

[†]Here, we have quoted “ $\overline{\text{MS}}$ masses” for u, d, s, c, b , and the “pole mass” for t .

angular momentum (including both constituent spins and orbital angular momentum) $J = 1/2$ are listed in Table 1.4.

$J = 1/2$ baryon		Charge	Mass (GeV/ c^2)	Lifetime (sec)
p	(uud)	+1	0.938272	$> 6.6 \times 10^{36}$
n	(udd)	0	0.939565	880.3
Λ	(uds)	0	1.11568	2.63×10^{-10}
Σ^+	(uus)	+1	1.18937	8.02×10^{-11}
Σ^0	(uds)	0	1.19264	7.4×10^{-20}
Σ^-	(dds)	-1	1.19745	1.48×10^{-10}
Ξ^0	(uss)	0	1.31486	2.9×10^{-10}
Ξ^-	(dss)	-1	1.32171	1.64×10^{-10}

Table 1.4: Baryons with $J = 1/2$ made from light (u, d, s) quarks.

The quarks listed in parentheses are the valence quarks of the bound state, but there are also virtual (or “sea”) quark-antiquark pairs and virtual gluons in each of these and other hadrons. The proton may be absolutely stable; experiments to try to observe its decays have not found any, resulting in only a very high lower bound on the mean lifetime. The neutron lifetime is also relatively long, but it decays into a proton, electron, and antineutrino ($n \rightarrow pe^-\bar{\nu}_e$). The other $J = 1/2$ baryons decay in times of order 10^{-10} seconds by weak interactions, except for the Σ^0 baryon, which decays extremely quickly by an electromagnetic interaction into the Λ , which has the same valence quark content: $\Sigma^0 \rightarrow \Lambda\gamma$. In that sense, one can think of the Σ^0 as being an excited state of the Λ . There are other excited states of these baryons, not listed here. The mass of the baryons in Table 1.4 increases with the number of valence strange quarks contained.

Note that the masses of the proton and the neutron (and all other hadrons) are much larger than the sums of the masses of the valence quarks that make them up. These nucleon masses come about from the strong interactions by a mechanism known as chiral symmetry breaking. Nucleons dominate the visible mass of particles in the universe. Therefore, it is only partially correct to say that the Higgs boson is needed to understand the “origin of mass”. Most of the masses of the W^\pm and Z bosons and the top, bottom, charm, and strange quarks and the leptons are indeed believed to come from the Higgs mechanism, to be discussed below. However, the Higgs mechanism is by no means necessary to understand the origin of *all* mass, and in particular it is definitely not the explanation for most of the mass that is directly observed in the universe.

There are also $J = 3/2$ baryons, with some of the more common ones listed in Table 1.5.

$J = 3/2$ baryon		Charge	Mass (GeV/ c^2)	Γ (GeV/ c^2)	Lifetime (seconds)
Δ^{++}	(uuu)	+2	1.232	0.117	5.6×10^{-24}
Δ^+	(uud)	+1	""	""	""
Δ^0	(udd)	0	""	""	""
Δ^-	(ddd)	-1	""	""	""
Σ^{*+}	(suu)	+1	1.383	0.036	1.8×10^{-23}
Σ^{*0}	(sud)	0	1.384	0.036	1.8×10^{-23}
Σ^{*-}	(sdd)	-1	1.387	0.039	1.7×10^{-23}
Ξ^{*0}	(ssu)	0	1.532	0.0091	7.2×10^{-23}
Ξ^{*-}	(ssd)	-1	1.535	0.0099	6.6×10^{-23}
Ω^-	(sss)	-1	1.672	8.0×10^{-15}	8.21×10^{-11}

Table 1.5: $J = 3/2$ baryons.

The RPP uses a slightly different notation for the Σ^* and Ξ^* $J = 3/2$ baryons. Instead of the $*$ notation to differentiate these states from the corresponding $J = 1/2$ baryons with the same quantum numbers, the RPP chooses to denote them by their approximate mass in MeV (as determined by older experiments, so a little off from the present best values) in parentheses, so $\Sigma(1385)$ and $\Xi(1530)$. Very narrow resonances correspond to very long-lived states; the Ω^- is by far the narrowest and most stable of the ten $J = 3/2$ baryon ground states listed.

There are also baryons containing heavy (c or b) quarks. The only ones that have been definitively observed so far have $J = 1/2$ and contain exactly one heavy quark. The lowest lying states with a charm quark include the Λ_c^+ , Σ_c^{++} , Σ_c^+ , Σ_c^0 , Ξ_c^+ , Ξ_c^0 , and Ω_c^0 resonances with masses ranging from 2.29 GeV/ c^2 to 2.7 GeV/ c^2 , and those with a bottom quark include the Λ_b^0 , Ξ_b^0 , Ξ_b^- , Ω_b^- , Σ_b^+ , and Σ_b^- , with masses ranging from 5.62 GeV/ c^2 to 5.82 GeV/ c^2 . More information about them can be found in the RPP. Again, there are other baryons, generally with heavier masses, that can be thought of as excited states of the more common ones listed above.

Bound states of a valence quark and antiquark are called mesons. They always carry integer total angular momentum J . The most common $J = 0$ mesons are listed in Table 1.6.

Here the bar over a quark name denotes the corresponding antiquark. The charged pions π^\pm are antiparticles of each other, as are the charged kaons K^\pm , so they are exactly degenerate mass pairs with the same lifetime. However, the K^0 and \bar{K}^0 mesons are mixed and not quite exactly degenerate in mass. One of the interaction eigenstates (K_L^0) is actually much longer-lived than the other (K_S^0); the mean lifetimes are respectively 5.12×10^{-8} and 8.95×10^{-11} seconds. The lifetimes (and the widths) of the other $J = 0$ mesons are not listed here; you can find them

$J = 0$ meson		Charge	Mass (GeV/ c^2)
π^0	$(u\bar{u}, d\bar{d})$	0	0.134977
π^\pm	$(u\bar{d}); (d\bar{u})$	± 1	0.139570
K^\pm	$(u\bar{s}); (s\bar{u})$	± 1	0.493677
K^0, \bar{K}^0	$(d\bar{s}); (s\bar{d})$	0	0.497614
η	$(u\bar{u}, d\bar{d}, s\bar{s})$	0	0.54786
η'	$(u\bar{u}, d\bar{d}, s\bar{s})$	0	0.95778

Table 1.6: $J = 0$ mesons containing light (u, d, s) quarks and antiquarks.

yourself in the RPP.

Besides the $J = 0$ mesons listed above, there are counterparts containing a single heavy (charm or bottom) quark or antiquark, with the other antiquark or quark light (up, down or strange). The most common ones are listed in Table 1.7.

$J = 0$ meson		Charge	Mass (GeV/ c^2)
D^0, \bar{D}^0	$(c\bar{u}); (u\bar{c})$	0	1.8648
D^\pm	$(c\bar{d}); (d\bar{c})$	± 1	1.8696
D_s^\pm	$(c\bar{s}); (s\bar{c})$	± 1	1.9683
B^\pm	$(u\bar{b}); (b\bar{u})$	± 1	5.279
B^0, \bar{B}^0	$(d\bar{b}); (b\bar{d})$	0	5.280
B_s^0, \bar{B}_s^0	$(s\bar{b}); (b\bar{s})$	0	5.367

Table 1.7: $J = 0$ mesons containing one heavy and one light quark and antiquark.

There are also $J = 0$ mesons containing only charm and bottom quarks and antiquarks. The ones with the lowest masses are listed in Table 1.8.

$J = 0$ meson		Charge	Mass (GeV/ c^2)
η_c “charmonium”	$(c\bar{c})$	0	2.984
B_c^\pm	$(c\bar{b}); (b\bar{c})$	± 1	6.275
η_b “bottomonium”	$(b\bar{b})$	0	9.398

Table 1.8: $J = 0$ mesons containing a heavy quark and a heavy antiquark.

Vector ($J = 1$) mesons are also very important. Table 1.9 lists the most common ones that contain only light (u, d, s) valence quarks and antiquarks.

$J = 1$ meson		Charge	Mass (GeV/ c^2)
ρ^\pm	$(u\bar{d}); (d\bar{u})$	± 1	0.7752
ρ^0	$(u\bar{u}, d\bar{d})$	0	" "
ω^0	$(u\bar{u}, d\bar{d})$	0	0.7827
$K^{*\pm}$	$(u\bar{s}); (s\bar{u})$	± 1	0.8917
K^{*0}, \bar{K}^{*0}	$(d\bar{s}); (s\bar{d})$	0	0.8958
ϕ	$(u\bar{u}, d\bar{d}, s\bar{s})$	0	1.01946

Table 1.9: $J = 1$ mesons containing light quarks and antiquarks.

The most common $J = 1$ mesons containing one heavy (c or b) quark or antiquark are likewise shown in Table 1.10.

$J = 1$ meson		Charge	Mass (GeV/ c^2)
D^{*0}, \bar{D}^{*0}	$(c\bar{u}); (u\bar{c})$	0	2.007
$D^{*\pm}$	$(c\bar{d}); (d\bar{c})$	± 1	2.010
$D_s^{*\pm}$	$(c\bar{s}); (s\bar{c})$	± 1	2.112
B^{*0}, \bar{B}^{*0}	$(d\bar{b}); (b\bar{d})$	0	5.325
$B^{*\pm}$	$(u\bar{b}); (b\bar{u})$	± 1	5.325
B_s^{*0}, \bar{B}_s^{*0}	$(s\bar{b}); (b\bar{s})$	0	5.415

Table 1.10: $J = 1$ mesons containing one heavy and one light quark and antiquark.

Note that these have the same charges and slightly larger masses than the corresponding $J = 0$ mesons in Table 1.7. Mesons with $J = 1$ and with both quark and antiquark heavy are shown in Table 1.11.

$J = 1$ meson		Charge	Mass (GeV/ c^2)
J/ψ “charmonium”	$(c\bar{c})$	0	3.096916
Υ “bottomonium”	$(b\bar{b})$	0	9.4603

Table 1.11: $J = 1$ mesons containing a heavy quark and a heavy antiquark.

In principle, there should also be $J = 1$ $B_c^{*\pm}$ mesons, but (unlike their $J = 0$ counterparts in Table 1.8) their existence has not been established experimentally. The heavy quarkonium ($c\bar{c}$ and $b\bar{b}$) systems have other states besides the η_c , J/ψ and η_b , Υ from Tables 1.8 and 1.11. For the $c\bar{c}$ system, there are $J = 0$ mesons $\chi_{c0,1,2}$ that have the quark and antiquark in P -wave

orbital angular momentum states. There are also states $\eta_c(2S)$, $\psi(2S)$, $\psi(3770)$, $\psi(3872)$ that are similar to the η_c and J/ψ , but with excited radial bound-state wavefunctions. Similarly, in the $b\bar{b}$ system, there are excited bottomonium states $\Upsilon(2S)$, $\Upsilon(3S)$, $\Upsilon(4S)$, $\Upsilon(10860)$, and $\Upsilon(11020)$ with $J = 1$, and P -wave orbital angular momentum states with total $J = 0$, $\chi_{b0,1,2}(1P)$ and $\chi_{b0,1,2}(2P)$. The spectroscopy of these states provides a striking confirmation of the quark model for hadrons and of the strong force.

Much more detailed information on all of these hadronic bound states (and many others not listed above), including the decay widths and the decay products, can be found in the RPP. Theoretically, one also expects exotic mesons that are mostly “gluonium” or glueballs, that is, bound states of gluons. However, these states are expected to mix with excited quark-antiquark bound states, and they will be extremely difficult to identify experimentally.

In collider experiments, hadrons are most often produced in groups called jets. Roughly speaking, each jet can be thought of as originating, at the shortest distance scales, from individual gluons and quarks (partons) which then hadronize by complicated processes into collections of final state particles that share the energy and momentum of the original parton. The hadrons in a given jet have momenta in approximately the same direction as their parent parton.

1.5 Decays and branching ratios

In some cases, hadrons can decay through the strong interactions, with widths of order tens or hundreds of MeV. Some examples include:

$$\Delta^{++} \rightarrow p\pi^+ \quad (1.5.1)$$

$$\rho^- \rightarrow \pi^0\pi^- \quad (1.5.2)$$

$$\omega \rightarrow \pi^+\pi^-\pi^0 \quad (1.5.3)$$

$$\phi \rightarrow K^+K^-. \quad (1.5.4)$$

There are also decays that are mediated by electromagnetic interactions, for example:

$$\pi^0 \rightarrow \gamma\gamma \quad (1.5.5)$$

$$\Delta^+ \rightarrow p\gamma \quad (1.5.6)$$

$$\Sigma^0 \rightarrow \Lambda\gamma \quad (1.5.7)$$

$$\rho^0 \rightarrow \pi^+\pi^-\gamma. \quad (1.5.8)$$

The smallest decay widths for hadrons are those mediated by the weak interactions, for example:

$$n \rightarrow pe^-\bar{\nu}_e \quad (1.5.9)$$

$$\pi^- \rightarrow \mu^-\bar{\nu}_\mu \quad (1.5.10)$$

$$K^+ \rightarrow \pi^+\pi^0 \quad (1.5.11)$$

$$B^+ \rightarrow \bar{D}^0\mu^+\nu_\tau \quad (1.5.12)$$

$$\Omega^- \rightarrow K^-\Lambda. \quad (1.5.13)$$

The weak interactions are also entirely responsible for the decays of the charged leptons:

$$\mu^- \rightarrow \nu_\mu e^- \bar{\nu}_e \quad (1.5.14)$$

$$\tau^- \rightarrow \nu_\tau e^- \bar{\nu}_e \quad (1.5.15)$$

$$\tau^- \rightarrow \nu_\tau \mu^- \bar{\nu}_\mu \quad (1.5.16)$$

$$\tau^- \rightarrow \nu_\tau + \text{hadrons}. \quad (1.5.17)$$

Experimentally, the hadronic τ decays are classified by the number of charged hadrons present in the final state, as either “1-prong” (if exactly one charged hadron), “3-prong” (if exactly three charged hadrons), etc.

In most cases, a variety of different decay modes contribute to each total decay width. The fraction that each final state contributes to the total decay width is known as the branching ratio (or branching fraction), usually abbreviated as BR or B. As a randomly chosen example, in the case of the ω meson the strong interaction accounts for most, but not all, of the decays:

$$\text{BR}(\omega \rightarrow \pi^+ \pi^- \pi^0) = (89.2 \pm 0.7)\% \quad (\text{strong}) \quad (1.5.18)$$

$$\text{BR}(\omega \rightarrow \pi^0 \gamma) = (8.3 \pm 0.3)\% \quad (\text{EM}) \quad (1.5.19)$$

$$\text{BR}(\omega \rightarrow \pi^+ \pi^-) = (1.53 \pm 0.13)\% \quad (\text{EM}) \quad (1.5.20)$$

with other final states totaling less than 1%.

It is also common to present this information in terms of the partial widths into various final states. If the total decay width for a parent particle X is $\Gamma(X)$, then the partial decay width of X into a particular final state Y is

$$\Gamma(X \rightarrow Y) = \text{BR}(X \rightarrow Y) \Gamma(X). \quad (1.5.21)$$

The sum of all of the branching ratios is equal to 1, and the sum of the partial widths is equal to the total decay width.

There are two roads to enlightenment regarding the Standard Model and its future replacement. The experimental road, which is highly successful as indicated by the impressive volume and detail in the RPP, finds the answers to masses, decay rates, branching ratios, production rates, and even more detailed information like kinematic and angular distributions directly from data in high-energy collisions. The theoretical road aims to match these results onto predictions of quantum field theories specified in terms of a small number of parameters. In the case of electromagnetic interactions, quantum field theory is extremely successful, providing amazingly accurate predictions for observable quantities such as magnetic moments and interaction rates. In other applications, quantum field theory is only partly successful. For some calculations, perturbation theory and other known methods are too difficult to carry out, or do not converge even in principle. In some cases, lattice gauge theory provides useful information; this approach

is based on a discretized approximation to quantum field theory and stochastic methods. In other cases, only rough or even qualitative results are possible. However, quantum field theory is systematic and elegant, and provides understanding that is often elusive in the raw data. In the following notes, we will try to understand some of the basic calculation methods of quantum field theory as a general framework, and eventually the description of the Standard Model in terms of it.

2 Special Relativity and Lorentz Transformations

2.1 Lorentz transformations

A successful description of elementary particles must be consistent with the two pillars of modern physics: special relativity and quantum mechanics. Let us begin by reviewing some important features of special relativity.

Spacetime has four dimensions. For any given event (for example, a firecracker explodes, or a particle decays to two other particles) one can assign a four-vector position:

$$(ct, x, y, z) = (x^0, x^1, x^2, x^3) = x^\mu \quad (2.1.1)$$

The Greek indices μ, ν, ρ, \dots run over the values 0, 1, 2, 3, and c is the speed of light in vacuum. As a matter of terminology, x^μ is an example of a contravariant four-vector.

The laws of physics should not depend on what coordinate system we use, as long as it is an “inertial reference frame”, which means that the coordinates describing the position of a free classical particle do not accelerate. This invariance of the laws of physics is a guiding principle in making a sensible theory. It is often useful to change our coordinate system from one inertial reference frame to another, according to

$$x^\mu \rightarrow x'^\mu = L^\mu{}_\nu x^\nu. \quad (2.1.2)$$

Here $L^\mu{}_\nu$ is a constant 4×4 real matrix that parameterizes the Lorentz transformation. It is not arbitrary, however, as we will soon see. Such a change of coordinates is called a Lorentz transformation.

As a simple example of a Lorentz transformation, suppose we rotate our coordinate system about the z -axis by an angle α . Then in the new coordinate system:

$$x'^\mu = (ct', x', y', z') \quad (2.1.3)$$

where

$$\begin{aligned} ct' &= ct \\ x' &= x \cos \alpha + y \sin \alpha \\ y' &= -x \sin \alpha + y \cos \alpha \\ z' &= z. \end{aligned} \quad (2.1.4)$$

Alternatively, we could go to a frame moving with respect to the original frame with velocity v along the z direction, with the origins of the two frames coinciding at time $t = t' = 0$. Then:

$$ct' = \gamma(ct - \beta z)$$

$$\begin{aligned}
x' &= x \\
y' &= y \\
z' &= \gamma(z - \beta ct).
\end{aligned}
\tag{2.1.5}$$

where

$$\beta = v/c; \quad \gamma = 1/\sqrt{1 - \beta^2}.$$
(2.1.6)

Another way of rewriting this is to define the rapidity ρ by $\beta = \tanh \rho$, so that $\gamma = \cosh \rho$ and $\beta\gamma = \sinh \rho$. Then we can rewrite eq. (2.1.5),

$$\begin{aligned}
x'^0 &= x^0 \cosh \rho - x^3 \sinh \rho \\
x'^1 &= x^1 \\
x'^2 &= x^2 \\
x'^3 &= -x^0 \sinh \rho + x^3 \cosh \rho.
\end{aligned}
\tag{2.1.7}$$

This change of coordinates is called a boost (with rapidity ρ and in the \hat{z} direction).

Another example of a contravariant four-vector is given by the 4-momentum formed from the energy E and spatial momentum \vec{p} of a particle:

$$p^\mu = (E/c, \vec{p}).$$
(2.1.8)

In the rest frame of a particle of mass m , its 4-momentum is given by $p^\mu = (mc, 0, 0, 0)$. All contravariant four-vectors transform the same way under a Lorentz transformation:

$$a'^\mu = L^\mu{}_\nu a^\nu.$$
(2.1.9)

The 4-momentum of a particle is related to its mass by the Lorentz transformation that relates the frame of reference in which it is measured and the rest frame. In the example of eq. (2.1.5), one has:

$$L^\mu{}_\nu = \begin{pmatrix} \gamma & 0 & 0 & -\beta\gamma \\ 0 & 1 & 0 & 0 \\ 0 & 0 & 1 & 0 \\ -\beta\gamma & 0 & 0 & \gamma \end{pmatrix},$$
(2.1.10)

and the inverse Lorentz transformation is

$$a^\mu = (L^{-1})^\mu{}_\nu a'^\nu, \quad (L^{-1})^\mu{}_\nu = \begin{pmatrix} \gamma & 0 & 0 & \beta\gamma \\ 0 & 1 & 0 & 0 \\ 0 & 0 & 1 & 0 \\ \beta\gamma & 0 & 0 & \gamma \end{pmatrix}.$$
(2.1.11)

A key property of special relativity is that for any two events one can define a proper interval, which is independent of the Lorentz frame, and which tells us how far apart the two events are in a coordinate-independent sense. So, consider two events occurring at x^μ and $x^\mu + d^\mu$, where d^μ is some four-vector displacement. The proper interval between the events is

$$(\Delta\tau)^2 = (d^0)^2 - (d^1)^2 - (d^2)^2 - (d^3)^2 = g_{\mu\nu}d^\mu d^\nu \quad (2.1.12)$$

where

$$g_{\mu\nu} = \begin{pmatrix} 1 & 0 & 0 & 0 \\ 0 & -1 & 0 & 0 \\ 0 & 0 & -1 & 0 \\ 0 & 0 & 0 & -1 \end{pmatrix} \quad (2.1.13)$$

is known as the metric tensor. Here, and from now on, we adopt the Einstein summation convention, in which repeated indices μ, ν, \dots are taken to be summed over. It is an assumption of special relativity that $g_{\mu\nu}$ is the same in every inertial reference frame.

The existence of the metric tensor allows us to define covariant four-vectors by lowering an index:

$$x_\mu = g_{\mu\nu}x^\nu = (ct, -x, -y, -z), \quad (2.1.14)$$

$$p_\mu = g_{\mu\nu}p^\nu = (E/c, -p_x, -p_y, -p_z). \quad (2.1.15)$$

Furthermore, one can define an inverse metric $g^{\mu\nu}$ so that

$$g^{\mu\nu}g_{\nu\rho} = \delta_\rho^\mu, \quad (2.1.16)$$

where $\delta_\nu^\mu = 1$ if $\mu = \nu$, and otherwise $= 0$. It follows that

$$g^{\mu\nu} = \begin{pmatrix} 1 & 0 & 0 & 0 \\ 0 & -1 & 0 & 0 \\ 0 & 0 & -1 & 0 \\ 0 & 0 & 0 & -1 \end{pmatrix}. \quad (2.1.17)$$

Then one has, for any vector a^μ ,

$$a_\mu = g_{\mu\nu}a^\nu; \quad a^\mu = g^{\mu\nu}a_\nu. \quad (2.1.18)$$

It follows that covariant four-vectors transform as

$$a'_\mu = L_\mu{}^\nu a_\nu \quad (2.1.19)$$

where (note the positions of the indices!)

$$L_\mu{}^\nu = g_{\mu\rho}g^{\nu\sigma}L^\rho{}_\sigma. \quad (2.1.20)$$

Because one can always use the metric to go between contravariant and covariant four-vectors, people often use a harmlessly sloppy terminology and neglect the distinction, simply referring to them as four-vectors.

If a^μ and b^μ are any four-vectors, then

$$a^\mu b^\nu g_{\mu\nu} = a_\mu b_\nu g^{\mu\nu} = a_\mu b^\mu = a^\mu b_\mu \equiv a \cdot b \quad (2.1.21)$$

is a scalar quantity. For example, if p^μ and q^μ are the four-momenta of any two particles, then $p \cdot q$ is a Lorentz-invariant; it does not depend on which inertial reference frame it is measured in. In particular, a particle with mass m satisfies the on-shell condition

$$p^2 = p^\mu p_\mu = E^2/c^2 - \vec{p}^2 = m^2 c^2. \quad (2.1.22)$$

The Lorentz invariance of dot products of pairs of 4-momenta, plus the conservation of total four-momentum, plus the on-shell condition (2.1.22), is enough to solve most problems in relativistic kinematics.

2.2 Relativistic kinematics

Let us pause to illustrate this with an example. Consider the situation of two particles, each of mass m , colliding. Suppose the result of the collision is two final-state particles each of mass M . Let us find the threshold energy and momentum 4-vectors for this process in the COM (center-of-momentum) frame and in the frame in which one of the initial-state particles is at rest. Throughout most of the following, we will take $c = 1$, by a choice of units.

Relativistic kinematics problems are often more easily analyzed in the COM frame, so let us consider that case first. Without loss of generality, we can take the colliding initial-state particles to be moving along the z -axis. Then their 4-momenta are:

$$p_1^\mu = (E, 0, 0, \sqrt{E^2 - m^2}) \quad (2.2.1)$$

$$p_2^\mu = (E, 0, 0, -\sqrt{E^2 - m^2}). \quad (2.2.2)$$

The spatial momenta are required to be opposite by the definition of the COM frame, which in turn requires the energies to be the same, using eq. (2.1.22) and the fact that the masses are assumed equal. The total 4-momentum of the initial state is $p^\mu = (2E, 0, 0, 0)$, and so this must be equal to the total 4-momentum of the final state in the COM frame as well. Furthermore,

$$p^2 = 4E^2 \quad (2.2.3)$$

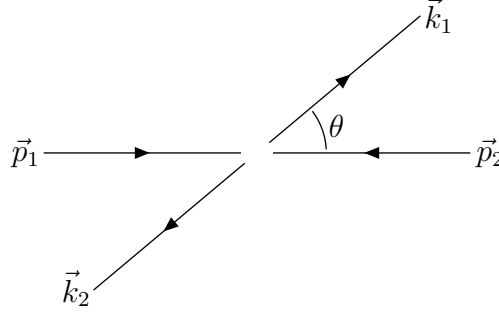
is a Lorentz invariant, the same in any inertial frame.

Similarly, in the COM frame, the final state 4-momenta can be written as:

$$k_1^\mu = (E_f, 0, \sin \theta \sqrt{E_f^2 - M^2}, \cos \theta \sqrt{E_f^2 - M^2}) \quad (2.2.4)$$

$$k_2^\mu = (E_f, 0, -\sin \theta \sqrt{E_f^2 - M^2}, -\cos \theta \sqrt{E_f^2 - M^2}). \quad (2.2.5)$$

The angle θ parametrizes the arbitrary direction of the scattering. Without loss of generality, we have taken the scattering to occur within the yz plane, as shown:



The fact that we are in the COM frame again requires the spatial momenta to be opposite, and thus the energies to be equal to a common value E_f because of the assumed equal masses M . Now, requiring conservation of total 4-momentum gives $k_1^\mu + k_2^\mu = p_1^\mu + p_2^\mu$, so $E_f = E$. In order for the spatial momentum components to be real, we therefore find the energy threshold condition in the COM frame

$$E > E_{\text{thresh}} = M. \quad (2.2.6)$$

Now let us reconsider the problem in a frame where one of the initial-state particles is at rest, corresponding to a fixed-target experiment. In the Lab frame,

$$p_1'^\mu = (E', 0, 0, \sqrt{E'^2 - m^2}), \quad (2.2.7)$$

$$p_2'^\mu = (m, 0, 0, 0) \quad (2.2.8)$$

are the 4-momenta of the two initial-state particles, and E' is the Lab frame energy of the moving particle. The total initial state 4-momentum is therefore $p'^\mu = (E' + m, 0, 0, \sqrt{E'^2 - m^2})$, leading to a Lorentz invariant

$$p'^2 = (E' + m)^2 - (E'^2 - m^2) = 2m(E' + m). \quad (2.2.9)$$

This must be the same as eq. (2.2.3), so the Lab frame energy is related to the COM energy of each particle by

$$m(E' + m) = 2E^2. \quad (2.2.10)$$

Because we already found $E > M$, the Lab frame threshold energy condition for the scattering event to be possible is $m(E' + m) > 2M^2$, or

$$E' > E'_{\text{thresh}} = \frac{2M^2 - m^2}{m}. \quad (2.2.11)$$

Let us also relate the Lab frame 4-momenta to those in the COM frame. To find the Lorentz transformation needed to go from the COM frame to the Lab frame, consider the 0, 3 components of the equation $p_2'^\mu = \Lambda^\mu{}_\nu p_2^\nu$:

$$\begin{pmatrix} m \\ 0 \end{pmatrix} = \begin{pmatrix} \gamma & \beta\gamma \\ \beta\gamma & \gamma \end{pmatrix} \begin{pmatrix} E \\ -\sqrt{E^2 - m^2} \end{pmatrix}. \quad (2.2.12)$$

It follows that

$$\beta = \sqrt{1 - m^2/E^2} = \sqrt{\frac{E' - m}{E' + m}}, \quad (2.2.13)$$

$$\gamma = \frac{1}{\sqrt{1 - \beta^2}} = E/m = \sqrt{\frac{E' + m}{2m}}, \quad (2.2.14)$$

$$\beta\gamma = \sqrt{E^2/m^2 - 1} = \sqrt{\frac{E' - m}{2m}}. \quad (2.2.15)$$

Now we can apply this Lorentz boost to the final-state momenta as found in the COM frame to obtain the Lab frame momenta. For the first final-state particle:

$$k_1'^\mu = \begin{pmatrix} \gamma & 0 & 0 & \beta\gamma \\ 0 & 1 & 0 & 0 \\ 0 & 0 & 1 & 0 \\ \beta\gamma & 0 & 0 & \gamma \end{pmatrix} \begin{pmatrix} E \\ 0 \\ \sin \theta \sqrt{E^2 - M^2} \\ \cos \theta \sqrt{E^2 - M^2} \end{pmatrix} \quad (2.2.16)$$

$$= (E^2/m) \begin{pmatrix} 1 + \cos \theta \sqrt{1 - m^2/E^2} \sqrt{1 - M^2/E^2} \\ 0 \\ \sin \theta (m/E) \sqrt{1 - M^2/E^2} \\ \sqrt{1 - m^2/E^2} + \cos \theta \sqrt{1 - M^2/E^2} \end{pmatrix}. \quad (2.2.17)$$

Note that for $M > m$, the z -component of the momentum is always positive (in the same direction as the incoming particle in the Lab frame), regardless of the sign of $\cos \theta$. (The other final-state momentum is obtained by just flipping the signs of $\cos \theta$ and $\sin \theta$.) The Lab-frame scattering angle with respect to the original collision axis (the z -axis in both frames) is determined by

$$\tan \theta' = \frac{(m/E) \sin \theta}{\sqrt{1 - m^2/E^2} / \sqrt{1 - M^2/E^2} + \cos \theta}. \quad (2.2.18)$$

For fixed θ in the COM frame, $|\theta'|$ in the Lab frame decreases with increasing E/m , as the produced particles go more in the forward direction.

Notice from eqs. (2.2.6) and (2.2.11) that while the production of a pair of heavy particles of mass M requires beam energies in symmetric collisions that scale like M , in fixed-target collisions the energy required scales like $2M^2/m \gg M$, where m is the beam particle mass. This is why fixed-target collisions are no longer an option for frontier physics discoveries of very heavy particles or high-energy phenomena.

In collider applications, it is common to see the direction of a final-state particle with respect to the colliding beams described either by the pseudo-rapidity η or the longitudinal rapidity y . Suppose that the two colliding beams are oriented so that Beam 1 is going in the \hat{z} direction and Beam 2 is going in the $-\hat{z}$ direction. A final state particle (or group of particles) emerging at an angle θ with respect to Beam 1 in general has a four-vector momentum given by:

$$p^\mu = (E, p_T \cos \phi, p_T \sin \phi, p_z), \quad (2.2.19)$$

where $p_T = |\vec{p}| \sin \theta$ is the transverse momentum, $p_z = |\vec{p}| \cos \theta$ is the longitudinal momentum, and $E = \sqrt{|\vec{p}|^2 + m^2}$ is the energy, with m the mass and \vec{p} the three-vector momentum. (In hadron colliders, this four-vector is generally defined in the lab frame, not in the center-of-momentum frame of the scattering event, which is often unknown.) Then the pseudo-rapidity is defined by

$$\eta = \frac{1}{2} \ln \left(\frac{|\vec{p}| + p_z}{|\vec{p}| - p_z} \right) = -\ln [\tan(\theta/2)]. \quad (2.2.20)$$

Thus $\eta = 0$ corresponds to a particle coming out perpendicular to the beam line ($\theta = 90^\circ$), while $\eta = \pm\infty$ correspond to the directions along the beams ($\theta = 0, 180^\circ$). Particles at small $|\eta|$ (less than 1 or 2 or so, depending on the situation) are said to be central, while those at large $|\eta|$ are said to be forward. Note that the pseudo-rapidity depends only on the direction of the particle, not on its energy. The longitudinal rapidity is defined somewhat similarly by

$$y = \frac{1}{2} \ln \left(\frac{E + p_z}{E - p_z} \right). \quad (2.2.21)$$

In fact, $\eta = y$ in the special case of a massless particle, and they are very nearly equal for a particle whose energy is large compared to its mass. However, in general y does depend on the energy. For the same particle, the ordinary rapidity is given by:

$$\rho = \frac{1}{2} \ln \left(\frac{E + |\vec{p}|}{E - |\vec{p}|} \right). \quad (2.2.22)$$

The quantity y is the rapidity of the boost needed to move to a frame where the particle has no longitudinal momentum along the beam direction, while ρ is the rapidity of the boost needed to move to the particle's rest frame. Confusingly, it has become a standard abuse of language

among collider physicists to call y simply the rapidity, and among non-collider physicists it is common to see the letter η used to refer to the ordinary rapidity, called ρ here. Some care is needed to ensure that one is using and interpreting these quantities consistently.

2.3 Tensors and Lorentz invariant quantities

Now let us return to the study of the properties of Lorentz transformations. The Lorentz-invariance of equation (2.1.21) implies that, if a^μ and b^μ are constant four-vectors, then

$$g_{\mu\nu}a'^\mu b'^\nu = g_{\mu\nu}a^\mu b^\nu, \quad (2.3.1)$$

so that

$$g_{\mu\nu}L^\mu{}_\rho L^\nu{}_\sigma a^\rho b^\sigma = g_{\rho\sigma}a^\rho b^\sigma. \quad (2.3.2)$$

Since a^μ and b^ν are arbitrary, it must be that:

$$g_{\mu\nu}L^\mu{}_\rho L^\nu{}_\sigma = g_{\rho\sigma}. \quad (2.3.3)$$

This is the fundamental constraint that a Lorentz transformation matrix must satisfy. In matrix form, it could be written as $L^T g L = g$. If we contract eq. (2.3.3) with $g^{\rho\kappa}$, we obtain

$$L_\nu{}^\kappa L^\nu{}_\sigma = \delta_\sigma^\kappa \quad (2.3.4)$$

Applying this to eqs. (2.1.2) and (2.1.19), we find that the inverse Lorentz transformation of any four-vector is

$$a^\nu = a'^\mu L_\mu{}^\nu \quad (2.3.5)$$

$$a_\nu = a'_\mu L^\mu{}_\nu \quad (2.3.6)$$

Let us now consider some more particular Lorentz transformations. To begin, we note that as a matrix, $\det(L) = \pm 1$. (See homework problem.) An example of a “large” Lorentz transformation with $\det(L) = -1$ is:

$$L^\mu{}_\nu = \begin{pmatrix} -1 & 0 & 0 & 0 \\ 0 & 1 & 0 & 0 \\ 0 & 0 & 1 & 0 \\ 0 & 0 & 0 & 1 \end{pmatrix}. \quad (2.3.7)$$

This just flips the sign of the time coordinate, and is therefore known as time reversal:

$$x'^0 = -x^0 \quad x'^1 = x^1 \quad x'^2 = x^2 \quad x'^3 = x^3. \quad (2.3.8)$$

Another “large” Lorentz transformation is parity, or space inversion:

$$L^\mu{}_\nu = \begin{pmatrix} 1 & 0 & 0 & 0 \\ 0 & -1 & 0 & 0 \\ 0 & 0 & -1 & 0 \\ 0 & 0 & 0 & -1 \end{pmatrix}, \quad (2.3.9)$$

so that:

$$x'^0 = x^0 \quad x'^1 = -x^1 \quad x'^2 = -x^2 \quad x'^3 = -x^3. \quad (2.3.10)$$

It was once thought that the laws of physics have to be invariant under these operations. However, it was shown experimentally in the 1950’s that parity is violated in the weak interactions, specifically in the weak decays of the ^{60}Co nucleus and the K^\pm mesons. Likewise, experiments in the 1960’s on the decays of K^0 mesons showed that time-reversal invariance is violated (at least if very general properties of quantum mechanics and special relativity are assumed).

However, all experiments up to now are consistent with invariance of the laws of physics under the subset of Lorentz transformations that are continuously connected to the identity; these are known as “proper” Lorentz transformations and have $\det(L) = +1$. They can be built up out of infinitesimal Lorentz transformations:

$$L^\mu{}_\nu = \delta^\mu_\nu + \omega^\mu{}_\nu + \mathcal{O}(\omega^2), \quad (2.3.11)$$

where we agree to drop everything with more than one $\omega^\mu{}_\nu$. Then, according to eq. (2.3.3),

$$g_{\mu\nu}(\delta^\mu_\rho + \omega^\mu{}_\rho + \dots)(\delta^\nu_\sigma + \omega^\nu{}_\sigma + \dots) = g_{\rho\sigma}, \quad (2.3.12)$$

or

$$g_{\rho\sigma} + \omega_{\sigma\rho} + \omega_{\rho\sigma} + \dots = g_{\rho\sigma}. \quad (2.3.13)$$

Therefore

$$\omega_{\sigma\rho} = -\omega_{\rho\sigma} \quad (2.3.14)$$

is an antisymmetric 4×4 matrix, with $4 \cdot 3/2 \cdot 1 = 6$ independent entries. These correspond to 3 rotations ($\rho, \sigma = 1, 2$ or $1, 3$ or $2, 3$) and 3 boosts ($\rho, \sigma = 0, 1$ or $0, 2$ or $0, 3$). It is a mathematical fact that any Lorentz transformation can be built up out of repeated infinitesimal boosts and rotations, combined with the operations of time-reversal and space inversion.

Lorentz transformations obey the mathematical properties of a group, known as the Lorentz group. The subset of Lorentz transformations that can be built out of repeated infinitesimal boosts and rotations form a smaller group, called the proper Lorentz group. In the Standard

Model of particle physics and generalizations of it, all interesting objects, including operators, states, particles, and fields, transform as well-defined representations of the Lorentz group. We will study these group representations in more detail later.

So far we have considered constant four-vectors. However, one can also consider four-vectors that depend on position in spacetime. For example, suppose that $F(x)$ is a scalar function of x^μ . It is usual to leave the index μ off of x^μ when it is used as the argument of a function, so $F(x)$ really means $F(x^0, x^1, x^2, x^3)$. Under a Lorentz transformation from coordinates $x^\mu \rightarrow x'^\mu$, at a given fixed point in spacetime the value of the function F' reported by an observer using the primed coordinate system is taken to be equal to the value of the original function F in the original coordinates:

$$F'(x') = F(x). \quad (2.3.15)$$

Then

$$\partial_\mu F \equiv \frac{\partial F}{\partial x^\mu} = \left(\frac{1}{c} \frac{\partial F}{\partial t}, \vec{\nabla} F \right) \quad (2.3.16)$$

is a covariant four-vector. This is because:

$$(\partial_\mu F)'(x') \equiv \frac{\partial}{\partial x'^\mu} F'(x') = \frac{\partial x^\nu}{\partial x'^\mu} \frac{\partial}{\partial x^\nu} F(x) = L_\mu{}^\nu (\partial_\nu F)(x), \quad (2.3.17)$$

showing that it transforms according to eq. (2.1.19). [The second equality uses the chain rule and eq. (2.3.15); the last equality uses eq. (2.3.5) with $a^\mu = x^\mu$.] By raising the index, one obtains a contravariant four-vector function

$$\partial^\mu F = g^{\mu\nu} \partial_\nu F = \left(\frac{1}{c} \frac{\partial F}{\partial t}, -\vec{\nabla} F \right). \quad (2.3.18)$$

One can obtain another scalar function by acting twice with the 4-dimensional derivative operator on F , contracting the indices on the derivatives:

$$\partial^\mu \partial_\mu F = \frac{1}{c^2} \frac{\partial^2 F}{\partial t^2} - \nabla^2 F. \quad (2.3.19)$$

The object $-\partial^\mu \partial_\mu F$ is a 4-dimensional generalization of the Laplacian.

A tensor is an object that can carry an arbitrary number of spacetime vector indices, and transforms appropriately when one goes to a new reference frame. The objects $g^{\mu\nu}$ and $g_{\mu\nu}$ and δ^μ_ν are constant tensors. Four-vectors and scalar functions and 4-derivatives of them are also tensors. In general, the defining characteristic of a tensor function $T^{\mu_1\mu_2\cdots}_{\nu_1\nu_2\cdots}(x)$ is that under a change of reference frame, it transforms so that in the primed coordinate system, the corresponding tensor T' is:

$$T'^{\mu_1\mu_2\cdots}_{\nu_1\nu_2\cdots}(x') = L^{\mu_1}{}_{\rho_1} L^{\mu_2}{}_{\rho_2} \cdots L^{\sigma_1}{}_{\nu_1} L^{\sigma_2}{}_{\nu_2} \cdots T^{\rho_1\rho_2\cdots}_{\sigma_1\sigma_2\cdots}(x). \quad (2.3.20)$$

A special and useful constant tensor is the totally antisymmetric Levi-Civita tensor:

$$\epsilon_{\mu\nu\rho\sigma} = \begin{cases} +1 & \text{if } \mu\nu\rho\sigma \text{ is an even permutation of } 0123 \\ -1 & \text{if } \mu\nu\rho\sigma \text{ is an odd permutation of } 0123 \\ 0 & \text{otherwise} \end{cases} \quad (2.3.21)$$

One use for the Levi-Civita tensor is in understanding the Lorentz invariance of four-dimensional integration. Define 4 four-vectors so that in a particular frame they are given by the infinitesimal differentials:

$$A^\mu = (cdt, 0, 0, 0); \quad (2.3.22)$$

$$B^\mu = (0, dx, 0, 0); \quad (2.3.23)$$

$$C^\mu = (0, 0, dy, 0); \quad (2.3.24)$$

$$D^\mu = (0, 0, 0, dz). \quad (2.3.25)$$

Then the 4-dimensional volume element

$$d^4x \equiv dx^0 dx^1 dx^2 dx^3 = A^\mu B^\nu C^\rho D^\sigma \epsilon_{\mu\nu\rho\sigma} \quad (2.3.26)$$

is Lorentz-invariant, since in the last expression it has no uncontracted four-vector indices. It follows that if $F(x)$ is a Lorentz scalar function of x^μ , then the integral

$$I[F] = \int d^4x F(x) \quad (2.3.27)$$

is invariant under Lorentz transformations. This is good because eventually we will learn to define theories in terms of such an integral, known as the *action*.

2.4 Maxwell's equations and electromagnetism

An example of a relativistic theory that we are familiar with is electricity and magnetism. It is instructive to recast Maxwell's equations into a manifestly relativistic form. This will give us familiarity with four-component gauge field formulation of the relativistic wave equations governing electromagnetic fields. We will also see the relativistic version of gauge invariance and concept of gauge transformations for the electromagnetic field, which will be explored more completely in later sections.

Recall that Maxwell's equations can be written in the form:

$$\vec{\nabla} \cdot \vec{E} = e\rho, \quad (2.4.1)$$

$$\vec{\nabla} \times \vec{B} - \frac{\partial \vec{E}}{\partial t} = e\vec{J}, \quad (2.4.2)$$

$$\vec{\nabla} \cdot \vec{B} = 0, \quad (2.4.3)$$

$$\vec{\nabla} \times \vec{E} + \frac{\partial \vec{B}}{\partial t} = 0, \quad (2.4.4)$$

where ρ is the local charge density and \vec{J} is the current density, with the magnitude of the electron's charge, e , factored out. These equations can be rewritten in a manifestly relativistic form, using the following observations. First, suppose we add together the equations obtained by taking $\partial/\partial t$ of eq. (2.4.1) and $\vec{\nabla} \cdot$ of eq. (2.4.2). Since the divergence of a curl vanishes identically, this yields the Law of Local Conservation of Charge:

$$\frac{\partial \rho}{\partial t} + \vec{\nabla} \cdot \vec{J} = 0. \quad (2.4.5)$$

To put this into a Lorentz-invariant form, we can form a four-vector charge and current density:

$$J^\mu = (\rho, \vec{J}), \quad (2.4.6)$$

so that eq. (2.4.5) becomes

$$\partial_\mu J^\mu = 0. \quad (2.4.7)$$

Furthermore, eqs. (2.4.3) and (2.4.4) imply that we can write the electric and magnetic fields as derivatives of the electric and magnetic potentials V and \vec{A} :

$$\vec{E} = -\vec{\nabla}V - \frac{\partial \vec{A}}{\partial t}, \quad (2.4.8)$$

$$\vec{B} = \vec{\nabla} \times \vec{A}. \quad (2.4.9)$$

Now if we assemble the potentials into a four-vector:

$$A^\mu = (V, \vec{A}), \quad (2.4.10)$$

then eqs. (2.4.8) and (2.4.9) mean that we can write the electric and magnetic fields as components of an antisymmetric tensor:

$$F_{\mu\nu} = \partial_\mu A_\nu - \partial_\nu A_\mu \quad (2.4.11)$$

$$= \begin{pmatrix} 0 & E_x & E_y & E_z \\ -E_x & 0 & -B_z & B_y \\ -E_y & B_z & 0 & -B_x \\ -E_z & -B_y & B_x & 0 \end{pmatrix}. \quad (2.4.12)$$

Now the Maxwell equations (2.4.1) and (2.4.2) correspond to the relativistic wave equation

$$\partial_\mu F^{\mu\nu} = eJ^\nu, \quad (2.4.13)$$

or equivalently,

$$\partial_\mu \partial^\mu A^\nu - \partial^\nu \partial_\mu A^\mu = eJ^\nu. \quad (2.4.14)$$

The remaining Maxwell equations (2.4.3) and (2.4.4) are equivalent to the identity:

$$\partial_\rho F_{\mu\nu} + \partial_\mu F_{\nu\rho} + \partial_\nu F_{\rho\mu} = 0, \quad (2.4.15)$$

for $\mu, \nu, \rho = \text{any of } 0, 1, 2, 3$. Note that this equation is automatically true because of eq. (2.4.11). Also, because $F^{\mu\nu}$ is antisymmetric and partial derivatives commute, $\partial_\mu \partial_\nu F^{\mu\nu} = 0$, so that the Law of Local Conservation of Charge eq. (2.4.7) follows from eq. (2.4.13).

The potential $A^\mu(x)$ may be thought of as fundamental, and the fields \vec{E} and \vec{B} as derived from it. The theory of electromagnetism as described by $A^\mu(x)$ is subject to a redundancy known as gauge invariance. To see this, we note that eq. (2.4.14) is unchanged if we do the transformation

$$A^\mu(x) \rightarrow A^\mu(x) + \partial^\mu \lambda(x), \quad (2.4.16)$$

where $\lambda(x)$ is any function of position in spacetime. In components, this amounts to:

$$V \rightarrow V + \frac{\partial \lambda}{\partial t}, \quad (2.4.17)$$

$$\vec{A} \rightarrow \vec{A} - \vec{\nabla} \lambda. \quad (2.4.18)$$

This transformation leaves $F^{\mu\nu}$ (or equivalently \vec{E} and \vec{B}) unchanged. Therefore, the new A^μ is just as good as the old A^μ for the purposes of describing a particular physical situation.

3 Relativistic Quantum Mechanics of Single Particles

3.1 Klein-Gordon and Dirac equations

Any realistic theory must be consistent with quantum mechanics. In this section, we consider how to formulate a theory of quantum mechanics that is consistent with special relativity.

Suppose that $\Phi(x)$ is the wavefunction of a free particle in 4-dimensional spacetime. A fundamental principle of quantum mechanics is that the time dependence of Φ is determined by a Hamiltonian operator, according to:

$$H\Phi = i\hbar \frac{\partial}{\partial t} \Phi. \quad (3.1.1)$$

Now, the three-momentum operator is given by

$$\vec{P} = -i\hbar \vec{\nabla}. \quad (3.1.2)$$

Because H and \vec{P} commute, one can take Φ to be one of the basis of wavefunctions for eigenstates with energy and momentum eigenvalues E and \vec{p} respectively:

$$H\Phi = E\Phi; \quad \vec{P}\Phi = \vec{p}\Phi. \quad (3.1.3)$$

One can now turn this into a relativistic Schrodinger wave equation for free particle states, by using the fact that special relativity implies:

$$E = \sqrt{m^2 c^4 + \vec{p}^2 c^2}, \quad (3.1.4)$$

where m is the mass of the particle. To make sense of this as an operator equation, we could try expanding it in an infinite series, treating \vec{p}^2 as small compared to $m^2 c^2$:

$$i\hbar \frac{\partial}{\partial t} \Phi = mc^2 \left(1 + \frac{\vec{p}^2}{2m^2 c^2} - \frac{\vec{p}^4}{8m^4 c^4} + \dots \right) \Phi \quad (3.1.5)$$

$$= \left[mc^2 - \frac{\hbar^2}{2m} \nabla^2 - \frac{\hbar^4}{8m^3 c^2} (\nabla^2)^2 + \dots \right] \Phi \quad (3.1.6)$$

If we keep only the first two terms, then we recover the standard non-relativistic quantum mechanics of a free particle; the first term mc^2 is an unobservable constant contribution to the Hamiltonian, proportional to the rest energy, and the second term is the usual non-relativistic kinetic energy. However, the presence of an infinite number of derivatives leads to horrible problems, including apparently non-local effects.

Instead, one can consider the operator H^2 acting on Φ , avoiding the square root. It follows that

$$H^2 \Phi = E^2 \Phi = (c^2 \vec{p}^2 + m^2 c^4) \Phi = (c^2 \vec{P}^2 + m^2 c^4) \Phi, \quad (3.1.7)$$

so that:

$$-\frac{\partial^2 \Phi}{\partial t^2} = -\nabla^2 \Phi + m^2 \Phi. \quad (3.1.8)$$

Here and from now on we have set $c = 1$ and $\hbar = 1$ by a choice of units. This convention means that mass, energy, and momentum all have the same units (GeV), while time and distance have units of GeV^{-1} , and velocity is dimensionless. These conventions greatly simplify the equations of particle physics. One can always recover the usual metric system units using the following conversion table for energy, mass, distance, and time, respectively:

$$1 \text{ GeV} = 1.6022 \times 10^{-3} \text{ erg} = 1.6022 \times 10^{-10} \text{ Joules}, \quad (3.1.9)$$

$$(1 \text{ GeV})/c^2 = 1.7827 \times 10^{-24} \text{ g} = 1.7827 \times 10^{-27} \text{ kg}, \quad (3.1.10)$$

$$(1 \text{ GeV})^{-1}(\hbar c) = 1.9733 \times 10^{-14} \text{ cm} = 1.9733 \times 10^{-16} \text{ m}, \quad (3.1.11)$$

$$(1 \text{ GeV})^{-1}\hbar = 6.58212 \times 10^{-25} \text{ sec}. \quad (3.1.12)$$

Using eq. (2.3.19), the wave-equation eq. (3.1.8) can be rewritten in a manifestly Lorentz-invariant way as

$$(\partial^\mu \partial_\mu + m^2)\Phi = 0. \quad (3.1.13)$$

This relativistic generalization of the Schrodinger equation is known as the Klein-Gordon equation.

It is easy to guess the solutions of the Klein-Gordon equation. If we try:

$$\Phi(x) = \Phi_0 e^{-ik \cdot x}, \quad (3.1.14)$$

where Φ_0 is a constant and k^μ is a four-vector, then $\partial_\mu \Phi = -ik_\mu \Phi$ and so

$$\partial^\mu \partial_\mu \Phi = -k^\mu k_\mu \Phi = -k^2 \Phi. \quad (3.1.15)$$

Therefore, we only need to impose $k^2 = m^2$ to have a solution. It is then easy to check that this is an eigenstate of H and \vec{P} with energy $E = k^0$ and three-momentum $\vec{p} = \vec{k}$, satisfying $E^2 = \vec{p}^2 + m^2$.

However, there is a big problem with this. If $k^\mu = (E, \vec{p})$ gives a solution, then so does $k^\mu = (-E, \vec{p})$. By increasing $|\vec{p}|$, one can have $|E|$ arbitrarily large. This is a disaster, because the energy is not bounded from below. If the particle can interact, it will make transitions from higher energy states to lower energy states. This would seem to lead to the release of an infinite amount of energy as the particle acquires a larger and larger three-momentum, without bound!

In 1927, Dirac suggested an alternative, based on the observation that the problem with the Klein-Gordon equation seems to be that it is quadratic in H or equivalently $\partial/\partial t$; this leads

to the sign ambiguity for E . Dirac could also have been[†] motivated by the fact that particles like the electron have spin; since they have more than one intrinsic degree of freedom, trying to explain them with a single wavefunction $\Phi(x)$ is doomed to failure. Instead, Dirac proposed to write a relativistic Schrodinger equation, for a multi-component wavefunction $\Psi_a(x)$, where the spinor index $a = 1, 2, \dots, n$ runs over the components. The wave equation should be linear in $\partial/\partial t$; since relativity places t on the same footing as x, y, z , it should also be linear in derivatives of the spatial coordinates. Therefore, the equation ought to take the form

$$i\frac{\partial}{\partial t}\Psi = H\Psi = (\vec{\alpha} \cdot \vec{P} + \beta m)\Psi, \quad (3.1.16)$$

where $\alpha_x, \alpha_y, \alpha_z$, and β are $n \times n$ matrices acting in “spinor space”.

To determine what $\vec{\alpha}$ and β have to be, consider $H^2\Psi$. There are two ways to evaluate the result. First, by exactly the same reasoning as for the Klein-Gordon equation, one finds

$$-\frac{\partial^2}{\partial t^2}\Psi = (-\nabla^2 + m^2)\Psi. \quad (3.1.17)$$

On the other hand, expressing H in terms of the right-hand side of eq. (3.1.16), we find:

$$-\frac{\partial^2}{\partial t^2}\Psi = \left[-\sum_{j,k=1}^3 \alpha_j \alpha_k \frac{\partial}{\partial x^j} \frac{\partial}{\partial x^k} - im \sum_j (\alpha_j \beta + \beta \alpha_j) \frac{\partial}{\partial x^j} + \beta^2 m^2 \right] \Psi. \quad (3.1.18)$$

Since partial derivatives commute, one can write:

$$\sum_{j,k=1}^3 \alpha_j \alpha_k \frac{\partial}{\partial x^j} \frac{\partial}{\partial x^k} = \frac{1}{2} \sum_{j,k=1}^3 (\alpha_j \alpha_k + \alpha_k \alpha_j) \frac{\partial}{\partial x^j} \frac{\partial}{\partial x^k}. \quad (3.1.19)$$

Then comparing eqs. (3.1.17) and (3.1.18), one finds that the two agree if, for $j, k = 1, 2, 3$:

$$\beta^2 = 1, \quad (3.1.20)$$

$$\alpha_j \beta + \beta \alpha_j = 0, \quad (3.1.21)$$

$$\alpha_j \alpha_k + \alpha_k \alpha_j = 2\delta_{jk}. \quad (3.1.22)$$

The simplest solution turns out to require $n = 4$ spinor indices. This may be somewhat surprising, since naively one only needs $n = 2$ to describe a spin-1/2 particle like the electron. As we will see, the Dirac equation automatically describes positrons as well as electrons, accounting for the doubling. It is easiest to write the solution in terms of 2×2 Pauli matrices:

$$\sigma^1 = \begin{pmatrix} 0 & 1 \\ 1 & 0 \end{pmatrix}, \quad \sigma^2 = \begin{pmatrix} 0 & -i \\ i & 0 \end{pmatrix}, \quad \sigma^3 = \begin{pmatrix} 1 & 0 \\ 0 & -1 \end{pmatrix}, \quad \text{and} \quad \sigma^0 = \begin{pmatrix} 1 & 0 \\ 0 & 1 \end{pmatrix}. \quad (3.1.23)$$

[†]Apparently, he realized this only in hindsight.

Then one can check that the 4×4 matrices

$$\beta = \begin{pmatrix} 0 & \sigma^0 \\ \sigma^0 & 0 \end{pmatrix}, \quad \alpha_j = \begin{pmatrix} -\sigma^j & 0 \\ 0 & \sigma^j \end{pmatrix}, \quad (j = 1, 2, 3) \quad (3.1.24)$$

obey the required conditions. The matrices β, α_j are written in 2×2 block form, so “0” actually denotes a 2×2 block of 0’s. Equation (3.1.16) is known as the Dirac equation, and the 4-component object is known as a Dirac spinor. Note that the fact that Dirac spinor space is 4-dimensional, just like ordinary spacetime, is really just a coincidence.[‡] One must be careful not to confuse the two types of 4-dimensional spaces!

It is convenient and traditional to rewrite the Dirac equation in a nicer way by multiplying it on the left by the matrix β , and defining

$$\gamma^0 = \beta, \quad \gamma^j = \beta \alpha_j, \quad (j = 1, 2, 3). \quad (3.1.25)$$

The result is

$$\left[i(\gamma^0 \frac{\partial}{\partial x^0} + \gamma^1 \frac{\partial}{\partial x^1} + \gamma^2 \frac{\partial}{\partial x^2} + \gamma^3 \frac{\partial}{\partial x^3}) - m \right] \Psi = 0, \quad (3.1.26)$$

or, even more nicely:

$$(i\gamma^\mu \partial_\mu - m)\Psi = 0. \quad (3.1.27)$$

The γ^μ matrices are explicitly given, in 2×2 blocks, by:

$$\gamma^0 = \begin{pmatrix} 0 & \sigma^0 \\ \sigma^0 & 0 \end{pmatrix}, \quad \gamma^j = \begin{pmatrix} 0 & \sigma^j \\ -\sigma^j & 0 \end{pmatrix}, \quad (j = 1, 2, 3). \quad (3.1.28)$$

[The solution found above for the γ^μ is not unique. To see this, suppose U is any constant unitary 4×4 matrix satisfying $U^\dagger U = 1$. Then the Dirac equation implies:

$$U(i\gamma^\mu \partial_\mu - m)U^\dagger U\Psi = 0, \quad (3.1.29)$$

from which it follows that, writing $\gamma'^\mu = U\gamma^\mu U^\dagger$, and $\Psi' = U\Psi$,

$$(i\gamma'^\mu \partial_\mu - m)\Psi' = 0. \quad (3.1.30)$$

So, the new γ'^μ matrices together with the new spinor Ψ' are just as good as the old pair γ^μ, Ψ ; there are an infinite number of different, equally valid choices. The set we’ve given above is called the chiral or Weyl representation. Another popular choice used by some textbooks (but not here) is the Pauli-Dirac representation.]

[‡]For example, if we lived in 10 dimensional spacetime, it turns out that Dirac spinors would have 32 components.

Many problems involving fermions in high-energy physics involve many gamma matrices dotted into partial derivatives or momentum four-vectors. To keep the notation from getting too bloated, it is often useful to use the Feynman slash notation:

$$\gamma^\mu a_\mu = \not{a} \quad (3.1.31)$$

for any four-vector a^μ . Then the Dirac equation takes the even more compact form:

$$(i\not{\partial} - m)\Psi = 0. \quad (3.1.32)$$

Some important properties of the γ^μ matrices are:

$$\gamma^{0\dagger} = \gamma^0, \quad \gamma^{j\dagger} = -\gamma^j, \quad (j = 1, 2, 3), \quad (3.1.33)$$

$$\gamma^0 \gamma^{\mu\dagger} \gamma^0 = \gamma^\mu, \quad (3.1.34)$$

$$\text{Tr}(\gamma_\mu \gamma_\nu) = 4g_{\mu\nu}, \quad (3.1.35)$$

$$\gamma^\mu \gamma_\mu = 4, \quad (3.1.36)$$

$$\gamma_\mu \gamma_\nu + \gamma_\nu \gamma_\mu = \{\gamma_\mu, \gamma_\nu\} = 2g_{\mu\nu}. \quad (3.1.37)$$

Note that on the right-hand sides of each of eqs. (3.1.36) and (3.1.37), there is an implicit 4×4 unit matrix. It turns out that one almost never needs to know the explicit form of the γ^μ . Instead, the equations above can be used to derive identities needed in practical work. (You will get some practice with this from the homework.)

How does a Dirac spinor $\Psi_a(x)$ transform under a Lorentz transformation? It carries no vector index, so it is not a tensor. On the other hand, the fact that the Hamiltonian “mixes up” the components of $\Psi_a(x)$ is a clue that it doesn’t transform like an ordinary scalar function either. Instead, we might expect that the spinor reported by an observer in the primed frame is given by

$$\Psi'(x') = \Lambda \Psi(x), \quad (3.1.38)$$

where Λ is a 4×4 matrix that depends on the Lorentz transformation matrix $L^\mu{}_\nu$. In fact, you will show for homework that for an infinitesimal Lorentz transformation $L^\mu{}_\nu = \delta^\mu{}_\nu + \omega^\mu{}_\nu$, one has:

$$\Psi'(x') = (1 - \frac{i}{2} \omega_{\mu\nu} S^{\mu\nu}) \Psi(x), \quad (3.1.39)$$

where

$$S^{\mu\nu} = \frac{i}{4} [\gamma^\mu, \gamma^\nu]. \quad (3.1.40)$$

To obtain the result for a non-infinitesimal proper Lorentz transformation, we can apply the same infinitesimal transformation a large number of times N , with $N \rightarrow \infty$. Letting $\Omega_{\mu\nu} = N\omega_{\mu\nu}$, we obtain, after N iterations of the Lorentz transformation parameterized by $\omega^\mu{}_\nu$:

$$L^\mu{}_\nu = (\delta^\mu{}_\nu + \Omega^\mu{}_\nu/N)^N \rightarrow [\exp(\Omega)]^\mu{}_\nu \quad (3.1.41)$$

as $N \rightarrow \infty$. Here we are using the identity:

$$\lim_{N \rightarrow \infty} (1 + x/N)^N = \exp(x), \quad (3.1.42)$$

with the exponential of a matrix to be interpreted in the power series sense:

$$\exp(M) = 1 + M + M^2/2 + M^3/6 + \dots \quad (3.1.43)$$

For the Dirac spinor, one has in the same way:

$$\Psi'(x') = \left(1 - \frac{i}{2}\Omega_{\mu\nu}S^{\mu\nu}/N\right)^N \Psi(x) \rightarrow \exp\left(-\frac{i}{2}\Omega_{\mu\nu}S^{\mu\nu}\right) \Psi(x). \quad (3.1.44)$$

So, we have found the Λ that appears in eq. (3.1.38) corresponding to the $L^\mu{}_\nu$ that appears in eq. (3.1.41):

$$\Lambda = \exp\left(-\frac{i}{2}\Omega_{\mu\nu}S^{\mu\nu}\right). \quad (3.1.45)$$

As an example, consider a boost in the z direction:

$$\Omega^\mu{}_\nu = \begin{pmatrix} 0 & 0 & 0 & -\rho \\ 0 & 0 & 0 & 0 \\ 0 & 0 & 0 & 0 \\ -\rho & 0 & 0 & 0 \end{pmatrix}. \quad (3.1.46)$$

Then

$$\Omega^2 = \begin{pmatrix} \rho^2 & 0 & 0 & 0 \\ 0 & 0 & 0 & 0 \\ 0 & 0 & 0 & 0 \\ 0 & 0 & 0 & \rho^2 \end{pmatrix}, \quad \Omega^3 = \begin{pmatrix} 0 & 0 & 0 & -\rho^3 \\ 0 & 0 & 0 & 0 \\ 0 & 0 & 0 & 0 \\ -\rho^3 & 0 & 0 & 0 \end{pmatrix}, \quad \text{etc.} \quad (3.1.47)$$

so that from eqs. (3.1.41) and (3.1.43),

$$\begin{aligned} L^\mu{}_\nu &= \begin{pmatrix} 1 & 0 & 0 & 0 \\ 0 & 1 & 0 & 0 \\ 0 & 0 & 1 & 0 \\ 0 & 0 & 0 & 1 \end{pmatrix} + \left(\frac{\rho^2}{2} + \frac{\rho^4}{24} + \dots\right) \begin{pmatrix} 1 & 0 & 0 & 0 \\ 0 & 0 & 0 & 0 \\ 0 & 0 & 0 & 0 \\ 0 & 0 & 0 & 1 \end{pmatrix} - \left(\rho + \frac{\rho^3}{6} + \dots\right) \begin{pmatrix} 0 & 0 & 0 & 1 \\ 0 & 0 & 0 & 0 \\ 0 & 0 & 0 & 0 \\ 1 & 0 & 0 & 0 \end{pmatrix} \\ &= \begin{pmatrix} \cosh \rho & 0 & 0 & -\sinh \rho \\ 0 & 1 & 0 & 0 \\ 0 & 0 & 1 & 0 \\ -\sinh \rho & 0 & 0 & \cosh \rho \end{pmatrix}, \end{aligned} \quad (3.1.48)$$

in agreement with eq. (2.1.7). Meanwhile, $\Omega_{03} = -\Omega_{30} = -\rho$, so

$$-\frac{i}{2}\Omega_{\mu\nu}S^{\mu\nu} = -\frac{\rho}{4}[\gamma^0, \gamma^3] = \frac{\rho}{2} \begin{pmatrix} \sigma^3 & 0 \\ 0 & -\sigma^3 \end{pmatrix} \quad (3.1.49)$$

in 2×2 blocks. Since this matrix is diagonal, it is particularly easy to exponentiate, and eq. (3.1.45) gives:

$$\Lambda = \exp \begin{pmatrix} \rho/2 & 0 & 0 & 0 \\ 0 & -\rho/2 & 0 & 0 \\ 0 & 0 & -\rho/2 & 0 \\ 0 & 0 & 0 & \rho/2 \end{pmatrix} = \begin{pmatrix} e^{\rho/2} & 0 & 0 & 0 \\ 0 & e^{-\rho/2} & 0 & 0 \\ 0 & 0 & e^{-\rho/2} & 0 \\ 0 & 0 & 0 & e^{\rho/2} \end{pmatrix}. \quad (3.1.50)$$

Therefore, this is the matrix that boosts a Dirac spinor in the z direction with rapidity ρ , in eq. (3.1.38).

Since Ψ is not a scalar, it is natural to ask whether one can use it to construct a scalar quantity. A tempting guess is to get rid of all the pesky spinor indices by

$$\Psi^\dagger \Psi(x) \equiv \sum_{a=1}^4 \Psi_a^\dagger \Psi_a. \quad (3.1.51)$$

However, under a Lorentz transformation, $\Psi'(x') = \Lambda \Psi(x)$ and $\Psi'^\dagger(x') = \Psi^\dagger(x) \Lambda^\dagger$, so:

$$\Psi'^\dagger \Psi'(x') = \Psi^\dagger \Lambda^\dagger \Lambda \Psi(x). \quad (3.1.52)$$

This will therefore be a scalar function if $\Lambda^\dagger \Lambda = 1$, in other words if Λ is a unitary matrix. However, this is not true, as the example of eq. (3.1.50) clearly illustrates.

Instead, with amazing foresight, let us consider the object

$$\Psi^\dagger \gamma^0 \Psi. \quad (3.1.53)$$

Under a Lorentz transformation:

$$\Psi'^\dagger \gamma^0 \Psi'(x') = \Psi^\dagger \Lambda^\dagger \gamma^0 \Lambda \Psi(x). \quad (3.1.54)$$

Therefore, $\Psi^\dagger \gamma^0 \Psi$ will transform as a scalar if:

$$\Lambda^\dagger \gamma^0 \Lambda = \gamma^0. \quad (3.1.55)$$

One can check that this is indeed true for the special case of eq. (3.1.50). More importantly, eq. (3.1.55) is true for any

$$\Lambda = 1 - \frac{i}{2} \omega_{\mu\nu} S^{\mu\nu} \quad (3.1.56)$$

that is infinitesimally close to the identity, using eqs. (3.1.33) and (3.1.34). Therefore, it is true for any proper Lorentz transformation built out of infinitesimal ones.

Motivated by this, one defines, for any Dirac spinor Ψ ,

$$\bar{\Psi} \equiv \Psi^\dagger \gamma^0. \quad (3.1.57)$$

One should think of Ψ as a column vector in spinor space, and $\bar{\Psi}$ as a row vector. Then their inner product

$$\bar{\Psi}\Psi, \quad (3.1.58)$$

with all spinor indices contracted, transforms as a scalar function under proper Lorentz transformations. Similarly, one can show that

$$\bar{\Psi}\gamma^\mu\Psi \quad (3.1.59)$$

transforms as a four-vector. One should think of eq. (3.1.59) as a (row vector) \times (matrix) \times (column vector) in spinor-index space, with a spacetime vector index μ hanging around.

3.2 Solutions of the Dirac equation

Our next task is to construct solutions to the Dirac equation. Let us separate out the x^μ -dependent part as a plane wave, by trying

$$\Psi(x) = u(p, s)e^{-ip \cdot x}. \quad (3.2.1)$$

Here p^μ is a four-vector momentum, with $p^0 = E > 0$. A solution to the Dirac equation must also satisfy the Klein-Gordon equation, so $p^2 = E^2 - \vec{p}^2 = m^2$. The object $u(p, s)$ is a spinor, labeled by the 4-momentum p and s . For now s just distinguishes between distinct solutions, but it will turn out to be related to the spin. Plugging this into the Dirac equation (3.1.32), we obtain a 4×4 eigenvalue equation to be solved for $u(p, s)$:

$$(\not{p} - m)u(p, s) = 0. \quad (3.2.2)$$

To simplify things, first consider this equation in the rest frame of the particle, where $p^\mu = (m, 0, 0, 0)$. In that frame,

$$m(\gamma^0 - 1)u(p, s) = 0. \quad (3.2.3)$$

Using the explicit form of γ^0 , we can therefore write in 2×2 blocks:

$$\begin{pmatrix} -1 & 1 \\ 1 & -1 \end{pmatrix} u(p, s) = 0, \quad (3.2.4)$$

where each “1” means a 2×2 unit matrix. The solutions are clearly

$$u(p, s) = \sqrt{m} \begin{pmatrix} \chi_s \\ \chi_s \end{pmatrix}, \quad (3.2.5)$$

where χ_s can be any 2-vector, and the \sqrt{m} normalization is a convention. In practice, it is best to choose the χ_s orthonormal, satisfying $\chi_s^\dagger \chi_r = \delta_{rs}$ for $r, s = 1, 2$. A particularly nice choice is:

$$\chi_1 = \begin{pmatrix} 1 \\ 0 \end{pmatrix}, \quad \chi_2 = \begin{pmatrix} 0 \\ 1 \end{pmatrix}. \quad (3.2.6)$$

As we will see, these just correspond to spin eigenstates $S_z = 1/2$ and $-1/2$.

Now, to construct the corresponding solution in any other frame, one can just boost the spinor using eqs. (3.1.45). For example, consider the solution

$$\Psi'(x') = u(p, 1)e^{-ip \cdot x'} = \sqrt{m} \begin{pmatrix} 1 \\ 0 \\ 1 \\ 0 \end{pmatrix} e^{-imt'} \quad (3.2.7)$$

in a frame where the particle is at rest; we have called it the primed frame for convenience. We suppose the primed frame is moving with respect to the unprimed frame with rapidity ρ in the z direction. Thus, the particle has, in the unprimed frame:

$$E = p^0 = m \cosh \rho; \quad p_z = p^3 = m \sinh \rho. \quad (3.2.8)$$

Now, $\Psi(x) = \Lambda^{-1} \Psi'(x')$ from eq. (3.1.38), so using the inverse of eq. (3.1.50):

$$\Psi(x) = \sqrt{m} \begin{pmatrix} e^{-\rho/2} \\ 0 \\ e^{\rho/2} \\ 0 \end{pmatrix} e^{-ip \cdot x}. \quad (3.2.9)$$

We can rewrite this, noting that from eq. (3.2.8),

$$\sqrt{m}e^{\rho/2} = \sqrt{E + p_z}, \quad \sqrt{m}e^{-\rho/2} = \sqrt{E - p_z}. \quad (3.2.10)$$

Therefore, one solution of the Dirac equation for a particle moving in the z direction, with energy E and three-momentum $p_z = \sqrt{E^2 - m^2}$, is:

$$\Psi(x) = \begin{pmatrix} \sqrt{E - p_z} \\ 0 \\ \sqrt{E + p_z} \\ 0 \end{pmatrix} e^{-ip \cdot x}, \quad (3.2.11)$$

so that

$$u(p, 1) = \begin{pmatrix} \sqrt{E - p_z} \\ 0 \\ \sqrt{E + p_z} \\ 0 \end{pmatrix} \quad (3.2.12)$$

in this frame.

Similarly, if we use instead $\chi_2 = \begin{pmatrix} 0 \\ 1 \end{pmatrix}$ in eq. (3.2.5) in the rest frame, and apply the same procedure, we find a solution:

$$\Psi(x) = \sqrt{m} \begin{pmatrix} 0 \\ e^{\rho/2} \\ 0 \\ e^{-\rho/2} \end{pmatrix} e^{-ip \cdot x} = \begin{pmatrix} 0 \\ \sqrt{E + p_z} \\ 0 \\ \sqrt{E - p_z} \end{pmatrix} e^{-ip \cdot x}, \quad (3.2.13)$$

so that

$$u(p, 2) = \begin{pmatrix} 0 \\ \sqrt{E + p_z} \\ 0 \\ \sqrt{E - p_z} \end{pmatrix} \quad (3.2.14)$$

in this frame. Note that p_z in eqs. (3.2.11) and (3.2.13) can have either sign, corresponding to the wavefunction for a particle moving in either the $+z$ or $-z$ directions.

In order to make a direct connection between spin and the various components of a Dirac spinor, let us now consider how to construct the spin operator \vec{S} . To do this, recall that by definition, spin is the difference between the total angular momentum operator \vec{J} and the orbital angular momentum operator \vec{L} :

$$\vec{J} = \vec{L} + \vec{S}. \quad (3.2.15)$$

Now,

$$\vec{L} = \vec{x} \times \vec{P}, \quad (3.2.16)$$

where \vec{x} and \vec{P} are the three-dimensional position and momentum operators. The total angular momentum must be conserved, or in other words it must commute with the Hamiltonian:

$$[H, \vec{J}] = 0. \quad (3.2.17)$$

Using the Dirac Hamiltonian given in eq. (3.1.16), we have

$$[H, \vec{L}] = [\vec{\alpha} \cdot \vec{P} + \beta m, \vec{x} \times \vec{P}] = -i\vec{\alpha} \times \vec{P}, \quad (3.2.18)$$

where we have used the canonical commutation relation (with $\hbar = 1$) $[P_j, x_k] = -i\delta_{jk}$. So, comparing eqs. (3.2.15), (3.2.17) and (3.2.18), it must be true that:

$$[H, \vec{S}] = i\vec{\alpha} \times \vec{P} = i \begin{pmatrix} -\vec{\sigma} \times \vec{P} & 0 \\ 0 & \vec{\sigma} \times \vec{P} \end{pmatrix}. \quad (3.2.19)$$

One can now observe that the matrix:

$$\vec{S} = \frac{1}{2} \begin{pmatrix} \vec{\sigma} & 0 \\ 0 & \vec{\sigma} \end{pmatrix} \quad (3.2.20)$$

obeys eq. (3.2.19). So, it must be the spin operator acting on Dirac spinors.

In particular, the z -component of the spin operator for Dirac spinors is given by the diagonal matrix:

$$S_z = \frac{1}{2} \begin{pmatrix} 1 & 0 & 0 & 0 \\ 0 & -1 & 0 & 0 \\ 0 & 0 & 1 & 0 \\ 0 & 0 & 0 & -1 \end{pmatrix}. \quad (3.2.21)$$

Therefore, the solutions in eqs. (3.2.11) and (3.2.13) can be identified to have spin eigenvalues $S_z = +1/2$ and $S_z = -1/2$, respectively. In general, a Dirac spinor eigenstate with $S_z = +1/2$ will have only the first and third components non-zero, and one with $S_z = -1/2$ will have only the second and fourth components non-zero, regardless of the direction of the momentum. Note that, as promised, $S_z = 1/2$ ($-1/2$) exactly corresponds to the use of χ_1 (χ_2) in eq. (3.2.5).

The helicity operator gives the relative orientation of the spin of the particle and its momentum. It is defined to be:

$$h = \frac{\vec{p} \cdot \vec{S}}{|\vec{p}|}. \quad (3.2.22)$$

Like S_z , helicity has possible eigenvalues $\pm 1/2$ for a spin-1/2 particle. For example, if $p_z > 0$, then eqs. (3.2.11) and (3.2.13) represent states with helicity $+1/2$ and $-1/2$ respectively. The helicity is not invariant under Lorentz transformations for massive particles. This is because one can always boost to a different frame in which the 3-momentum is flipped but the spin remains the same. (Also, note that unlike S_z , helicity is not even well-defined for a particle exactly at rest, due to the $|\vec{p}| = 0$ in the denominator.) However, a massless particle moves at the speed of light in any inertial frame, so one can never boost to a frame in which its 3-momentum direction is flipped. This means that for massless (or very energetic, so that $E \gg m$) particles, the helicity is fixed and invariant under Lorentz transformations. In any frame, a particle with \vec{p} and \vec{S} parallel has helicity $h = 1/2$, and a particle with \vec{p} and \vec{S} antiparallel has helicity $h = -1/2$.

Helicity is particularly useful in the high-energy limit. For example, we can consider four solutions obtained from the $E, p_z \gg m$ limits of eqs. (3.2.11) and (3.2.13), so that $|p_z| = E$:

$$\Psi_{p_z > 0, S_z = +1/2} = \begin{pmatrix} 0 \\ 0 \\ \sqrt{2E} \\ 0 \end{pmatrix} e^{-iE(t-z)} \quad [\vec{p} \uparrow, \vec{S} \uparrow, h = +1/2] \quad (3.2.23)$$

$$\Psi_{p_z > 0, S_z = -1/2} = \begin{pmatrix} 0 \\ \sqrt{2E} \\ 0 \\ 0 \end{pmatrix} e^{-iE(t-z)} \quad [\vec{p} \uparrow, \vec{S} \downarrow, h = -1/2] \quad (3.2.24)$$

$$\Psi_{p_z < 0, S_z = +1/2} = \begin{pmatrix} \sqrt{2E} \\ 0 \\ 0 \\ 0 \end{pmatrix} e^{-iE(t+z)} \quad [\vec{p} \downarrow, \vec{S} \uparrow, h = -1/2] \quad (3.2.25)$$

$$\Psi_{p_z < 0, S_z = -1/2} = \begin{pmatrix} 0 \\ 0 \\ 0 \\ \sqrt{2E} \end{pmatrix} e^{-iE(t+z)} \quad [\vec{p} \downarrow, \vec{S} \downarrow, h = +1/2] \quad (3.2.26)$$

In this high-energy limit, a Dirac spinor with $h = +1/2$ is called right-handed (R) and one with $h = -1/2$ is called left-handed (L). Notice that a high-energy L state is one that has the last two entries zero, while a high-energy R state always has the first two entries zero.

It is useful to define matrices that project onto L and R states in the high-energy or massless limit. In 2×2 blocks:

$$P_L = \begin{pmatrix} 1 & 0 \\ 0 & 0 \end{pmatrix}; \quad P_R = \begin{pmatrix} 0 & 0 \\ 0 & 1 \end{pmatrix}, \quad (3.2.27)$$

where 1 and 0 mean the 2×2 unit and zero matrices, respectively. Then P_L acting on any Dirac spinor gives back a left-handed spinor, by just killing the last two components. The projectors obey the rules:

$$P_L^2 = P_L; \quad P_R^2 = P_R; \quad P_R P_L = P_L P_R = 0. \quad (3.2.28)$$

It is traditional to write P_L and P_R in terms of a “fifth” gamma matrix, which in our conventions is given in 2×2 blocks by:

$$\gamma_5 = \begin{pmatrix} -1 & 0 \\ 0 & 1 \end{pmatrix}. \quad (3.2.29)$$

Then

$$P_L = \frac{1 - \gamma_5}{2}; \quad P_R = \frac{1 + \gamma_5}{2}. \quad (3.2.30)$$

The matrix γ_5 satisfies the equations:

$$\gamma_5^2 = 1; \quad \gamma_5^\dagger = \gamma_5; \quad \{\gamma_5, \gamma_\mu\} = 0. \quad (3.2.31)$$

So far, we have been considering Dirac spinor wavefunction solutions of the form

$$\Psi(x) = u(p, s) e^{-ip \cdot x} \quad (3.2.32)$$

with $p^0 = E > 0$. We have successfully interpreted these solutions in terms of a spin-1/2 particle, say, the electron. However, there is nothing mathematically wrong with these solutions

for p^μ with $p^0 < 0$ and $p^2 = m^2$. So, like the Klein-Gordon equation, the Dirac equation has the embarrassment of negative energy solutions.

Dirac proposed to get around the problem of negative energy states by using the fact that spin-1/2 particles are fermions. The Pauli exclusion principle dictates that two fermions cannot occupy the same quantum state. Therefore, Dirac proposed that all of the negative energy states are occupied. This prevents electrons with positive energy from making disastrous transitions to the $E < 0$ states. The infinite number of filled $E < 0$ states is called the Dirac sea.

If one of the states in the Dirac sea becomes unoccupied, it leaves behind a “hole”. Since a hole is the absence of an $E < 0$ state, it effectively has energy $-E > 0$. An electron has charge[†] $-e$, so the hole corresponding to its absence effectively has the opposite charge, $+e$. Since both electrons and holes obey $p^2 = m^2$, they have the same mass. Dirac’s proposal therefore predicts the existence of “anti-electrons” or positrons, with positive energy and positive charge. The positron was indeed discovered in 1932 in cosmic ray experiments.

Feynman and Stückelberg noted that one can reinterpret the positron as a negative energy electron moving backwards in time, so that $p^\mu \rightarrow -p^\mu$ and $\vec{S} \rightarrow -\vec{S}$. According to this interpretation, the wavefunction for a positron with 4-momentum p^μ with $p^0 = E > 0$ is

$$\Psi(x) = v(p, s)e^{ip \cdot x}. \quad (3.2.33)$$

Now, using the Dirac equation (3.1.32), $v(p, s)$ must satisfy the eigenvalue equation:

$$(\not{p} + m)v(p, s) = 0. \quad (3.2.34)$$

We can now construct solutions to this equation just as before. First, in the rest (primed) frame of the particle, we have in 2×2 blocks:

$$\begin{pmatrix} m & m \\ m & m \end{pmatrix} v(p, s) = 0. \quad (3.2.35)$$

So, the solutions are

$$\Psi'(x') = \sqrt{m} \begin{pmatrix} \xi_s \\ -\xi_s \end{pmatrix} e^{imt'} \quad (3.2.36)$$

for any two-vector ξ_s .

One must be careful in interpreting the quantum numbers of the positron solutions to the Dirac equation. This is because the Hamiltonian, 3-momentum, and spin operators of a positron described by the wavefunction eq. (3.2.33) are all given by the negative of the expressions one

[†]Here, e is always defined to be positive, so that the electron has charge $-e$. (Some references define e to be negative.)

would use for an electron wavefunction. Thus, acting on a positron wavefunction, one has

$$H\Psi = -i\frac{\partial}{\partial t}\Psi, \quad (3.2.37)$$

$$\vec{P}\Psi = i\vec{\nabla}\Psi, \quad (3.2.38)$$

$$\vec{S}\Psi = -\frac{1}{2}\begin{pmatrix} \vec{\sigma} & 0 \\ 0 & \vec{\sigma} \end{pmatrix}\Psi, \quad (3.2.39)$$

where H , \vec{P} , and \vec{S} are the operators whose eigenvalues are to be interpreted as the energy, 3-momentum, and spin of the positive-energy positron antiparticle. Therefore, to describe a positron with spin $S_z = +1/2$ or $-1/2$, one should use, respectively,

$$\xi_1 = \begin{pmatrix} 0 \\ 1 \end{pmatrix}; \quad \text{or} \quad \xi_2 = \begin{pmatrix} 1 \\ 0 \end{pmatrix}, \quad (3.2.40)$$

in eq. (3.2.36).

Now we can boost to the unprimed frame just as before, yielding the solutions:

$$v(p, 1) = \begin{pmatrix} 0 \\ \sqrt{E + p_z} \\ 0 \\ -\sqrt{E - p_z} \end{pmatrix}, \quad (3.2.41)$$

$$v(p, 2) = \begin{pmatrix} \sqrt{E - p_z} \\ 0 \\ -\sqrt{E + p_z} \\ 0 \end{pmatrix}. \quad (3.2.42)$$

Here $v(p, 1)$ corresponds to a positron moving in the $+z$ direction with 3-momentum p_z and energy $E = \sqrt{p_z^2 + m^2}$ and $S_z = +1/2$, hence helicity $h = +1/2$ if $p_z > 0$. Similarly, $v(p, 2)$ corresponds to a positron with the same energy and 3-momentum, but with $S_z = -1/2$, and therefore helicity $h = -1/2$ if $p_z > 0$.

Note that for positron wavefunctions, P_L projects onto states that describe *right*-handed positrons in the high-energy limit, and P_R projects onto states that describe *left*-handed positrons in the high-energy limit. If we insist that P_L projects on to left-handed spinors, and P_R projects on to right-handed spinors, then we must simply remember that a right-handed positron is described by a left-handed spinor (annihilated by P_R), and vice versa!

Later we will also need to use the Dirac row spinors:

$$\bar{u}(p, s) = u(p, s)^\dagger \gamma^0, \quad \bar{v}(p, s) = v(p, s)^\dagger \gamma^0. \quad (3.2.43)$$

The quantities $\bar{u}(p, s)u(k, r)$ and $\bar{u}(p, s)v(k, r)$ and $\bar{v}(p, s)u(k, r)$ and $\bar{v}(p, s)v(k, r)$ are all Lorentz scalars. For example, in the rest frame of a particle with mass m and spin $S_z = +1/2$, one has

$$\bar{u}(p, 1) = u(p, 1)^\dagger \gamma^0 = \sqrt{m} \begin{pmatrix} 1 & 0 & 1 & 0 \end{pmatrix} \begin{pmatrix} 0 & \sigma^0 \\ \sigma^0 & 0 \end{pmatrix} = (\sqrt{m} & 0 & \sqrt{m} & 0), \quad (3.2.44)$$

so that

$$\bar{u}(p, 1)u(p, 1) = \begin{pmatrix} \sqrt{m} & 0 & \sqrt{m} & 0 \end{pmatrix} \begin{pmatrix} \sqrt{m} \\ 0 \\ \sqrt{m} \\ 0 \end{pmatrix} = 2m. \quad (3.2.45)$$

Since this quantity is a scalar, it must be true that $\bar{u}(p, 1)u(p, 1) = 2m$ in any Lorentz frame, in other words, for any p^μ . More generally, if $s, r = 1, 2$ represent orthonormal spin state labels, then the u and v spinors obey:

$$\bar{u}(p, s)u(p, r) = 2m\delta_{sr}, \quad (3.2.46)$$

$$\bar{v}(p, s)v(p, r) = -2m\delta_{sr}, \quad (3.2.47)$$

$$\bar{v}(p, s)u(p, r) = \bar{u}(p, s)v(p, r) = 0. \quad (3.2.48)$$

Similarly, one can show that $\bar{u}(p, s)\gamma^\mu u(p, r) = 2(m, \vec{0})\delta_{sr}$ in the rest frame. Since it is a four-vector, it must be that in any frame:

$$\bar{u}(p, s)\gamma^\mu u(p, r) = 2p^\mu\delta_{sr}. \quad (3.2.49)$$

But the most useful identities that we will use later on are the spin-sum equations:

$$\sum_{s=1}^2 u(p, s)\bar{u}(p, s) = \not{p} + m; \quad (3.2.50)$$

$$\sum_{s=1}^2 v(p, s)\bar{v}(p, s) = \not{p} - m. \quad (3.2.51)$$

Here the spin state label s is summed over. These equations are to be interpreted in the sense of a column vector times a row vector giving a 4×4 matrix, like:

$$\begin{pmatrix} a_1 \\ a_2 \\ a_3 \\ a_4 \end{pmatrix} \begin{pmatrix} b_1 & b_2 & b_3 & b_4 \end{pmatrix} = \begin{pmatrix} a_1b_1 & a_1b_2 & a_1b_3 & a_1b_4 \\ a_2b_1 & a_2b_2 & a_2b_3 & a_2b_4 \\ a_3b_1 & a_3b_2 & a_3b_3 & a_3b_4 \\ a_4b_1 & a_4b_2 & a_4b_3 & a_4b_4 \end{pmatrix}. \quad (3.2.52)$$

We will use eqs. (3.2.50) and (3.2.51) often when calculating cross-sections and decay rates involving fermions.

As a check, note that if we act on the left of eq. (3.2.50) with $\not{p} - m$, the left hand side vanishes because of eq. (3.2.2), and the right hand side vanishes because of

$$(\not{p} - m)(\not{p} + m) = \not{p}\not{p} - m^2 = 0. \quad (3.2.53)$$

This relies on the identity

$$\not{p}\not{p} = p^2, \quad (3.2.54)$$

which follows from

$$\not{p}\not{p} = p^\mu p^\nu \gamma_\mu \gamma_\nu = p^\mu p^\nu (-\gamma_\nu \gamma_\mu + 2g_{\mu\nu}) = -\not{p}\not{p} + 2p^2, \quad (3.2.55)$$

where eq. (3.1.37) was used. A similar consistency check works if we act on the left of eq. (3.2.51) with $\not{p} + m$.

The Dirac spinors given above only describe electrons and positrons with both momentum and spin aligned along the $\pm z$ direction. More generally, we could construct $u(p, s)$ and $v(p, s)$ for states describing electrons or positrons with any \vec{p} and spin. However, in general that is quite a mess, and it turns out to be not particularly useful in most practical applications, as we will see.

3.3 The Weyl equation

It turns out that the Dirac equation can be replaced by something simpler and more fundamental in the special case $m = 0$. If we go back to Dirac's guess for the Hamiltonian, we now have just

$$H = \vec{\alpha} \cdot \vec{P}, \quad (3.3.1)$$

and there is no need for the matrix β . Therefore, eqs. (3.1.20) and (3.1.21) are not applicable, and we have only the one requirement:

$$\alpha_j \alpha_k + \alpha_k \alpha_j = 2\delta_{jk}. \quad (3.3.2)$$

Now there are two distinct solutions involving 2×2 matrices, namely $\vec{\alpha} = \vec{\sigma}$ or $\vec{\alpha} = -\vec{\sigma}$. So we have two possible quantum mechanical wave equations:

$$i \frac{\partial}{\partial t} \psi = \pm i \vec{\sigma} \cdot \vec{\nabla} \psi. \quad (3.3.3)$$

If we now define

$$\sigma^\mu = (\sigma^0, \sigma^1, \sigma^2, \sigma^3), \quad (3.3.4)$$

$$\bar{\sigma}^\mu = (\sigma^0, -\sigma^1, -\sigma^2, -\sigma^3), \quad (3.3.5)$$

then we can write the two possible equations in the form:

$$i \bar{\sigma}^\mu \partial_\mu \psi_L = 0, \quad (3.3.6)$$

$$i \sigma^\mu \partial_\mu \psi_R = 0. \quad (3.3.7)$$

Here I have attached labels L and R because the solutions to these equations turn out to have left and right helicity, respectively, as we will see in a moment. Each of these equations is called

a Weyl equation. They are similar to the Dirac equation, but only apply to massless spin-1/2 particles, and are 2×2 matrix equations rather than 4×4 . The two-component objects ψ_L and ψ_R are called Weyl spinors.

We can understand the relationship of the Dirac equation to the Weyl equations if we notice that the γ^μ matrices can be written as

$$\gamma^\mu = \begin{pmatrix} 0 & \sigma^\mu \\ \bar{\sigma}^\mu & 0 \end{pmatrix}. \quad (3.3.8)$$

[Compare eq. (3.1.28).] If we now write a Dirac spinor in its L and R helicity components,

$$\Psi = \begin{pmatrix} \Psi_L \\ \Psi_R \end{pmatrix}, \quad (3.3.9)$$

then the Dirac equation (3.1.27) becomes:

$$i \begin{pmatrix} 0 & \sigma^\mu \\ \bar{\sigma}^\mu & 0 \end{pmatrix} \partial_\mu \begin{pmatrix} \Psi_L \\ \Psi_R \end{pmatrix} = m \begin{pmatrix} \Psi_L \\ \Psi_R \end{pmatrix}, \quad (3.3.10)$$

or

$$i\sigma^\mu \partial_\mu \Psi_R = m\Psi_L, \quad (3.3.11)$$

$$i\bar{\sigma}^\mu \partial_\mu \Psi_L = m\Psi_R. \quad (3.3.12)$$

Comparing with eqs. (3.3.6) and (3.3.7) when $m = 0$, we can indeed identify Ψ_R as a right-handed helicity Weyl fermion, and Ψ_L as a left-handed helicity Weyl fermion.

Note that if $m = 0$, one can consistently set $\Psi_R = 0$ as an identity in the Dirac spinor without violating eqs. (3.3.11) and (3.3.12). Then only the left-handed helicity fermion exists. This is how neutrinos originally appeared in the Standard Model; a massless neutrino corresponds to a left-handed Weyl fermion. Recent evidence shows that neutrinos *do* have small masses, so that this discussion has to be modified slightly. However, for experiments in which neutrino masses can be neglected, it is still proper to treat a neutrino as a Weyl fermion, or equivalently as the left-handed part of a Dirac neutrino with no right-handed part.

The two versions of the Weyl equation, eqs. (3.3.6) and (3.3.7), are actually not distinct. To see this, suppose we take the Hermitian conjugate of eq. (3.3.7). Since $(\vec{\nabla})^\dagger = -\vec{\nabla}$ and $(\sigma^\mu)^\dagger = \sigma^\mu$, we obtain:

$$i(\sigma^0 \frac{\partial}{\partial t} - \vec{\sigma} \cdot \vec{\nabla})\psi_R^\dagger = 0 \quad (3.3.13)$$

or:

$$i\bar{\sigma}^\mu \partial_\mu \psi_R^\dagger = 0. \quad (3.3.14)$$

In other words, a right-handed Weyl spinor is the Hermitian conjugate of a left-handed Weyl spinor, and vice versa. The modern point of view is that the Weyl equation is fundamental, and all 4-component Dirac fermions can be thought of as consisting of two 2-component Weyl fermions coupled together by a mass. This is because in the Standard Model, all fermions are massless until they are provided with a mass term by the spontaneous breaking of the electroweak symmetry, as described in section 11.2. Since a right-handed Weyl fermion is the Hermitian conjugate of a left-handed Weyl fermion, all one really needs is the single Weyl equation (3.3.6). A Dirac fermion is then written as

$$\Psi = \begin{pmatrix} \chi \\ \xi^\dagger \end{pmatrix}, \quad (3.3.15)$$

where χ and ξ are independent left-handed two-component Weyl fermions. All fermion degrees of freedom can thus be thought of in terms of left-handed Weyl fermions.

3.4 Majorana fermions

A Majorana fermion can be obtained from a massive Dirac fermion by reducing the number of degrees of freedom. This is done by identifying the right-handed part with the conjugate of the left-handed part, imposed as a constraint, expressed by:

$$\psi \equiv \Psi_L = \Psi_R^\dagger. \quad (3.4.1)$$

In four-component notation, a Majorana spinor has the form

$$\Psi_M = \begin{pmatrix} \psi \\ \psi^\dagger \end{pmatrix}, \quad (3.4.2)$$

and obeys the same wave equation as a Dirac fermion, $(i\gamma^\mu\partial_\mu - m)\Psi_M = 0$. However, it has only half as many degrees of freedom; the Majorana condition (3.4.1) ensures that a Majorana fermion is its own antiparticle. From eqs. (3.3.11), (3.3.12), one sees that in the two-component form a classical Majorana fermion obeys the wave equation:

$$i\bar{\sigma}^\mu\partial_\mu\psi - m\psi^\dagger = 0, \quad (3.4.3)$$

or, in complex-conjugated form,

$$i\sigma^\mu\partial_\mu\psi^\dagger - m\psi = 0. \quad (3.4.4)$$

As we will see in section 11.4, the experimental fact that neutrinos have small masses suggests that they are likely to be Majorana fermions (and thus their own antiparticles), although this expectation is based partly on theoretical prejudice and it is also quite possible that they may be Dirac. In the minimal supersymmetric extension of the Standard Model, there are new fermions called neutralinos and the gluino, which are predicted to be Majorana fermions.

4 Field Theory and Lagrangians

4.1 The field concept and Lagrangian dynamics

It is now time to make a conceptual break from our earlier treatment of relativistic quantum-mechanical wave equations for scalar and Dirac particles. There are two reasons for doing this. First, the existence of negative energy solutions has lead us to the concept of antiparticles. Now, a hole in the Dirac sea, representing a positron, can be removed if the state is occupied by a positive energy electron, releasing an energy of at least $2m$. This forces us to admit that the total number of particles is not conserved. The Klein-Gordon wavefunction $\phi(x)$ and the Dirac wavefunction $\Psi(x)$ were designed to describe single-particle probability amplitudes, but the correct theory of nature evidently must describe a variable number of particles. Secondly, we note that in the electromagnetic theory, $A^\mu(x)$ are not just quantum mechanical wavefunctions; they exist classically too. If we follow this example with scalar and spinor particles, we are lead to abandon $\phi(x)$ and $\Psi(x)$ as quantum wavefunctions representing single-particle states, and reinterpret them as fields that have meaning even classically.

Specifically, a scalar particle is described by a field $\phi(x)$. Classically, this just means that for every point x^μ , the object $\phi(x)$ returns a number. Quantum mechanically, $\phi(x)$ becomes an operator (rather than a state or wavefunction). There is a distinct operator for each x^μ . Therefore, we no longer have a position operator x^μ ; instead, it is just an ordinary number label that tells us which operator ϕ we are talking about.

If $\phi(x)$ is now an operator, what states will it act on? To answer this, we can start with a vacuum state

$$|0\rangle \tag{4.1.1}$$

that describes an empty universe with no particles in it. If we now act with our field operator, we obtain a state:

$$\phi(x)|0\rangle, \tag{4.1.2}$$

which, at the time $t = x^0$, contains one particle at \vec{x} . (What this state describes at other times is a much more complicated question!) If we act again with our field operator at a different point y^μ , we get a state

$$\phi(y)\phi(x)|0\rangle, \tag{4.1.3}$$

which in general can be a linear combination of states containing any number of particles. [The operator $\phi(y)$ can either add another particle, or remove the particle added to the vacuum state

by $\phi(x)$. But, in addition, the particles can interact to change their number.] In general, the field operator $\phi(x)$ acts on any state by adding or subtracting particles. So this is the right framework to describe the quantum mechanics of a system with a variable number of particles.

Similarly, to describe spin-1/2 particles and their antiparticles, like the electron and the positron, or quarks and antiquarks, we will want to use a Dirac field $\Psi(x)$. Classically, $\Psi(x)$ is a set of four functions (one for each of the Dirac spinor components). Quantum mechanically, $\Psi(x)$ is a set of four operators. We can build up any state we want, containing any number of electrons and positrons, by acting on the vacuum state $|0\rangle$ enough times with the fields $\Psi(x)$ and $\bar{\Psi}(x) = \Psi^\dagger \gamma^0$.

The vector field $A^\mu(x)$ associated with electromagnetism is already very familiar in the classical theory, as the electrical and vector potentials. In the quantum theory of electromagnetism, $A^\mu(x)$ becomes an operator which can add or subtract photons from the vacuum.

This way of dealing with theories of multi-particle physics is called field theory. In order to describe how particles in a field theory evolve and interact, we need to specify a single object called the action.

Let us first review how the action principle works in a simple, non-field-theory setting. Let the variables $q_n(t)$ describe the configuration of a physical system. (For example, a single $q(t)$ could describe the displacement of a harmonic oscillator from equilibrium, as a function of time.) Here n is just a label distinguishing the different configuration variables. Classically, we could specify the equations of motion for the q_n , which we could get from knowing what forces were acting on it. A clever way of summarizing this information is to specify the action

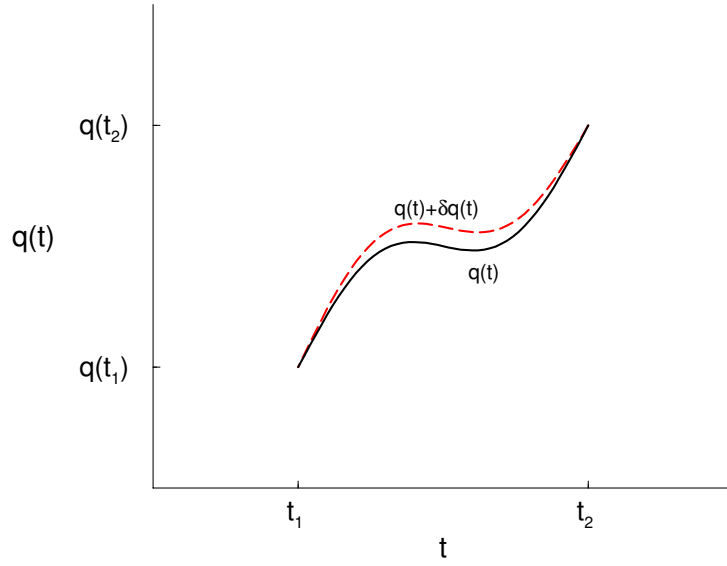
$$S = \int_{t_i}^{t_f} L(q_n, \dot{q}_n) dt. \quad (4.1.4)$$

Here t_i and t_f are fixed initial and final times, and L is the Lagrangian. It is given in simple systems by

$$L = T - V, \quad (4.1.5)$$

where T is the total kinetic energy and V is the total potential energy. Thus the action S is a functional of q_n ; if you specify a particular trajectory $q_n(t)$, then the action returns a single number. The Lagrangian is a function of $q_n(t)$ and its first derivative.

The usefulness of the action is given by Hamilton's principle, which states that if $q_n(t_i)$ and $q_n(t_f)$ are held fixed as boundary conditions, then S is minimized when $q_n(t)$ satisfy the equations of motion. Since S is at an extremum, this means that any small variation in $q_n(t)$ will lead to no change in S , so that $q_n(t) \rightarrow q_n(t) + \delta q_n(t)$ implies $\delta S = 0$, provided that $q_n(t)$ obeys the equations of motion. Here $\delta q_n(t)$ is any small function of t that vanishes at both t_i and t_f , as shown in the figure below:



Let us therefore compute δS . First, note that by the chain rule, we have:

$$\delta L = \sum_n \left(\delta q_n \frac{\partial L}{\partial q_n} + \delta \dot{q}_n \frac{\partial L}{\partial \dot{q}_n} \right). \quad (4.1.6)$$

Now, since

$$\delta \dot{q}_n = \frac{d}{dt}(\delta q_n), \quad (4.1.7)$$

we obtain

$$\delta S = \sum_n \int_{t_i}^{t_f} \left[\delta q_n \frac{\partial L}{\partial q_n} + \frac{d}{dt}(\delta q_n) \frac{\partial L}{\partial \dot{q}_n} \right] dt. \quad (4.1.8)$$

Now integrating by parts yields:

$$\delta S = \sum_n \int_{t_i}^{t_f} \delta q_n \left[\frac{\partial L}{\partial q_n} - \frac{d}{dt} \left(\frac{\partial L}{\partial \dot{q}_n} \right) \right] dt + \sum_n \delta q_n \frac{\partial L}{\partial \dot{q}_n} \Big|_{t=t_i}^{t=t_f}. \quad (4.1.9)$$

The last term vanishes because of the boundary conditions $\delta q_n(t_i) = \delta q_n(t_f) = 0$. Since the variation δS is supposed to vanish for any $\delta q_n(t)$, it must be that

$$\frac{\partial L}{\partial q_n} - \frac{d}{dt} \left(\frac{\partial L}{\partial \dot{q}_n} \right) = 0, \quad (4.1.10)$$

which is the equation of motion for $q_n(t)$, for each n .

As a simple example, suppose there is only one $q_n(t) = x(t)$, the position of some particle moving in one dimension in a potential $V(x)$. Then

$$L = T - V = \frac{1}{2} m \dot{x}^2 - V(x), \quad (4.1.11)$$

from which there follows:

$$\frac{\partial L}{\partial x} = -\frac{\partial V}{\partial x} = F, \quad (4.1.12)$$

which we recognize as the Newtonian force, and

$$\frac{d}{dt} \left(\frac{\partial L}{\partial \dot{x}} \right) = \frac{d}{dt} (m\dot{x}) = m\ddot{x}. \quad (4.1.13)$$

So the equation of motion is Newton's second law:

$$F = m\ddot{x}. \quad (4.1.14)$$

Everything we need to know about the dynamics of a physical system is encoded in the action S , or equivalently the Lagrangian L . In quantum field theory, it will tell us what the particle masses are, how they interact, how they decay, and what symmetries provide selection rules on their behavior.

As a first example of an action for a relativistic field theory, consider a scalar field $\phi(x) = \phi(t, \vec{x})$. Then, in the previous discussion, we identify the label n with the spatial position \vec{x} , and $q_n(t) = \phi(t, \vec{x})$. The action is obtained by summing contributions from each x :

$$S = \int_{t_i}^{t_f} dt L(\phi, \dot{\phi}) = \int_{t_i}^{t_f} dt \int d^3\vec{x} \mathcal{L}(\phi, \dot{\phi}). \quad (4.1.15)$$

Now, since this expression depends on $\dot{\phi}$, it must also depend on $\vec{\nabla}\phi$ in order to be Lorentz invariant. This just means that the form of the Lagrangian allows it to depend on the differences between the field evaluated at infinitesimally nearby points. So, a better way to write the action is:

$$S = \int d^4x \mathcal{L}(\phi, \partial_\mu \phi). \quad (4.1.16)$$

The object \mathcal{L} is known as the Lagrangian density. Specifying a particular form for \mathcal{L} defines the theory.

To find the classical equations of motion for the field, we must find $\phi(x)$ so that S is extremized; in other words, for any small variation $\phi(x) \rightarrow \phi(x) + \delta\phi(x)$, we must have $\delta S = 0$. By a similar argument as above, this implies the equations of motion:

$$\frac{\delta \mathcal{L}}{\delta \phi} - \partial_\mu \left(\frac{\delta \mathcal{L}}{\delta(\partial_\mu \phi)} \right) = 0. \quad (4.1.17)$$

Here, we use $\frac{\delta \mathcal{L}}{\delta \phi}$ to mean the partial derivative of \mathcal{L} with respect to ϕ ; δ is used rather than ∂ to avoid confusing between derivatives with respect to ϕ and spacetime partial derivatives with

respect to x^μ . Likewise, $\frac{\delta \mathcal{L}}{\delta(\partial_\mu \phi)}$ means a partial derivative of \mathcal{L} with respect to the object $\partial_\mu \phi$, upon which it depends.

As an example, consider the choice:

$$\mathcal{L} = \frac{1}{2} \partial_\mu \phi \partial^\mu \phi - \frac{1}{2} m^2 \phi^2. \quad (4.1.18)$$

It follows that:

$$\frac{\delta \mathcal{L}}{\delta \phi} = -m^2 \phi \quad (4.1.19)$$

and

$$\frac{\delta \mathcal{L}}{\delta(\partial_\mu \phi)} = \frac{\delta}{\delta(\partial_\mu \phi)} \left[\frac{1}{2} g^{\alpha\beta} \partial_\alpha \phi \partial_\beta \phi \right] = \frac{1}{2} g^{\mu\beta} \partial_\beta \phi + \frac{1}{2} g^{\alpha\mu} \partial_\alpha \phi = \partial^\mu \phi. \quad (4.1.20)$$

Therefore,

$$\partial_\mu \left(\frac{\delta \mathcal{L}}{\delta(\partial_\mu \phi)} \right) = \partial_\mu \partial^\mu \phi, \quad (4.1.21)$$

and so the equation of motion following from eq. (4.1.17) is:

$$\partial_\mu \partial^\mu \phi + m^2 \phi = 0. \quad (4.1.22)$$

This we recognize as the Klein-Gordon wave equation for a scalar particle of mass m ; compare to eq. (3.1.13). This equation was originally introduced with the interpretation as the equation governing the quantum wavefunction of a single scalar particle. Now it has reappeared with a totally different interpretation, as the classical equation of motion for the scalar field.

The previous discussion for scalar fields can be extended to other types of fields as well. Consider a general list of fields $\Phi_j(x)$, which could include scalar fields $\phi(x)$, Dirac or Majorana fields $\Psi(x)$ with four components, Weyl fields $\psi(x)$ with two components, or vector fields $A^\mu(x)$ with four components, or several copies of any of these. The Lagrangian density $\mathcal{L}(\Phi_j, \partial_\mu \Phi_j)$ determines the classical equations of motion through the principle that $S = \int d^4x \mathcal{L}$ should be stationary to first order when a deviation $\Phi_j(x) \rightarrow \Phi_j(x) + \delta \Phi_j(x)$ is made, with boundary conditions that $\delta \Phi_j(x)$ vanishes on the boundary of the spacetime region on which S is evaluated. (Typically one evaluates S between two times t_i and t_f , and over all of space, so this means that $\delta \Phi(x)$ vanishes very far away from some region of interest.) The Lagrangian density \mathcal{L} should be a real quantity that transforms under proper Lorentz transformations as a scalar.

Similarly to eq. (4.1.6), we have by the chain rule:

$$\delta S = \int d^4x \sum_j \left[\delta \Phi_j \frac{\delta \mathcal{L}}{\delta \Phi_j} + \delta(\partial_\mu \Phi_j) \left(\frac{\delta \mathcal{L}}{\delta(\partial_\mu \Phi_j)} \right) \right]. \quad (4.1.23)$$

Now using $\delta(\partial_\mu \Phi_j) = \partial_\mu(\delta\Phi_j)$, and integrating the second term by parts (this is where the boundary conditions come in), one obtains

$$\delta S = \int d^4x \sum_j \delta\Phi_j \left[\frac{\delta\mathcal{L}}{\delta\Phi_j} - \partial_\mu \left(\frac{\delta\mathcal{L}}{\delta(\partial_\mu \Phi_j)} \right) \right]. \quad (4.1.24)$$

If we require this to vanish for each and every arbitrary variation $\delta\Phi_j$, we obtain the Euler-Lagrange equations of motion:

$$\frac{\delta\mathcal{L}}{\delta\Phi_j} - \partial_\mu \left(\frac{\delta\mathcal{L}}{\delta(\partial_\mu \Phi_j)} \right) = 0, \quad (4.1.25)$$

for each j .

For example, let us consider how to make a Lagrangian density for a Dirac field $\Psi(x)$. Under Lorentz transformations, $\Psi(x)$ transforms exactly like the wavefunction solution to the Dirac equation. But now it is interpreted instead as a field; classically it is a function on spacetime, and quantum mechanically it is an operator for each point x^μ . Now, $\Psi(x)$ is a complex 4-component object, so $\Psi^\dagger(x)$ is also a field. One should actually treat $\Psi(x)$ and $\Psi^\dagger(x)$ as independent fields, in the same way that in complex analysis one often treats $z = x + iy$ and $z^* = x - iy$ as independent variables. As we found in section 3.1, if we want to build Lorentz scalar quantities, it is useful to use $\bar{\Psi}(x) = \Psi^\dagger \gamma^0$ as a building block.

A good (and correct) guess for the Lagrangian for a Dirac field is:

$$\mathcal{L} = i\bar{\Psi}\gamma^\mu\partial_\mu\Psi - m\bar{\Psi}\Psi, \quad (4.1.26)$$

which can also be written as:

$$\mathcal{L} = i\Psi^\dagger\gamma^0\gamma^\mu\partial_\mu\Psi - m\Psi^\dagger\gamma^0\Psi. \quad (4.1.27)$$

This is a Lorentz scalar, so that when integrated $\int d^4x$ it will give a Lorentz-invariant number. Let us now compute the equations of motion that follow from it. First, let us find the equations of motion obtained by varying with respect to Ψ^\dagger . For this, we need:

$$\frac{\delta\mathcal{L}}{\delta\Psi^\dagger} = i\gamma^0\gamma^\mu\partial_\mu\Psi - m\gamma^0\Psi, \quad (4.1.28)$$

$$\frac{\delta\mathcal{L}}{\delta(\partial_\mu\Psi^\dagger)} = 0. \quad (4.1.29)$$

The second equation just reflects the fact that the Lagrangian only contains the derivative of Ψ , not the derivative of Ψ^\dagger . So, by plugging in to the general result eq. (4.1.25), the equation of motion is simply:

$$i\gamma^\mu\partial_\mu\Psi - m\Psi = 0, \quad (4.1.30)$$

where we have multiplied $\frac{\delta \mathcal{L}}{\delta \Psi^\dagger} = 0$ on the left by γ^0 and used the fact that $(\gamma^0)^2 = 1$. This is, of course, the Dirac equation.

We can also find the equations of motion obtained from the Lagrangian by varying with respect to Ψ . For that, we need:

$$\frac{\delta \mathcal{L}}{\delta \Psi} = -m\bar{\Psi}, \quad (4.1.31)$$

$$\frac{\delta \mathcal{L}}{\delta(\partial_\mu \Psi)} = i\bar{\Psi}\gamma^\mu. \quad (4.1.32)$$

Plugging these into eq. (4.1.25), we obtain:

$$-i\partial_\mu \bar{\Psi}\gamma^\mu - m\bar{\Psi} = 0. \quad (4.1.33)$$

However, this is nothing new; it is just the Hermitian conjugate of eq. (4.1.30), multiplied on the right by γ^0 and using eq. (3.1.34).

The Lagrangian density for an electromagnetic field is:

$$\mathcal{L}_{\text{EM}} = -\frac{1}{4}F_{\mu\nu}F^{\mu\nu} = -\frac{1}{4}(\partial_\mu A_\nu - \partial_\nu A_\mu)(\partial^\mu A^\nu - \partial^\nu A^\mu). \quad (4.1.34)$$

To find the equations of motion that follow from this Lagrangian, we compute:

$$\frac{\delta \mathcal{L}_{\text{EM}}}{\delta A_\nu} = 0, \quad (4.1.35)$$

since A^μ doesn't appear in the Lagrangian without a derivative acting on it, and

$$\begin{aligned} \frac{\delta \mathcal{L}_{\text{EM}}}{\delta(\partial_\mu A_\nu)} &= \frac{\delta}{\delta(\partial_\mu A_\nu)} \left[-\frac{1}{4}(\partial_\alpha A_\beta - \partial_\beta A_\alpha)(\partial_\rho A_\sigma - \partial_\sigma A_\rho)g^{\alpha\rho}g^{\beta\sigma} \right] \\ &= -\frac{1}{4} \left[(\partial_\rho A_\sigma - \partial_\sigma A_\rho)g^{\mu\rho}g^{\nu\sigma} - (\partial_\rho A_\sigma - \partial_\sigma A_\rho)g^{\nu\rho}g^{\mu\sigma} \right. \\ &\quad \left. + (\partial_\alpha A_\beta - \partial_\beta A_\alpha)g^{\mu\alpha}g^{\beta\sigma} - (\partial_\alpha A_\beta - \partial_\alpha A_\beta)g^{\nu\alpha}g^{\mu\beta} \right] \\ &= -\partial^\mu A^\nu + \partial^\nu A^\mu \\ &= -F^{\mu\nu}. \end{aligned} \quad (4.1.36)$$

So, the equations of motion,

$$\frac{\delta \mathcal{L}_{\text{EM}}}{\delta A_\nu} - \partial_\mu \left(\frac{\delta \mathcal{L}_{\text{EM}}}{\delta(\partial_\mu A_\nu)} \right) = 0 \quad (4.1.37)$$

reduce to

$$\partial_\mu F^{\mu\nu} = 0, \quad (4.1.38)$$

which we recognize as Maxwell's equations in the case of vanishing J^μ [see eq. (2.4.13)]. In order to include the effects of a 4-current J^μ , we can simply add a term

$$\mathcal{L}_{\text{current}} = -eJ^\mu A_\mu \quad (4.1.39)$$

to the Lagrangian density. Then, since

$$\frac{\delta \mathcal{L}_{\text{current}}}{\delta A_\nu} = -eJ^\nu; \quad (4.1.40)$$

$$\frac{\delta \mathcal{L}_{\text{current}}}{\delta (\partial_\mu A_\nu)} = 0, \quad (4.1.41)$$

the classical equations of motion for the vector field become

$$\partial_\mu F^{\mu\nu} - eJ^\nu = 0, \quad (4.1.42)$$

in agreement with eq. (2.4.13). The current density J^μ may be regarded as an external source of unspecified origin for the electromagnetic field; or, it can be built out of the fields for charged particles, as we will see.

4.2 Quantization of free scalar field theory

Let us now turn to the question of quantizing a field theory. To begin, let us recall how one quantizes a simple generic system based on variables $q_n(t)$, given the Lagrangian $L(q_n, \dot{q}_n)$. First, one defines the canonical momenta conjugate to each q_n :

$$p_n \equiv \frac{\partial L}{\partial \dot{q}_n}. \quad (4.2.1)$$

The classical Hamiltonian is then defined by

$$H(q_n, p_n) \equiv \sum_n p_n \dot{q}_n - L(q_n, \dot{q}_n), \quad (4.2.2)$$

where the \dot{q}_n are to be eliminated using eq. (4.2.1). To go to the corresponding quantum theory, the q_n and p_n and H are reinterpreted as Hermitian operators acting on a Hilbert space of states. The operators obey canonical equal-time commutation relations:

$$[p_n, p_m] = 0; \quad (4.2.3)$$

$$[q_n, q_m] = 0; \quad (4.2.4)$$

$$[p_n, q_m] = -i\hbar\delta_{nm}, \quad (4.2.5)$$

and the time evolution of the system is determined by the Hamiltonian operator H .

Let us now apply this to the theory of a scalar field $\phi(x)$ with the Lagrangian density given by eq. (4.1.18). Then $\phi(x) = \phi(t, \vec{x})$ plays the role of $q_n(t)$, with \vec{x} playing the role of the label n ; there is a different field at each point in space. The momentum conjugate to ϕ is:

$$\pi(\vec{x}) \equiv \frac{\delta \mathcal{L}}{\delta \dot{\phi}} = \frac{\delta}{\delta \dot{\phi}} \left[\frac{1}{2} \dot{\phi}^2 + \dots \right] = \dot{\phi}. \quad (4.2.6)$$

It should be emphasized that $\pi(\vec{x})$, the momentum conjugate to the field $\phi(\vec{x})$, is not in any way the mechanical momentum of the particle. Notice that $\pi(\vec{x})$ is a scalar function, not a three-vector or a four-vector!

The Hamiltonian is obtained by summing over the fields at each point \vec{x} :

$$H = \int d^3\vec{x} \pi(\vec{x}) \dot{\phi}(\vec{x}) - L \quad (4.2.7)$$

$$= \int d^3\vec{x} \pi(\vec{x}) \dot{\phi}(\vec{x}) - \int d^3\vec{x} \frac{1}{2} [\dot{\phi}^2 - (\vec{\nabla}\phi)^2 - m^2\phi^2] \quad (4.2.8)$$

$$= \frac{1}{2} \int d^3\vec{x} [\pi^2 + (\vec{\nabla}\phi)^2 + m^2\phi^2]. \quad (4.2.9)$$

Notice that a nice feature has emerged: this Hamiltonian is a sum of squares, and is therefore always ≥ 0 . There are no dangerous solutions with arbitrarily large negative energy, unlike the case of the single-particle Klein-Gordon wave equation.

At any given fixed time t , the field operators $\phi(\vec{x})$ and their conjugate momenta $\pi(\vec{x})$ are Hermitian operators satisfying commutation relations exactly analogous to eqs. (4.2.3)-(4.2.5):

$$[\phi(\vec{x}), \phi(\vec{y})] = 0; \quad (4.2.10)$$

$$[\pi(\vec{x}), \pi(\vec{y})] = 0; \quad (4.2.11)$$

$$[\pi(\vec{x}), \phi(\vec{y})] = -i\hbar\delta^{(3)}(\vec{x} - \vec{y}). \quad (4.2.12)$$

As we will see, it turns out to be profitable to analyze the system in a way similar to the way one treats the harmonic oscillator in one-dimensional nonrelativistic quantum mechanics. In that system, one defines “creation” and “annihilation” (or “raising” and “lowering”) operators a^\dagger and a as complex linear combinations of the position and momentum operators x and p . Similarly, here we will define:

$$a_{\vec{p}} = \int d^3\vec{x} e^{-i\vec{p}\cdot\vec{x}} [E_{\vec{p}}\phi(\vec{x}) + i\pi(\vec{x})], \quad (4.2.13)$$

where

$$E_{\vec{p}} = \sqrt{\vec{p}^2 + m^2}, \quad (4.2.14)$$

with the positive square root always taken. The overall coefficient in front of eq. (4.2.13) reflects an arbitrary choice (and in fact it is chosen differently by various books). Equation (4.2.13) defines a distinct annihilation operator for each three-momentum \vec{p} . Taking the Hermitian conjugate yields:

$$a_{\vec{p}}^\dagger = \int d^3\vec{x} e^{i\vec{p}\cdot\vec{x}} [E_{\vec{p}}\phi(\vec{x}) - i\pi(\vec{x})]. \quad (4.2.15)$$

To see the usefulness of these definitions, compute the commutator:

$$[a_{\vec{p}}, a_{\vec{k}}^\dagger] = \int d^3\vec{x} \int d^3\vec{y} e^{-i\vec{p}\cdot\vec{x}} e^{i\vec{k}\cdot\vec{y}} [E_{\vec{p}}\phi(\vec{x}) + i\pi(\vec{x}), E_{\vec{k}}\phi(\vec{y}) - i\pi(\vec{y})] \quad (4.2.16)$$

$$= \int d^3\vec{x} \int d^3\vec{y} e^{-i\vec{p}\cdot\vec{x}} e^{i\vec{k}\cdot\vec{y}} (E_{\vec{k}} + E_{\vec{p}}) \delta^{(3)}(\vec{x} - \vec{y}), \quad (4.2.17)$$

where eqs. (4.2.10)-(4.2.12) have been used. Now performing the \vec{y} integral using the definition of the delta function, one obtains:

$$[a_{\vec{p}}, a_{\vec{k}}^\dagger] = (E_{\vec{k}} + E_{\vec{p}}) \int d^3\vec{x} e^{i(\vec{k}-\vec{p})\cdot\vec{x}}. \quad (4.2.18)$$

This can be further reduced by using the important identity:

$$\int d^3\vec{x} e^{i\vec{q}\cdot\vec{x}} = (2\pi)^3 \delta^{(3)}(\vec{q}), \quad (4.2.19)$$

valid for any 3-vector \vec{q} , to obtain the final result:

$$[a_{\vec{p}}, a_{\vec{k}}^\dagger] = (2\pi)^3 2E_{\vec{p}} \delta^{(3)}(\vec{k} - \vec{p}). \quad (4.2.20)$$

Here we have put $E_{\vec{k}} = E_{\vec{p}}$, using the fact that the delta function vanishes except when $\vec{k} = \vec{p}$. In a similar way, one can check the commutators:

$$[a_{\vec{p}}, a_{\vec{k}}] = [a_{\vec{p}}^\dagger, a_{\vec{k}}^\dagger] = 0. \quad (4.2.21)$$

Up to a constant factor on the right-hand side of eq. (4.2.20), these results have the same form as the harmonic oscillator algebra familiar from non-relativistic quantum mechanics: $[a, a^\dagger] = 1$; $[a, a] = [a^\dagger, a^\dagger] = 0$. Therefore, the quantum mechanics of a scalar field behaves like an infinite collection of harmonic oscillators, one associated with each three-momentum \vec{p} .

Now we can understand the Hilbert space of states for the quantum field theory. We start with the vacuum state $|0\rangle$, which is taken to be annihilated by all of the lowering operators:

$$a_{\vec{k}}|0\rangle = 0. \quad (4.2.22)$$

Acting on the vacuum state with any raising operator produces

$$a_{\vec{k}}^\dagger|0\rangle = |\vec{k}\rangle, \quad (4.2.23)$$

which describes a state with a single particle with three-momentum \vec{k} (and no definite position). Acting multiple times with raising operators produces a state with multiple particles. So

$$a_{\vec{k}_1}^\dagger a_{\vec{k}_2}^\dagger \dots a_{\vec{k}_n}^\dagger |0\rangle = |\vec{k}_1, \vec{k}_2, \dots, \vec{k}_n\rangle \quad (4.2.24)$$

describes a state of the universe with n ϕ -particles with momenta $\vec{k}_1, \vec{k}_2, \dots, \vec{k}_n$. Note that these states are automatically symmetric under interchange of any two of the momentum labels \vec{k}_i ,

because of the identity $[a_{\vec{k}_i}^\dagger, a_{\vec{k}_j}^\dagger] = 0$. This is another way of saying that the multiparticle states obey Bose-Einstein statistics for identical particles with integer (in this case, 0) spin.

In order to check our interpretation of the quantum theory, let us now evaluate the Hamiltonian operator in terms of the raising and lowering operators, and then determine how H acts on the space of states. First, let us invert the definitions eqs. (4.2.13) and (4.2.15) to find $\phi(\vec{x})$ and $\pi(\vec{y})$ in terms of the $a_{\vec{p}}^\dagger$ and $a_{\vec{p}}$. We begin by noting that:

$$a_{\vec{p}} + a_{-\vec{p}}^\dagger = \int d^3\vec{x} e^{-i\vec{p}\cdot\vec{x}} 2E_{\vec{p}} \phi(\vec{x}). \quad (4.2.25)$$

Now we act on both sides by:

$$\int d\tilde{p} e^{i\vec{p}\cdot\vec{y}}, \quad (4.2.26)$$

where we have introduced the very convenient shorthand notation:

$$\int d\tilde{p} \equiv \int \frac{d^3\vec{p}}{(2\pi)^3 2E_{\vec{p}}}, \quad (4.2.27)$$

used often from now on. The result is that eq. (4.2.25) becomes

$$\int d\tilde{p} e^{i\vec{p}\cdot\vec{y}} (a_{\vec{p}} + a_{-\vec{p}}^\dagger) = \int d^3\vec{x} \phi(\vec{x}) \left\{ \int \frac{d^3\vec{p}}{(2\pi)^3} e^{i\vec{p}\cdot(\vec{y}-\vec{x})} \right\}. \quad (4.2.28)$$

Since the \vec{p} integral in braces is equal to $\delta^{(3)}(\vec{y}-\vec{x})$ [see eq. (4.2.19)], one obtains after performing the \vec{x} integral:

$$\phi(\vec{y}) = \int d\tilde{p} e^{i\vec{p}\cdot\vec{y}} (a_{\vec{p}} + a_{-\vec{p}}^\dagger), \quad (4.2.29)$$

or, renaming $\vec{y} \rightarrow \vec{x}$, and $\vec{p} \rightarrow -\vec{p}$ in the second term on the right:

$$\phi(\vec{x}) = \int d\tilde{p} (e^{i\vec{p}\cdot\vec{x}} a_{\vec{p}} + e^{-i\vec{p}\cdot\vec{x}} a_{\vec{p}}^\dagger). \quad (4.2.30)$$

This expresses the original field in terms of raising and lowering operators. Similarly, for the conjugate momentum field, one finds:

$$\pi(\vec{x}) = -i \int d\tilde{p} E_{\vec{p}} (e^{i\vec{p}\cdot\vec{x}} a_{\vec{p}} - e^{-i\vec{p}\cdot\vec{x}} a_{\vec{p}}^\dagger). \quad (4.2.31)$$

Now we can plug the results of eqs. (4.2.30) and (4.2.31) into the expression eq. (4.2.9) for the Hamiltonian. The needed terms are:

$$\frac{1}{2} \int d^3\vec{x} \pi(x)^2 = \frac{1}{2} \int d^3\vec{x} \int d\tilde{k} \int d\tilde{p} (-i)^2 E_{\vec{k}} E_{\vec{p}} (e^{i\vec{k}\cdot\vec{x}} a_{\vec{k}} - e^{-i\vec{k}\cdot\vec{x}} a_{\vec{k}}^\dagger) (e^{i\vec{p}\cdot\vec{x}} a_{\vec{p}} - e^{-i\vec{p}\cdot\vec{x}} a_{\vec{p}}^\dagger), \quad (4.2.32)$$

$$\frac{1}{2} \int d^3\vec{x} (\vec{\nabla} \phi)^2 = \frac{1}{2} \int d^3\vec{x} \int d\tilde{k} \int d\tilde{p} (i\vec{k} e^{i\vec{k}\cdot\vec{x}} a_{\vec{k}} - i\vec{k} e^{-i\vec{k}\cdot\vec{x}} a_{\vec{k}}^\dagger) \cdot (i\vec{p} e^{i\vec{p}\cdot\vec{x}} a_{\vec{p}} - i\vec{p} e^{-i\vec{p}\cdot\vec{x}} a_{\vec{p}}^\dagger), \quad (4.2.33)$$

$$\frac{m^2}{2} \int d^3\vec{x} \phi(x)^2 = \frac{m^2}{2} \int d^3\vec{x} \int d\tilde{k} \int d\tilde{p} (e^{i\vec{k}\cdot\vec{x}} a_{\vec{k}} + e^{-i\vec{k}\cdot\vec{x}} a_{\vec{k}}^\dagger) (e^{i\vec{p}\cdot\vec{x}} a_{\vec{p}} + e^{-i\vec{p}\cdot\vec{x}} a_{\vec{p}}^\dagger). \quad (4.2.34)$$

Adding up the pieces, one finds:

$$H = \frac{1}{2} \int d\vec{k} \int d\vec{p} \int d^3\vec{x} \left\{ (m^2 - \vec{k} \cdot \vec{p} - E_{\vec{k}} E_{\vec{p}}) [a_{\vec{k}} a_{\vec{p}} e^{i(\vec{k}+\vec{p}) \cdot \vec{x}} + a_{\vec{k}}^\dagger a_{\vec{p}}^\dagger e^{-i(\vec{k}+\vec{p}) \cdot \vec{x}}] \right. \\ \left. + (m^2 + \vec{k} \cdot \vec{p} + E_{\vec{k}} E_{\vec{p}}) [a_{\vec{k}}^\dagger a_{\vec{p}} e^{i(\vec{p}-\vec{k}) \cdot \vec{x}} + a_{\vec{k}} a_{\vec{p}}^\dagger e^{i(\vec{k}-\vec{p}) \cdot \vec{x}}] \right\} . \quad (4.2.35)$$

Now one can do the \vec{x} integration using:

$$\int d^3\vec{x} e^{\pm i(\vec{k}+\vec{p}) \cdot \vec{x}} = (2\pi)^3 \delta^{(3)}(\vec{k} + \vec{p}), \quad (4.2.36)$$

$$\int d^3\vec{x} e^{\pm i(\vec{k}-\vec{p}) \cdot \vec{x}} = (2\pi)^3 \delta^{(3)}(\vec{k} - \vec{p}). \quad (4.2.37)$$

As a result, the coefficient $(m^2 - \vec{k} \cdot \vec{p} - E_{\vec{k}} E_{\vec{p}})$ of the aa and $a^\dagger a^\dagger$ terms vanishes after plugging in $\vec{k} = -\vec{p}$ as enforced by the delta function. Meanwhile, for the aa^\dagger and $a^\dagger a$ terms one has $\vec{k} = \vec{p}$ from the delta function, so that

$$(m^2 + \vec{k} \cdot \vec{p} + E_{\vec{k}} E_{\vec{p}}) \delta^{(3)}(\vec{k} - \vec{p}) = 2E_{\vec{p}}^2 \delta^{(3)}(\vec{k} - \vec{p}). \quad (4.2.38)$$

Now performing the \vec{k} integral in eq. (4.2.35), one finds:

$$H = \frac{1}{2} \int d\vec{p} E_{\vec{p}} (a_{\vec{p}}^\dagger a_{\vec{p}} + a_{\vec{p}} a_{\vec{p}}^\dagger). \quad (4.2.39)$$

Finally, we can rearrange the second term, using

$$a_{\vec{p}} a_{\vec{p}}^\dagger = a_{\vec{p}}^\dagger a_{\vec{p}} + (2\pi)^3 2E_{\vec{p}} \delta^{(3)}(\vec{p} - \vec{p}) \quad (4.2.40)$$

from eq. (4.2.20). The last term is infinite, so

$$H = \int d\vec{p} E_{\vec{p}} a_{\vec{p}}^\dagger a_{\vec{p}} + \infty, \quad (4.2.41)$$

where “ ∞ ” means an infinite, but constant, contribution to the energy. Since a uniform constant contribution to the energy of all states is unobservable and commutes with all other operators, we are free to drop it, by a redefinition of the Hamiltonian. This is a simple example of the process known as renormalization. (In a more careful treatment, one could “regulate” the theory by quantizing the theory confined to a box of finite volume, and neglecting all contributions coming from momenta greater than some very large cutoff $|\vec{p}|_{\text{max}}$. Then the infinite constant would be rendered finite. Since we are going to ignore the constant anyway, we won’t bother doing this.) So, from now on,

$$H = \int d\vec{p} E_{\vec{p}} a_{\vec{p}}^\dagger a_{\vec{p}} \quad (4.2.42)$$

is the Hamiltonian operator.

Acting on the vacuum state,

$$H|0\rangle = 0, \quad (4.2.43)$$

since all $a_{\vec{p}}$ annihilate the vacuum. This shows that the infinite constant we dropped from H is actually the infinite energy density associated with an infinite universe of empty space, filled with the zero-point energies of an infinite number of oscillators, one for each possible momentum 3-vector \vec{p} . But we've already agreed to ignore it, so let it go. One can show that:

$$[H, a_{\vec{k}}^\dagger] = E_{\vec{k}} a_{\vec{k}}^\dagger. \quad (4.2.44)$$

Acting with H on a one-particle state, we therefore obtain

$$H|\vec{k}\rangle = H a_{\vec{k}}^\dagger |0\rangle = [H, a_{\vec{k}}^\dagger] |0\rangle = E_{\vec{k}} a_{\vec{k}}^\dagger |0\rangle = E_{\vec{k}} |\vec{k}\rangle. \quad (4.2.45)$$

This proves that the one-particle state with 3-momentum \vec{k} has energy eigenvalue $E_{\vec{k}} = \sqrt{\vec{k}^2 + m^2}$, as expected from special relativity. More generally, a multi-particle state

$$|\vec{k}_1, \vec{k}_2, \dots, \vec{k}_n\rangle = a_{\vec{k}_1}^\dagger a_{\vec{k}_2}^\dagger \dots a_{\vec{k}_n}^\dagger |0\rangle \quad (4.2.46)$$

is easily shown to be an eigenstate of H with eigenvalue $E_{\vec{k}_1} + E_{\vec{k}_2} + \dots + E_{\vec{k}_n}$. Note that it is not possible to construct a state with a negative energy eigenvalue!

4.3 Quantization of free Dirac fermion field theory

Let us now apply the wisdom obtained by the quantization of a scalar field in the previous subsection to the problem of quantizing a Dirac fermion field that describes electrons and positrons. A sensible strategy is to expand the fields Ψ and Ψ^\dagger in terms of operators that act on states by creating and destroying particles with a given 3-momentum. Now, since Ψ is a spinor with four components, one must expand it in a basis for the four-dimensional spinor space. A convenient such basis is the solutions we found to the Dirac equation, $u(p, s)$ and $v(p, s)$. So we expand the Dirac field, at a given fixed time t , as:

$$\Psi(\vec{x}) = \sum_{s=1}^2 \int d\vec{p} \left[u(p, s) e^{i\vec{p}\cdot\vec{x}} b_{\vec{p},s} + v(p, s) e^{-i\vec{p}\cdot\vec{x}} d_{\vec{p},s}^\dagger \right]. \quad (4.3.1)$$

Here s labels the two possible spin states in some appropriate basis (for example, $S_z = \pm 1/2$). The operator $b_{\vec{p},s}$ will be interpreted as an annihilation operator, which removes an electron, with 3-momentum \vec{p} and spin state s , from whatever state it acts on. The operator $d_{\vec{p},s}^\dagger$ is a creation operator, which adds a positron to whatever state it acts on. We are using b, b^\dagger and d, d^\dagger rather than a, a^\dagger in order to distinguish the fermion and antifermion creation and annihilation

operators from the scalar field versions. Taking the Hermitian conjugate of eq. (4.3.1), and multiplying by γ^0 on the right, we get:

$$\bar{\Psi}(\vec{x}) = \sum_{s=1}^2 \int d\vec{p} \left[\bar{u}(p, s) e^{-i\vec{p}\cdot\vec{x}} b_{\vec{p},s}^\dagger + \bar{v}(p, s) e^{i\vec{p}\cdot\vec{x}} d_{\vec{p},s} \right]. \quad (4.3.2)$$

The operator $b_{\vec{p},s}^\dagger$ creates an electron, and $d_{\vec{p},s}$ destroys a positron, with the corresponding 3-momentum and spin.

More generally, if the Dirac field describes some fermions other than the electron-positron system, then you can substitute “particle” for electron and “antiparticle” for positron. So b^\dagger, b act on states to create and destroy particles, while d^\dagger, d create and destroy antiparticles.

Just as in the case of a scalar field, we assume the existence of a vacuum state $|0\rangle$, which describes a universe of empty space with no electrons or positrons present. The annihilation operators yield 0 when acting on the vacuum state:

$$b_{\vec{p},s}|0\rangle = d_{\vec{p},s}|0\rangle = 0 \quad (4.3.3)$$

for all \vec{p} and s . To make a state describing a single electron with 3-momentum \vec{p} and spin state s , just act on the vacuum with the corresponding creation operator:

$$b_{\vec{p},s}^\dagger|0\rangle = |e_{\vec{p},s}^-\rangle. \quad (4.3.4)$$

Similarly,

$$b_{\vec{k},r}^\dagger b_{\vec{p},s}^\dagger|0\rangle = |e_{\vec{k},r}^-; e_{\vec{p},s}^-\rangle \quad (4.3.5)$$

is a state containing two electrons, etc.

Now, electrons are fermions; they must obey Fermi-Dirac statistics for identical particles. This means that if we interchange the momentum and spin labels for the two electrons in the state of eq. (4.3.5), we must get a minus sign:

$$|e_{\vec{k},r}^-; e_{\vec{p},s}^-\rangle = -|e_{\vec{p},s}^-; e_{\vec{k},r}^-\rangle. \quad (4.3.6)$$

A corollary of this is the Pauli exclusion principle, which states that two electrons cannot be in exactly the same state. In the present case, that means that we cannot add to the vacuum two electrons with exactly the same 3-momentum and spin. Taking $\vec{k} = \vec{p}$ and $r = s$ in eq. (4.3.6):

$$|e_{\vec{p},s}^-; e_{\vec{p},s}^-\rangle = -|e_{\vec{p},s}^-; e_{\vec{p},s}^-\rangle, \quad (4.3.7)$$

which can only be true if $|e_{\vec{p},s}^-; e_{\vec{p},s}^-\rangle = 0$, in other words there is no such state.

Writing eq. (4.3.6) in terms of creation operators, we have:

$$b_{\vec{k},r}^\dagger b_{\vec{p},s}^\dagger |0\rangle = -b_{\vec{p},s}^\dagger b_{\vec{k},r}^\dagger |0\rangle. \quad (4.3.8)$$

So, instead of the commutation relation

$$[b_{\vec{k},r}^\dagger, b_{\vec{p},s}^\dagger] = 0 \quad (\text{Wrong!}) \quad (4.3.9)$$

that one might expect from comparison with the scalar field, we must have an anticommutation relation:

$$b_{\vec{k},r}^\dagger b_{\vec{p},s}^\dagger + b_{\vec{p},s}^\dagger b_{\vec{k},r}^\dagger = \{b_{\vec{k},r}^\dagger, b_{\vec{p},s}^\dagger\} = 0. \quad (4.3.10)$$

Taking the Hermitian conjugate, we must also have:

$$\{b_{\vec{k},r}, b_{\vec{p},s}\} = 0. \quad (4.3.11)$$

Similarly, applying the same thought process to identical positron fermions, one must have:

$$\{d_{\vec{k},r}^\dagger, d_{\vec{p},s}^\dagger\} = \{d_{\vec{k},r}, d_{\vec{p},s}\} = 0. \quad (4.3.12)$$

Note that in the classical limit, $\hbar \rightarrow 0$, these equations are unaffected, since \hbar doesn't appear anywhere. So it must be true that b , b^\dagger , d , and d^\dagger anticommute even classically. So, as classical fields, one must have

$$\{\Psi(x), \Psi(y)\} = 0, \quad (4.3.13)$$

$$\{\Psi^\dagger(x), \Psi^\dagger(y)\} = 0, \quad (4.3.14)$$

$$\{\Psi(x), \Psi^\dagger(y)\} = 0. \quad (4.3.15)$$

Evidently, the classical Dirac field is not a normal number, but rather an anticommuting or Grassmann number. Interchanging the order of any two Grassmann numbers results in an overall minus sign.

In order to discover how the classical equations (4.3.13) and (4.3.15) are modified when one goes to the quantum theory, let us construct the momentum conjugate to $\Psi(\vec{x})$. It is:

$$\mathcal{P}(\vec{x}) = \frac{\delta \mathcal{L}}{\delta(\partial_0 \Psi)} = i\bar{\Psi}\gamma^0 = i\Psi^\dagger\gamma^0\gamma^0 = i\Psi^\dagger. \quad (4.3.16)$$

So the momentum conjugate to the Dirac spinor field is just i times its Hermitian conjugate. Now, naively following the path of canonical quantization, one might expect the equal-time commutation relation:

$$[\mathcal{P}(\vec{x}), \Psi(\vec{y})] = -i\hbar\delta^{(3)}(\vec{x} - \vec{y}). \quad (\text{Wrong!}) \quad (4.3.17)$$

However, this clearly cannot be correct, since these are anticommuting fields; in the classical limit $\hbar \rightarrow 0$, eq. (4.3.17) disagrees with eq. (4.3.15). So, instead we postulate a canonical anticommutation relation for the Dirac field operator and its conjugate momentum operator:

$$\{\mathcal{P}(\vec{x}), \Psi(\vec{y})\} = -i\hbar\delta^{(3)}(\vec{x} - \vec{y}). \quad (4.3.18)$$

Now just rewriting $\mathcal{P} = i\Psi^\dagger$, this becomes:

$$\{\Psi^\dagger(\vec{x}), \Psi(\vec{y})\} = -\hbar\delta^{(3)}(\vec{x} - \vec{y}). \quad (4.3.19)$$

From this, using a strategy similar to that used for scalar fields, one can obtain:

$$\{b_{\vec{p},s}, b_{\vec{k},r}^\dagger\} = \{d_{\vec{p},s}, d_{\vec{k},r}^\dagger\} = (2\pi)^3 2E_{\vec{p}} \delta^{(3)}(\vec{p} - \vec{k}) \delta_{sr}, \quad (4.3.20)$$

and all other anticommutators of $b, b^\dagger, d, d^\dagger$ operators vanish.

One also can check that the Hamiltonian is

$$H = \sum_{s=1}^2 \int d\tilde{p} E_{\vec{p}} (b_{\vec{p},s}^\dagger b_{\vec{p},s} + d_{\vec{p},s}^\dagger d_{\vec{p},s}) \quad (4.3.21)$$

in a way very similar to the way we found the Hamiltonian for a scalar field in terms of a, a^\dagger operators. In doing so, one must again drop an infinite constant contribution (negative, this time) which is unobservable because it is the same for all states. Note that H again has energy eigenvalues that are ≥ 0 . One can show that:

$$[H, b_{\vec{k},s}^\dagger] = E_{\vec{k}} b_{\vec{k},s}^\dagger, \quad (4.3.22)$$

$$[H, d_{\vec{k},s}^\dagger] = E_{\vec{k}} d_{\vec{k},s}^\dagger. \quad (4.3.23)$$

(Note that these equations are commutators rather than anticommutators!) It follows that the eigenstates of energy and 3-momentum are given in general by:

$$b_{\vec{p}_1,s_1}^\dagger \dots b_{\vec{p}_n,s_n}^\dagger d_{\vec{k}_1,r_1}^\dagger \dots d_{\vec{k}_m,r_m}^\dagger |0\rangle, \quad (4.3.24)$$

which describes a state with n electrons (particles) and m positrons (antiparticles) with the obvious 3-momenta and spins, and total energy $E_{\vec{p}_1} + \dots + E_{\vec{p}_n} + E_{\vec{k}_1} + \dots + E_{\vec{k}_m}$.

4.4 Scalar field with ϕ^4 coupling

So far, we have been dealing with free field theories. These are theories in which the Lagrangian density is quadratic in the fields, so that the Euler-Lagrange equations obtained by varying \mathcal{L} are linear wave equations in the fields, with exact solutions that are not too hard to find. At the quantum level, this nice feature shows up in the simple time evolution of the states. In field

theory, as in any quantum system, the time evolution of a state $|X\rangle$ is given in the Schrodinger picture by

$$i\hbar \frac{d}{dt}|X\rangle = H|X\rangle. \quad (4.4.1)$$

So, in the case of a multiparticle state with an energy eigenvalue E as described above, the solution is just

$$|X(t)\rangle = e^{-i(t-t_0)H}|X(t_0)\rangle = e^{-i(t-t_0)E}|X(t_0)\rangle. \quad (4.4.2)$$

In other words, the state at some time t is just the same as the state at some previous time t_0 , up to a phase. So nothing ever happens to the particles in a free theory; their number does not change, and their momenta and spins remain the same.

We are interested in describing a more interesting situation where particles can scatter off each other, perhaps inelastically to create new particles, and in which some particles can decay into other sets of particles. To describe this, we need a Lagrangian density that contains terms with more than two fields. At the classical level, this will lead to non-linear equations of motion that have to be solved approximately. At the quantum level, finding exact energy eigenstates of the Hamiltonian is not possible, so one usually treats the non-quadratic part of the Hamiltonian as a perturbation on the quadratic part, giving an approximate answer.

As an example, consider the free Lagrangian for a scalar field ϕ , as given in eq. (4.1.18), and add to it an interaction term:

$$\mathcal{L} = \mathcal{L}_0 + \mathcal{L}_{\text{int}}; \quad (4.4.3)$$

$$\mathcal{L}_{\text{int}} = -\frac{\lambda}{24}\phi^4. \quad (4.4.4)$$

Here λ is a dimensionless number, a parameter of the theory known as a coupling. It governs the strength of interactions; if we set $\lambda = 0$, we would be back to the free theory in which nothing interesting ever happens. The factor of $1/4! = 1/24$ is a convention, and the reason for it will be apparent later. Now canonical quantization can proceed as before, except that now the Hamiltonian is

$$H = H_0 + H_{\text{int}}, \quad (4.4.5)$$

where

$$H_{\text{int}} = - \int d^3\vec{x} \mathcal{L}_{\text{int}} = \frac{\lambda}{24} \int d^3\vec{x} \phi(\vec{x})^4. \quad (4.4.6)$$

Let us write this in terms of creation and annihilation operators, using eq. (4.2.30):

$$H_{\text{int}} = \frac{\lambda}{24} \int d^3\vec{x} \int d\vec{q}_1 \int d\vec{q}_2 \int d\vec{q}_3 \int d\vec{q}_4 \left(a_{\vec{q}_1} e^{i\vec{q}_1 \cdot \vec{x}} + a_{\vec{q}_1}^\dagger e^{-i\vec{q}_1 \cdot \vec{x}} \right) \left(a_{\vec{q}_2} e^{i\vec{q}_2 \cdot \vec{x}} + a_{\vec{q}_2}^\dagger e^{-i\vec{q}_2 \cdot \vec{x}} \right) \\ \left(a_{\vec{q}_3} e^{i\vec{q}_3 \cdot \vec{x}} + a_{\vec{q}_3}^\dagger e^{-i\vec{q}_3 \cdot \vec{x}} \right) \left(a_{\vec{q}_4} e^{i\vec{q}_4 \cdot \vec{x}} + a_{\vec{q}_4}^\dagger e^{-i\vec{q}_4 \cdot \vec{x}} \right). \quad (4.4.7)$$

Now we can perform the $d^3\vec{x}$ integration, using eq. (4.2.19). The result is:

$$\begin{aligned}
H_{\text{int}} = \frac{\lambda}{24}(2\pi)^3 \int d\vec{q}_1 \int d\vec{q}_2 \int d\vec{q}_3 \int d\vec{q}_4 \left[a_{\vec{q}_1}^\dagger a_{\vec{q}_2}^\dagger a_{\vec{q}_3}^\dagger a_{\vec{q}_4}^\dagger \delta^{(3)}(\vec{q}_1 + \vec{q}_2 + \vec{q}_3 + \vec{q}_4) \right. \\
+ 4a_{\vec{q}_1}^\dagger a_{\vec{q}_3}^\dagger a_{\vec{q}_2}^\dagger a_{\vec{q}_4}^\dagger \delta^{(3)}(\vec{q}_1 + \vec{q}_2 + \vec{q}_3 - \vec{q}_4) \\
+ 6a_{\vec{q}_1}^\dagger a_{\vec{q}_2}^\dagger a_{\vec{q}_3}^\dagger a_{\vec{q}_4}^\dagger \delta^{(3)}(\vec{q}_1 + \vec{q}_2 - \vec{q}_3 - \vec{q}_4) \\
+ 4a_{\vec{q}_1}^\dagger a_{\vec{q}_2}^\dagger a_{\vec{q}_3}^\dagger a_{\vec{q}_4}^\dagger \delta^{(3)}(\vec{q}_1 - \vec{q}_3 - \vec{q}_2 - \vec{q}_4) \\
\left. + a_{\vec{q}_1} a_{\vec{q}_2} a_{\vec{q}_3} a_{\vec{q}_4} \delta^{(3)}(\vec{q}_1 + \vec{q}_2 + \vec{q}_3 + \vec{q}_4) \right]. \quad (4.4.8)
\end{aligned}$$

Here we have combined several like terms, by relabeling the momenta, giving rise to the factors of 4, 6, and 4. This involves reordering the a 's and a^\dagger 's. In doing so, we have ignored the fact that a 's do not commute with a^\dagger 's when the 3-momenta are exactly equal. This should not cause any worry, because it just corresponds to the situation where a particle is “scattered” without changing its momentum at all, which is the same as no scattering, and therefore not of interest.

To see how to use the interaction Hamiltonian, it is useful to tackle a specific process. For example, consider a scattering problem in which we have two scalar particles with 4-momenta p_a, p_b that interact, producing two scalar particles with 4-momenta k_1, k_2 :

$$p_a p_b \rightarrow k_1 k_2. \quad (4.4.9)$$

We will work in the Schrodinger picture of quantum mechanics, in which operators are time-independent and states evolve in time according to eq. (4.4.1). Nevertheless, in the far past, we assume that the incoming particles were far apart, so the system is accurately described by the free Hamiltonian and its energy eigenstates. The same applies to the outgoing particles in the far future. So, we can pretend that H_{int} is “turned off” in both the far past and the far future. The states that are simple two-particle states are

$$|p_a, p_b\rangle_{\text{IN}} = a_{\vec{p}_a}^\dagger a_{\vec{p}_b}^\dagger |0\rangle, \quad (4.4.10)$$

in the far past, and

$$|k_1, k_2\rangle_{\text{OUT}} = a_{\vec{k}_1}^\dagger a_{\vec{k}_2}^\dagger |0\rangle, \quad (4.4.11)$$

in the far future. These are built out of creation and annihilation operators just as before, so they are eigenstates of the free Hamiltonian H_0 , but not of the full Hamiltonian. Now, we are interested in computing the probability amplitude that the state $|p_a, p_b\rangle_{\text{IN}}$ evolves to the state $|k_1, k_2\rangle_{\text{OUT}}$. According to the rules of quantum mechanics this is given by their overlap at a common time, say in the far future:

$${}_{\text{OUT}}\langle k_1, k_2 | p_a, p_b \rangle_{\text{OUT}}. \quad (4.4.12)$$

The state $|p_a, p_b\rangle_{\text{OUT}}$ is the time evolution of $|p_a, p_b\rangle_{\text{IN}}$ from the far past to the far future:

$$|p_a, p_b\rangle_{\text{OUT}} = e^{-iTH} |p_a, p_b\rangle_{\text{IN}}, \quad (4.4.13)$$

where T is the long time between the far past time when the initial state was created and the far future time at which the overlap is computed. So we have:

$${}_{\text{OUT}}\langle k_1, k_2 | p_a, p_b \rangle_{\text{OUT}} = {}_{\text{OUT}}\langle k_1, k_2 | e^{-iTH} | p_a, p_b \rangle_{\text{IN}}. \quad (4.4.14)$$

The states appearing on the right-hand side are simple; see eqs. (4.4.10) and (4.4.11). The complications are hidden in the operator e^{-iTH} .

In general, e^{-iTH} cannot be written exactly in a useful way in terms of creation and annihilation operators. However, we can do it perturbatively, order by order in the coupling λ . For example, let us consider the contribution linear in λ . We use the definition of the exponential to write:

$$e^{-iTH} = [1 - iHT/N]^N = [1 - i(H_0 + H_{\text{int}})T/N]^N, \quad (4.4.15)$$

for $N \rightarrow \infty$. Now, the part of this that is linear in H_{int} can be expanded as:

$$e^{-iTH} = \sum_{n=0}^{N-1} [1 - iH_0T/N]^{N-n-1} (-iH_{\text{int}}T/N) [1 - iH_0T/N]^n. \quad (4.4.16)$$

(Here we have dropped the 0th order part, e^{-iTH_0} , as uninteresting; it just corresponds to the particles evolving as free particles.) We can now turn this discrete sum into an integral, by letting $t = nT/N$ and $dt = T/N$ in the limit of large N :

$$e^{-iTH} = -i \int_0^T dt e^{-i(T-t)H_0} H_{\text{int}} e^{-itH_0}. \quad (4.4.17)$$

Next we can use the fact that we know what H_0 is when acting on the simple states of eqs. (4.4.10) and (4.4.11):

$$e^{-itH_0} |p_a, p_b\rangle_{\text{IN}} = e^{-itE_i} |p_a, p_b\rangle_{\text{IN}}, \quad (4.4.18)$$

$${}_{\text{OUT}}\langle k_1, k_2 | e^{-i(T-t)H_0} = {}_{\text{OUT}}\langle k_1, k_2 | e^{-i(T-t)E_f}, \quad (4.4.19)$$

where

$$E_i = E_{\vec{p}_a} + E_{\vec{p}_b}, \quad E_f = E_{\vec{k}_1} + E_{\vec{k}_2} \quad (4.4.20)$$

are the energies of the initial and final states, respectively. So we have:

$${}_{\text{OUT}}\langle k_1, k_2 | e^{-iTH} | p_a, p_b \rangle_{\text{IN}} = -i \int_0^T dt e^{-i(T-t)E_f} e^{-itE_i} {}_{\text{OUT}}\langle k_1, k_2 | H_{\text{int}} | p_a, p_b \rangle_{\text{IN}}. \quad (4.4.21)$$

First let us do the t integral:

$$\int_0^T dt e^{-i(T-t)E_f} e^{-itE_i} = e^{-i(E_f+E_i)T/2} \int_{-T/2}^{T/2} dt' e^{it'(E_f-E_i)} \quad (4.4.22)$$

where we have redefined the integration variable by $t = t' + T/2$. As we take $T \rightarrow \infty$, we can use the integral identity

$$\int_{-\infty}^{\infty} dx e^{ixA} = 2\pi\delta(A) \quad (4.4.23)$$

to obtain:

$$\int_0^T dt e^{-i(T-t)E_f} e^{-itE_i} = 2\pi\delta(E_f - E_i) e^{-i(E_f+E_i)T/2}. \quad (4.4.24)$$

This tells us that energy conservation will be enforced, and (dropping the phase factor $e^{-i(E_f+E_i)T/2}$, which will just give 1 when we take the complex square of the probability amplitude):

$${}_{\text{OUT}}\langle k_1, k_2 | p_a, p_b \rangle_{\text{OUT}} = -i 2\pi \delta(E_f - E_i) {}_{\text{OUT}}\langle k_1, k_2 | H_{\text{int}} | p_a, p_b \rangle_{\text{IN}}. \quad (4.4.25)$$

Now we are ready to use our expression for H_{int} in eq. (4.4.8). The action of H_{int} on eigenstates of the free Hamiltonian can be read off from the different types of terms. The $aaaa$ -type term will remove four particles from the state. Clearly we don't have to worry about that, because there were only two particles in the state to begin with! The same goes for the $a^\dagger aaa$ -type term. The terms of type $a^\dagger a^\dagger a^\dagger a^\dagger$ and $a^\dagger a^\dagger a^\dagger a$ create more than the two particles we know to be in the final state, so we can ignore them too. Therefore, the only term that will play a role in this example is the $a^\dagger a^\dagger aa$ contribution:

$$H_{\text{int}} = \frac{\lambda}{4} (2\pi)^3 \int d\tilde{q}_1 \int d\tilde{q}_2 \int d\tilde{q}_3 \int d\tilde{q}_4 \delta^{(3)}(\vec{q}_1 + \vec{q}_2 - \vec{q}_3 - \vec{q}_4) a_{\vec{q}_1}^\dagger a_{\vec{q}_2}^\dagger a_{\vec{q}_3} a_{\vec{q}_4}, \quad (4.4.26)$$

Therefore, we have:

$${}_{\text{OUT}}\langle k_1, k_2 | p_a, p_b \rangle_{\text{OUT}} = -i(2\pi)^4 \frac{\lambda}{4} \int d\tilde{q}_1 \int d\tilde{q}_2 \int d\tilde{q}_3 \int d\tilde{q}_4 \delta^{(4)}(q_1 + q_2 - q_3 - q_4) {}_{\text{OUT}}\langle k_1, k_2 | a_{\vec{q}_1}^\dagger a_{\vec{q}_2}^\dagger a_{\vec{q}_3} a_{\vec{q}_4} | p_a, p_b \rangle_{\text{IN}}. \quad (4.4.27)$$

Here we have combined the three-momenta delta function from eq. (4.4.26) with the energy delta function from eq. (4.4.25) to give a 4-momentum delta function.

It remains to evaluate:

$${}_{\text{OUT}}\langle k_1, k_2 | a_{\vec{q}_1}^\dagger a_{\vec{q}_2}^\dagger a_{\vec{q}_3} a_{\vec{q}_4} | p_a, p_b \rangle_{\text{IN}}, \quad (4.4.28)$$

which, according to eqs. (4.4.10) and (4.4.11), is equal to

$$\langle 0 | a_{\vec{k}_1} a_{\vec{k}_2} a_{\vec{q}_1}^\dagger a_{\vec{q}_2}^\dagger a_{\vec{q}_3} a_{\vec{q}_4} a_{\vec{p}_a}^\dagger a_{\vec{p}_b}^\dagger | 0 \rangle. \quad (4.4.29)$$

This can be done using the commutation relations of eqs. (4.2.20) and (4.2.21). The strategy is to commute $a_{\vec{q}_3}$ and $a_{\vec{q}_4}$ to the right, so they can give 0 when acting on $|0\rangle$, and commute $a_{\vec{q}_1}^\dagger$ and $a_{\vec{q}_2}^\dagger$ to the left so they can give 0 when acting on $\langle 0|$. Along the way, one picks up delta functions whenever the 3-momenta of an a and a^\dagger match. One contribution occurs when $\vec{q}_3 = \vec{p}_a$ and $\vec{q}_4 = \vec{p}_b$ and $\vec{q}_1 = \vec{k}_1$ and $\vec{q}_2 = \vec{k}_2$. It yields:

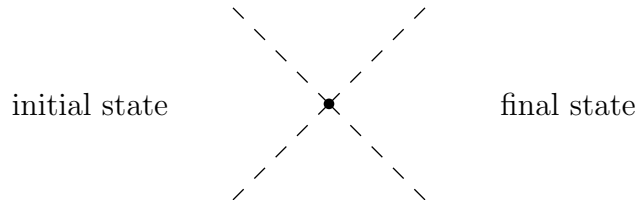
$$(2\pi)^3 2E_{\vec{q}_3} \delta^{(3)}(\vec{q}_3 - \vec{p}_a) (2\pi)^3 2E_{\vec{q}_4} \delta^{(3)}(\vec{q}_4 - \vec{p}_b) (2\pi)^3 2E_{\vec{q}_1} \delta^{(3)}(\vec{q}_1 - \vec{k}_1) (2\pi)^3 2E_{\vec{q}_2} \delta^{(3)}(\vec{q}_2 - \vec{k}_2). \quad (4.4.30)$$

There are 3 more similar terms. You can check that each of them gives a contribution equal to eq. (4.4.30) when put into eq. (4.4.27), after relabeling momenta; this cancels the factor of $1/4$ in eq. (4.4.27). Now, the factors of $(2\pi)^3 2E_{\vec{q}_3}$ etc. all neatly cancel against the corresponding factors in the denominator of $d\vec{q}_3$, etc. [See eq. (4.2.27).] The three-momentum delta functions then make the remaining $d^3\vec{q}_1$, $d^3\vec{q}_2$, $d^3\vec{q}_3$, and $d^3\vec{q}_4$ integrations trivial; they just set the four-vectors $q_3 = p_a$, $q_4 = p_b$, $q_1 = k_1$, and $q_2 = k_2$ in the remaining 4-momentum delta function that was already present in eq. (4.4.27).

Putting it all together, we are left with the remarkably simple result:

$${}_{\text{OUT}}\langle k_1, k_2 | p_a, p_b \rangle_{\text{OUT}} = -i\lambda(2\pi)^4 \delta^{(4)}(k_1 + k_2 - p_a - p_b). \quad (4.4.31)$$

Rather than go through this whole messy procedure every time we invent a new interaction term for the Lagrangian density, or every time we think of a new scattering process, one can instead summarize the procedure with a simple set of diagrammatic rules. These rules, called Feynman rules, are useful both as a precise summary of a matrix element calculation, and as a heuristic guide to what physical process the calculation represents. In the present case, the Feynman diagram for the process is:



Here the two lines coming from the left represent the incoming state scalar particles, which get “destroyed” by the annihilation operators in H_{int} . The vertex where the four lines meet represents the interaction itself, and is associated with the factor $-i\lambda$. The two lines outgoing to the right represent the two final state scalar particles, which are resurrected by the two creation operators in H_{int} .

This is just the simplest of many Feynman diagrams one could write down for the process of two particle scattering in this theory. But all other diagrams represent contributions that are higher order in λ , so if λ is small we can ignore them.

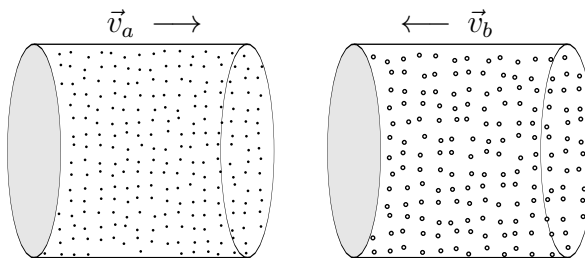
4.5 Scattering processes and cross-sections

In subsection 4.4, we found that the matrix element corresponding to 2 particle to 2 particle scattering in a scalar field theory with interaction Lagrangian $-\frac{\lambda}{24}\phi^4$ is:

$${}_{\text{OUT}}\langle k_1 k_2 | p_a p_b \rangle_{\text{OUT}} = -i\lambda(2\pi)^4 \delta^{(4)}(k_1 + k_2 - p_a - p_b). \quad (4.5.1)$$

Now we would like to learn how to translate this information into something physically meaningful that could in principle be measured in an experiment. The matrix element itself is infinite whenever 4-momentum is conserved, and zero otherwise. So clearly we must do some work to relate it to an appropriate physically measurable quantity, namely the cross-section.

The cross-section is the observable that gives the expected number of scattering events N_S that will occur if two large sets of particles are allowed to collide. Suppose that we have N_a particles of type a and N_b of type b , formed into large packets of uniform density that move completely through each other as shown:



The two packets are assumed to have the same area A (shaded gray) perpendicular to their motion. The total number of scattering events occurring while the packets move through each other should be proportional to each of the numbers N_a and N_b , and inversely proportional to the area A . The equation

$$N_S = \frac{N_a N_b}{A} \sigma \quad (4.5.2)$$

defines the cross-section σ . The rate at which the effective $N_a N_b / A$ is increasing with time in an experiment is called the luminosity L (or instantaneous luminosity), and the same quantity integrated over time is called the integrated luminosity. Therefore,

$$N_S = \sigma \int L dt. \quad (4.5.3)$$

The dimensions for cross-section are the same as area, and the official unit is 1 barn = 10^{-24} cm² = 2568 GeV⁻². However, from the point of view of modern high-energy experiments, a barn is a very large cross-section,[†] so more commonly-used units are obtained by using the prefixes nano-, pico-, and femto-:

$$1 \text{ nb} = 10^{-33} \text{ cm}^2 = 2.568 \times 10^{-6} \text{ GeV}^{-2}, \quad (4.5.4)$$

$$1 \text{ pb} = 10^{-36} \text{ cm}^2 = 2.568 \times 10^{-9} \text{ GeV}^{-2}, \quad (4.5.5)$$

$$1 \text{ fb} = 10^{-39} \text{ cm}^2 = 2.568 \times 10^{-12} \text{ GeV}^{-2}. \quad (4.5.6)$$

As an example, the Tevatron collided protons (p) and antiprotons (\bar{p}) with a center-of-momentum (CM) energy of $E_{\text{CM}} = 1960$ GeV and each experiment received a total integrated luminosity of about

$$\int L dt = 12 \text{ fb}^{-1} = 12,000 \text{ pb}^{-1}, \quad (4.5.7)$$

although not all of that data is useable in any given analysis. The Large Hadron Collider (LHC) at CERN is a pp machine that previously collected 23.3 fb^{-1} of integrated luminosity per experiment (ATLAS and CMS) at center-of-mass energy $\sqrt{s} = 8 \text{ TeV}$. The LHC has been running at $\sqrt{s} = 13 \text{ TeV}$ since 2015, with the goal of reaching several hundred fb^{-1} of integrated luminosity in the coming years. As of this writing (August 2018), about 130 fb^{-1} have already been delivered to each LHC experiment at $\sqrt{s} = 13 \text{ TeV}$, with the record highest luminosity in a single day being about 860 pb^{-1} . The highest instantaneous luminosity so far is about $2.1 \times 10^{34} \text{ cm}^{-2} \text{ sec}^{-1}$, exceeding the LHC design target.

To figure out how many scattering events one expects at a collider, one needs to know the corresponding cross-section for that type of event, which depends on the final state. The total cross-section for any type of scattering at hadron colliders is quite large. By one estimate at the Tevatron it was approximately

$$\sigma(p\bar{p} \rightarrow \text{anything}) = 0.075 \text{ barns}. \quad (4.5.8)$$

However, this estimate is quite fuzzy, because it depends on detection variables such as the minimum momentum transfer that one requires in order to say that a scattering event has occurred. For arbitrarily small momentum transfer in elastic scattering of charged particles, the cross-section actually becomes arbitrarily large due to the long-range nature of the Coulomb force, as we will see in section 5.2.4. Also, the vast majority of the scattering events reflected in eq. (4.5.8) are extremely uninteresting, featuring final states of well-known and well-understood hadrons.

[†]The joke is that achieving an event with such a cross-section is “as easy as hitting the broad side of a barn”.

An example of a more interesting final state would be anything involving a top quark (t) and anti-top quark (\bar{t}) pair, for which the Tevatron cross-section was about

$$\sigma(p\bar{p} \rightarrow t\bar{t} + \text{anything}) = 7.5 \text{ pb.} \quad (4.5.9)$$

This means that about 96,000 top pairs were produced at the Tevatron. However, only a small fraction of these were identified as such. At the LHC, the cross-section for producing top-antitop pairs is about

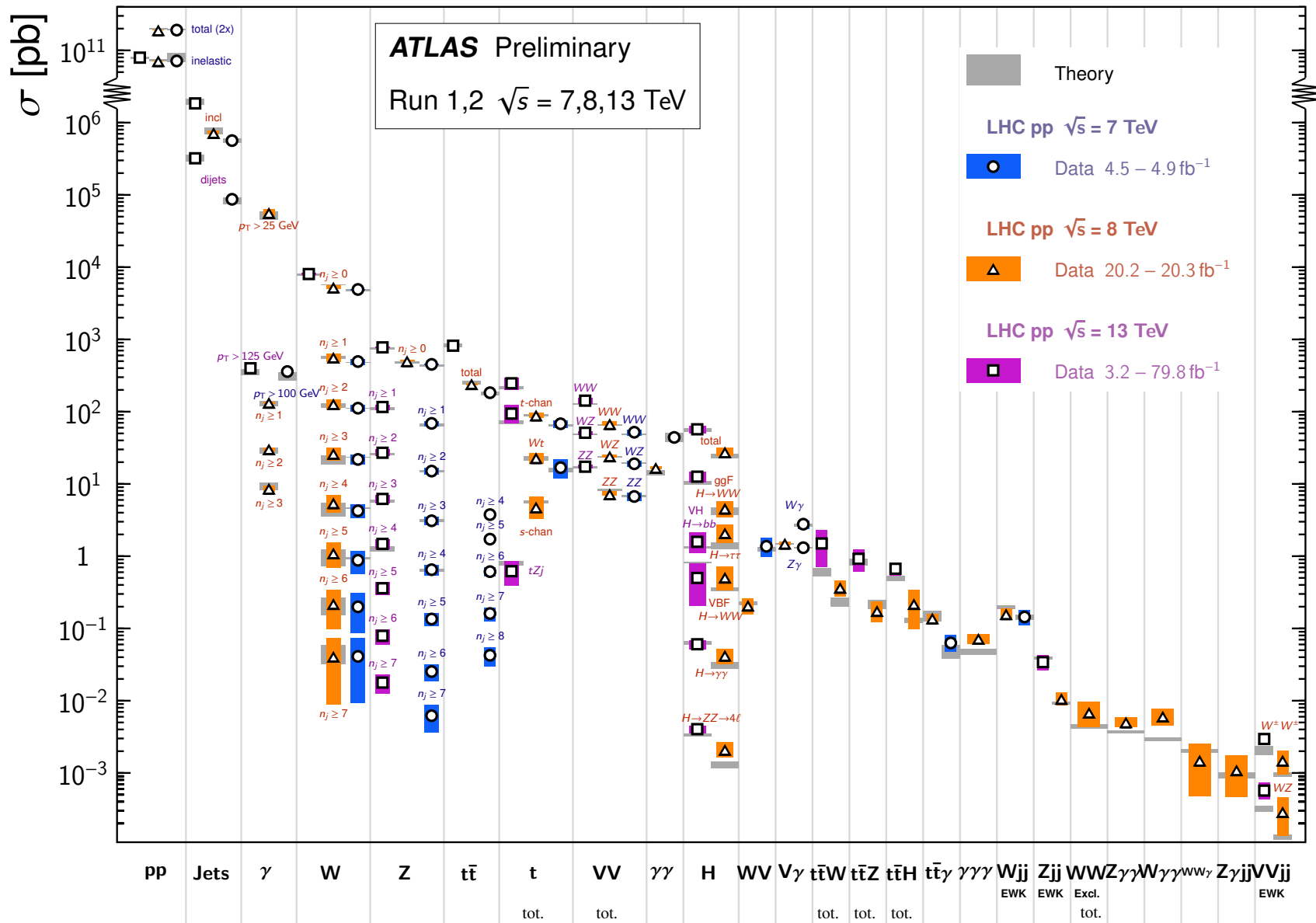
$$\sigma(pp \rightarrow t\bar{t} + \text{anything}) = (175, 250, 830) \text{ pb,} \quad (4.5.10)$$

for center-of-mass energies $\sqrt{s} = (7, 8, 13)$ TeV, respectively. This means that tens of millions of $t\bar{t}$ pairs have already been produced, enabling unprecedented precision studies of top quark properties. Those studies will continue as the integrated luminosity increases.

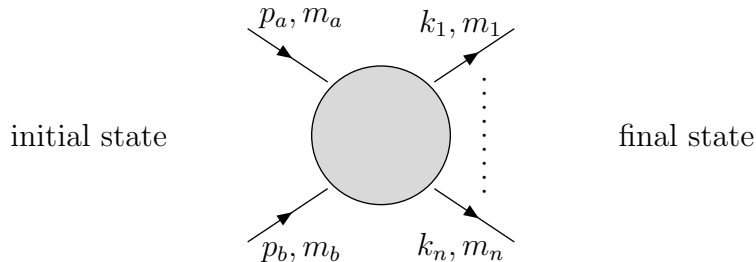
A propaganda plot summarizing the theoretical predictions and experimental measurements of cross-sections for a selection of some of the more important processes involving Standard Model particles is shown on the next page for LHC energies of 7, 8, and 13 TeV. Besides the very large total and the inelastic total, also shown are the cross-sections for producing ≥ 1 or ≥ 2 hadronic jets, a photon, a W boson, a Z boson, $t\bar{t}$ pairs, a single top quark, combinations of vector bosons WW , WZ , ZZ , and $\gamma\gamma$, the Higgs boson, and other even rarer processes as labeled. In some cases, the cross-sections are given independently for sub-cases in which at least a certain number of hadronic jets n_j is required in the final state. Note that the ranges for these cross-sections span many orders of magnitude. The plot shows both experimental results and theoretical predictions for these cross-section. It is both gratifying and reassuring that the theoretical predictions of the Standard Model are in good agreement with the experimental results.

Standard Model Production Cross Section Measurements

Status: July 2018



In general, our task is to figure out how to relate the matrix element for a given collision process to the corresponding cross-section. Let us consider a general situation in which two particles a and b with masses m_a and m_b and 4-momenta p_a and p_b collide, producing n final-state particles with masses m_i and 4-momenta k_i , where $i = 1, 2, \dots, n$:



As an abbreviation, we can call the initial state $|i\rangle = |p_a, m_a; p_b, m_b\rangle_{\text{IN}}$ and the final state $|f\rangle = |k_1, m_1; \dots; k_n, m_n\rangle_{\text{OUT}}$. In general, all of the particles could be different, so that a different species of creation and annihilation operators might be used for each. They can be either fermions or bosons, provided that the process conserves angular momentum, charge, and color, and is consistent with other symmetries of the Standard Model. If the particles are not scalars, then $|i\rangle$ and $|f\rangle$ should also carry labels that specify the spin of each particle. Now, because of four-momentum conservation, we can always write:

$$\langle f|i\rangle = \mathcal{M}_{i\rightarrow f} (2\pi)^4 \delta^{(4)}(p_a + p_b - \sum_{i=1}^n k_i). \quad (4.5.11)$$

Here $\mathcal{M}_{i\rightarrow f}$ is called the reduced matrix element for the process. In the example in subsection 4.4, the reduced matrix element we found to first order in the coupling λ was simply a constant: $\mathcal{M}_{\phi\phi\rightarrow\phi\phi} = -i\lambda$. However, in general, \mathcal{M} can be a non-trivial Lorentz-scalar function of the various 4-momenta and spin eigenvalues of the particles in the problem. In practice, it is computed order-by-order in perturbation theory, so it is only known approximately.

According to the postulates of quantum mechanics, the probability of a transition from the state $|i\rangle$ to the state $|f\rangle$ is:

$$\mathcal{P}_{i\rightarrow f} = \frac{|\langle f|i\rangle|^2}{\langle f|f\rangle\langle i|i\rangle}. \quad (4.5.12)$$

The matrix element has been divided by the norms of the states, which are not unity; they will be computed below. Now, the total number of scattering events expected to occur is:

$$N_S = N_a N_b \sum_f \mathcal{P}_{i\rightarrow f}. \quad (4.5.13)$$

Here $N_a N_b$ represents the total number of initial states, one for each possible pair of incoming particles. The sum \sum_f is over all possible final states f . To evaluate this, recall that if one puts

particles in a large box of volume V , then the density of one-particle states with 3-momentum \vec{k} is

$$\text{density of states} = V \frac{d^3 \vec{k}}{(2\pi)^3}. \quad (4.5.14)$$

So, including a sum over the n final-state particles implies

$$\sum_f \rightarrow \prod_{i=1}^n \left[V \int \frac{d^3 \vec{k}_i}{(2\pi)^3} \right]. \quad (4.5.15)$$

Putting this into eq. (4.5.13) and comparing with the definition eq. (4.5.2), we have for the differential contribution to the total cross-section:

$$d\sigma = \mathcal{P}_{i \rightarrow f} A \prod_{i=1}^n \left[V \frac{d^3 \vec{k}_i}{(2\pi)^3} \right]. \quad (4.5.16)$$

Let us now suppose that each packet of particles consists of a cylinder with a large volume V . Then the total time T over which the particles can collide is given by the time it takes for the two packets to move through each other:

$$T = \frac{V}{A|\vec{v}_a - \vec{v}_b|}. \quad (4.5.17)$$

(Assume that the volume V and area A of each bunch are very large compared to the cube and square of the particles' Compton wavelengths.) It follows that the differential contribution to the cross-section is:

$$d\sigma = \mathcal{P}_{i \rightarrow f} \frac{V}{T|\vec{v}_a - \vec{v}_b|} \prod_{i=1}^n \left[V \frac{d^3 \vec{k}_i}{(2\pi)^3} \right]. \quad (4.5.18)$$

The total cross-section is obtained by integrating over 3-momenta of the final state particles. Note that the differential cross-section $d\sigma$ depends only on the collision process being studied. So in the following we expect that the arbitrary volume V and packet collision time T should cancel out.

To see how that happens in the example of $\phi\phi \rightarrow \phi\phi$ scattering with a ϕ^4 interaction, let us first compute the normalizations of the states appearing in $\mathcal{P}_{i \rightarrow f}$. For the initial state $|i\rangle$ of eq. (4.4.10), one has:

$$\langle i|i\rangle = \langle 0|a_{\vec{p}_b} a_{\vec{p}_a}^\dagger a_{\vec{p}_a}^\dagger a_{\vec{p}_b}^\dagger |0\rangle. \quad (4.5.19)$$

To compute this, one can commute the a^\dagger operators to the left:

$$\langle i|i\rangle = \langle 0|a_{\vec{p}_b} [a_{\vec{p}_a} a_{\vec{p}_a}^\dagger] a_{\vec{p}_b}^\dagger |0\rangle + \langle 0|a_{\vec{p}_b} a_{\vec{p}_a}^\dagger a_{\vec{p}_a} a_{\vec{p}_b}^\dagger |0\rangle. \quad (4.5.20)$$

Now the incoming particle momenta \vec{p}_a and \vec{p}_b are always different, so in the last term the $a_{\vec{p}_a}^\dagger$ just commutes with $a_{\vec{p}_b}$ according to eq. (4.2.20), yielding 0 when acting on $\langle 0|$. The first term can be simplified using the commutator eq. (4.2.20):

$$\langle i|i \rangle = \langle 0|a_{\vec{p}_b}a_{\vec{p}_b}^\dagger|0 \rangle (2\pi)^3 2E_a \delta^{(3)}(\vec{p}_a - \vec{p}_a). \quad (4.5.21)$$

Commuting $a_{\vec{p}_b}^\dagger$ to the left in the same way yields the norm of the state $|i\rangle$:

$$\langle i|i \rangle = (2\pi)^6 4E_a E_b \delta^{(3)}(\vec{p}_a - \vec{p}_a) \delta^{(3)}(\vec{p}_b - \vec{p}_b). \quad (4.5.22)$$

This result is doubly infinite, since the arguments of each delta function vanish! In order to successfully interpret it, let us recall the origin of the 3-momentum delta functions. One can write

$$(2\pi)^3 \delta^{(3)}(\vec{p} - \vec{p}) = \int d^3\vec{x} e^{i\vec{0}\cdot\vec{x}} = V, \quad (4.5.23)$$

showing that a 3-momentum delta-function with vanishing argument corresponds to $V/(2\pi)^3$, where V is the volume that the particles occupy. So we obtain

$$\langle i|i \rangle = 4E_a E_b V^2 \quad (4.5.24)$$

for the norm of the incoming state.

Similarly, the norm of the state $|f\rangle$ is:

$$\langle f|f \rangle = \prod_{i=1}^n (2\pi)^3 2E_i \delta^{(3)}(\vec{k}_i - \vec{k}_i) = \prod_{i=1}^n (2E_i V). \quad (4.5.25)$$

In doing this, there is one subtlety; unlike the colliding particles, it could be that two identical outgoing particles have exactly the same momentum. This seemingly could produce “extra” contributions when we commute a^\dagger operators to the left. However, at least for massive particles, one can usually ignore this, since the probability that two outgoing particles will have *exactly* the same momentum is vanishingly small in the limit $V \rightarrow \infty$.

Next we turn to the square of the matrix element:

$$|\langle f|i \rangle|^2 = |\mathcal{M}_{i \rightarrow f}|^2 \left[(2\pi)^4 \delta^{(4)}(p_a + p_b - \sum k_i) \right]^2. \quad (4.5.26)$$

This also is apparently the square of an infinite quantity. To interpret it, we again recall the origin of the delta functions:

$$2\pi \delta(E_f - E_i) = \int_{-T/2}^{T/2} dt e^{it(E_f - E_i)} = T \quad (\text{for } E_f = E_i), \quad (4.5.27)$$

$$(2\pi)^3 \delta(\sum \vec{k} - \sum \vec{p}) = \int d^3\vec{x} e^{i\vec{x} \cdot (\sum \vec{k} - \sum \vec{p})} = V \quad (\text{for } \sum \vec{k} = \sum \vec{p}). \quad (4.5.28)$$

So we can write:

$$(2\pi)^4 \delta^{(4)}(p_a + p_b - \sum_{i=1}^n k_i) = TV. \quad (4.5.29)$$

Now if we use this to replace one of the two 4-momentum delta functions in eq. (4.5.26), we have:

$$|\langle f|i \rangle|^2 = |\mathcal{M}_{i \rightarrow f}|^2 (2\pi)^4 T V \delta^{(4)}(p_a + p_b - \sum_{i=1}^n k_i). \quad (4.5.30)$$

Plugging the results of eqs. (4.5.24), (4.5.25) and (4.5.30) into eq. (4.5.12), we obtain an expression for the transition probability:

$$\mathcal{P}_{i \rightarrow f} = |\mathcal{M}_{i \rightarrow f}|^2 (2\pi)^4 \delta^{(4)}(p_a + p_b - \sum_{i=1}^n k_i) \frac{T}{4E_a E_b V} \prod_{i=1}^n \left(\frac{1}{2E_i V} \right). \quad (4.5.31)$$

Putting this in turn into eq. (4.5.18), we finally obtain:

$$d\sigma = \frac{|\mathcal{M}_{i \rightarrow f}|^2}{4E_a E_b |\vec{v}_a - \vec{v}_b|} d\Phi_n, \quad (4.5.32)$$

where $d\Phi_n$ is a short-hand notation for

$$d\Phi_n = (2\pi)^4 \delta^{(4)}(p_a + p_b - \sum_{i=1}^n k_i) \prod_{i=1}^n \left(\frac{d^3 \vec{k}_i}{(2\pi)^3 2E_i} \right), \quad (4.5.33)$$

and is known as the n -body differential Lorentz-invariant phase space: As expected, all factors of T and V have canceled out of the formula eq. (4.5.32) for the differential cross-section.

In the formula eq. (4.5.32), one can write for the velocities:

$$\vec{v}_a = \frac{\vec{p}_a}{E_a}, \quad \vec{v}_b = \frac{\vec{p}_b}{E_b}. \quad (4.5.34)$$

Now, assuming that the collision is head-on so that \vec{v}_b is opposite to \vec{v}_a (or 0), the denominator in eq. (4.5.32) is:

$$4E_a E_b |\vec{v}_a - \vec{v}_b| = 4(E_a |\vec{p}_b| + E_b |\vec{p}_a|). \quad (4.5.35)$$

The most common case one encounters is two-particle scattering to a final state with two particles. In the center-of-momentum frame, $\vec{p}_b = -\vec{p}_a$, so that the 2-body Lorentz-invariant phase space becomes:

$$d\Phi_2 = (2\pi)^4 \delta^{(3)}(\vec{k}_1 + \vec{k}_2) \delta(E_a + E_b - E_1 - E_2) \frac{d^3 \vec{k}_1}{(2\pi)^3 2E_1} \frac{d^3 \vec{k}_2}{(2\pi)^3 2E_2} \quad (4.5.36)$$

$$= \frac{\delta^{(3)}(\vec{k}_1 + \vec{k}_2) \delta(\sqrt{\vec{k}_1^2 + m_1^2} + \sqrt{\vec{k}_2^2 + m_2^2} - E_{\text{CM}})}{16\pi^2 \sqrt{\vec{k}_1^2 + m_1^2} \sqrt{\vec{k}_2^2 + m_2^2}} d^3 \vec{k}_1 d^3 \vec{k}_2, \quad (4.5.37)$$

where

$$E_{\text{CM}} \equiv E_a + E_b \quad (4.5.38)$$

is the center-of-momentum energy of the process. Now one can do the \vec{k}_2 integral; the 3-momentum delta function just sets $\vec{k}_2 = -\vec{k}_1$ (as it must be in the CM frame). If we define

$$K \equiv |\vec{k}_1| \quad (4.5.39)$$

for convenience, then

$$d^3\vec{k}_1 = K^2 dK d\Omega = K^2 dK d\phi d(\cos\theta), \quad (4.5.40)$$

where $\Omega = (\theta, \phi)$ are the spherical coordinate angles for \vec{k}_1 . So

$$\int \dots d\Phi_2 = \int \dots \frac{\delta(\sqrt{K^2 + m_1^2} + \sqrt{K^2 + m_2^2} - E_{\text{CM}})}{\sqrt{K^2 + m_1^2} \sqrt{K^2 + m_2^2}} K^2 dK d\phi d(\cos\theta), \quad (4.5.41)$$

where \dots represents any quantity. To do the remaining dK integral, it is convenient to change variables to the argument of the delta function. So, defining

$$W = \sqrt{K^2 + m_1^2} + \sqrt{K^2 + m_2^2} - E_{\text{CM}}, \quad (4.5.42)$$

we find

$$dW = \frac{\sqrt{K^2 + m_1^2} + \sqrt{K^2 + m_2^2}}{\sqrt{K^2 + m_1^2} \sqrt{K^2 + m_2^2}} K dK. \quad (4.5.43)$$

Noticing that the delta function predestines $\sqrt{K^2 + m_1^2} + \sqrt{K^2 + m_2^2}$ to be replaced by E_{CM} , we can write:

$$\frac{K^2 dK}{\sqrt{K^2 + m_1^2} \sqrt{K^2 + m_2^2}} = \frac{K dW}{E_{\text{CM}}}. \quad (4.5.44)$$

Using this in eq. (4.5.41), and integrating dW using the delta function $\delta(W)$, we obtain:

$$d\Phi_2 = \frac{K}{16\pi^2 E_{\text{CM}}} d\phi d(\cos\theta) \quad (4.5.45)$$

for the Lorentz-invariant phase space of a two-particle final state.

Meanwhile, in the CM frame, eq. (4.5.35) simplifies according to:

$$4E_a E_b |\vec{v}_a - \vec{v}_b| = 4(E_a |\vec{p}_b| + E_b |\vec{p}_a|) = 4|\vec{p}_a|(E_a + E_b) = 4|\vec{p}_a|E_{\text{CM}}. \quad (4.5.46)$$

Therefore, using the results of eqs. (4.5.45) and (4.5.46) in eq. (4.5.32), we have:

$$d\sigma = |\mathcal{M}_{i \rightarrow f}|^2 \frac{|\vec{k}_1|}{64\pi^2 E_{\text{CM}}^2 |\vec{p}_a|} d\Omega \quad (4.5.47)$$

for the differential cross-section for two-particle scattering to two particles.

The matrix element is almost always symmetric under rotations about the collision axis determined by the incoming particle momenta. If so, then everything is independent of ϕ , and one can do $\int d\phi = 2\pi$, leaving:

$$d\sigma = |\mathcal{M}_{i \rightarrow f}|^2 \frac{|\vec{k}_1|}{32\pi E_{\text{CM}}^2 |\vec{p}_a|} d(\cos \theta). \quad (4.5.48)$$

If the particle masses satisfy $m_a = m_1$ and $m_b = m_2$ (or they are very small), then one has the further simplification $|\vec{k}_1| = |\vec{p}_a|$, so that

$$d\sigma = |\mathcal{M}_{i \rightarrow f}|^2 \frac{1}{32\pi E_{\text{CM}}^2} d(\cos \theta). \quad (4.5.49)$$

The formulas eqs. (4.5.47)-(4.5.49) will be used often in the following.

We can finally interpret the meaning of the result eq. (4.4.31) that we obtained for scalar ϕ^4 theory. Since we found $\mathcal{M}_{\phi\phi \rightarrow \phi\phi} = -i\lambda$, the differential cross-section in the CM frame is:

$$d\sigma_{\phi\phi \rightarrow \phi\phi} = \frac{\lambda^2}{32\pi E_{\text{CM}}^2} d(\cos \theta). \quad (4.5.50)$$

Now we can integrate over θ using $\int_{-1}^1 d(\cos \theta) = 2$. However, there is a double-counting problem that we must take into account. The angles (θ, ϕ) that we have integrated over represent the direction of the 3-momentum of one of the final state particles. The other particle must then have 3-momentum in the opposite direction $(\pi - \theta, -\phi)$. The two possible final states with \vec{k}_1 along those two opposite directions are therefore actually the *same* state, because the two particles are identical. So, we have actually counted each state twice when integrating over all $d\Omega$. To take this into account, we have to divide by 2, arriving at the result for the total cross-section:

$$\sigma_{\phi\phi \rightarrow \phi\phi} = \frac{\lambda^2}{32\pi E_{\text{CM}}^2}. \quad (4.5.51)$$

In the system of units with $c = \hbar = 1$, energy has the same units as 1/distance. Since λ is dimensionless, it checks that σ indeed has units of area. This is a very useful thing to check whenever one has found a cross-section!

4.6 Scalar field with ϕ^3 coupling

For our next example, let us consider a theory with a single scalar field as before, but with an interaction Lagrangian that is cubic in the field:

$$\mathcal{L}_{\text{int}} = -\frac{\mu}{6}\phi^3, \quad (4.6.1)$$

instead of eq. (4.4.4). Here μ is a coupling that has the same dimensions as mass. As before, let us compute the matrix element for 2 particle to particle scattering, $\phi\phi \rightarrow \phi\phi$.

The definition and quantization of the free Hamiltonian proceeds exactly as before, with equal time commutators given by eqs. (4.2.20) and (4.2.21), and the free Hamiltonian by eq. (4.2.42). The interaction part of the Hamiltonian can be obtained in exactly the same way as the discussion leading up to eq. (4.4.8), yielding:

$$\begin{aligned} H_{\text{int}} = \frac{\mu}{6}(2\pi)^3 \int d\vec{q}_1 \int d\vec{q}_2 \int d\vec{q}_3 \left[a_{\vec{q}_1}^\dagger a_{\vec{q}_2}^\dagger a_{\vec{q}_3}^\dagger \delta^{(3)}(\vec{q}_1 + \vec{q}_2 + \vec{q}_3) \right. \\ + 3a_{\vec{q}_1}^\dagger a_{\vec{q}_2}^\dagger a_{\vec{q}_3} \delta^{(3)}(\vec{q}_1 + \vec{q}_2 - \vec{q}_3) \\ + 3a_{\vec{q}_1}^\dagger a_{\vec{q}_2} a_{\vec{q}_3} \delta^{(3)}(\vec{q}_1 - \vec{q}_2 - \vec{q}_3) \\ \left. + a_{\vec{q}_1} a_{\vec{q}_2} a_{\vec{q}_3} \delta^{(3)}(\vec{q}_1 + \vec{q}_2 + \vec{q}_3) \right]. \end{aligned} \quad (4.6.2)$$

As before, we want to calculate:

$${}_{\text{OUT}}\langle \vec{k}_1, \vec{k}_2 | \vec{p}_a \vec{p}_b \rangle_{\text{OUT}} = {}_{\text{OUT}}\langle \vec{k}_1, \vec{k}_2 | e^{-iTH} | \vec{p}_a, \vec{p}_b \rangle_{\text{IN}} = \langle 0 | a_{\vec{k}_1} a_{\vec{k}_2} e^{-iTH} a_{\vec{p}_a}^\dagger a_{\vec{p}_b}^\dagger | 0 \rangle, \quad (4.6.3)$$

where $H = H_0 + H_{\text{int}}$ is the total Hamiltonian. However, this time if we expand e^{-iTH} only to first order in H_{int} , the contribution is clearly zero, because the net number of particles created or destroyed by H_{int} is always odd. Therefore we must work to second order in H_{int} , or equivalently in the coupling μ .

The operator e^{-iTH} can be written as [compare to eq. (4.4.15) and the surrounding discussion]:

$$e^{-iTH} = \left[1 - i(H_0 + H_{\text{int}}) \frac{T}{N} \right]^N, \quad (4.6.4)$$

in the large N limit. Keeping only terms that are of order H_{int}^2 , this becomes:

$$e^{-iTH} = \sum_{n=0}^{N-2} \sum_{m=0}^{N-n-2} \left[1 - iH_0 \frac{T}{N} \right]^{N-n-m-2} \left(-iH_{\text{int}} \frac{T}{N} \right) \left[1 - iH_0 \frac{T}{N} \right]^m \left(-iH_{\text{int}} \frac{T}{N} \right) \left[1 - iH_0 \frac{T}{N} \right]^n.$$

Now, in the large N limit, we can convert the discrete sums into integrals over the variables $t = Tn/N$ and $t' = Tm/N + t$ with $\Delta t = \Delta t' = T/N$. Since most of the contribution comes from large n, m when $N \rightarrow \infty$, the result becomes:

$$e^{-iTH} = \int_0^T dt \int_t^T dt' e^{-iH_0(T-t')} (-iH_{\text{int}}) e^{-iH_0(t'-t)} (-iH_{\text{int}}) e^{-iH_0 t}. \quad (4.6.5)$$

When we sandwich this between the states $\langle \vec{k}_1, \vec{k}_2 |$ and $|\vec{p}_a, \vec{p}_b\rangle$, we can substitute

$$e^{-iH_0(T-t')} \rightarrow e^{-iE_f(T-t')}; \quad (4.6.6)$$

$$e^{-iH_0 t} \rightarrow e^{-iE_i t}, \quad (4.6.7)$$

where $E_i = E_{\vec{p}_a} + E_{\vec{p}_b}$ is the initial state energy eigenvalue and $E_f = E_{\vec{k}_1} + E_{\vec{k}_2}$ is the final state energy eigenvalue. Now, $(-iH_{\text{int}})|\vec{p}_a, \vec{p}_b\rangle$ will consist of a linear combination of eigenstates $|X\rangle$ of H_0 with different energies E_X . So we can also substitute

$$e^{-iH_0(t'-t)} \rightarrow e^{-iE_X(t'-t)} \quad (4.6.8)$$

provided that in place of E_X we will later put in the appropriate energy eigenvalue of the state created by each particular term in $-iH_{\text{int}}$ acting on the initial state. So, we have:

$$e^{-iTH} = (-iH_{\text{int}}) I (-iH_{\text{int}}) \quad (4.6.9)$$

where

$$I = \int_0^T dt \int_t^T dt' e^{-iE_f(T-t')} e^{-iE_X(t'-t)} e^{-iE_i t}. \quad (4.6.10)$$

To evaluate the integral I , we can first define shifted integration variables $\bar{t} = t - T/2$ and $\bar{t}' = t' - T/2$, so that with due care to the limits of integration,

$$I = e^{-iT(E_i+E_f)/2} \int_{-T/2}^{T/2} d\bar{t} e^{i\bar{t}(E_X-E_i)} \int_{\bar{t}}^{T/2} d\bar{t}' e^{i\bar{t}'(E_f-E_X)}. \quad (4.6.11)$$

Now $e^{-iT(E_i+E_f)/2}$ is just a constant phase that will go away when we take the complex square of the matrix element, so we drop it. Then, relabeling $\bar{t} \rightarrow t$ and $\bar{t}' \rightarrow t'$, and taking the limit of a very long time $T \rightarrow \infty$:

$$I = \int_{-\infty}^{\infty} dt e^{it(E_X-E_i)} \int_t^{\infty} dt' e^{it'(E_f-E_X+i\epsilon)}. \quad (4.6.12)$$

The t' integral does not have the form of a delta function because its lower limit of integration is t . Therefore we have inserted an infinitesimal factor $e^{-\epsilon t'}$ so that the integral converges for $t' \rightarrow \infty$; we will take $\epsilon \rightarrow 0$ at the end. Performing the t' integration, we get:

$$I = \left(\frac{i}{E_f - E_X + i\epsilon} \right) \int_{-\infty}^{\infty} dt e^{it(E_f-E_i)} \quad (4.6.13)$$

$$= 2\pi \delta(E_f - E_i) \left(\frac{i}{E_f - E_X + i\epsilon} \right). \quad (4.6.14)$$

As usual, energy conservation between the initial and final states is thus automatic.

Putting together the results above, we have so far:

$$\begin{aligned} \text{OUT} \langle \vec{k}_1, \vec{k}_2 | \vec{p}_a, \vec{p}_b \rangle_{\text{OUT}} &= \\ 2\pi\delta(E_f - E_i) \langle 0 | a_{\vec{k}_1} a_{\vec{k}_2} (-iH_{\text{int}}) \left(\frac{i}{E_f - E_X + i\epsilon} \right) (-iH_{\text{int}}) a_{\vec{p}_a}^\dagger a_{\vec{p}_b}^\dagger | 0 \rangle. \end{aligned} \quad (4.6.15)$$

Let us now evaluate the matrix element in eq. (4.6.15). To do this, we can divide the calculation up into pieces, depending on how many a and a^\dagger operators are contained in each factor of H_{int} . First, let us consider the contribution when the right H_{int} contains $a^\dagger a a$ terms acting on the initial state, and the left H_{int} contains $a^\dagger a^\dagger a$ terms. Taking these pieces from eq. (4.6.2), the contribution from eq. (4.6.15) is:

$$\begin{aligned} \text{OUT} \langle \vec{k}_1, \vec{k}_2 | \vec{p}_a, \vec{p}_b \rangle_{\text{OUT}} \Big|_{(a^\dagger a^\dagger a)(a^\dagger a a) \text{ part}} &= \\ \left[-i\frac{\mu}{2}(2\pi)^3 \right]^2 2\pi\delta(E_f - E_i) \int d\vec{r}_1 \int d\vec{r}_2 \int d\vec{r}_3 \int d\vec{q}_1 \int d\vec{q}_2 \int d\vec{q}_3 & \\ \delta^{(3)}(\vec{r}_1 + \vec{r}_2 - \vec{r}_3) \delta^{(3)}(\vec{q}_1 - \vec{q}_2 - \vec{q}_3) & \\ \langle 0 | a_{\vec{k}_1} a_{\vec{k}_2} a_{\vec{r}_1}^\dagger a_{\vec{r}_2}^\dagger a_{\vec{r}_3} \left(\frac{i}{E_f - E_X} \right) a_{\vec{q}_1}^\dagger a_{\vec{q}_2}^\dagger a_{\vec{q}_3} a_{\vec{p}_a}^\dagger a_{\vec{p}_b}^\dagger | 0 \rangle. \end{aligned} \quad (4.6.16)$$

The factor involving E_X is left inserted within the matrix element to remind us that E_X should be replaced by the eigenvalue of the free Hamiltonian H_0 acting on the state to its right.

The last line in eq. (4.6.16) can be calculated using the following general strategy. We commute a 's to the right and a^\dagger 's to the left, using eqs. (4.2.20) and (4.2.21). In doing so, we will get a non-zero contribution with a delta function whenever the 3-momentum of an a equals that of an a^\dagger with which it is commuted, removing that a, a^\dagger pair. In the end, every a must “contract” with some a^\dagger in this way (and vice versa), because an a acting on $|0\rangle$ or an a^\dagger acting on $\langle 0|$ vanishes.

This allows us to identify what E_X is. The $a_{\vec{q}_2}$ and $a_{\vec{q}_3}$ operators must be contracted with $a_{\vec{p}_a}^\dagger$ and $a_{\vec{p}_b}^\dagger$ if a non-zero result is to be obtained. There are two ways to do this: either pair up $[a_{\vec{q}_2}, a_{\vec{p}_a}^\dagger]$ and $[a_{\vec{q}_3}, a_{\vec{p}_b}^\dagger]$, or pair up $[a_{\vec{q}_2}, a_{\vec{p}_b}^\dagger]$ and $[a_{\vec{q}_3}, a_{\vec{p}_a}^\dagger]$. In both cases, the result can be non-zero only if $\vec{q}_2 + \vec{q}_3 = \vec{p}_a + \vec{p}_b$. The delta-function $\delta^{(3)}(\vec{q}_1 - \vec{q}_2 - \vec{q}_3)$ then insures that there will be a non-zero contribution only when

$$\vec{q}_1 = \vec{p}_a + \vec{p}_b \equiv \vec{Q}. \quad (4.6.17)$$

So the energy eigenvalue of the state $a_{\vec{q}_1}^\dagger a_{\vec{q}_2} a_{\vec{q}_3} a_{\vec{p}_a}^\dagger a_{\vec{p}_b}^\dagger | 0 \rangle$ must be replaced by

$$E_X = E_{\vec{Q}} = \sqrt{|\vec{p}_a + \vec{p}_b|^2 + m^2} \quad (4.6.18)$$

whenever there is a non-zero contribution.

Evaluating the quantity

$$\langle 0 | a_{\vec{k}_1} a_{\vec{k}_2} a_{\vec{r}_1}^\dagger a_{\vec{r}_2}^\dagger a_{\vec{r}_3} a_{\vec{q}_1}^\dagger a_{\vec{q}_2} a_{\vec{q}_3} a_{\vec{p}_a}^\dagger a_{\vec{p}_b}^\dagger | 0 \rangle \quad (4.6.19)$$

now yields four distinct non-zero terms, corresponding to the following ways of contracting a 's and a^\dagger 's:

$$[a_{\vec{k}_1}, a_{\vec{r}_1}^\dagger] [a_{\vec{k}_2}, a_{\vec{r}_2}^\dagger] [a_{\vec{q}_2}, a_{\vec{p}_a}^\dagger] [a_{\vec{q}_3}, a_{\vec{p}_b}^\dagger] [a_{\vec{r}_3}, a_{\vec{q}_1}^\dagger], \text{ or} \quad (4.6.20)$$

$$[a_{\vec{k}_1}, a_{\vec{r}_2}^\dagger] [a_{\vec{k}_2}, a_{\vec{r}_1}^\dagger] [a_{\vec{q}_2}, a_{\vec{p}_a}^\dagger] [a_{\vec{q}_3}, a_{\vec{p}_b}^\dagger] [a_{\vec{r}_3}, a_{\vec{q}_1}^\dagger], \text{ or} \quad (4.6.21)$$

$$[a_{\vec{k}_1}, a_{\vec{r}_1}^\dagger] [a_{\vec{k}_2}, a_{\vec{r}_2}^\dagger] [a_{\vec{q}_2}, a_{\vec{p}_b}^\dagger] [a_{\vec{q}_3}, a_{\vec{p}_a}^\dagger] [a_{\vec{r}_3}, a_{\vec{q}_1}^\dagger], \text{ or} \quad (4.6.22)$$

$$[a_{\vec{k}_1}, a_{\vec{r}_2}^\dagger] [a_{\vec{k}_2}, a_{\vec{r}_1}^\dagger] [a_{\vec{q}_2}, a_{\vec{p}_b}^\dagger] [a_{\vec{q}_3}, a_{\vec{p}_a}^\dagger] [a_{\vec{r}_3}, a_{\vec{q}_1}^\dagger]. \quad (4.6.23)$$

For the first of these contributions to eq. (4.6.19), we get:

$$\begin{aligned} & (2\pi)^3 2E_{\vec{r}_1} \delta^{(3)}(\vec{r}_1 - \vec{k}_1) \quad (2\pi)^3 2E_{\vec{r}_2} \delta^{(3)}(\vec{r}_2 - \vec{k}_2) \quad (2\pi)^3 2E_{\vec{q}_2} \delta^{(3)}(\vec{q}_2 - \vec{p}_a) \\ & (2\pi)^3 2E_{\vec{q}_3} \delta^{(3)}(\vec{q}_3 - \vec{p}_b) \quad (2\pi)^3 2E_{\vec{r}_3} \delta^{(3)}(\vec{r}_3 - \vec{q}_1). \end{aligned} \quad (4.6.24)$$

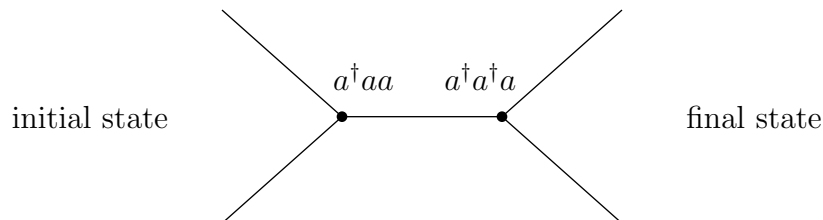
Now, the various factors of $(2\pi)^2 2E$ just cancel the factors in the denominators of the definition of $d\tilde{q}_i$ and $d\tilde{r}_i$. One can do the \vec{q}_1 , \vec{q}_2 , \vec{q}_3 , \vec{r}_1 , \vec{r}_2 , and \vec{r}_3 integrations trivially, using the 3-momentum delta functions, resulting in the following contribution to eq. (4.6.16):

$$\left(-i\frac{\mu}{2}\right)^2 \left(\frac{i}{E_f - E_{\vec{Q}}}\right) \frac{1}{2E_{\vec{Q}}} (2\pi)^4 \delta(E_f - E_i) \delta^{(3)}(\vec{k}_1 + \vec{k}_2 - \vec{p}_a - \vec{p}_b). \quad (4.6.25)$$

The two delta functions can be combined into $\delta^{(4)}(k_1 + k_2 - p_a - p_b)$. Now, the other three sets of contractions listed in eqs. (4.6.21)-(4.6.23) are exactly the same, after a relabeling of momenta. This gives a factor of 4, so (replacing $E_f \rightarrow E_i$ in the denominator, as allowed by the delta function) we have:

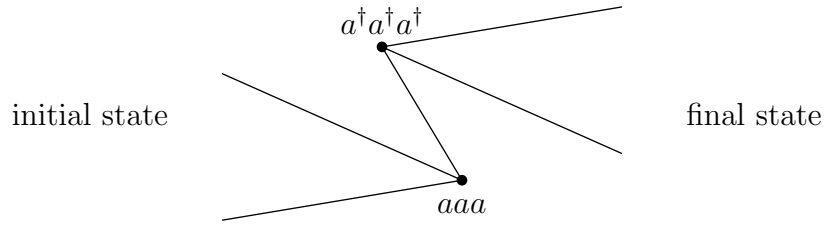
$$\begin{aligned} & \text{OUT} \langle \vec{k}_1, \vec{k}_2 | \vec{p}_a, \vec{p}_b \rangle_{\text{OUT}} \Big|_{(a^\dagger a^\dagger a)(a^\dagger a a) \text{ part}} = \\ & (-i\mu)^2 \frac{i}{(E_i - E_{\vec{Q}})(2E_{\vec{Q}})} (2\pi)^4 \delta^{(4)}(k_1 + k_2 - p_a - p_b). \end{aligned} \quad (4.6.26)$$

One can draw a simple picture illustrating what has happened in the preceding formulas:



The initial state contains two particles, denoted by the lines on the left. Acting with the first factor of H_{int} (on the right in the formula, and represented by the vertex on the left in the figure) destroys the two particles and creates a virtual particle in their place. The second factor of H_{int} destroys the virtual particle and creates the two final state particles, represented by the lines on the right. The three-momentum carried by the intermediate virtual particle is $\vec{Q} = \vec{p}_a + \vec{p}_b = \vec{k}_1 + \vec{k}_2$, so momentum is conserved at the two vertices.

However, there are other contributions that must be included. Another one occurs if the H_{int} on the right in eq. (4.6.15) contains $a^\dagger a^\dagger a^\dagger$ operators, and the other H_{int} contains aaa operators. The corresponding picture is this:



Here the H_{int} carrying $a^\dagger a^\dagger a^\dagger$ (the rightmost one in the formula) is represented by the upper left vertex in the figure, and the one carrying aaa is represented by the lower right vertex. The explicit formula corresponding to this picture is:

$$\begin{aligned}
& \text{OUT} \langle \vec{k}_1, \vec{k}_2 | \vec{p}_a, \vec{p}_b \rangle_{\text{OUT}} \Big|_{(aaa)(a^\dagger a^\dagger a^\dagger) \text{ part}} = \\
& \left[-i \frac{\mu}{6} (2\pi)^3 \right]^2 2\pi \delta(E_f - E_i) \int d\tilde{r}_1 \int d\tilde{r}_2 \int d\tilde{r}_3 \int d\tilde{q}_1 \int d\tilde{q}_2 \int d\tilde{q}_3 \\
& \delta^{(3)}(\vec{r}_1 + \vec{r}_2 + \vec{r}_3) \delta^{(3)}(\vec{q}_1 + \vec{q}_2 + \vec{q}_3) \\
& \langle 0 | a_{\vec{k}_1} a_{\vec{k}_2} a_{\vec{r}_1} a_{\vec{r}_2} a_{\vec{r}_3} \left(\frac{i}{E_f - E_X} \right) a_{\vec{q}_1}^\dagger a_{\vec{q}_2}^\dagger a_{\vec{q}_3}^\dagger a_{\vec{p}_a}^\dagger a_{\vec{p}_b}^\dagger | 0 \rangle. \tag{4.6.27}
\end{aligned}$$

As before, we can calculate this by commuting a 's to the right and a^\dagger 's to the left. In the end, non-zero contributions arise only when each a is contracted with some a^\dagger . In doing so, we should ignore any terms that arise whenever a final state state $a_{\vec{k}}$ is contracted with an initial state $a_{\vec{p}}^\dagger$. That would correspond to a situation with no scattering, since the initial state particle and the final state particle would be exactly the same.

The result contains 36 distinct contributions, corresponding to the 6 ways of contracting $a_{\vec{k}_1}$ and $a_{\vec{k}_2}$ with any two of $a_{\vec{q}_1}^\dagger$, $a_{\vec{q}_2}^\dagger$, and $a_{\vec{q}_3}^\dagger$, times the 6 ways of contracting $a_{\vec{p}_a}^\dagger$ and $a_{\vec{p}_b}^\dagger$ with any two of $a_{\vec{r}_1}$, $a_{\vec{r}_2}$, $a_{\vec{r}_3}$. However, all 36 of these contributions are identical under relabeling of momentum, so we can just calculate one of them and multiply the answer by 36. This will neatly convert the factor of $(-i\mu/6)^2$ to $(-i\mu)^2$. We also note that E_X must be replaced by the

free Hamiltonian energy eigenvalue of the state $a_{\vec{q}_1}^\dagger a_{\vec{q}_2}^\dagger a_{\vec{q}_3}^\dagger a_{\vec{p}_a}^\dagger a_{\vec{p}_b}^\dagger |0\rangle$, namely:

$$E_X = E_{\vec{q}_1} + E_{\vec{q}_2} + E_{\vec{q}_3} + E_{\vec{p}_a} + E_{\vec{p}_b}. \quad (4.6.28)$$

For example consider the term obtained from the following contractions of a 's and a^\dagger 's:

$$[a_{\vec{k}_1}, a_{\vec{q}_1}^\dagger] [a_{\vec{k}_2}, a_{\vec{q}_2}^\dagger] [a_{\vec{r}_1}, a_{\vec{p}_a}^\dagger] [a_{\vec{r}_2}, a_{\vec{p}_b}^\dagger] [a_{\vec{r}_3}, a_{\vec{q}_3}^\dagger]. \quad (4.6.29)$$

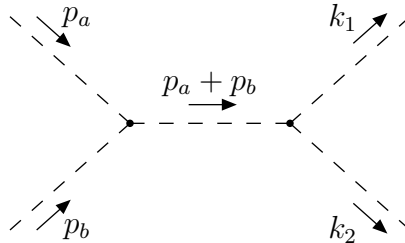
This leads to factors of $(2\pi)^3 2E$ and momentum delta functions just as before. So we can do the 3-momentum $\vec{q}_{1,2}$ and $\vec{r}_{1,2,3}$ integrals using the delta functions, in the process setting $\vec{q}_1 = \vec{k}_1$ and $\vec{q}_2 = \vec{k}_2$ and $\vec{r}_1 = \vec{p}_a$ and $\vec{r}_2 = \vec{p}_b$ and $\vec{r}_3 = \vec{q}_3$. Finally, we can do the \vec{q}_3 integral using one of the delta functions already present in eq. (4.6.27), resulting in $\vec{q}_3 = -\vec{p}_a - \vec{p}_b = -\vec{k}_1 - \vec{k}_2 = -\vec{Q}$, with \vec{Q} the same as was defined in eq. (4.6.17). This allows us to identify in this case:

$$E_X = E_{\vec{k}_1} + E_{\vec{k}_2} + E_{\vec{p}_a} + E_{\vec{p}_b} + E_{\vec{Q}} = 2E_i + E_{\vec{Q}}. \quad (4.6.30)$$

The end result is:

$$\begin{aligned} \text{OUT} \langle \vec{k}_1, \vec{k}_2 | \vec{p}_a, \vec{p}_b \rangle_{\text{OUT}} \Big|_{(aaa)(a^\dagger a^\dagger a^\dagger) \text{ part}} &= \\ (-i\mu)^2 \frac{-i}{(E_i + E_{\vec{Q}})(2E_{\vec{Q}})} (2\pi)^4 \delta^{(4)}(k_1 + k_2 - p_a - p_b). \end{aligned} \quad (4.6.31)$$

It is now profitable to combine the two contributions we have found. One hint that this is a good idea is the fact that the two cartoon figures we have drawn for them are topologically the same; the second one just has a line that moves backwards. So if we just ignore the distinction between internal lines that move backwards and those that move forwards, we can draw a single Feynman diagram to represent both results combined:



The initial state is on the left, and the final state is on the right, and the flow of 4-momentum is indicated by the arrows, with 4-momentum conserved at each vertex.

The result of combining these two contributions is called the s -channel contribution, to distinguish it from still more contributions that we will get to soon. Using a common denominator for $(E_i - E_{\vec{Q}})$ and $(E_i + E_{\vec{Q}})$, we get:

$$\text{OUT} \langle \vec{k}_1, \vec{k}_2 | \vec{p}_a, \vec{p}_b \rangle_{\text{OUT}} \Big|_{s\text{-channel}} = (-i\mu)^2 \frac{i}{E_i^2 - E_{\vec{Q}}^2} (2\pi)^4 \delta^{(4)}(k_1 + k_2 - p_a - p_b). \quad (4.6.32)$$

If we now consider the four-vector

$$p_a^\mu + p_b^\mu = (\sqrt{|\vec{p}_a|^2 + m^2} + \sqrt{|\vec{p}_b|^2 + m^2}, \vec{p}_a + \vec{p}_b) = (E_i, \vec{Q}), \quad (4.6.33)$$

then we recognize that

$$(p_a + p_b)^2 = E_i^2 - |\vec{Q}|^2 = E_i^2 - E_{\vec{Q}}^2 + m^2. \quad (4.6.34)$$

[Note that $p_a^\mu + p_b^\mu$ is *not* equal to $(E_{\vec{Q}}, \vec{Q})$.] So we can rewrite the term

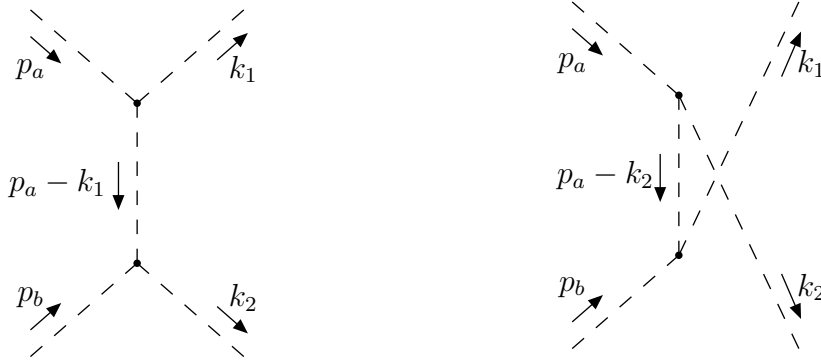
$$\frac{i}{E_i^2 - E_{\vec{Q}}^2} = \frac{i}{(p_a + p_b)^2 - m^2}, \quad (4.6.35)$$

The final result is that the s -channel contribution to the matrix element is:

$${}_{\text{OUT}}\langle \vec{k}_1, \vec{k}_2 | \vec{p}_a, \vec{p}_b \rangle_{\text{OUT}} \Big|_{s\text{-channel}} = (-i\mu)^2 \frac{i}{(p_a + p_b)^2 - m^2} (2\pi)^4 \delta^{(4)}(k_1 + k_2 - p_a - p_b). \quad (4.6.36)$$

Note that one could just as well have put $(k_1 + k_2)^2$ in place of $(p_a + p_b)^2$ in this expression, because of the delta function.

Now one can go through the same whole process with contributions that come from the rightmost H_{int} (acting first on the initial state) consisting of $a^\dagger a^\dagger a$ terms, and the leftmost H_{int} containing $a^\dagger a a$ terms. One can draw Feynman diagrams that represent these terms, which look like:



These are referred to as the t -channel and u -channel contributions respectively. Here we have combined all topologically-identical diagrams. This is a standard procedure that is always followed; the diagrams we have drawn with dashed lines for the scalar field are the Feynman diagrams for the process. [The solid-line diagrams appearing between eqs. (4.6.26) and (4.6.27) above are sometimes known as “old-fashioned Feynman diagrams”, but it is very rare to see them in the modern literature.]

After much juggling of factors of $(2\pi)^3$ and doing 3-momentum integrals using delta functions, but using no new concepts, the contributions of the t -channel and u -channel Feynman diagrams can be found to be simply:

$${}_{\text{OUT}}\langle \vec{k}_1, \vec{k}_2 | \vec{p}_a, \vec{p}_b \rangle_{\text{OUT}} \Big|_{t\text{-channel}} = (-i\mu)^2 \frac{i}{(p_a - k_1)^2 - m^2} (2\pi)^4 \delta^{(4)}(k_1 + k_2 - p_a - p_b), \quad (4.6.37)$$

and

$${}_{\text{OUT}}\langle \vec{k}_1, \vec{k}_2 | \vec{p}_a, \vec{p}_b \rangle_{\text{OUT}} \Big|_{u\text{-channel}} = (-i\mu)^2 \frac{i}{(p_a - k_2)^2 - m^2} (2\pi)^4 \delta^{(4)}(k_1 + k_2 - p_a - p_b). \quad (4.6.38)$$

The reduced matrix element can now be obtained by just stripping off the factors of $(2\pi)^4 \delta^{(4)}(k_1 + k_2 - p_a - p_b)$, as demanded by the definition eq. (4.5.11). So the total reduced matrix element, suitable for plugging into the formula for the cross-section, is:

$$\mathcal{M}_{\phi\phi \rightarrow \phi\phi} = \mathcal{M}_s + \mathcal{M}_t + \mathcal{M}_u \quad (4.6.39)$$

where:

$$\mathcal{M}_s = (-i\mu)^2 \frac{i}{(p_a + p_b)^2 - m^2}, \quad (4.6.40)$$

$$\mathcal{M}_t = (-i\mu)^2 \frac{i}{(p_a - k_1)^2 - m^2}, \quad (4.6.41)$$

$$\mathcal{M}_u = (-i\mu)^2 \frac{i}{(p_a - k_2)^2 - m^2}. \quad (4.6.42)$$

The reason for the terminology s , t , and u is because of the standard kinematic variables for 2→2 scattering known as Mandelstam variables:

$$s = (p_a + p_b)^2 = (k_1 + k_2)^2, \quad (4.6.43)$$

$$t = (p_a - k_1)^2 = (k_2 - p_b)^2, \quad (4.6.44)$$

$$u = (p_a - k_2)^2 = (k_1 - p_b)^2. \quad (4.6.45)$$

The s -, t -, and u -channel diagrams are simple functions of the corresponding Mandelstam variables:

$$\mathcal{M}_s = (-i\mu)^2 \frac{i}{s - m^2}, \quad (4.6.46)$$

$$\mathcal{M}_t = (-i\mu)^2 \frac{i}{t - m^2}, \quad (4.6.47)$$

$$\mathcal{M}_u = (-i\mu)^2 \frac{i}{u - m^2}. \quad (4.6.48)$$

Typically, if one instead scatters fermions or vector particles or some combination of them, the s - t - and u - channel diagrams will have a similar form, with m always the mass of the particle on the internal line, but with more junk in the numerators coming from the appropriate reduced matrix elements.

4.7 Feynman rules

It is now possible to abstract what we have found, to obtain the general Feynman rules for calculating reduced matrix elements in a scalar field theory. Evidently, the reduced matrix

calculation. There are additional rules that apply to diagrams with closed loops (loop diagrams) which have not arisen explicitly in the preceding discussion, but could be inferred from more complicated calculations. For them, the additional rules are:

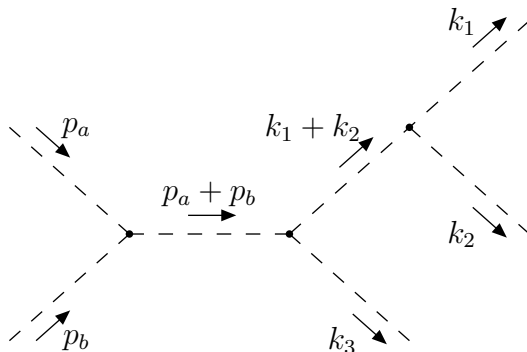
- For each closed loop in a Feynman diagram, there is an undetermined 4-momentum ℓ^μ . These loop momenta should be integrated over according to:

$$\int \frac{d^4\ell}{(2\pi)^4}. \quad (4.7.2)$$

Loop diagrams quite often diverge because of the integration over all ℓ^μ , because of the contribution from very large $|\ell^2|$. This can be fixed by introducing a cutoff $|\ell^2|_{\text{max}}$ in the integral, or by other more rigorous methods, which can make the integrals finite. The techniques of getting physically meaningful answers out of this are known as regularization (making the integrals finite) and renormalization (redefining coupling constants and masses so that the physical observables do not depend explicitly on the unknown cutoff).

- If a Feynman diagram with one or more closed loops can be transformed into an exact copy of itself by interchanging any number of internal lines through a smooth deformation, without moving the external lines, then there is an additional factor of $1/N$, where N is the number of distinct permutations of that type. (This is known as the “symmetry factor” for the loop diagram.)

Some examples might be useful. In the ϕ^3 theory, there are quite a few Feynman diagrams that will describe the scattering of 2 particles to 3 particles. One of them is shown below:

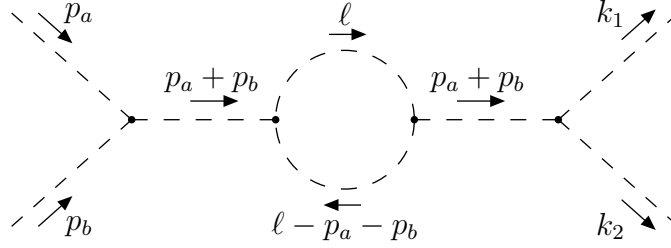


For this diagram, according to the rules, the contribution to the reduced matrix element is just

$$\mathcal{M} = (-i\mu)^3 \left[\frac{i}{(p_a + p_b)^2 - m^2} \right] \left[\frac{i}{(k_1 + k_2)^2 - m^2} \right]. \quad (4.7.3)$$

Imagine having to calculate this starting from scratch with creation and annihilation operators, and tremble with fear! Feynman rules are good.

An example of a Feynman diagram with a closed loop in the ϕ^3 theory is:



There is a symmetry factor of $1/2$ for this diagram, because one can smoothly interchange the two lines carrying 4-momenta ℓ^μ and $\ell^\mu - p_a^\mu - p_b^\mu$ to get back to the original diagram, without moving the external lines. So the reduced matrix element for this diagram is:

$$\mathcal{M} = \frac{1}{2}(-i\mu)^4 \left[\frac{i}{(p_a + p_b)^2 - m^2} \right]^2 \int \frac{d^4\ell}{(2\pi)^4} \left[\frac{i}{(\ell - p_a - p_b)^2 - m^2 + i\epsilon} \right] \left[\frac{i}{\ell^2 - m^2 + i\epsilon} \right]. \quad (4.7.4)$$

Again, deriving this result starting from the creation and annihilation operators is possible, but extraordinarily unpleasant! In the future, we will simply state the Feynman rules for any theory from staring at the Lagrangian density. The general procedure for doing this is rather simple (although the proof is not), and is outlined below.

A Feynman diagram is a precise representation of a contribution to the reduced matrix element \mathcal{M} for a given physical process. The diagrams are built out of three types of building blocks:

$$\text{vertices} \longleftrightarrow \text{interactions} \quad (4.7.5)$$

$$\text{internal lines} \longleftrightarrow \text{free virtual particle propagation} \quad (4.7.6)$$

$$\text{external lines} \longleftrightarrow \text{initial, final states.} \quad (4.7.7)$$

The Feynman rules specify a mathematical expression for each of these objects. They follow from the Lagrangian density, which defines a particular theory.[†]

To generalize what we have found for scalar fields, let us consider a set of generic fields Φ_i , which can include both commuting bosons and anticommuting fermions. They might include real or complex scalars, Dirac or Weyl fermions, and vector fields of various types. The index i runs over a list of all the fields, and over their spinor or vector indices. Now, it is always possible to obtain the Feynman rules by writing an interaction Hamiltonian and computing matrix elements. Alternatively, one can use powerful path integral techniques that are beyond the scope of this course to derive the Feynman rules. However, in the end the rules can be summarized very simply in a way that could be guessed from the examples of real scalar field

[†]It is tempting to suggest that the Feynman rules themselves should be taken as the definition of the theory. However, this would only be sufficient to describe phenomena that occur in a perturbative weak-coupling expansion.

theory that we have already worked out. In these notes, we will simply state the relevant results; more rigorous derivations can be found in field theory textbooks.

For interactions, we have now found in two cases that the Feynman rule for n scalar lines to meet at a vertex is equal to $-i$ times the coupling of n scalar fields in the Lagrangian with a factor of $1/n!$. More generally, consider an interaction Lagrangian term:

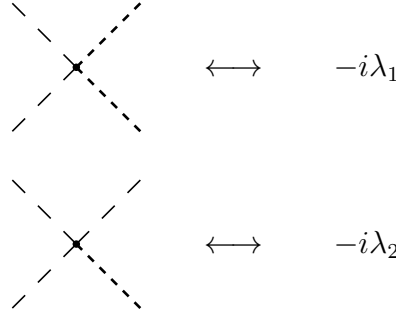
$$\mathcal{L}_{\text{int}} = -\frac{X_{i_1 i_2 \dots i_N}}{P} \Phi_{i_1} \Phi_{i_2} \dots \Phi_{i_N}, \quad (4.7.8)$$

where P is the product of $n!$ for each set of n identical fields in the list $\Phi_{i_1}, \Phi_{i_2}, \dots, \Phi_{i_N}$, and $X_{i_1 i_2 \dots i_N}$ is the coupling constant that determines the strength of the interaction. The corresponding Feynman rule attaches N lines together at a vertex. Then the mathematical expression assigned to this vertex is $-iX_{i_1 i_2 \dots i_N}$. The lines for distinguishable fields among i_1, i_2, \dots, i_N should be labeled as such, or otherwise distinguished by drawing them differently from each other.

For example, consider a theory with two real scalar fields ϕ and ρ . If the interaction Lagrangian includes terms, say,

$$\mathcal{L}_{\text{int}} = -\frac{\lambda_1}{4} \phi^2 \rho^2 - \frac{\lambda_2}{6} \phi^3 \rho, \quad (4.7.9)$$

then there are Feynman rules:

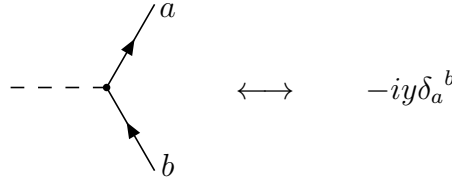


Here the longer-dashed lines correspond to the field ϕ , and the shorter-dashed lines to the field ρ .

As another example, consider a theory in which a real scalar field ϕ couples to a Dirac fermion Ψ according to:

$$\mathcal{L}_{\text{int}} = -y\phi\bar{\Psi}\Psi. \quad (4.7.10)$$

In this case, we must distinguish between lines for all three fields, because $\bar{\Psi} = \Psi^\dagger \gamma^0$ is independent of Ψ . For Dirac fermions, one draws solid lines with an arrow coming in to a vertex representing Ψ in H_{int} , and an arrow coming out representing $\bar{\Psi}$. So the Feynman rule for this interaction is:



Note that this Feynman rule is proportional to a 4×4 identity matrix in Dirac spinor space. This is because the interaction Lagrangian can be written $-y\delta_a^b \phi \bar{\Psi}^a \Psi_b$, where a is the Dirac spinor index for $\bar{\Psi}$ and b for Ψ . Often, one just suppresses the spinor indices, and writes simply $-iy$ for the Feynman rule, with the identity matrix implicit.

The interaction Lagrangian eq. (4.7.10) is called a Yukawa coupling. This theory has a real-world physical application: it is precisely the type of interaction that applies between the Standard Model Higgs boson $\phi = h$ and each Dirac fermion Ψ , with the coupling y proportional to the mass of that fermion. We will return to this interaction when we discuss the decays of the Higgs boson into fermion-antifermion pairs.

Let us turn next to the topic of internal lines in Feynman diagrams. These are determined by the free (quadratic) part of the Lagrangian density. Recall that for a scalar field, we can write the free Lagrangian after integrating by parts as:

$$\mathcal{L}_0 = \frac{1}{2} \phi (-\partial_\mu \partial^\mu - m^2) \phi. \quad (4.7.11)$$

This corresponded to a Feynman propagator rule for internal scalar lines $i/(p^2 - m^2 + i\epsilon)$. So, up to the $i\epsilon$ factor, the propagator is just proportional to i divided by the inverse of the coefficient of the quadratic piece of the Lagrangian density, with the replacement

$$\partial_\mu \longrightarrow -ip_\mu. \quad (4.7.12)$$

The free Lagrangian density for generic fields Φ_i can always be put into either the form

$$\mathcal{L}_0 = \frac{1}{2} \sum_{i,j} \Phi_i P_{ij} \Phi_j, \quad (4.7.13)$$

for real fields, or the form

$$\mathcal{L}_0 = \sum_{i,j} (\Phi^\dagger)_i P_{ij} \Phi_j, \quad (4.7.14)$$

for complex fields (including, for example, Dirac spinors). To accomplish this, one may need to integrate the action by parts, throwing away a total derivative in \mathcal{L}_0 which will not contribute to $S = \int d^4x \mathcal{L}$. Here P_{ij} is a matrix that involves spacetime derivatives and masses. Then it turns out that the Feynman propagator can be found by making the replacement eq. (4.7.12) and taking i times the inverse of the matrix P_{ij} :

$$i(P^{-1})_{ij}. \quad (4.7.15)$$

This corresponds to an internal line in the Feynman diagram labeled by i at one end and j at the other.

As an example, consider the free Lagrangian for a Dirac spinor Ψ , as given by eq. (4.1.26). According to the prescription of eqs. (4.7.14) and (4.7.15), the Feynman propagator connecting vertices with spinor indices a and b should be:

$$i[(\not{p} - m)^{-1}]_a^b. \quad (4.7.16)$$

In order to make sense of the inverse matrix, we can write it as a fraction, then multiply numerator and denominator by $(\not{p} + m)$, and use the fact that $\not{p}\not{p} = p^2$ from eq. (3.2.54):

$$\frac{i}{\not{p} - m} = \frac{i(\not{p} + m)}{(\not{p} - m)(\not{p} + m)} = \frac{i(\not{p} + m)}{p^2 - m^2 + i\epsilon}. \quad (4.7.17)$$

In the last line we have put in the $i\epsilon$ factor needed for loop diagrams as a prescription for handling the possible singularity at $p^2 = m^2$. So the Feynman rule for a Dirac fermion internal line is:

$$\begin{array}{c} b \quad \xrightarrow{p} \quad a \\ \hline \end{array} \quad \longleftrightarrow \quad \frac{i([\not{p}]_a^b + m\delta_a^b)}{p^2 - m^2 + i\epsilon}$$

Here the arrow direction on the fermion line distinguishes the direction of particle flow, with particles (anti-particles) moving with (against) the arrow. For electrons and positrons, this means that the arrow on the propagator points in the direction of the flow of negative charge. As indicated, the 4-momentum p^μ appearing in the propagator is also assigned to be in the direction of the arrow on the internal fermion line.

Next we turn to the question of Feynman rules for external particle and anti-particle lines. At a fixed time $t = 0$, a generic field Φ is written as an expansion of the form:

$$\Phi(\vec{x}) = \sum_n \int d\vec{p} \left[i(\vec{p}, n) e^{i\vec{p}\cdot\vec{x}} a_{\vec{p},n} + f(\vec{p}, n) e^{-i\vec{p}\cdot\vec{x}} b_{\vec{p},n}^\dagger \right], \quad (4.7.18)$$

where $a_{\vec{p},n}$ and $b_{\vec{p},n}^\dagger$ are annihilation and creation operators (which may or may not be Hermitian conjugates of each other); n is an index running over spins and perhaps other labels for different particle types; and $i(\vec{p}, n)$ and $f(\vec{p}, n)$ are expansion coefficients. In general, we build an interaction Hamiltonian out of the fields Φ . When acting on an initial state $a_{\vec{k},m}^\dagger |0\rangle$ on the right, H_{int} will therefore produce a factor of $i(\vec{k}, m)$ after commuting (or anticommuting, for fermions) the $a_{\vec{p},n}$ operator in Φ to the right, removing the $a_{\vec{k},m}^\dagger$. Likewise, when acting on a final state $\langle 0|b_{\vec{k},m}$ on the left, the interaction Hamiltonian will produce a factor of $f(\vec{k}, m)$. Therefore, initial and final state lines just correspond to the appropriate coefficient of annihilation and creation operators in the Fourier mode expansion for that field.

For example, comparing eq. (4.7.18) to eq. (4.2.30) in the scalar case, we find that $i(\vec{p}, n)$ and $f(\vec{p}, n)$ are both just equal to 1.

For Dirac fermions, we see from eq. (4.3.1) that the coefficient for an initial state particle (electron) carrying 4-momentum p^μ and spin state s is $u(p, s)_a$, where a is a spinor index. Similarly, the coefficient for a final state antiparticle (positron) is $v(p, s)_a$. So the Feynman rules for these types of external particle lines are:

$$\begin{aligned}
 \text{initial state electron:} \quad & \xrightarrow[a]{p \rightarrow} \text{blob} \quad \longleftrightarrow \quad u(p, s)_a \\
 \text{final state positron:} \quad & \text{blob} \xleftarrow[p]{p \rightarrow} \quad \longleftrightarrow \quad v(p, s)_a
 \end{aligned}$$

Here the blobs represent the rest of the Feynman diagram in each case. Similarly, considering the expansion of the field $\bar{\Psi}$ in eq. (4.3.2), we see that the coefficient for an initial state antiparticle (positron) is $\bar{v}(p, s)^a$ and that for a final state particle (electron) is $\bar{u}(p, s)^a$. So the Feynman rules for these external states are:

$$\begin{aligned}
 \text{initial state positron:} \quad & \xleftarrow[a]{p \rightarrow} \text{blob} \quad \longleftrightarrow \quad \bar{v}(p, s)^a \\
 \text{final state electron:} \quad & \text{blob} \xrightarrow[p]{p \rightarrow} \quad \longleftrightarrow \quad \bar{u}(p, s)^a
 \end{aligned}$$

Note that in these rules, the p^μ label of an external state is always the physical 4-momentum of that particle or anti-particle; this means that with the standard convention of initial state on the left and final state on the right, the p^μ associated with each of $u(p, s)$, $v(p, s)$, $\bar{u}(p, s)$ and $\bar{v}(p, s)$ is always taken to be pointing to the right. For $v(p, s)$ and $\bar{v}(p, s)$, this is in the opposite direction to the arrow on the fermion line itself.

5 Quantum Electro-Dynamics (QED)

5.1 QED Lagrangian and Feynman rules

Let us now see how all of these general rules apply in the case of Quantum Electrodynamics. This is the quantum field theory governing photons (quantized electromagnetic waves) and charged fermions and antifermions. The fermions in the theory are represented by Dirac spinor fields Ψ carrying electric charge Qe , where e is the magnitude of the charge of the electron. Thus $Q = -1$ for electrons and positrons, $+2/3$ for up, charm and top quarks and their anti-quarks, and $-1/3$ for down, strange and bottom quarks and their antiquarks. (Recall that a single Dirac field, assigned a single value of Q , is used to describe both particles and their anti-particles.) The free Lagrangian for the theory is:

$$\mathcal{L}_0 = -\frac{1}{4}F^{\mu\nu}F_{\mu\nu} + \bar{\Psi}(i\gamma^\mu\partial_\mu - m)\Psi. \quad (5.1.1)$$

Now, earlier we found that the electromagnetic field A^μ couples to the 4-current density $J^\mu = (\rho, \vec{J})$ by a term in the Lagrangian $-eJ^\mu A_\mu$ [see eq. (4.1.39)]. Since J^μ must be a four-vector built out of the charged fermion fields Ψ and $\bar{\Psi}$, we can guess that

$$J^\mu = Q\bar{\Psi}\gamma^\mu\Psi. \quad (5.1.2)$$

The interaction Lagrangian density for a fermion with charge Qe and electromagnetic fields is therefore

$$\mathcal{L}_{\text{int}} = -eQ\bar{\Psi}\gamma^\mu\Psi A_\mu. \quad (5.1.3)$$

The value of e is determined by experiment. However, it is a running coupling constant, which means that effectively its value has a logarithmic dependence on the characteristic energy of the process. For very low energy experiments, the numerical value is $e \approx 0.30282$, corresponding to the experimental result for the fine structure constant:

$$\alpha \equiv \frac{e^2}{4\pi} \approx 1/137.036. \quad (5.1.4)$$

For experiments done at energies near 100 GeV, the appropriate value is a little larger, more like $e \approx 0.313$.

Let us take a small detour to check that eq. (5.1.2) really has the correct form and normalization to be the electromagnetic current density. Consider the total charge operator:

$$\hat{Q} = \int d^3\vec{x} \rho(\vec{x}) = \int d^3\vec{x} J^0(\vec{x}) = Q \int d^3\vec{x} \bar{\Psi}\gamma^0\Psi = Q \int d^3\vec{x} \Psi^\dagger\Psi. \quad (5.1.5)$$

Plugging in eqs. (4.3.1) and (4.3.2), and doing the \vec{x} integration, and one of the momentum integrations using the resulting delta function, one finds

$$\hat{Q} = Q \sum_{s=1}^2 \sum_{r=1}^2 \int d\vec{p} \frac{1}{2E_{\vec{p}}} [u^\dagger(p, s) b_{\vec{p}, s}^\dagger + v^\dagger(p, s) d_{\vec{p}, s}^\dagger] [u(p, r) b_{\vec{p}, r} + v(p, r) d_{\vec{p}, r}^\dagger]. \quad (5.1.6)$$

This can be simplified using some spinor identities:

$$u^\dagger(p, s) u(p, r) = v^\dagger(p, s) v(p, r) = 2E_{\vec{p}} \delta_{sr}; \quad (5.1.7)$$

$$u^\dagger(p, s) v(p, r) = v^\dagger(p, s) u(p, r) = 0. \quad (5.1.8)$$

Taking into account that the operators d, d^\dagger satisfy the anticommutation relation eqs. (4.3.20), the result is

$$\hat{Q} = Q \sum_{s=1}^2 \int d\vec{p} [b_{\vec{p}, s}^\dagger b_{\vec{p}, s} - d_{\vec{p}, s}^\dagger d_{\vec{p}, s}]. \quad (5.1.9)$$

Here we have dropped an infinite contribution, much like we had to do in getting to eqs. (4.2.42) and eqs. (4.3.21). This represents a uniform and constant (and therefore unobservable) infinite charge density throughout all space. The result is that the total charge eigenvalue of the vacuum vanishes:

$$\hat{Q}|0\rangle = 0. \quad (5.1.10)$$

One can now check that

$$[\hat{Q}, b_{\vec{k}, r}^\dagger] = Q b_{\vec{k}, r}^\dagger, \quad (5.1.11)$$

$$[\hat{Q}, d_{\vec{k}, r}^\dagger] = -Q d_{\vec{k}, r}^\dagger. \quad (5.1.12)$$

Therefore,

$$\hat{Q} b_{\vec{k}, r}^\dagger |0\rangle = Q b_{\vec{k}, r}^\dagger |0\rangle \quad (5.1.13)$$

for single-particle states, and

$$\hat{Q} d_{\vec{k}, r}^\dagger |0\rangle = -Q d_{\vec{k}, r}^\dagger |0\rangle \quad (5.1.14)$$

for single anti-particle states. More generally, the eigenvalue of \hat{Q} acting on a state with N particles and \bar{N} antiparticles is $(N - \bar{N})Q$. From eq. (5.1.5), this verifies that the charge density ρ is indeed the time-like component of the four-vector $Q\bar{\Psi}\gamma^\mu\Psi$, which must therefore be equal to J^μ .

The full QED Lagrangian is invariant under gauge transformations:

$$A_\mu(x) \rightarrow A_\mu(x) - \frac{1}{e} \partial_\mu \theta(x), \quad (5.1.15)$$

$$\Psi(x) \rightarrow e^{iQ\theta} \Psi(x), \quad (5.1.16)$$

$$\bar{\Psi}(x) \rightarrow e^{-iQ\theta} \bar{\Psi}(x), \quad (5.1.17)$$

where $\theta(x)$ is an arbitrary function of spacetime [equal to $-e\lambda(x)$ in eq. (2.4.16)]. A nice way to see this invariance is to define the covariant derivative:

$$D_\mu \Psi \equiv (\partial_\mu + iQeA_\mu)\Psi. \quad (5.1.18)$$

Here the term “covariant” refers to the gauge transformation symmetry, not the Lorentz transformation symmetry as it did when we introduced covariant four-vectors. Note that the covariant derivative actually depends on the charge of the field it acts on. Now one can write the full Lagrangian density as

$$\mathcal{L} = \mathcal{L}_0 + \mathcal{L}_{\text{int}} = -\frac{1}{4}F^{\mu\nu}F_{\mu\nu} + i\bar{\Psi}\gamma^\mu D_\mu \Psi - m\bar{\Psi}\Psi. \quad (5.1.19)$$

The ordinary derivative of the spinor transforms under the gauge transformation with an “extra” term:

$$\partial_\mu \Psi \rightarrow \partial_\mu (e^{iQ\theta} \Psi) = e^{iQ\theta} \partial_\mu \Psi + iQ\Psi \partial_\mu \theta. \quad (5.1.20)$$

The point of the covariant derivative of Ψ is that it transforms under the gauge transformation the same way Ψ does, by acquiring a phase:

$$D_\mu \Psi \rightarrow e^{iQ\theta} D_\mu \Psi. \quad (5.1.21)$$

Here the contribution from the transformation of A_μ in D_μ cancels the extra term in eq. (5.1.20). Using eqs. (5.1.15)-(5.1.17) and (5.1.21), it is easy to see that \mathcal{L} is invariant under the gauge transformation, since the multiplicative phase factors just cancel.

Returning to the interaction term eq. (5.1.3), we can now identify the Feynman rule for QED interactions, by following the general prescription outlined with eq. (4.7.8):

$$\longleftrightarrow -iQe\gamma^\mu$$

This one interaction vertex governs all physical processes in QED.

To find the Feynman rules for initial and final state photons, consider the Fourier expansion of the vector field at a fixed time:

$$A_\mu = \sum_{\lambda=0}^3 \int d\tilde{p} \left[\epsilon_\mu(p, \lambda) e^{i\vec{p}\cdot\vec{x}} a_{\vec{p},\lambda} + \epsilon_\mu^*(p, \lambda) e^{-i\vec{p}\cdot\vec{x}} a_{\vec{p},\lambda}^\dagger \right]. \quad (5.1.22)$$

Here $\epsilon_\mu(p, \lambda)$ is a basis of four polarization four-vectors labeled by $\lambda = 0, 1, 2, 3$. They satisfy the orthonormality condition:

$$\epsilon^\mu(p, \lambda) \epsilon_\mu^*(p, \lambda') = \begin{cases} -1 & \text{for } \lambda = \lambda' = 1, 2, \text{ or } 3 \\ +1 & \text{for } \lambda = \lambda' = 0 \\ 0 & \text{for } \lambda \neq \lambda' \end{cases} \quad (5.1.23)$$

The operators $a_{\vec{p},\lambda}^\dagger$ and $a_{\vec{p},\lambda}$ act on the vacuum state by creating and destroying photons with momentum \vec{p} and polarization vector $\epsilon_\mu(p, \lambda)$.

However, not all of the four degrees of freedom labeled by λ can be physical. From classical electromagnetism, we know that electromagnetic waves are transversely polarized. This means that the electric and magnetic fields are perpendicular to the 3-momentum direction of propagation. In terms of the potentials, it means that one can always choose a gauge in which $A^0 = 0$ and the Lorenz gauge condition $\partial_\mu A^\mu = 0$ is satisfied. Therefore, physical electromagnetic wave quanta corresponding to the classical solutions to Maxwell's equations $A^\mu = \epsilon^\mu e^{-ip \cdot x}$ with $p^2 = 0$ can be taken to obey:

$$\epsilon^\mu = (0, \vec{\epsilon}), \quad (5.1.24)$$

$$p_\mu \epsilon^\mu = 0 \quad (5.1.25)$$

(or, equivalent to the last condition, $\vec{\epsilon} \cdot \vec{p} = 0$). After imposing these two conditions, only two of the four λ 's will survive as valid initial or final states for any given p^μ .

For example, suppose that a state contains a photon with 3-momentum $\vec{p} = p\hat{z}$, so $p^\mu = (p, 0, 0, p)$. Then we can choose a basis of transverse linearly-polarized vectors with $\lambda = 1, 2$:

$$\epsilon^\mu(p, 1) = (0, 1, 0, 0) \quad x\text{-polarized}, \quad (5.1.26)$$

$$\epsilon^\mu(p, 2) = (0, 0, 1, 0) \quad y\text{-polarized}. \quad (5.1.27)$$

However, in high-energy physics it is often more useful to instead use a basis of left- and right-handed circular polarizations that carry definite helicities $\lambda = R, L$:

$$\epsilon^\mu(p, R) = \frac{1}{\sqrt{2}}(0, 1, i, 0) \quad \text{right-handed}, \quad (5.1.28)$$

$$\epsilon^\mu(p, L) = \frac{1}{\sqrt{2}}(0, 1, -i, 0) \quad \text{left-handed}. \quad (5.1.29)$$

In general, incoming photon lines have a Feynman rule $\epsilon_\mu(p, \lambda)$ and outgoing photon lines have a Feynman rule $\epsilon_\mu^*(p, \lambda)$, where $\lambda = 1, 2$ in some convenient basis of choice. Often, we will sum or average over the polarization labels λ , so the $\epsilon_\mu(p, \lambda)$ will not need to be listed explicitly for a given momentum.

Let us next construct the Feynman propagator for photon lines. The free Lagrangian density given in eq. (4.1.34) can be rewritten as:

$$\mathcal{L}_0 = \frac{1}{2} A^\mu (g_{\mu\nu} \partial_\rho \partial^\rho - \partial_\mu \partial_\nu) A^\nu, \quad (5.1.30)$$

where we have dropped a total derivative. (The action, obtained by integrating \mathcal{L}_0 , does not depend on total derivative terms.) Therefore, following the prescription of eq. (4.7.15), it appears that we ought to find the propagator by finding the inverse of the 4×4 matrix

$$P_{\mu\nu} = -p^2 g_{\mu\nu} + p_\mu p_\nu. \quad (5.1.31)$$

Unfortunately, however, this matrix is not invertible. The reason for this can be traced to the gauge invariance of the theory; not all of the physical states we are attempting to propagate are really physical.

This problem can be avoided using a trick, due to Fermi, called “gauge fixing”. As long as we agree to stick to the Lorenz gauge, $\partial_\mu A^\mu = 0$, we can add a term to the Lagrangian density proportional to $(\partial_\mu A^\mu)^2$:

$$\mathcal{L}_0^{(\xi)} = \mathcal{L}_0 - \frac{1}{2\xi} (\partial_\mu A^\mu)^2. \quad (5.1.32)$$

In Lorenz gauge, not only does the extra term vanish, but also its contribution to the equations of motion vanishes. Here ξ is an arbitrary new gauge-fixing parameter; it can be picked at will. Intermediate steps in a calculation may depend on it, but physical results should not depend on the choice of ξ . The new term in the modified free Lagrangian $\mathcal{L}_0^{(\xi)}$ is called the gauge-fixing term. Now the matrix to be inverted is:

$$P_{\mu\nu} = -p^2 g_{\mu\nu} + \left(1 - \frac{1}{\xi}\right) p_\mu p_\nu. \quad (5.1.33)$$

To find the inverse, one notices that as a tensor, $(P^{-1})^{\nu\rho}$ can only be a linear combination of terms proportional to $g^{\nu\rho}$ and to $p^\nu p^\rho$. So, writing the most general possible form for the answer:

$$(P^{-1})^{\nu\rho} = C_1 g^{\nu\rho} + C_2 p^\nu p^\rho \quad (5.1.34)$$

and requiring that

$$P_{\mu\nu} (P^{-1})^{\nu\rho} = \delta_\mu^\rho, \quad (5.1.35)$$

one finds the solution

$$C_1 = -\frac{1}{p^2}; \quad C_2 = \frac{1-\xi}{(p^2)^2}. \quad (5.1.36)$$

It follows that the desired Feynman propagator for a photon with momentum p^μ is:

$$\frac{i}{p^2 + i\epsilon} \left[-g_{\mu\nu} + (1-\xi) \frac{p_\mu p_\nu}{p^2} \right]. \quad (5.1.37)$$

(Here we have put in the $i\epsilon$ factor in the denominator as usual.) In a Feynman diagram, this propagator corresponds to an internal wavy line, labeled by μ and ν at opposite ends, and carrying 4-momentum p . The gauge-fixing parameter ξ can be chosen at the convenience or whim of the person computing the Feynman diagram. The most popular choice for simple calculations is $\xi = 1$, called Feynman gauge. Then the Feynman propagator for photons is simply:

$$\frac{-ig_{\mu\nu}}{p^2 + i\epsilon} \quad (\text{Feynman gauge}). \quad (5.1.38)$$

Another common choice is $\xi = 0$, known as Landau gauge, for which the Feynman propagator is:

$$\frac{-i}{p^2 + i\epsilon} \left[g_{\mu\nu} - \frac{p_\mu p_\nu}{p^2} \right] \quad (\text{Landau gauge}). \quad (5.1.39)$$

[Comparing to eq. (5.1.32), we see that this is really obtained as a formal limit $\xi \rightarrow 0$.] The Landau gauge photon propagator has the nice property that it vanishes when contracted with either p^μ or p^ν , which can make some calculations simpler (especially certain loop diagram calculations). Sometimes it is useful to just leave ξ unspecified. Even though this means having to calculate more terms, the payoff is that in the end one can see if the final answer for the reduced matrix element is independent of ξ , providing a consistency check.


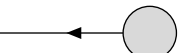
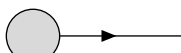
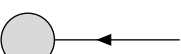


We have now encountered most of the Feynman rules for QED. There are some additional rules having to do with minus signs because of Fermi-Dirac statistics; these can be understood by carefully considering the effects of anticommutation relations for fermionic operators. In practice, one usually does not write out the spinor indices explicitly. All of the rules are summarized in the following two pages in a cookbook form. Of course, the best way to understand how the rules work is to do some examples. That will be the subject of the next few subsections.

FEYNMAN RULES FOR QED

To find the contributions to the reduced matrix element \mathcal{M} for a physical process involving charged Dirac fermions and photons:

1. Draw all topologically distinct Feynman diagrams, with wavy lines representing photons, and solid lines with arrows representing fermions, using the rules below for external lines, internal lines, and interaction vertices. The arrow direction is preserved when following each fermion line. Enforce four-momentum conservation at each vertex.

2. For external lines, write (with 4-momentum p^μ always to the right, and spin polarization s or λ as appropriate):

initial-state fermion:		\longleftrightarrow	$u(p, s)$
initial-state antifermion:		\longleftrightarrow	$\bar{v}(p, s)$
final-state fermion:		\longleftrightarrow	$\bar{u}(p, s)$
final-state antifermion:		\longleftrightarrow	$v(p, s)$
initial-state photon:		\longleftrightarrow	$\epsilon_\mu(p, \lambda)$
final-state photon:		\longleftrightarrow	$\epsilon_\mu^*(p, \lambda)$

3. For internal fermion lines, write Feynman propagators:

$$\text{---}\longrightarrow\text{---} \longleftrightarrow \frac{i(\not{p} + m)}{p^2 - m^2 + i\epsilon}$$

with 4-momentum p^μ along the arrow direction, and m the mass of the fermion. For internal photon lines, write:

$$\text{---}\overset{\mu}{\sim}\text{---}\overset{\nu}{\sim}\text{---} \longleftrightarrow \frac{i}{p^2 + i\epsilon} \left[-g_{\mu\nu} + (1 - \xi) \frac{p_\mu p_\nu}{p^2} \right]$$

with 4-momentum p^μ along either direction in the wavy line. (Use $\xi = 1$ for Feynman gauge and $\xi = 0$ for Landau gauge.)

4. For the interaction vertex of a fermion f of charge Q_f , write:

$$\longleftrightarrow -iQ_f e \gamma^\mu$$

The vector index μ is to be contracted with the corresponding index on the photon line to which it is connected. This will be either an external photon line factor of ϵ_μ or ϵ_μ^* , or on an internal photon line propagator index. Note that the fermion f coming into the vertex must be the same flavor as the fermion coming out of the vertex; for example, there is no photon-muon-positron vertex.

5. For each loop momentum ℓ^μ that is undetermined by four-momentum conservation with fixed external-state momenta, perform an integration

$$\int \frac{d^4 \ell}{(2\pi)^4}. \quad (5.1.40)$$

Getting a finite answer from these loop integrations often requires that they be regularized by introducing a cutoff or some other trick.

6. Put a factor of (-1) for each closed fermion loop.

7. To take into account suppressed spinor indices on fermion lines, write terms involving spinors as follows. For fermion lines that go all the way through the diagram, start at the end of each fermion line (as defined by the arrow direction) with a factor \bar{u} or \bar{v} , and write down factors of γ^μ or $(\not{p} + m)$ consecutively, following the line backwards until a u or v spinor is reached. For closed fermion loops, start at an arbitrary vertex on the loop, and follow the fermion line backwards until the original point is reached; take a trace over the gamma matrices in the closed loop.

8. If a Feynman diagram with one or more closed loops can be transformed into an exact copy of itself by interchanging any number of internal lines through a smooth deformation without moving the external lines, then there is an additional symmetry factor of $1/N$, where N is the number of distinct permutations of that type.

9. After writing down the contributions from each diagram to the reduced matrix element \mathcal{M} according to the preceding rules, assign an additional relative minus sign between different diagram contributions whenever the written ordering of external state spinor wavefunctions u, v, \bar{u}, \bar{v} differs by an odd permutation.

5.2 Electron-positron scattering

5.2.1 $e^-e^+ \rightarrow \mu^-\mu^+$

In the next few subsections we will study some of the basic scattering processes in QED, using the Feynman rules found in the previous section and the general discussion of cross-sections given in section 4.5. These calculations will involve several thematic tricks that are common to many Feynman diagram evaluations.

We begin with electron-positron annihilation into a muon-antimuon pair:

$$e^-e^+ \rightarrow \mu^-\mu^+.$$

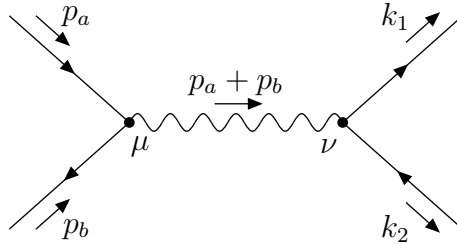
We will calculate the differential and total cross-sections for this process in the center-of-momentum frame, to leading order in the coupling e . Since the mass of the muon (and the anti-muon) is about $m_\mu = 105.66$ MeV, this process requires a center-of-momentum energy of at least $\sqrt{s} = 211.3$ MeV. By contrast, the mass of the electron is only about $m_e = 0.511$ MeV, which we can therefore safely neglect. The error made in doing so is far less than the error made by not including higher-order corrections.

A good first step is to label the momentum and spin data for the initial state electron and positron and the final state muon and anti-muon:

Particle	Momentum	Spin	Spinor
e^-	p_a	s_a	$u(p_a, s_a)$
e^+	p_b	s_b	$\bar{v}(p_b, s_b)$
μ^-	k_1	s_1	$\bar{u}(k_1, s_1)$
μ^+	k_2	s_2	$v(k_2, s_2)$

(5.2.1)

At order e^2 , there is only one Feynman diagram for this process. Here it is:



Applying the rules for QED to turn this picture into a formula for the reduced matrix element, we find:

$$\mathcal{M} = [\bar{v}(p_b, s_b) (ie\gamma^\mu) u(p_a, s_a)] \left[\frac{-ig_{\mu\nu}}{(p_a + p_b)^2} \right] [\bar{u}(k_1, s_1) (ie\gamma^\nu) v(k_2, s_2)]. \quad (5.2.2)$$

The $\bar{v}(p_b, s_b) (ie\gamma^\mu) u(p_a, s_a)$ part is obtained by starting at the end of the electron-positron line with the positron external state spinor, and following it back to its beginning. The interaction

vertex is $-iQe\gamma^\mu = ie\gamma^\mu$, since the charge of the electron and muon is $Q = -1$. Likewise, the $\bar{u}(k_1, s_1) (ie\gamma^\nu) v(k_2, s_2)$ part is obtained by starting at the end of the muon-antimuon line with the muon external state spinor, and following it backwards. The photon propagator is written in Feynman gauge, for simplicity, and carries indices μ and ν that connect to the two fermion lines at their respective interaction vertices.

We can write this result more compactly by using abbreviations $\bar{v}(p_b, s_b) = \bar{v}_b$ and $u(p_a, s_a) \equiv u_a$, etc. Writing the denominator of the photon propagator as the Mandelstam variable $s = (p_a + p_b)^2 = (k_1 + k_2)^2$, and using the metric in the photon propagator to lower the index on one of the gamma matrices, we get:

$$\mathcal{M} = i\frac{e^2}{s}(\bar{v}_b\gamma_\mu u_a)(\bar{u}_1\gamma^\mu v_2). \quad (5.2.3)$$

The differential cross-section involves the complex square of \mathcal{M} :

$$|\mathcal{M}|^2 = \frac{e^4}{s^2}(\bar{v}_b\gamma_\mu u_a)(\bar{u}_1\gamma^\mu v_2)(\bar{v}_b\gamma_\nu u_a)^*(\bar{u}_1\gamma^\nu v_2)^*. \quad (5.2.4)$$

Evaluating the complex conjugated terms in parentheses can be done systematically by taking the Hermitian conjugate of the Dirac spinors and matrices they are made of, taking care to write them in the reverse order. So, for example,

$$(\bar{v}_b\gamma_\nu u_a)^* = (v_b^\dagger\gamma^0\gamma_\nu u_a)^* = u_a^\dagger\gamma_\nu^\dagger\gamma^0 v_b = u_a^\dagger\gamma^0\gamma_\nu v_b = \bar{u}_a\gamma_\nu v_b. \quad (5.2.5)$$

The third equality follows from the identity (A.2.5), which implies $\gamma_\nu^\dagger\gamma^0 = \gamma^0\gamma_\nu$. Similarly,

$$(\bar{u}_1\gamma^\nu v_2)^* = \bar{v}_2\gamma^\nu u_1. \quad (5.2.6)$$

[Following the same strategy, one can show that in general,

$$(\bar{x}\gamma_\mu\gamma_\nu\cdots\gamma_\rho y)^* = \bar{y}\gamma_\rho\cdots\gamma_\nu\gamma_\mu x \quad (5.2.7)$$

where x and y are any u and v spinors.] Therefore we have:

$$|\mathcal{M}|^2 = \frac{e^4}{s^2}(\bar{v}_b\gamma_\mu u_a)(\bar{u}_a\gamma_\nu v_b)(\bar{u}_1\gamma^\mu v_2)(\bar{v}_2\gamma^\nu u_1). \quad (5.2.8)$$

At this point, we could work out explicit forms for the external state spinors and plug eq. (5.2.8) into eq. (4.5.47) to find the differential cross-section for any particular set of spins. However, this is not very convenient, and fortunately it is not necessary either. In a real experiment, the final state spins of the muon and anti-muon are typically not measured. Therefore, to find the total cross-section for all possible final states, we should sum over s_1 and s_2 . Also, if the initial-state electron spin states are unknown, we should average over s_a and s_b . (One must

average, not sum, over the initial-state spins, because s_a and s_b cannot simultaneously take on both spin-up and spin-down values; there is only one initial state, even if it is unknown.) These spin sums and averages will allow us to exploit the identities (3.2.50) and (3.2.51) [also listed in Appendix B as (A.2.29) and (A.2.30)], so that the explicit forms for the spinors are never needed.

After doing the spin sum and average, the differential cross-section must be symmetric under rotations about the collision axis. This is because the only special directions in the problem are the momenta of the particles, so that the cross-section can only depend on the angle θ between the collision axis determined by the two initial-state particles and the scattering axis determined by the two final-state particles. So, we can apply eq. (4.5.48) to obtain:

$$\frac{d\sigma}{d(\cos\theta)} = \frac{1}{2} \sum_{s_a} \frac{1}{2} \sum_{s_b} \sum_{s_1} \sum_{s_2} |\mathcal{M}|^2 \frac{|\vec{k}_1|}{32\pi s |\vec{p}_a|} \quad (5.2.9)$$

in the center-of-momentum frame, with the effects of initial state spin averaging and final state spin summing now included.

We can now use eqs. (A.2.29) and (A.2.30), which in the present situation imply

$$\sum_{s_a} u_a \bar{u}_a = \not{p}_a + m_e, \quad (5.2.10)$$

$$\sum_{s_2} v_2 \bar{v}_2 = \not{k}_2 - m_\mu. \quad (5.2.11)$$

Neglecting m_e as promised earlier, we obtain:

$$\frac{1}{2} \sum_{s_a} \frac{1}{2} \sum_{s_b} \sum_{s_1} \sum_{s_2} |\mathcal{M}|^2 = \frac{e^4}{4s^2} \sum_{s_b} \sum_{s_1} (\bar{v}_b \gamma_\mu \not{p}_a \gamma_\nu v_b) (\bar{u}_1 \gamma^\mu [\not{k}_2 - m_\mu] \gamma^\nu u_1). \quad (5.2.12)$$

Now we apply another trick. A dot product of two vectors is equal to the trace of the vectors multiplied in the opposite order to form a matrix:

$$(a_1 \ a_2 \ a_3 \ a_4) \begin{pmatrix} b_1 \\ b_2 \\ b_3 \\ b_4 \end{pmatrix} = \text{Tr} \left[\begin{pmatrix} b_1 \\ b_2 \\ b_3 \\ b_4 \end{pmatrix} (a_1 \ a_2 \ a_3 \ a_4) \right] \equiv \text{Tr} \begin{pmatrix} b_1 a_1 & b_1 a_2 & b_1 a_3 & b_1 a_4 \\ b_2 a_1 & b_2 a_2 & b_2 a_3 & b_2 a_4 \\ b_3 a_1 & b_3 a_2 & b_3 a_3 & b_3 a_4 \\ b_4 a_1 & b_4 a_2 & b_4 a_3 & b_4 a_4 \end{pmatrix} \quad (5.2.13)$$

Applying this to each expression in parentheses in eq. (5.2.12), we move the barred spinor (thought of as a row vector) to the end and take the trace over the resulting 4×4 Dirac spinor matrix. So:

$$\bar{v}_b \gamma_\mu \not{p}_a \gamma_\nu v_b = \text{Tr}[\gamma_\mu \not{p}_a \gamma_\nu v_b \bar{v}_b], \quad (5.2.14)$$

$$\bar{u}_1 \gamma^\mu [\not{k}_2 - m_\mu] \gamma^\nu u_1 = \text{Tr}[\gamma^\mu (\not{k}_2 - m_\mu) \gamma^\nu u_1 \bar{u}_1], \quad (5.2.15)$$

so that

$$\frac{1}{4} \sum_{\text{spins}} |\mathcal{M}|^2 = \frac{e^4}{4s^2} \sum_{s_b} \sum_{s_1} \text{Tr}[\gamma_\mu \not{p}_a \gamma_\nu v_b \bar{v}_b] \text{Tr}[\gamma^\mu (\not{k}_2 - m_\mu) \gamma^\nu u_1 \bar{u}_1]. \quad (5.2.16)$$

The reason this trick of rearranging into a trace is useful is that now we can once again exploit the spin-sum identities (A.2.29) and (A.2.30), this time in the form:

$$\sum_{s_b} v_b \bar{v}_b = \not{p}_b - m_e, \quad (5.2.17)$$

$$\sum_{s_1} u_1 \bar{u}_1 = \not{k}_1 + m_\mu. \quad (5.2.18)$$

The result, again neglecting m_e , is:

$$\frac{1}{4} \sum_{\text{spins}} |\mathcal{M}|^2 = \frac{e^4}{4s^2} \text{Tr}[\gamma_\mu \not{p}_a \gamma_\nu \not{p}_b] \text{Tr}[\gamma^\mu (\not{k}_2 - m_\mu) \gamma^\nu (\not{k}_1 + m_\mu)]. \quad (5.2.19)$$

Next we must evaluate the traces. First,

$$\text{Tr}[\gamma_\mu \not{p}_a \gamma_\nu \not{p}_b] = p_a^\alpha p_b^\beta \text{Tr}[\gamma_\mu \gamma_\alpha \gamma_\nu \gamma_\beta] \quad (5.2.20)$$

$$= p_a^\alpha p_b^\beta (4g_{\mu\alpha} g_{\nu\beta} - 4g_{\mu\nu} g_{\alpha\beta} + 4g_{\mu\beta} g_{\nu\alpha}) \quad (5.2.21)$$

$$= 4p_{a\mu} p_{b\nu} - 4g_{\mu\nu} p_a \cdot p_b + 4p_{b\mu} p_{a\nu}, \quad (5.2.22)$$

where we have used the general result for the trace of four gamma matrices found in the homework, and listed in eq. (A.2.10). Similarly, making use of the fact that the trace of an odd number of gamma matrices is zero:

$$\text{Tr}[\gamma^\mu (\not{k}_2 - m_\mu) \gamma^\nu (\not{k}_1 + m_\mu)] = \text{Tr}[\gamma^\mu \not{k}_2 \gamma^\nu \not{k}_1] - m_\mu^2 \text{Tr}[\gamma^\mu \gamma^\nu] \quad (5.2.23)$$

$$= 4k_2^\mu k_1^\nu - 4g^{\mu\nu} k_1 \cdot k_2 + 4k_1^\mu k_2^\nu - 4g^{\mu\nu} m_\mu^2, \quad (5.2.24)$$

where eqs. (A.2.8)-(A.2.10) have been used. Taking the product of the two traces, one finds that the answer reduces to simply:

$$\frac{1}{4} \sum_{\text{spins}} |\mathcal{M}|^2 = \frac{e^4}{s^2} 8 \left[(p_a \cdot k_2)(p_b \cdot k_1) + (p_a \cdot k_1)(p_b \cdot k_2) + (p_a \cdot p_b) m_\mu^2 \right]. \quad (5.2.25)$$

Our next task is to work out the kinematic quantities appearing in eq. (5.2.25). Let us call P and K the magnitudes of the 3-momenta of the electron and the muon, respectively. We assume that the electron is initially moving in the $+z$ direction, and the muon makes an angle θ with respect to the positive z axis, within the yz plane. The on-shell conditions for the particles are:

$$p_a^2 = p_b^2 = m_e^2 \approx 0, \quad (5.2.26)$$

$$k_1^2 = k_2^2 = m_\mu^2. \quad (5.2.27)$$

Then we have:

$$p_a = (P, 0, 0, P), \quad (5.2.28)$$

$$p_b = (P, 0, 0, -P), \quad (5.2.29)$$

$$k_1 = (\sqrt{K^2 + m_\mu^2}, 0, K \sin \theta, K \cos \theta), \quad (5.2.30)$$

$$k_2 = (\sqrt{K^2 + m_\mu^2}, 0, -K \sin \theta, -K \cos \theta). \quad (5.2.31)$$

Since $(p_a + p_b)^2 = (k_1 + k_2)^2 = s$, it follows that

$$P = \sqrt{\frac{s}{4}}, \quad (5.2.32)$$

$$K = \sqrt{\frac{s}{4} - m_\mu^2}, \quad (5.2.33)$$

and

$$p_a \cdot p_b = 2P^2 = \frac{s}{2}, \quad (5.2.34)$$

$$p_a \cdot k_1 = p_b \cdot k_2 = P\sqrt{K^2 + m_\mu^2} - PK \cos \theta = \frac{s}{4} \left[1 - \cos \theta \sqrt{1 - \frac{4m_\mu^2}{s}} \right], \quad (5.2.35)$$

$$p_a \cdot k_2 = p_b \cdot k_1 = P\sqrt{K^2 + m_\mu^2} + PK \cos \theta = \frac{s}{4} \left[1 + \cos \theta \sqrt{1 - \frac{4m_\mu^2}{s}} \right]. \quad (5.2.36)$$

Putting these results into eq. (5.2.25), we get:

$$\begin{aligned} \frac{1}{4} \sum_{\text{spins}} |\mathcal{M}|^2 &= \frac{8e^4}{s^2} \left\{ \left(\frac{s}{4} \right)^2 \left[1 + \cos \theta \sqrt{1 - \frac{4m_\mu^2}{s}} \right]^2 + \left(\frac{s}{4} \right)^2 \left[1 - \cos \theta \sqrt{1 - \frac{4m_\mu^2}{s}} \right]^2 + \frac{sm_\mu^2}{2} \right\} \\ &= e^4 \left[1 + \frac{4m_\mu^2}{s} + \left(1 - \frac{4m_\mu^2}{s} \right) \cos^2 \theta \right]. \end{aligned} \quad (5.2.37)$$

Finally we can plug this into eq. (5.2.9):

$$\frac{d\sigma}{d(\cos \theta)} = \frac{1}{4} \sum_{\text{spins}} |\mathcal{M}|^2 \frac{K}{32\pi s P} \quad (5.2.38)$$

$$= \frac{e^4}{32\pi s} \sqrt{1 - \frac{4m_\mu^2}{s}} \left[1 + \frac{4m_\mu^2}{s} + \left(1 - \frac{4m_\mu^2}{s} \right) \cos^2 \theta \right], \quad (5.2.39)$$

or, rewriting in terms of the fine structure constant $\alpha = e^2/4\pi$,

$$\frac{d\sigma}{d(\cos \theta)} = \frac{\pi\alpha^2}{2s} \sqrt{1 - \frac{4m_\mu^2}{s}} \left[1 + \frac{4m_\mu^2}{s} + \left(1 - \frac{4m_\mu^2}{s} \right) \cos^2 \theta \right]. \quad (5.2.40)$$

Doing the integral over $\cos \theta$ using $\int_{-1}^1 d(\cos \theta) = 2$ and $\int_{-1}^1 \cos^2 \theta d(\cos \theta) = 2/3$, we find the total cross-section:

$$\sigma = \frac{4\pi\alpha^2}{3s} \sqrt{1 - \frac{4m_\mu^2}{s}} \left(1 + \frac{2m_\mu^2}{s} \right). \quad (5.2.41)$$

It is a useful check that the cross-section has units of area; recall that when $c = \hbar = 1$, then $s = E_{\text{CM}}^2$ has units of mass² or length⁻².

Equations (5.2.40) and (5.2.41) have been tested in many experiments, and correctly predict the rate of production of muon-antimuon pairs at electron-positron colliders. Let us examine some special limiting cases. Near the energy threshold for $\mu^+\mu^-$ production, one may expand in the quantity

$$\Delta E = \sqrt{s} - 2m_\mu. \quad (5.2.42)$$

To leading order in small ΔE , eq. (5.2.41) becomes

$$\sigma \approx \frac{\pi\alpha^2}{2m_\mu^2} \sqrt{\frac{\Delta E}{m_\mu}}. \quad (5.2.43)$$

The cross-section therefore rises like the square root of the energy excess over the threshold. However, going to increasing energy, σ quickly levels off because of the $1/s$ factors in eq. (5.2.41). Maximizing with respect to s , one finds that the largest cross-section in eq. (5.2.41) is reached for $\sqrt{s} = \sqrt{1 + \sqrt{21}} m_\mu \approx 2.36m_\mu$, and is about

$$\sigma_{\text{max}} = 0.54\alpha^2/m_\mu^2 = 1000 \text{ nb}. \quad (5.2.44)$$

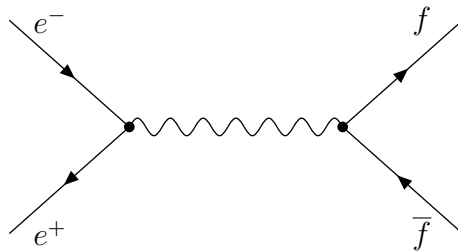
In the high energy limit $\sqrt{s} \gg m_\mu$, the cross-section decreases proportional to $1/s$:

$$\sigma \approx \frac{4\pi\alpha^2}{3s}. \quad (5.2.45)$$

However, this formula is not good for arbitrarily high values of the center-of-momentum energy, because there is another diagram in which the photon is replaced by a Z^0 boson. This effect becomes important when \sqrt{s} is not small compared to $m_Z = 91.1876 \text{ GeV}$.

5.2.2 $e^-e^+ \rightarrow f\bar{f}$.

In the last subsection, we calculated the cross-section for producing a muon-antimuon pair in e^-e^+ collisions. We can easily generalize this to the case of production of any charged fermion f and anti-fermion \bar{f} . The Feynman diagram for this process is obtained by simply replacing the muon-antimuon line by an $f\text{-}\bar{f}$ line:



The reduced matrix element for this process has exactly the same form as for $e^-e^+ \rightarrow f\bar{f}$, except that the photon- $\mu^-\mu^+$ vertex is replaced by a photon- $f\bar{f}$ vertex, with:

$$ie\gamma^\nu \longrightarrow -iQ_f e\gamma^\nu, \quad (5.2.46)$$

where Q_f is the charge of the fermion f . In the case of quarks, there are three indistinguishable colors for each flavor (up, down, strange, charm, bottom, top). The photon-quark-antiquark vertex is diagonal in color, so the three colors are simply summed over in order to find the total cross-section for a given flavor. In general, if we call n_f the number of colors (or perhaps other non-spin degrees of freedom) of the fermion f , then we have:

$$|\mathcal{M}_{e^-e^+ \rightarrow f\bar{f}}|^2 = n_f Q_f^2 |\mathcal{M}_{e^-e^+ \rightarrow \mu^-\mu^+}|^2, \quad (5.2.47)$$

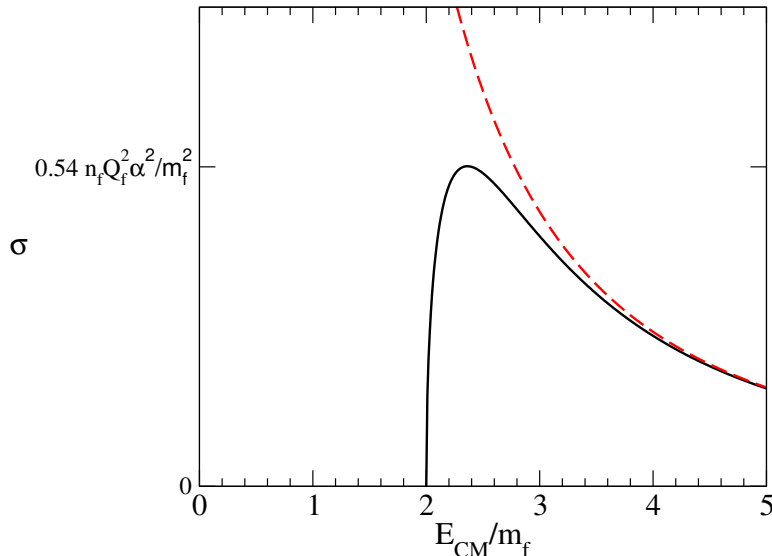
where it is understood that m_μ should be replaced by m_f everywhere in $|\mathcal{M}_{e^-e^+ \rightarrow f\bar{f}}|^2$. It follows that the differential and total cross-sections for $e^-e^+ \rightarrow f\bar{f}$ are obtained from eqs. (5.2.40) and (5.2.41) by just multiplying by $n_f Q_f^2$ and replacing $m_\mu \rightarrow m_f$:

$$\sigma_{e^-e^+ \rightarrow f\bar{f}} = n_f Q_f^2 \frac{4\pi\alpha^2}{3s} \sqrt{1 - \frac{4m_f^2}{s}} \left(1 + \frac{2m_f^2}{s}\right). \quad (5.2.48)$$

In the high-energy limit $\sqrt{s} \gg m_f$, we have:

$$\sigma_{e^-e^+ \rightarrow f\bar{f}} = n_f Q_f^2 \frac{4\pi\alpha^2}{3s}. \quad (5.2.49)$$

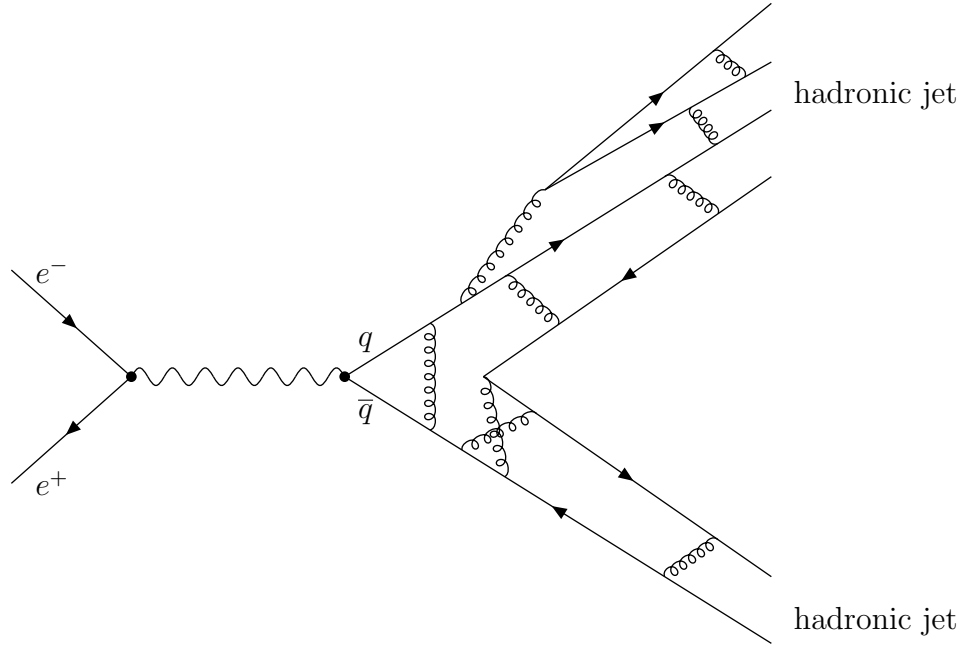
The following graph compares the total cross-section for $e^+e^- \rightarrow f\bar{f}$ (solid line) as given by eq. (5.2.48) to the asymptotic approximation (dashed line) given by eq. (5.2.49).



We see that the true cross-section is always less than the asymptotic approximation, but the two already agree fairly well when $\sqrt{s} \gtrsim 2.5m_f$. This means that when several fermions contribute, the total cross-section well above threshold is just equal to the sum of $n_f Q_f^2$ for the available states times a factor $4\pi\alpha^2/3s$. For example, the up quark has charge $Q_u = +2/3$, and there are three colors, so the prefactor indicated above is $3(2/3)^2 = 4/3$. The prefactors for all of the fundamental charged fermion types with masses less than m_Z are:

$$\begin{aligned}
\text{up, charm quarks:} \quad Q_f = 2/3, \quad n_f = 3 &\longrightarrow n_f Q_f^2 = 4/3 \\
\text{down, strange, bottom quarks:} \quad Q_f = -1/3, \quad n_f = 3 &\longrightarrow n_f Q_f^2 = 1/3 \\
\text{muon, tau leptons:} \quad Q_f = -1, \quad n_f = 1 &\longrightarrow n_f Q_f^2 = 1.
\end{aligned} \tag{5.2.50}$$

However, free quarks are not seen in nature because the QCD color force confines them within color-singlet hadrons. This means that the quark-antiquark production process $e^-e^+ \rightarrow Q\bar{Q}$ cross-section cannot easily be interpreted in terms of specific particles in the final state. Instead, one should view the quark production as a microscopic process, occurring at a distance scale much smaller than a typical hadron. Before we “see” them in macroscopic-sized detectors, the produced quarks then undergo further strong interactions that end up producing hadronic jets of particles with momenta close to those of the original quarks. This always involves at least the further production of a quark-antiquark pair in order to make the final state hadrons color singlets. A Feynman-diagram cartoon of the situation might look as follows:



Because the hadronic interactions are most important at the strong-interaction energy scale of a few hundred MeV, the calculation of the cross-section can only be trusted for energies that

are significantly higher than this. When $\sqrt{s} \gg 1$ GeV, one can make the approximation:

$$\sigma(e^-e^+ \rightarrow \text{hadrons}) \approx \sum_q \sigma(e^-e^+ \rightarrow q\bar{q}). \quad (5.2.51)$$

The final state can be quite complicated, so to test QED production of quarks, one can just measure the total cross-section for producing hadrons. The traditional measure of the total hadronic cross-section is the variable R_{hadrons} , defined as the ratio:

$$R_{\text{hadrons}} = \frac{\sigma(e^-e^+ \rightarrow \text{hadrons})}{\sigma(e^-e^+ \rightarrow \mu^-\mu^+)}. \quad (5.2.52)$$

When the approximation is valid, one can always produce up, down and strange quarks, which all have masses < 1 GeV. The threshold to produce charm-anticharm quarks occurs roughly when $\sqrt{s} > 2m_c \approx 3$ GeV, and that to produce bottom-antibottom quarks is at roughly $\sqrt{s} > 2m_b \approx 10$ GeV. As each of these thresholds is passed, one gets a contribution to R_{hadrons} that is approximately a constant proportional to $n_f Q_f^2$. So, for $\sqrt{s} < 3$ GeV, one has

$$R_{\text{hadrons}} = \frac{4}{3} + \frac{1}{3} + \frac{1}{3} = 2. \quad (u, d, s \text{ quarks}) \quad (5.2.53)$$

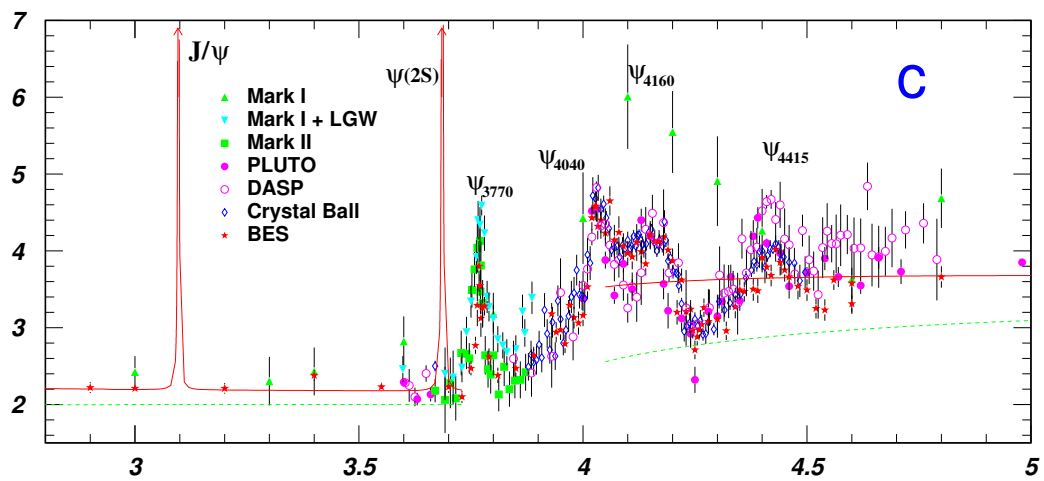
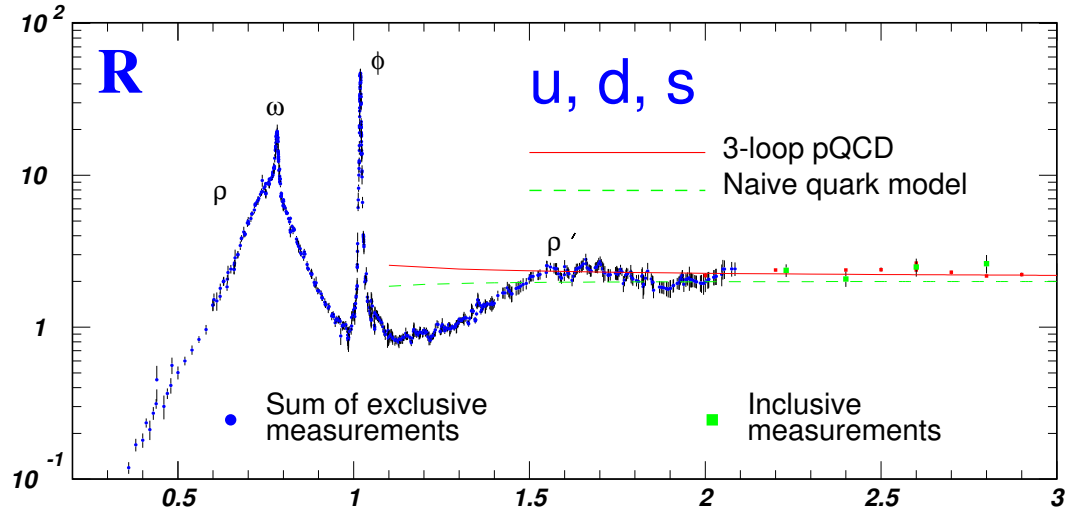
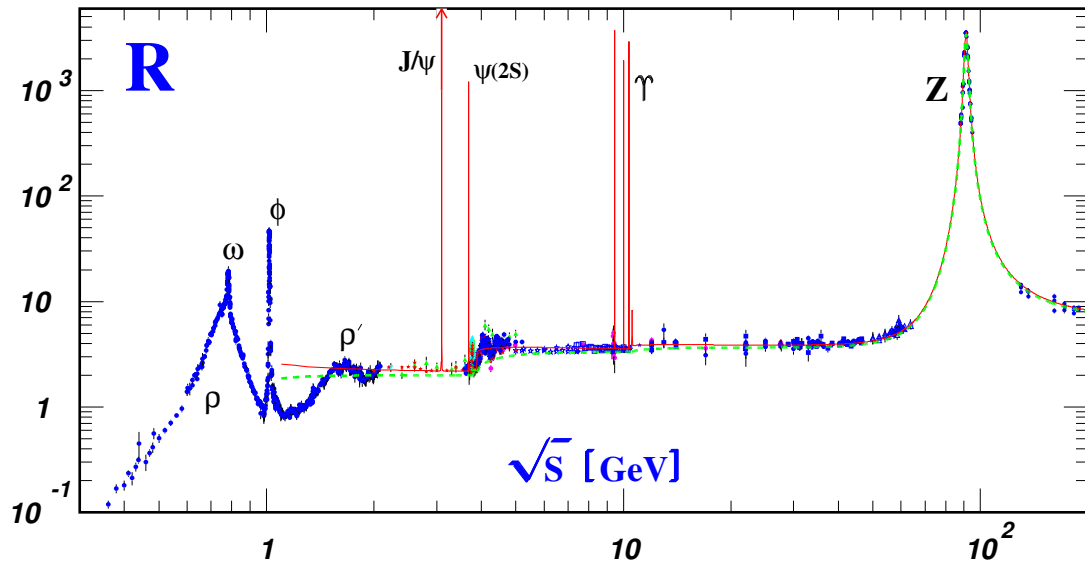
For $3 \text{ GeV} < \sqrt{s} < 10$ GeV, the charm quark contributes, and the ratio is

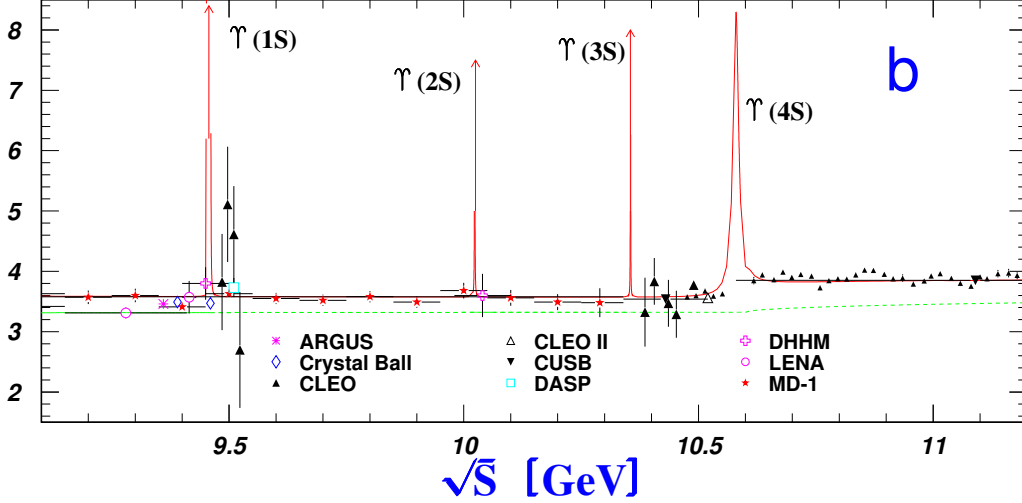
$$R_{\text{hadrons}} = \frac{4}{3} + \frac{1}{3} + \frac{1}{3} + \frac{4}{3} = \frac{10}{3}. \quad (u, d, s, c \text{ quarks}) \quad (5.2.54)$$

Finally, for $\sqrt{s} > 10$ GeV, we get

$$R_{\text{hadrons}} = \frac{4}{3} + \frac{1}{3} + \frac{1}{3} + \frac{4}{3} + \frac{1}{3} = \frac{11}{3}. \quad (u, d, s, c, b \text{ quarks}). \quad (5.2.55)$$

Besides these “continuum” contributions to R_{hadrons} , there are resonant contributions that come from $e^-e^+ \rightarrow \text{hadronic bound states}$. These bound states tend to have very large, but narrow, production cross-sections when \sqrt{s} is in just the right energy range to produce them. For example, when the bound state consists of a charm and anticharm quark, one gets the J/ψ particle resonance at $\sqrt{s} = 3.096916$ GeV, with a width of 0.00093 GeV. These resonances contribute very sharp peaks to the measured R_{hadrons} . Experimentally, R_{hadrons} is quite hard to measure, being plagued by systematic detector effects. Many of the older experiments at lower energy tended to underestimate the systematic uncertainties. Here are some plots of the data as of August 2007, from the online Review of Particle Properties, obtained from the COMPAS (Protvino) and HEPDATA (Durham) Groups, with corrections by P. Janot and M. Schmitt. The approximate agreement with the predictions for R_{hadrons} in eqs. (5.2.53)-(5.2.55) provides a crucial test of the quark model of hadrons, including the charges of the quarks and the number of colors.





5.2.3 Helicities in $e^-e^+ \rightarrow \mu^-\mu^+$

Up to now, we have computed the cross-section by averaging over the unknown spins of the initial state electron and positron. However, some e^-e^+ colliders can control the initial spin states, using polarized beams. This means that the beams are arranged to have an excess of either L-handed or R-handed helicity electrons and positrons. Practical realities make it impossible to achieve 100%-pure polarized beams, of course. At a proposed future Linear Collider, it is a very important part of the experimental program to be able to run with at least the electron beam polarized. Present estimates are that one might be able to get 90% or 95% pure polarization for the electron beam (either L or R), with perhaps 60% polarization for the positron beam. This terminology means that when the beam is operating in R mode, then a polarization of $X\%$ implies that

$$\mathcal{P}_R - \mathcal{P}_L = X\% \quad (5.2.56)$$

where \mathcal{P}_R and \mathcal{P}_L are the probabilities of measuring the spin pointing along and against the 3-momentum direction, respectively. This experimental capability shows that one needs to be able to calculate cross-sections without assuming that the initial spin state is random and averaged over.

We could redo the calculation of the previous subsections with particular spinors $u(p, s)$ and $\bar{v}(p, s)$ for the desired specific spin states s of initial state particles. However, then we would lose our precious trick of evaluating $\sum_s u\bar{u}$ and $\sum_s v\bar{v}$. A nicer way is to keep the sum over spins, but eliminate the “wrong” polarization from the sum using a projection matrix from eq. (3.2.30). So, for example, we can use

$$P_L u(p, s) \quad \longleftrightarrow \quad \text{L initial-state particle,} \quad (5.2.57)$$

$$P_R u(p, s) \longleftrightarrow \text{R initial-state particle,} \quad (5.2.58)$$

in place of the usual Feynman rules for an initial state particle. Summing over the spin s will not change the fact that the projection matrix allows only L- or R-handed electrons to contribute to the cross-section. Now our traces over gamma matrices will involve γ_5 , because of the explicit expressions for P_L and P_R [see eq. (3.2.30)].

To get the equivalent rules for an initial state antiparticle, we must remember that the spin operator acting on $v(p, s)$ spinors is the opposite of the spin operator acting on $u(p, s)$ spinors. Therefore, P_L acting on a $v(p, s)$ spinor projects onto a R-handed antiparticle. So if we form the object $\bar{v}(p, s)P_R = v^\dagger(p, s)\gamma^0 P_R = v^\dagger(p, s)P_L\gamma^0$, the result must describe a R-handed positron; in this case, the bar on the spinor for an antiparticle “corrects” the handedness. So, for an initial state antiparticle with either L or R polarization, we can use:

$$\bar{v}(p, s)P_L \longleftrightarrow \text{L initial-state anti-particle,} \quad (5.2.59)$$

$$\bar{v}(p, s)P_R \longleftrightarrow \text{R initial-state anti-particle.} \quad (5.2.60)$$

In some cases, one can also measure the polarizations of outgoing particles, for example by observing their decays. Tau leptons and anti-taus sometimes decay by the weak interaction processes:

$$\tau^- \rightarrow \ell^- \nu_\tau \bar{\nu}_\ell \quad (5.2.61)$$

$$, \tau^+ \rightarrow \ell^+ \bar{\nu}_\tau \nu_\ell, \quad (5.2.62)$$

where ℓ is either e or μ , with the angular distributions of the final state directions depending on the spin of the τ , which may be one of the final state fermions in a scattering or decay process of interest. If the polarization of a final-state fermion is fixed by measurement, then we need to use:

$$\bar{u}(p, s)P_R \longleftrightarrow \text{L final-state particle,} \quad (5.2.63)$$

$$\bar{u}(p, s)P_L \longleftrightarrow \text{R final-state particle,} \quad (5.2.64)$$

$$P_R v(p, s) \longleftrightarrow \text{L final-state anti-particle,} \quad (5.2.65)$$

$$P_L v(p, s) \longleftrightarrow \text{R final-state anti-particle,} \quad (5.2.66)$$

in order to be able to calculate cross-sections to final states with specific L or R spin polarization states. (As a result of the barred spinor notation, the general rule is that the projection matrix in an initial state has the same handedness as the incoming particle or antiparticle, while the projection matrix in a final state has the opposite handedness of the particle being produced.)

As an example, let us consider the process:

$$e_R^- e_R^+ \rightarrow \mu^- \mu^+, \quad (5.2.67)$$

where the helicities of the initial state particles are now assumed to be known perfectly. The reduced matrix element for this process, following from the same Feynman diagram as before, is:

$$\mathcal{M} = i \frac{e^2}{s} (\bar{v}_b P_R \gamma^\mu P_R u_a) (\bar{u}_2 \gamma_\mu v_1). \quad (5.2.68)$$

As you should have discovered in a homework problem, a projection matrix can be moved through a gamma matrix by changing $L \leftrightarrow R$:

$$P_R \gamma^\mu = \gamma^\mu P_L, \quad (5.2.69)$$

$$P_L \gamma^\mu = \gamma^\mu P_R. \quad (5.2.70)$$

This follows from the fact that γ_5 anticommutes with γ^μ :

$$P_R \gamma^\mu = \left(\frac{1 + \gamma_5}{2} \right) \gamma^\mu = \gamma^\mu \left(\frac{1 - \gamma_5}{2} \right) = \gamma^\mu P_L. \quad (5.2.71)$$

Therefore, eq. (5.2.68) simply vanishes, because

$$P_R \gamma^\mu P_R = \gamma^\mu P_L P_R = 0. \quad (5.2.72)$$

Therefore, the process $e_R^- e_R^+ \rightarrow \mu^- \mu^+$ does not occur in QED. Similarly, $e_L^- e_L^+ \rightarrow \mu^- \mu^+$ does not occur in QED. By the same type of argument, μ^- and μ^+ in the final state must have opposite L,R polarizations from each other in QED.

To study a non-vanishing reduced matrix element, let us therefore consider the process:

$$e_L^- e_R^+ \rightarrow \mu_L^- \mu_R^+, \quad (5.2.73)$$

in which we have now assumed that all helicities are perfectly known. To simplify matters, we will assume the high energy limit $\sqrt{s} \gg m_\mu$. The reduced matrix element can be simply obtained from eq. (5.2.3) by just putting in the appropriate L and R projection matrices acting on each external state spinor:

$$\mathcal{M} = i \frac{e^2}{s} (\bar{v}_b P_R \gamma^\mu P_L u_a) (\bar{u}_1 P_R \gamma_\mu P_L v_2). \quad (5.2.74)$$

This can be simplified slightly by using the properties of the projections matrices:

$$P_R \gamma^\mu P_L = \gamma^\mu P_L P_L = \gamma^\mu P_L, \quad (5.2.75)$$

so that

$$\mathcal{M} = i \frac{e^2}{s} (\bar{v}_b \gamma^\mu P_L u_a) (\bar{u}_1 \gamma_\mu P_L v_2), \quad (5.2.76)$$

and so

$$|\mathcal{M}|^2 = \frac{e^4}{s^2} (\bar{v}_b \gamma^\mu P_L u_a) (\bar{u}_1 \gamma_\mu P_L v_2) (\bar{v}_b \gamma^\nu P_L u_a)^* (\bar{u}_1 \gamma_\nu P_L v_2)^*. \quad (5.2.77)$$

To evaluate this, we compute:

$$(\bar{v}_b \gamma^\nu P_L u_a)^* = (v_b^\dagger \gamma^0 \gamma^\nu P_L u_a)^* = u_a^\dagger (P_L)^\dagger (\gamma^\nu)^\dagger \gamma^0 v_b \quad (5.2.78)$$

$$= u_a^\dagger P_L \gamma^0 \gamma^\nu v_b \quad (5.2.79)$$

$$= u_a^\dagger \gamma^0 P_R \gamma^\nu v_b \quad (5.2.80)$$

$$= \bar{u}_a P_R \gamma^\nu v_b. \quad (5.2.81)$$

Here we have used the facts that $(P_L)^\dagger = P_L$, and $(\gamma^\nu)^\dagger \gamma^0 = \gamma^0 \gamma^\nu$, and $P_L \gamma^0 = \gamma^0 P_R$, and $u_a^\dagger \gamma^0 = \bar{u}_a$. In a similar way,

$$(\bar{u}_1 \gamma_\nu P_L v_2)^* = \bar{v}_2 P_R \gamma_\nu u_1. \quad (5.2.82)$$

Therefore,

$$|\mathcal{M}|^2 = \frac{e^4}{s^2} (\bar{v}_b \gamma^\mu P_L u_a) (\bar{u}_a P_R \gamma^\nu v_b) (\bar{u}_1 \gamma_\mu P_L v_2) (\bar{v}_2 P_R \gamma_\nu u_1). \quad (5.2.83)$$

Because the spin projection matrices will only allow the specified set of spins to contribute anyway, we are free to sum over the spin labels s_a , s_b , s_1 , and s_2 , without changing anything. Let us do so, since it will allow us to apply the tricks

$$\sum_{s_a} u_a \bar{u}_a = \not{p}_a + m_e, \quad (5.2.84)$$

$$\sum_{s_2} v_2 \bar{v}_2 = \not{k}_2 - m_\mu. \quad (5.2.85)$$

Neglecting the masses because of the high-energy limit, we therefore have

$$|\mathcal{M}|^2 = \sum_{s_a} \sum_{s_b} \sum_{s_1} \sum_{s_2} |\mathcal{M}|^2 \quad (5.2.86)$$

$$= \frac{e^4}{s^2} \sum_{s_1} \sum_{s_b} (\bar{v}_b \gamma^\mu P_L \not{p}_a P_R \gamma^\nu v_b) (\bar{u}_1 \gamma_\mu P_L \not{k}_2 P_R \gamma_\nu u_1). \quad (5.2.87)$$

This can be simplified by eliminating excess projection matrices, using:

$$P_L \not{p}_a P_R = \not{p}_a P_R P_R = \not{p}_a P_R, \quad (5.2.88)$$

$$P_L \not{k}_2 P_R = \not{k}_2 P_R P_R = \not{k}_2 P_R, \quad (5.2.89)$$

to get

$$|\mathcal{M}|^2 = \frac{e^4}{s^2} \sum_{s_1} \sum_{s_b} (\bar{v}_b \gamma^\mu \not{p}_a P_R \gamma^\nu v_b) (\bar{u}_1 \gamma_\mu \not{k}_2 P_R \gamma_\nu u_1). \quad (5.2.90)$$

Again using the trick of putting the barred spinor at the end and taking the trace [see the discussion around eq. (5.2.13)] for each quantity in parentheses, this becomes:

$$|\mathcal{M}|^2 = \frac{e^4}{s^2} \sum_{s_1} \sum_{s_b} \text{Tr}[\gamma^\mu \not{p}_a P_R \gamma^\nu v_b \bar{v}_b] \text{Tr}[\gamma_\mu \not{k}_2 P_R \gamma_\nu u_1 \bar{u}_1]. \quad (5.2.91)$$

Doing the sums over s_1 and s_b using the usual trick gives:

$$|\mathcal{M}|^2 = \frac{e^4}{s^2} \text{Tr}[\gamma^\mu \not{p}_a P_R \gamma^\nu \not{p}_b] \text{Tr}[\gamma_\mu \not{k}_2 P_R \gamma_\nu \not{k}_1]. \quad (5.2.92)$$

Now it is time to evaluate the traces. We have

$$\text{Tr}[\gamma^\mu \not{p}_a P_R \gamma^\nu \not{p}_b] = \text{Tr}[\gamma^\mu \not{p}_a \left(\frac{1 + \gamma_5}{2}\right) \gamma^\nu \not{p}_b] \quad (5.2.93)$$

$$= \frac{1}{2} \text{Tr}[\gamma^\mu \not{p}_a \gamma^\nu \not{p}_b] + \frac{1}{2} \text{Tr}[\gamma^\mu \not{p}_a \gamma^\nu \not{p}_b \gamma_5], \quad (5.2.94)$$

where we have used the fact that γ_5 anticommutes with any gamma matrix to rearrange the order in the last term. The first of these traces was evaluated in section 5.2.1. The trace involving γ_5 is, from eq. (A.2.19):

$$\text{Tr}[\gamma^\mu \not{p}_a \gamma^\nu \not{p}_b \gamma_5] = p_{a\alpha} p_{b\beta} \text{Tr}[\gamma^\mu \gamma^\alpha \gamma^\nu \gamma^\beta \gamma_5] \quad (5.2.95)$$

$$= p_{a\alpha} p_{b\beta} (4i \epsilon^{\mu\alpha\nu\beta}). \quad (5.2.96)$$

where $\epsilon^{\mu\alpha\nu\beta}$ is the totally antisymmetric Levi-Civita tensor defined in eq. (2.3.21). Putting things together:

$$\text{Tr}[\gamma^\mu \not{p}_a P_R \gamma^\nu \not{p}_b] = 2 \left[p_a^\mu p_b^\nu - g^{\mu\nu} (p_a \cdot p_b) + p_b^\mu p_a^\nu + i p_{a\alpha} p_{b\beta} \epsilon^{\mu\alpha\nu\beta} \right]. \quad (5.2.97)$$

In exactly the same way, we get

$$\text{Tr}[\gamma_\mu \not{k}_2 P_R \gamma_\nu \not{k}_1] = 2 \left[k_{2\mu} k_{1\nu} - g_{\mu\nu} (k_2 \cdot k_1) + k_{1\mu} k_{2\nu} + i k_2^\rho k_1^\sigma \epsilon_{\rho\mu\nu\sigma} \right]. \quad (5.2.98)$$

Finally, we have to multiply these two traces together, contracting the indices μ and ν . Note that the cross-terms containing only one ϵ tensor vanish, because the epsilon tensors are antisymmetric under $\mu \leftrightarrow \nu$, while the other terms are symmetric. The term involving two epsilon tensors can be evaluated using the useful identity

$$\epsilon^{\mu\alpha\nu\beta} \epsilon_{\mu\rho\nu\sigma} = -2\delta_\rho^\alpha \delta_\sigma^\beta + 2\delta_\sigma^\alpha \delta_\rho^\beta, \quad (5.2.99)$$

which you can verify by brute force substitution of indices. The result is simply:

$$\text{Tr}[\gamma^\mu \not{p}_a P_R \gamma^\nu \not{p}_b] \text{Tr}[\gamma_\mu \not{k}_2 P_R \gamma_\nu \not{k}_1] = 16(p_a \cdot k_2)(p_b \cdot k_1), \quad (5.2.100)$$

so that

$$|\mathcal{M}|^2 = \frac{16e^4}{s^2}(p_a \cdot k_2)(p_b \cdot k_1). \quad (5.2.101)$$

This result should be plugged in to the formula for the differential cross-section:

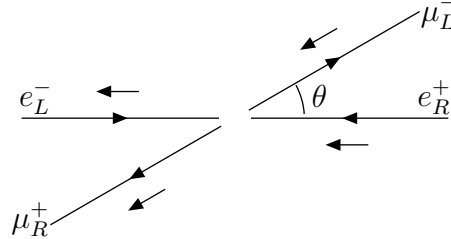
$$\frac{d\sigma_{e_L^- e_R^+ \rightarrow \mu_L^- \mu_R^+}}{d(\cos \theta)} = |\mathcal{M}|^2 \frac{|\vec{k}_1|}{32\pi s |\vec{p}_a|}. \quad (5.2.102)$$

Note that one does not average over initial-state spins in this case, because they have already been fixed. The kinematics is of course not affected by the fact that we have fixed the helicities, and so can be taken from the discussion in 5.2.1 with m_μ replaced by 0. It follows that:

$$\frac{d\sigma_{e_L^- e_R^+ \rightarrow \mu_L^- \mu_R^+}}{d(\cos \theta)} = \frac{e^4}{32\pi s} (1 + \cos \theta)^2 \quad (5.2.103)$$

$$= \frac{\pi \alpha^2}{2s} (1 + \cos \theta)^2. \quad (5.2.104)$$

The angular dependence of this result can be understood from considering the conservation of angular momentum in the event. Drawing a short arrow to represent the direction of the spin:



This shows that the total spin angular momentum of the initial state is $S_z = -1$ (taking the electron to be moving in the $+z$ direction). The total spin angular momentum of the final state is $S_{\hat{n}} = -1$, where \hat{n} is the direction of the μ^- . This explains why the cross-section vanishes if $\cos \theta = -1$; that corresponds to a final state with the total spin angular momentum in the opposite direction from the initial state. The quantum mechanical overlap for two states with measured angular momenta in exactly opposite directions must vanish. If we describe the initial and final states as eigenstates of angular momentum with $J = 1$:

$$\text{Initial state:} \quad |J_z = -1\rangle; \quad (5.2.105)$$

$$\text{Final state:} \quad |J_{\hat{n}} = -1\rangle, \quad (5.2.106)$$

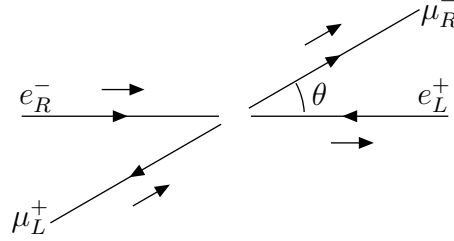
then the reduced matrix element squared is proportional to:

$$|\langle J_{\hat{n}} = -1 | J_{\hat{z}} = -1 \rangle|^2 = \frac{(1 + \cos \theta)^2}{4}. \quad (5.2.107)$$

Similarly, one can compute:

$$\frac{d\sigma_{e_R^- e_L^+ \rightarrow \mu_R^- \mu_L^+}}{d(\cos \theta)} = \frac{\pi \alpha^2}{2s} (1 + \cos \theta)^2, \quad (5.2.108)$$

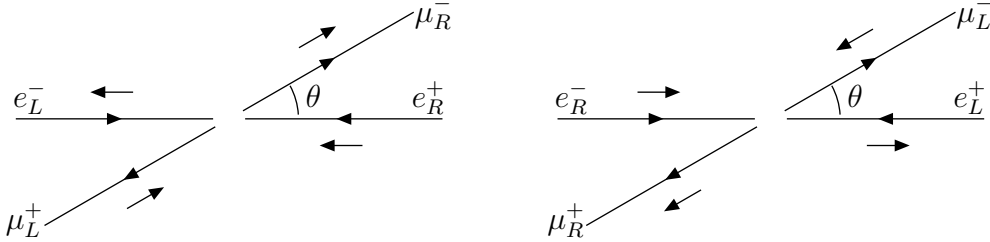
corresponding to the picture:



with all helicities reversed compared to the previous case. If we compute the cross-sections for the final state muon to have the opposite helicity from the initial state electron, we get

$$\frac{d\sigma_{e_L^- e_R^+ \rightarrow \mu_R^- \mu_L^+}}{d(\cos \theta)} = \frac{d\sigma_{e_R^- e_L^+ \rightarrow \mu_L^- \mu_R^+}}{d(\cos \theta)} = \frac{\pi \alpha^2}{2s} (1 - \cos \theta)^2, \quad (5.2.109)$$

corresponding to the pictures:



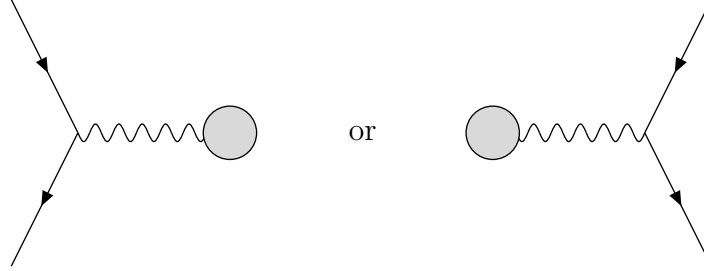
These are 4 of the possible $2^4 = 16$ possible helicity configurations for $e^- e^+ \rightarrow \mu^- \mu^+$. However, as we have already seen, the other 12 possible helicity combinations all vanish, because they contain either e^- and e^+ with the same helicity, or μ^- and μ^+ with the same helicity. If we take the average of the initial state helicities, and the sum of the possible final state helicities, we get:

$$\begin{aligned} & \frac{1}{4} \left[\frac{d\sigma_{e_L^- e_R^+ \rightarrow \mu_L^- \mu_R^+}}{d(\cos \theta)} + \frac{d\sigma_{e_R^- e_L^+ \rightarrow \mu_R^- \mu_L^+}}{d(\cos \theta)} + \frac{d\sigma_{e_L^- e_R^+ \rightarrow \mu_R^- \mu_L^+}}{d(\cos \theta)} + \frac{d\sigma_{e_R^- e_L^+ \rightarrow \mu_L^- \mu_R^+}}{d(\cos \theta)} + 12 \cdot 0 \right] \\ &= \frac{1}{4} \left(\frac{\pi \alpha^2}{2s} \right) [2(1 + \cos \theta)^2 + 2(1 - \cos \theta)^2] \end{aligned} \quad (5.2.110)$$

$$= \frac{\pi \alpha^2}{2s} (1 + \cos^2 \theta), \quad (5.2.111)$$

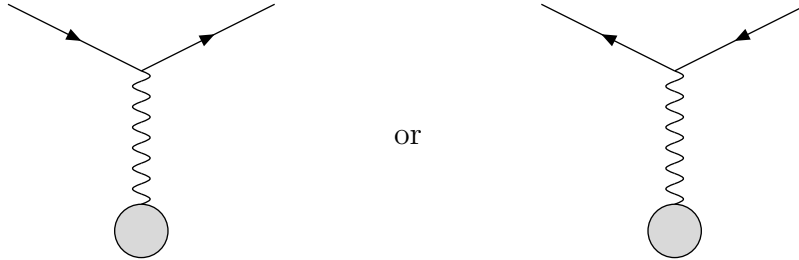
in agreement with the $\sqrt{s} \gg m_\mu$ limit of eq. (5.2.40).

The vanishing of the cross-sections for $e_L^- e_L^+$ and $e_R^- e_R^+$ in the above process can be generalized beyond this example and even beyond QED. Consider any field theory in which interactions are given by a fermion-antifermion-vector vertex with a Feynman rule proportional to a gamma matrix γ^μ . If an initial state fermion and antifermion merge into a vector, or a vector splits into a final state fermion and antifermion:



then by exactly the same argument as before, the fermion and antifermion must have *opposite* helicities, because of $\bar{v}P_L\gamma^\mu P_L u = \bar{v}P_R\gamma^\mu P_R u = 0$ and $\bar{u}P_L\gamma^\mu P_L v = \bar{u}P_R\gamma^\mu P_R v = 0$ and the rules of eqs. (5.2.57)-(5.2.60) and (5.2.63)-(5.2.66).

Moreover, if an initial state fermion (or anti-fermion) interacts with a vector and emerges as a final state fermion (or anti-fermion):



then the fermions (or anti-fermions) must have the *same* helicity, because of the identities $\bar{u}P_L\gamma^\mu P_L u = \bar{u}P_R\gamma^\mu P_R u = 0$ and $\bar{v}P_L\gamma^\mu P_L v = \bar{v}P_R\gamma^\mu P_R v = 0$. This is true even if the interaction with the vector changes the fermion from one type to another.

These rules embody the concept of helicity conservation in high energy scattering. They are obviously useful when the helicities of the particles are controlled or measured by the experimenter. They are also useful because, as we will see, the weak interactions only affect fermions with L helicity and antifermions with R helicity. The conservation of angular momentum together with helicity conservation often allows one to know in which direction a particle is most likely to emerge in a scattering or decay experiment, and in what cases one may expect the cross-section to vanish or be enhanced.

5.2.4 Bhabha scattering ($e^-e^+ \rightarrow e^-e^+$)

In this subsection we consider the process of Bhabha scattering:

$$e^-e^+ \rightarrow e^-e^+. \quad (5.2.112)$$

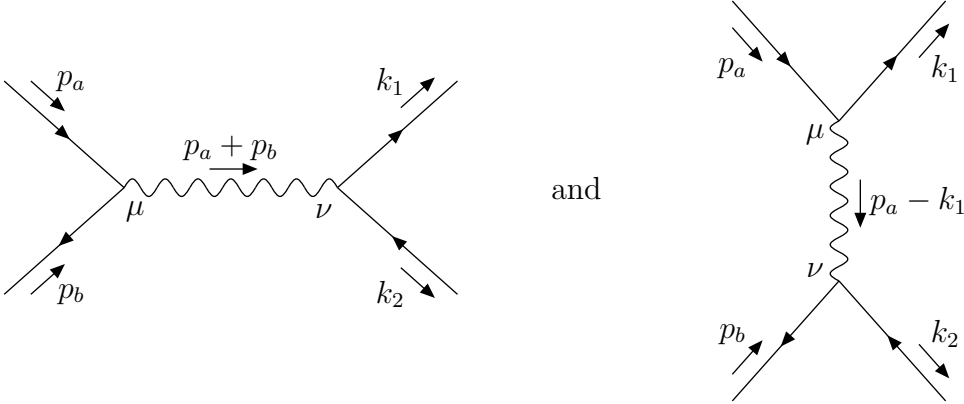
For simplicity we will only consider the case of high-energy scattering, with $\sqrt{s} = E_{\text{CM}} \gg m_e$, and we will consider all spins to be unknown (averaged over in the initial state, summed over in the final state).

Label the momentum and spin data as follows:

Particle	Momentum	Spin	Spinor
e^-	p_a	s_a	$u(p_a, s_a)$
e^+	p_b	s_b	$\bar{v}(p_b, s_b)$
e^-	k_1	s_1	$\bar{u}(k_1, s_1)$
e^+	k_2	s_2	$v(k_2, s_2)$

(5.2.113)

At order e^2 , there are two Feynman diagram for this process:



The first of these is called the s -channel diagram; it is exactly the same as the one we drew for $e^-e^+ \rightarrow \mu^-\mu^+$. The second one is called the t -channel diagram. Using the QED Feynman rules listed at the end of subsection 5.1, the corresponding contributions to the reduced matrix element for the process are:

$$\mathcal{M}_s = [\bar{v}_b(ie\gamma^\mu)u_a] \left[\frac{-ig_{\mu\nu}}{(p_a + p_b)^2} \right] [\bar{u}_1(ie\gamma^\nu)v_2], \quad (5.2.114)$$

and

$$\mathcal{M}_t = (-1) [\bar{u}_1(ie\gamma^\mu)u_a] \left[\frac{-ig_{\mu\nu}}{(p_a - k_1)^2} \right] [\bar{v}_b(ie\gamma^\nu)v_2]. \quad (5.2.115)$$

The additional (-1) factor in \mathcal{M}_t is due to Rule 9 in the QED Feynman rules at the end of section 5.1. It arises because the order of spinors in the written expression for \mathcal{M}_s is $b, a, 1, 2$,

but that in \mathcal{M}_t is 1, $a, b, 2$, and these differ from each other by an odd permutation. We could have just as well assigned the minus sign to \mathcal{M}_s instead; only the relative phases of terms in the matrix element are significant.

Therefore the full reduced matrix element for Bhabha scattering, written in terms of the Mandelstam variables $s = (p_a + p_b)^2$ and $t = (p_a - k_1)^2$, is:

$$\mathcal{M} = \mathcal{M}_s + \mathcal{M}_t = ie^2 \left\{ \frac{1}{s} (\bar{v}_b \gamma_\mu u_a) (\bar{u}_1 \gamma^\mu v_2) - \frac{1}{t} (\bar{u}_1 \gamma_\mu u_a) (\bar{v}_b \gamma^\mu v_2) \right\}. \quad (5.2.116)$$

Taking the complex conjugate of this gives:

$$\mathcal{M}^* = \mathcal{M}_s^* + \mathcal{M}_t^* \quad (5.2.117)$$

$$= -ie^2 \left\{ \frac{1}{s} (\bar{v}_b \gamma_\nu u_a)^* (\bar{u}_1 \gamma^\nu v_2)^* - \frac{1}{t} (\bar{u}_1 \gamma_\nu u_a)^* (\bar{v}_b \gamma^\nu v_2)^* \right\} \quad (5.2.118)$$

$$= -ie^2 \left\{ \frac{1}{s} (\bar{u}_a \gamma_\nu v_b) (\bar{v}_2 \gamma^\nu u_1) - \frac{1}{t} (\bar{u}_a \gamma_\nu u_1) (\bar{v}_2 \gamma^\nu v_b) \right\}. \quad (5.2.119)$$

The complex square of the reduced matrix element, $|\mathcal{M}|^2 = \mathcal{M}^* \mathcal{M}$, contains a pure s -channel piece proportional to $1/s^2$, a pure t -channel piece proportional to $1/t^2$, and an interference piece proportional to $1/st$. For organizational purposes, it is useful to calculate these pieces separately.

The pure s -channel contribution calculation is exactly the same as what we did before for $e^- e^+ \rightarrow \mu^- \mu^+$, except that now we can substitute $m_\mu \rightarrow m_e \rightarrow 0$. Therefore, plagiarizing the result of eq. (5.2.25), we have:

$$\frac{1}{4} \sum_{\text{spins}} |\mathcal{M}_s|^2 = \frac{8e^4}{s^2} [(p_a \cdot k_2)(p_b \cdot k_1) + (p_a \cdot k_1)(p_b \cdot k_2)]. \quad (5.2.120)$$

The pure t -channel contribution can be calculated in a very similar way. We have:

$$|\mathcal{M}_t|^2 = \frac{e^4}{t^2} (\bar{v}_2 \gamma_\nu v_b) (\bar{v}_b \gamma_\mu v_2) (\bar{u}_1 \gamma^\mu u_a) (\bar{u}_a \gamma^\nu u_1). \quad (5.2.121)$$

Taking the average of initial state spins and the sum over final state spins allows us to use the identities $\sum_{s_a} u_a \bar{u}_a = \not{p}_a$ and $\sum_{s_a} v_b \bar{v}_b = \not{p}_b$ (neglecting m_e). The result is:

$$\frac{1}{4} \sum_{\text{spins}} |\mathcal{M}_t|^2 = \frac{e^4}{4t^2} \sum_{s_1, s_2} (\bar{v}_2 \gamma_\nu \not{p}_b \gamma_\mu v_2) (\bar{u}_1 \gamma^\mu \not{p}_a \gamma^\nu u_1) \quad (5.2.122)$$

$$= \frac{e^4}{4t^2} \sum_{s_1, s_2} \text{Tr}[\gamma_\nu \not{p}_b \gamma_\mu v_2 \bar{v}_2] \text{Tr}[\gamma^\mu \not{p}_a \gamma^\nu u_1 \bar{u}_1], \quad (5.2.123)$$

in which we have turned the quantity into a trace by moving the \bar{u}_1 to the end. Now performing the sums over s_1, s_2 gives:

$$\frac{1}{4} \sum_{\text{spins}} |\mathcal{M}_t|^2 = \frac{e^4}{4t^2} \text{Tr}[\gamma_\nu \not{p}_b \gamma_\mu \not{k}_2] \text{Tr}[\gamma^\mu \not{p}_a \gamma^\nu \not{k}_1] \quad (5.2.124)$$

$$= \frac{e^4}{4t^2} \text{Tr}[\gamma_\mu \not{k}_2 \gamma_\nu \not{p}_b] \text{Tr}[\gamma^\mu \not{p}_a \gamma^\nu \not{k}_1]. \quad (5.2.125)$$

In the second line, the first trace has been rearranged using the cyclic property of traces. The point of doing so is that now these traces have exactly the same form that we encountered in eq. (5.2.19), but with $p_a \leftrightarrow k_2$ and $m_\mu \rightarrow 0$. Therefore we can obtain $\frac{1}{4} \sum_{\text{spins}} |\mathcal{M}_t|^2$ by simply making the same replacements $p_a \leftrightarrow k_2$ and $m_\mu \rightarrow 0$ in eq. (5.2.25):

$$\frac{1}{4} \sum_{\text{spins}} |\mathcal{M}_t|^2 = \frac{8e^4}{t^2} [(p_a \cdot k_2)(p_b \cdot k_1) + (k_2 \cdot k_1)(p_b \cdot p_a)]. \quad (5.2.126)$$

Next, consider the interference term:

$$\frac{1}{4} \sum_{\text{spins}} \mathcal{M}_t^* \mathcal{M}_s = -\frac{e^4}{4st} \sum_{\text{spins}} (\bar{v}_b \gamma_\mu u_a) (\bar{u}_a \gamma^\nu u_1) (\bar{u}_1 \gamma^\mu v_2) (\bar{v}_2 \gamma_\nu v_b). \quad (5.2.127)$$

We chose to write the factors parentheses in that order, so that now we can immediately use the tricks $\sum_{s_a} u_a \bar{u}_a = \not{p}_a$, and $\sum_{s_1} u_1 \bar{u}_1 = \not{k}_1$, and $\sum_{s_2} v_2 \bar{v}_2 = \not{k}_2$, to obtain:

$$\frac{1}{4} \sum_{\text{spins}} \mathcal{M}_t^* \mathcal{M}_s = -\frac{e^4}{4st} \sum_{s_b} (\bar{v}_b \gamma_\mu \not{p}_a \gamma^\nu \not{k}_1 \gamma^\mu \not{k}_2 \gamma_\nu v_b), \quad (5.2.128)$$

which can now be converted into a trace by the usual trick of moving the \bar{v}_b to the end:

$$\frac{1}{4} \sum_{\text{spins}} \mathcal{M}_t^* \mathcal{M}_s = -\frac{e^4}{4st} \sum_{s_b} \text{Tr}[\gamma_\mu \not{p}_a \gamma^\nu \not{k}_1 \gamma^\mu \not{k}_2 \gamma_\nu v_b \bar{v}_b] \quad (5.2.129)$$

$$= -\frac{e^4}{4st} \text{Tr}[\gamma_\mu \not{p}_a \gamma^\nu \not{k}_1 \gamma^\mu \not{k}_2 \gamma_\nu \not{p}_b]. \quad (5.2.130)$$

Now we are faced with the task of computing the trace of 8 gamma matrices. In principle, the trace of any number of gamma matrices can be performed with the algorithm of eq. (A.2.11). The procedure is to replace the trace over $2n$ gamma matrices by a sum over traces of $2n - 2$ gamma matrices, and repeat until all traces are short enough to evaluate using eqs. (A.2.8)-(A.2.11) and (A.2.15)-(A.2.19). However, in many cases including the present one it is easier to simplify the contents of the trace first, using eqs. (A.2.20)-(A.2.23). To evaluate the trace in eq. (5.2.130), we first use eq. (A.2.23) to write:

$$\gamma_\mu \not{p}_a \gamma^\nu \not{k}_1 \gamma^\mu = -2 \not{k}_1 \gamma^\nu \not{p}_a, \quad (5.2.131)$$

which implies that

$$\text{Tr}[\gamma_\mu \not{p}_a \gamma^\nu \not{k}_1 \gamma^\mu \not{k}_2 \gamma_\nu \not{p}_b] = -2 \text{Tr}[\not{k}_1 \gamma^\nu \not{p}_a \not{k}_2 \gamma_\nu \not{p}_b]. \quad (5.2.132)$$

This can be further simplified by now using eq. (A.2.22) to write:

$$\gamma^\nu \not{p}_a \not{k}_2 \gamma_\nu = 4 p_a \cdot k_2, \quad (5.2.133)$$

so that:

$$\text{Tr}[\gamma_\mu \not{p}_a \gamma^\nu \not{k}_1 \gamma^\mu \not{k}_2 \gamma_\nu \not{p}_b] = -8(p_a \cdot k_2) \text{Tr}[\not{k}_1 \not{p}_b] \quad (5.2.134)$$

$$= -32(p_a \cdot k_2)(k_1 \cdot p_b), \quad (5.2.135)$$

in which the trace has finally been performed using eq. (A.2.9). So, from eq. (5.2.130)

$$\frac{1}{4} \sum_{\text{spins}} \mathcal{M}_t^* \mathcal{M}_s = \frac{8e^4}{st} (p_a \cdot k_2)(p_b \cdot k_1). \quad (5.2.136)$$

Taking the complex conjugate of both sides, we also have:

$$\frac{1}{4} \sum_{\text{spins}} \mathcal{M}_s^* \mathcal{M}_t = \frac{8e^4}{st} (p_a \cdot k_2)(p_b \cdot k_1). \quad (5.2.137)$$

This completes the contributions to the total

$$\frac{1}{4} \sum_{\text{spins}} |\mathcal{M}|^2 = \frac{1}{4} \sum_{\text{spins}} [|\mathcal{M}_s|^2 + |\mathcal{M}_t|^2 + \mathcal{M}_t^* \mathcal{M}_s + \mathcal{M}_s^* \mathcal{M}_t]. \quad (5.2.138)$$

It remains to identify the dot products of momenta appearing in the above formulas. This can be done by carrying over the kinematic analysis for the case $e^- e^+ \rightarrow \mu^- \mu^+$ as worked out in eqs. (5.2.26)-(5.2.36), with $m_\mu, m_e \rightarrow 0$. Letting θ be the angle between the 3-momenta directions of the initial state electron and the final state electron, we have:

$$p_a \cdot p_b = k_1 \cdot k_2 = s/2, \quad (5.2.139)$$

$$p_a \cdot k_1 = p_b \cdot k_2 = -t/2, \quad (5.2.140)$$

$$p_a \cdot k_2 = p_b \cdot k_1 = -u/2, \quad (5.2.141)$$

with

$$t = -\frac{s}{2}(1 - \cos \theta), \quad (5.2.142)$$

$$u = -\frac{s}{2}(1 + \cos \theta). \quad (5.2.143)$$

It follows from eqs. (5.2.120), (5.2.126), (5.2.136), and (5.2.137) that:

$$\frac{1}{4} \sum_{\text{spins}} |\mathcal{M}_s|^2 = \frac{2e^4}{s^2} (u^2 + t^2) \quad (5.2.144)$$

$$\frac{1}{4} \sum_{\text{spins}} |\mathcal{M}_t|^2 = \frac{2e^4}{t^2} (u^2 + s^2) \quad (5.2.145)$$

$$\frac{1}{4} \sum_{\text{spins}} (\mathcal{M}_t^* \mathcal{M}_s + \mathcal{M}_s^* \mathcal{M}_t) = \frac{4e^4}{st} u^2. \quad (5.2.146)$$

Putting this into eq. (4.5.49), since $|\vec{p}_a| = |\vec{k}_1|$, we obtain the spin-averaged differential cross-section for Bhabha scattering:

$$\frac{d\sigma}{d(\cos\theta)} = \frac{e^4}{16\pi s} \left(\frac{u^2 + t^2}{s^2} + \frac{u^2 + s^2}{t^2} + \frac{2u^2}{st} \right) \quad (5.2.147)$$

$$= \frac{\pi\alpha^2}{2s} \left(\frac{3 + \cos^2\theta}{1 - \cos\theta} \right)^2. \quad (5.2.148)$$

This result actually diverges for $\cos\theta \rightarrow 1$, because of the t 's in the denominator. This is not an integrable singularity, because the differential cross-section blows up quadratically near $\cos\theta = 1$, so

$$\sigma = \int_{-1}^1 \frac{d\sigma}{d(\cos\theta)} d(\cos\theta) \rightarrow \infty. \quad (5.2.149)$$

The infinite total cross-section corresponds to the infinite range of the Coulomb potential between two charged particles. It arises entirely from the t -channel diagram, in which the electron and positron scatter off of each other in the forward direction ($\theta \approx 0$). It simply reflects that an infinite-range interaction will always produce *some* deflection, although it may be extremely small. This result is the relativistic generalization of the non-relativistic, classical Rutherford scattering problem, in which an electron or alpha particle (or some other light charged particle) scatters off of the classical electric field of a heavy nucleus. As worked out in many textbooks on classical physics (for example, H. Goldstein's *Classical Mechanics*, J.D. Jackson's *Classical Electrodynamics*), the differential cross-section for a non-relativistic light particle with charge Q_A and a heavy particle with charge Q_B , with center-of-momentum energy E_{CM} to scatter through their Coulomb interaction is:

$$\frac{d\sigma_{\text{Rutherford}}}{d(\cos\theta)} = \frac{\pi Q_A^2 Q_B^2 \alpha^2}{2E^2 (1 - \cos\theta)^2}. \quad (5.2.150)$$

(Here one must be careful in comparing results, because the charge e used by Goldstein and Jackson differs from the one used here by a factor of $\sqrt{4\pi}$.) Comparing the non-relativistic Rutherford result to the relativistic Bhabha result, we see that in both cases the small-angle behavior scales like $1/\theta^4$, and does not depend on the signs of the charges of the particles.

In a real experiment, there is always some minimum scattering angle that can be resolved. In a colliding-beam experiment, this is usually dictated by the fact that detectors cannot be placed within or too close to the beamline. In other experiments, one is limited by the angular resolution of detectors. Therefore, the true observable quantity is typically something more like:

$$\sigma_{\text{experiment}} = \int_{-\cos\theta_{\text{cut}}}^{\cos\theta_{\text{cut}}} \frac{d\sigma}{d(\cos\theta)} d(\cos\theta). \quad (5.2.151)$$

Of course, in the Real World, the minimum resolvable angle is just one of many practical factors that have to be included.

In terms of the Feynman diagram interpretation, the divergence for small θ corresponds to the photon propagator going on-shell; in other words, the situation where the square of the t -channel virtual photon's 4-momentum is nearly equal to 0, the classical value for a real massless photon. For any scattering angle $\theta > 0$, one has

$$(p_a - k_1)^2 = t = \frac{s}{2}(1 - \cos \theta) > 0, \quad (5.2.152)$$

so that the virtual photon is said to be off-shell. In general, any time that a virtual (internal line) particle can go on-shell, there will be a divergence in the cross-section due to the denominator of the Feynman propagator blowing up. Sometimes this is a real divergence with a physical interpretation, as in the case of Bhabha scattering. In other cases, the divergence is removed by higher-order effects, such as the finite life-time of the virtual particle, which will give an imaginary part to its squared mass, removing the singularity in the Feynman propagator.

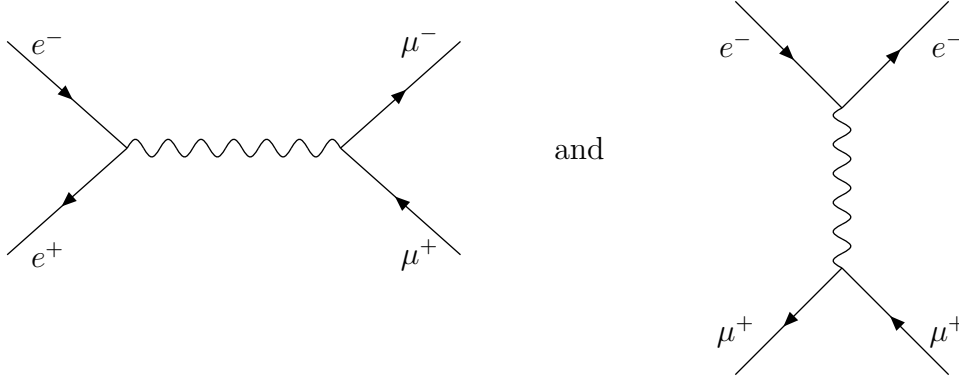
5.3 Crossing symmetry

Consider the two completely different processes:

$$e^- e^+ \rightarrow \mu^- \mu^+ \quad (5.3.1)$$

$$e^- \mu^+ \rightarrow e^- \mu^+. \quad (5.3.2)$$

The relevant Feynman diagrams for these two processes are very similar:



In fact, by stretching and twisting, one can turn the first process into the second by the transformation:

$$\text{initial } e^+ \rightarrow \text{final } e^- \quad (5.3.3)$$

$$\text{final } \mu^- \rightarrow \text{initial } \mu^+, \quad (5.3.4)$$

Two processes related to each other by exchanging some initial state particles with their antiparticles in the final state are said to be related by crossing. Not surprisingly, the reduced

matrix elements for these processes are also quite similar. For example, in the high-energy limit $\sqrt{s} \gg m_\mu$,

$$\frac{1}{4} \sum_{\text{spins}} |\mathcal{M}_{e^- e^+ \rightarrow \mu^- \mu^+}|^2 = 2e^4 \left(\frac{u^2 + t^2}{s^2} \right), \quad (5.3.5)$$

$$\frac{1}{4} \sum_{\text{spins}} |\mathcal{M}_{e^- \mu^+ \rightarrow e^- \mu^+}|^2 = 2e^4 \left(\frac{u^2 + s^2}{t^2} \right). \quad (5.3.6)$$

This similarity is generalized and made more precise by the following theorem.

Crossing Symmetry Theorem: Suppose two Feynman diagrams with reduced matrix elements \mathcal{M} and \mathcal{M}' are related by the exchange (“crossing”) of some initial state particles and antiparticles for the corresponding final state antiparticles and particles. If the crossed particles have 4-momenta P_1^μ, \dots, P_n^μ in \mathcal{M} , then $\sum_{\text{spins}} |\mathcal{M}|^2$ can be obtained by substituting $P_i'^\mu = -P_i^\mu$ into the mathematical expression for $\sum_{\text{spins}} |\mathcal{M}'|^2$, as follows:

$$\sum_{\text{spins}} |\mathcal{M}(P_1^\mu, \dots, P_n^\mu, \dots)|^2 = (-1)^F \sum_{\text{spins}} |\mathcal{M}'(P_1'^\mu, \dots, P_n'^\mu, \dots)|^2 \Big|_{P_i'^\mu \rightarrow -P_i^\mu}, \quad (5.3.7)$$

with the other (uncrossed) particle 4-momenta unaffected. Here F is the number of fermion lines that were crossed.

If $p^\mu = (E, \vec{p})$ is a valid physical 4-momentum, then $p'^\mu = (-E, -\vec{p})$ is never a physical 4-momentum, since it has negative energy. So the relation between the two diagrams is a formal one rather than a relation between physical reduced matrix elements that would actually be measured; when one of the matrix elements involves the 4-momenta appropriate for a physical process, the other one does not. However, it is still perfectly valid as a mathematical relation, and therefore extremely useful. In general, if one has calculated the cross-section or reduced matrix element for one process, one can obtain the results for several “crossed” processes by merely substituting momenta, with no additional labor. Equation (5.3.7) might look dubious at first, since it may look like the right-hand side is negative for odd F . However, the point is that when the expression for $|\mathcal{M}'|^2$ is analytically continued to unphysical momenta, it always flips sign for odd F . We will see this in some examples later.

5.3.1 $e^- \mu^+ \rightarrow e^- \mu^+$ and $e^- \mu^- \rightarrow e^- \mu^-$

Let us apply crossing symmetry to the example of eqs. (5.3.1) and (5.3.2) by assigning primed momenta to the Feynman diagram for $e^- e^+ \rightarrow \mu^- \mu^+$:

$$\text{initial state} \begin{cases} e^- & \leftrightarrow p'_a \\ e^+ & \leftrightarrow p'_b \end{cases} \quad (5.3.8)$$

$$\text{final state} \begin{cases} \mu^- & \leftrightarrow k'_1 \\ \mu^+ & \leftrightarrow k'_2. \end{cases} \quad (5.3.9)$$

Label the momenta in the crossed Feynman diagram (for $e^- \mu^+ \rightarrow e^- \mu^+$) without primes:

$$\text{initial state} \begin{cases} e^- & \leftrightarrow p_a \\ \mu^+ & \leftrightarrow p_b \end{cases} \quad (5.3.10)$$

$$\text{final state} \begin{cases} e^- & \leftrightarrow k_1 \\ \mu^+ & \leftrightarrow k_2. \end{cases} \quad (5.3.11)$$

Then the Crossing Symmetry Theorem tells us that we can get the reduced matrix element for the process $e^- \mu^+ \rightarrow e^- \mu^+$ as a function of physical momenta p_a, p_b, k_1, k_2 by substituting unphysical momenta

$$p'_a = p_a; \quad p'_b = -k_1; \quad k'_1 = -p_b; \quad k'_2 = k_2, \quad (5.3.12)$$

into the formula for the reduced matrix element for the process $e^- e^+ \rightarrow \mu^- \mu^+$. This means that we can identify:

$$s' = (p'_a + p'_b)^2 = (p_a - k_1)^2 = t, \quad (5.3.13)$$

$$t' = (p'_a - k'_1)^2 = (p_a + p_b)^2 = s, \quad (5.3.14)$$

$$u' = (p'_a - k'_2)^2 = (p_a - k_2)^2 = u. \quad (5.3.15)$$

In other words, crossing symmetry tells us that the formulas for the reduced matrix elements for these two processes are just related by the exchange of s and t , as illustrated in the high-energy limit in eqs. (5.3.5) and (5.3.6). Since we had already derived the result for the first process in section 5.2.1, the second result has been obtained for free. Note that we could have obtained the particular result (5.3.6) even more easily just by noting that the calculation for the reduced matrix element of $e^- \mu^+ \rightarrow e^- \mu^+$ is exactly the same as for Bhabha scattering, except that only the t -channel diagram exists in the former case. So one only keeps the contribution with t (not s or u) in the denominator, since that corresponds to the t -channel diagram.

We can carry this further by considering another process also related by crossing to the two just studied:

$$e^- \mu^- \rightarrow e^- \mu^-, \quad (5.3.16)$$

with physical momenta:

$$\text{initial state} \begin{cases} e^- & \leftrightarrow p_a \\ \mu^- & \leftrightarrow p_b \end{cases} \quad (5.3.17)$$

$$\text{final state} \begin{cases} e^- & \leftrightarrow k_1 \\ \mu^- & \leftrightarrow k_2 \end{cases} . \quad (5.3.18)$$

This time, the Crossing Symmetry Theorem tells us that we can identify the matrix element by again starting with the reduced matrix element for $e^-e^+ \rightarrow \mu^-\mu^+$ and replacing:

$$p'_a = p_a; \quad p'_b = -k_1; \quad k'_1 = k_2; \quad k'_2 = -p_b, \quad (5.3.19)$$

so that

$$s' = (p'_a + p'_b)^2 = (p_a - k_1)^2 = t, \quad (5.3.20)$$

$$t' = (p'_a - k'_1)^2 = (p_a - k_2)^2 = u, \quad (5.3.21)$$

$$u' = (p'_a - k'_2)^2 = (p_a + p_b)^2 = s. \quad (5.3.22)$$

Here the primed Mandelstam variable are the unphysical ones for the $e^-e^+ \rightarrow \mu^-\mu^+$ process, and the unprimed ones are for the desired process $e^-\mu^- \rightarrow e^-\mu^-$. We can therefore infer, from eq. (5.3.5), that

$$\frac{1}{4} \sum_{\text{spins}} |\mathcal{M}_{e^-\mu^- \rightarrow e^-\mu^-}|^2 = 2e^4 \left(\frac{s^2 + u^2}{t^2} \right), \quad (5.3.23)$$

by doing the substitutions indicated by eqs. (5.3.20)-(5.3.22).

By comparing eq. (5.3.6) to eq. (5.3.23), one sees that the spin averaged and summed squared matrix elements for the two processes are actually the same; the charge of the muon does not matter at leading order. Because we are neglecting the muon mass, the kinematics relating t and u to the scattering angle θ between the initial-state electron and the final state electron in these two cases is just the same as in Bhabha scattering:

$$t = -\frac{s}{2}(1 - \cos \theta); \quad u = -\frac{s}{2}(1 + \cos \theta). \quad (5.3.24)$$

Therefore, putting eq. (5.3.23) into eq. (4.5.49) with $|\vec{p}_a| = |\vec{k}_1|$ and using $e^2 = 4\pi\alpha$, we obtain the differential cross-section for $e^-\mu^\pm \rightarrow e^-\mu^\pm$:

$$\frac{d\sigma}{d(\cos \theta)} = \frac{\pi\alpha^2}{s} \left(\frac{u^2 + s^2}{t^2} \right) \quad (5.3.25)$$

$$= \frac{\pi\alpha^2}{2s} \frac{5 + 2\cos \theta + \cos^2 \theta}{(1 - \cos \theta)^2}. \quad (5.3.26)$$

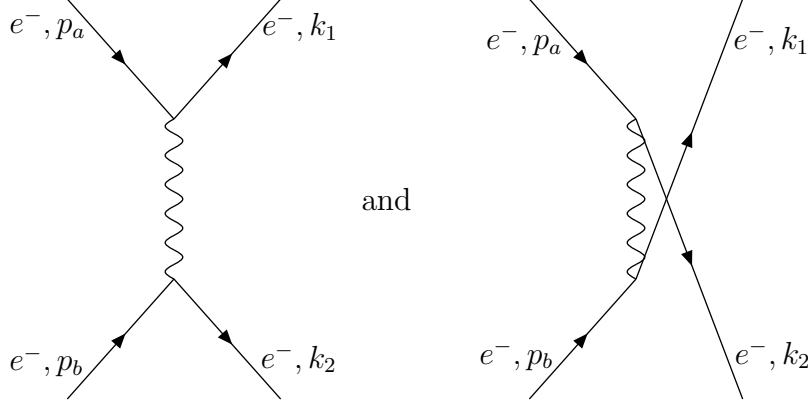
Note that this again diverges for forward scattering $\cos \theta \rightarrow 1$.

5.3.2 Møller scattering ($e^-e^- \rightarrow e^-e^-$)

As another example, let us consider the case of Møller scattering:

$$e^-e^- \rightarrow e^-e^-. \quad (5.3.27)$$

There are two Feynman diagrams for this process:



Now, nobody can stop us from getting the result for this process by applying the Feynman rules to get the reduced matrix element, taking the complex square, summing and averaging over spins, and computing the Dirac traces. However, an easier way is to note that this is a crossed version of Bhabha scattering, which we studied earlier. Making a table of the momenta:

Bhabha	Møller	(5.3.28)
--------	--------	----------

$e^- \leftrightarrow p'_a$	$e^- \leftrightarrow p_a$	(5.3.29)
----------------------------	---------------------------	----------

$e^+ \leftrightarrow p'_b$	$e^- \leftrightarrow p_b$	(5.3.30)
----------------------------	---------------------------	----------

$e^- \leftrightarrow k'_1$	$e^- \leftrightarrow k_1$	(5.3.31)
----------------------------	---------------------------	----------

$e^+ \leftrightarrow k'_2$	$e^- \leftrightarrow k_2,$	(5.3.32)
----------------------------	----------------------------	----------

we see that crossing symmetry allows us to compute the Møller scattering by identifying the (initial state positron, final state positron) in Bhabha scattering with the (final state electron, initial state electron) in Møller scattering, so that:

$$p'_a = p_a \quad p'_b = -k_2 \quad k'_1 = k_1 \quad k'_2 = -p_b. \quad (5.3.33)$$

Therefore, the Møller scattering reduced matrix element is obtained by putting

$$s' = (p'_a + p'_b)^2 = (p_a - k_2)^2 = u \quad (5.3.34)$$

$$t' = (p'_a - k'_1)^2 = (p_a - k_1)^2 = t \quad (5.3.35)$$

$$u' = (p'_a - k'_2)^2 = (p_a + p_b)^2 = s \quad (5.3.36)$$

into the corresponding result for Bhabha scattering. Using the results of eq. (5.2.144)-(5.2.146), we get:

$$\frac{1}{4} \sum_{\text{spins}} |\mathcal{M}_{e^-e^- \rightarrow e^-e^-}|^2 = 2e^2 \left(\frac{s^2 + t^2}{u^2} + \frac{s^2 + u^2}{t^2} + \frac{2s^2}{ut} \right). \quad (5.3.37)$$

Again, if we keep only the t -channel part (that is, the part with t^2 in the denominator), we recover the result for $e^-\mu^\pm \rightarrow e^-\mu^\pm$ in the previous section.

Applying eq. (4.5.49), we find the differential cross-section:

$$\frac{d\sigma_{e^-e^- \rightarrow e^-e^-}}{d(\cos\theta)} = \frac{1}{32\pi s} \left(\frac{1}{4} \sum_{\text{spins}} |\mathcal{M}_{e^-e^- \rightarrow e^-e^-}|^2 \right) \quad (5.3.38)$$

$$= \frac{\pi\alpha^2}{s} \left(\frac{s^2 + t^2}{u^2} + \frac{s^2 + u^2}{t^2} + \frac{2s^2}{ut} \right) \quad (5.3.39)$$

$$= \frac{2\pi\alpha^2}{s} \left(\frac{3 + \cos^2\theta}{1 - \cos^2\theta} \right)^2. \quad (5.3.40)$$

Just as in the cases in the previous sections, $t = -s(1 - \cos\theta)/2$ and $u = -2(1 + \cos\theta)/2$ where θ is the angle between the initial-state and final-state electrons. However, in this case there is a special feature, because the two electrons in the final state are indistinguishable particles. This means that the final state with an electron coming out at angles (θ, ϕ) is actually the *same* quantum state as the one with an electron coming out at angles $(\pi - \theta, -\phi)$. (As a check, note that eq. (5.3.40) is invariant under $\cos\theta \rightarrow -\cos\theta$. We have already integrated over the angle ϕ .) Therefore, to avoid overcounting we must only integrate over half the range of θ , or equivalently divide the total cross-section by 2. So, we have a tricky and crucial factor of $1/2$ in the total cross-section:

$$\sigma_{e^-e^- \rightarrow e^-e^-} = \frac{1}{2} \int_{-\cos\theta_{\text{cut}}}^{\cos\theta_{\text{cut}}} \frac{d\sigma_{e^-e^- \rightarrow e^-e^-}}{d(\cos\theta)} d(\cos\theta). \quad (5.3.41)$$

To obtain a finite value for the total cross-section, we had to also impose a cut on the minimum scattering angle θ_{cut} that we require in order to say that a scattering event should be counted.

5.4 Gauge invariance in Feynman diagrams

Let us now turn to the issue of gauge invariance as it is manifested in QED Feynman diagrams. Recall that when we found the Feynman propagator for a photon, it contained a term that depended on an arbitrary parameter ξ . We have been working with $\xi = 1$ (Feynman gauge). Consider what the matrix element for the process $e^-e^+ \rightarrow \mu^-\mu^+$ would be if instead we let ξ remain unfixed. Instead of eq. (5.2.2), we would have

$$\mathcal{M} = (\bar{v}_b \gamma^\mu u_a)(\bar{u}_1 \gamma^\nu v_2) \frac{ie^2}{(p_a + p_b)^2} \left[-g_{\mu\nu} + (1 - \xi) \frac{(p_a + p_b)_\mu (p_a + p_b)_\nu}{(p_a + p_b)^2} \right]. \quad (5.4.1)$$

If the answer is to be independent of ξ , then it must be true that the new term proportional to $(1 - \xi)$ gives no contribution. This can be easily proved by observing that it contains the factor

$$(\bar{v}_b \gamma^\mu u_a)(p_a + p_b)_\mu = \bar{v}_b \not{p}_a u_a + \bar{v}_b \not{p}_b u_a = m\bar{v}_b u_a - m\bar{v}_b u_a = 0. \quad (5.4.2)$$

Here we have applied the Dirac equation, as embodied in eqs. (A.2.24) and (A.2.25), to write $\not{p}_a u_a = m u_a$ and $\bar{v}_b \not{p}_b = -m \bar{v}_b$. For any photon propagator connected (at either end) to an external fermion line, the proof is similar. And, in general, one can show that the $1 - \xi$ term will always cancel when one includes all Feynman diagrams contributing to a particular process. So we can choose the most convenient value of ξ , which is usually $\xi = 1$.

Another aspect of gauge invariance involves a feature that we have not explored in an example so far: external state photons. Recall that the Feynman rules associate factors of $\epsilon^\mu(p, \lambda)$ and $\epsilon^{*\mu}(p, \lambda)$ to initial or final state photons, respectively. Now, making a gauge transformation on the photon field results in:

$$A^\mu \rightarrow A^\mu + \partial^\mu \Lambda \quad (5.4.3)$$

where Λ is any function. In momentum space, the derivative ∂^μ is proportional to p^μ . So, in terms of the polarization vector for the electromagnetic field, a gauge transformation is

$$\epsilon^\mu(p, \lambda) \rightarrow \epsilon^\mu(p, \lambda) + a p^\mu \quad (5.4.4)$$

where a is any quantity. The polarization vector and momentum for a physical photon satisfy $\epsilon^2 = -1$ and $\epsilon \cdot p = 0$ and $p^2 = 0$. As a consistency check, note that if these relations are satisfied, then they will also be obeyed after the gauge transformation (5.4.4).

Gauge invariance implies that the reduced matrix element should also be unchanged after the substitution in eq. (5.4.4). The reduced matrix element for a process with an external state photon with momentum p^μ and polarization label λ can always be written in the form:

$$\mathcal{M} = \mathcal{M}_\mu \epsilon^\mu(p, \lambda), \quad (5.4.5)$$

which defines \mathcal{M}_μ . Since \mathcal{M} must be invariant under a gauge transformation, it follows from eq. (5.4.4) that

$$\mathcal{M}_\mu p^\mu = 0. \quad (5.4.6)$$

This relation is known as the Ward identity for QED. It says that if we replace the polarization vector for any photon by the momentum of that photon, then the reduced matrix element should become 0. This is a nice consistency check on calculations.

Another nice consequence of the Ward identity is that it provides for a simplified way to sum or average over unmeasured photon polarization states. Consider a photon with momentum taken to be along the positive z axis, with $p^\mu = (P, 0, 0, P)$. Summing over the two polarization vectors in eqs. (5.1.26)-(5.1.27), we have:

$$\sum_{\lambda=1}^2 |\mathcal{M}|^2 = \sum_{\lambda=1}^2 \mathcal{M}_\mu \mathcal{M}_\nu^* \epsilon^\mu(p, \lambda) \epsilon^{*\nu}(p, \lambda) = |\mathcal{M}_1|^2 + |\mathcal{M}_2|^2, \quad (5.4.7)$$

where $\mathcal{M}_\mu = (\mathcal{M}_0, \mathcal{M}_1, \mathcal{M}_2, \mathcal{M}_3)$. The Ward identity implies that $p^\mu \mathcal{M}_\mu = P\mathcal{M}_0 + P\mathcal{M}_3 = 0$, so $|\mathcal{M}_0|^2 = |\mathcal{M}_3|^2$. Therefore, we can write $\sum_{\lambda=1}^2 |\mathcal{M}|^2 = -|\mathcal{M}_0|^2 + |\mathcal{M}_1|^2 + |\mathcal{M}_2|^2 + |\mathcal{M}_3|^2$, or

$$\sum_{\lambda=1}^2 |\mathcal{M}|^2 = -g^{\mu\nu} \mathcal{M}_\mu \mathcal{M}_\nu^*. \quad (5.4.8)$$

The last equation is written in a Lorentz invariant form, so it is true for any photon momentum direction, not just momenta oriented along the z direction. Gauge invariance, as expressed by the Ward identity, therefore implies that we can always sum over a photon's polarization states by the rule:

$$\sum_{\lambda=1}^2 \epsilon^\mu(p, \lambda) \epsilon^{*\nu}(p, \lambda) = -g^{\mu\nu} + (\text{irrelevant})^{\mu\nu}, \quad (5.4.9)$$

as long as we are taking the sum of the complex square of a reduced matrix element. Although the $(\text{irrelevant})^{\mu\nu}$ part is non-zero, it must vanish when contracted with $\mathcal{M}_\mu \mathcal{M}_\nu^*$, according to eq. (5.4.8).

5.5 External photon scattering

5.5.1 Compton scattering ($\gamma e^- \rightarrow \gamma e^-$)

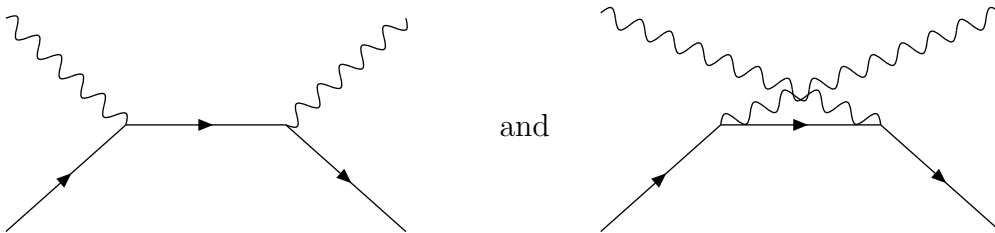
As our first example of a process with external-state photons, consider Compton scattering:

$$\gamma e^- \rightarrow \gamma e^-. \quad (5.5.1)$$

First let us assign the following labels to the external states:

initial γ	$\epsilon^\mu(p_a, \lambda_a)$
initial e^-	$u(p_b, s_b)$
final γ	$\epsilon^{\nu*}(k_1, \lambda_1)$
final e^-	$\bar{u}(k_2, s_2)$.

There are two Feynman diagrams for this process:



which are s -channel and u -channel, respectively. Applying the QED Feynman rules, we obtain:

$$\mathcal{M}_s = \bar{u}_2(ie\gamma^\nu) \left[\frac{i(\not{p}_a + \not{p}_b + m)}{(p_a + p_b)^2 - m^2} \right] (ie\gamma^\mu) u_b \epsilon_{1\nu}^* \epsilon_{a\mu} \quad (5.5.2)$$

$$= -i \frac{e^2}{s - m^2} \left[\bar{u}_2 \gamma^\nu (\not{p}_a + \not{p}_b + m) \gamma^\mu u_b \right] \epsilon_{1\nu}^* \epsilon_{a\mu} \quad (5.5.3)$$

and

$$\mathcal{M}_u = \bar{u}_2 (ie\gamma^\mu) \left[\frac{i(\not{p}_b - \not{k}_1 + m)}{(p_b - k_1)^2 - m^2} \right] (ie\gamma^\nu) u_b \epsilon_{1\nu}^* \epsilon_{a\mu} \quad (5.5.4)$$

$$= -i \frac{e^2}{u - m^2} \left[\bar{u}_2 \gamma^\mu (\not{p}_b - \not{k}_1 + m) \gamma^\nu u_b \right] \epsilon_{1\nu}^* \epsilon_{a\mu}. \quad (5.5.5)$$

Before squaring the total reduced matrix element, it is useful to simplify. So we note that:

$$(\not{p}_b + m) \gamma^\mu u_b = \{\not{p}_b, \gamma^\mu\} u_b - \gamma^\mu (\not{p}_b - m) u_b \quad (5.5.6)$$

$$= p_{b\sigma} \{\gamma^\sigma, \gamma^\mu\} u_b + 0 \quad (5.5.7)$$

$$= 2p_{b\sigma} g^{\sigma\mu} u_b \quad (5.5.8)$$

$$= 2p_b^\mu u_b, \quad (5.5.9)$$

where we have used eq. (A.2.24). So the reduced matrix element is:

$$\mathcal{M} = -ie^2 \epsilon_{1\nu}^* \epsilon_{a\mu} \bar{u}_2 \left[\frac{1}{s - m^2} (\gamma^\nu \not{p}_a \gamma^\mu + 2p_b^\mu \gamma^\nu) + \frac{1}{u - m^2} (-\gamma^\mu \not{k}_1 \gamma^\nu + 2p_b^\nu \gamma^\mu) \right] u_b. \quad (5.5.10)$$

Taking the complex conjugate of eq. (5.5.10) gives:

$$\mathcal{M}^* = ie^2 \epsilon_{1\sigma} \epsilon_{a\rho}^* \bar{u}_b \left[\frac{1}{s - m^2} (\gamma^\rho \not{p}_a \gamma^\sigma + 2p_b^\rho \gamma^\sigma) + \frac{1}{u - m^2} (-\gamma^\sigma \not{k}_1 \gamma^\rho + 2p_b^\sigma \gamma^\rho) \right] u_2. \quad (5.5.11)$$

Now we multiply together eqs. (5.5.10) and (5.5.11), and average over the initial photon polarization λ_a and sum over the final photon polarization λ_1 , using

$$\frac{1}{2} \sum_{\lambda_a=1}^2 \epsilon_{a\mu} \epsilon_{a\rho}^* = -\frac{1}{2} g_{\mu\rho} + \text{irrelevant}, \quad (5.5.12)$$

$$\sum_{\lambda_1=1}^2 \epsilon_{1\nu}^* \epsilon_{1\sigma} = -g_{\nu\sigma} + \text{irrelevant}, \quad (5.5.13)$$

to obtain:

$$\begin{aligned} \frac{1}{2} \sum_{\lambda_a, \lambda_1} |\mathcal{M}|^2 &= \frac{e^4}{2} \left\{ \bar{u}_2 \left[\frac{1}{s - m^2} (\gamma^\nu \not{p}_a \gamma^\mu + 2p_b^\mu \gamma^\nu) + \frac{1}{u - m^2} (-\gamma^\mu \not{k}_1 \gamma^\nu + 2p_b^\nu \gamma^\mu) \right] u_b \right\} \\ &\quad \left\{ \bar{u}_b \left[\frac{1}{s - m^2} (\gamma_\mu \not{p}_a \gamma_\nu + 2p_{b\mu} \gamma_\nu) + \frac{1}{u - m^2} (-\gamma_\nu \not{k}_1 \gamma_\mu + 2p_{b\nu} \gamma_\mu) \right] u_2 \right\}. \end{aligned} \quad (5.5.14)$$

Next we can average over s_b , and sum over s_2 , using the usual tricks:

$$\frac{1}{2} \sum_{s_b} u_b \bar{u}_b = \frac{1}{2} (\not{p}_b + m), \quad (5.5.15)$$

$$\sum_{s_2} \bar{u}_2 \dots u_2 = \text{Tr}[\dots (\not{k}_2 + m)]. \quad (5.5.16)$$

The result is a single spinor trace:

$$\begin{aligned} \frac{1}{4} \sum_{\text{spins}} |\mathcal{M}|^2 &= \frac{e^4}{4} \text{Tr} \left[\left\{ \frac{1}{s-m^2} (\gamma^\nu \not{p}_a \gamma^\mu + 2p_b^\mu \gamma^\nu) + \frac{1}{u-m^2} (-\gamma^\mu \not{k}_1 \gamma^\nu + 2p_b^\nu \gamma^\mu) \right\} (\not{p}_b + m) \right. \\ &\quad \left. \left\{ \frac{1}{s-m^2} (\gamma_\mu \not{p}_a \gamma_\nu + 2p_{b\mu} \gamma_\nu) + \frac{1}{u-m^2} (-\gamma_\nu \not{k}_1 \gamma_\mu + 2p_{b\nu} \gamma_\mu) \right\} (\not{k}_2 + m) \right]. \end{aligned} \quad (5.5.17)$$

Doing this trace requires a little patience and organization. The end result can be written compactly in terms of

$$p_a \cdot p_b = \frac{s-m^2}{2}, \quad (5.5.18)$$

$$p_b \cdot k_1 = \frac{m^2-u}{2}. \quad (5.5.19)$$

After some calculation, one finds:

$$\frac{1}{4} \sum_{\text{spins}} |\mathcal{M}|^2 = 2e^4 \left[\frac{p_a \cdot p_b}{p_b \cdot k_1} + \frac{p_b \cdot k_1}{p_a \cdot p_b} + 2m^2 \left(\frac{1}{p_a \cdot p_b} - \frac{1}{p_b \cdot k_1} \right) + m^4 \left(\frac{1}{p_a \cdot p_b} - \frac{1}{p_b \cdot k_1} \right)^2 \right]. \quad (5.5.20)$$

Equation (5.5.20) is a Lorentz scalar. We can now find the differential cross-section after choosing a reference frame. We will do this first in the center-of-momentum frame, and then redo it in the “lab” frame in which the initial electron is at rest.

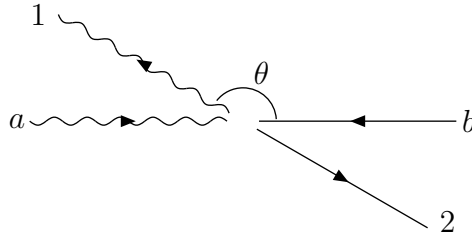
In the center-of-momentum frame, the kinematics is just like in the case $e\mu \rightarrow e\mu$ studied in a homework problem. Call the magnitude of the 3-momentum of the photon in the initial state P . Then using four-momentum conservation and the on-shell conditions $p_a^2 = k_1^2 = 0$ and $p_b^2 = k_2^2 = m^2$, and taking the initial state photon momentum to be in the $+z$ direction and the final state photon momentum to make an angle θ with the z -axis, we have:

$$p_a^\mu = (P, 0, 0, P), \quad (5.5.21)$$

$$p_b^\mu = (\sqrt{P^2 + m^2}, 0, 0, -P), \quad (5.5.22)$$

$$k_1^\mu = (P, 0, P \sin \theta, P \cos \theta), \quad (5.5.23)$$

$$k_2^\mu = (\sqrt{P^2 + m^2}, 0, -P \sin \theta, -P \cos \theta). \quad (5.5.24)$$



The initial and final state photons have the same energy, as do the initial and final state electrons, so define:

$$E_\gamma = P, \quad (5.5.25)$$

$$E_e = \sqrt{P^2 + m^2}. \quad (5.5.26)$$

Then we have:

$$s = (E_e + E_\gamma)^2, \quad (5.5.27)$$

$$p_a \cdot p_b = E_\gamma(E_e + E_\gamma), \quad (5.5.28)$$

$$p_b \cdot k_1 = E_\gamma(E_e + E_\gamma \cos \theta), \quad (5.5.29)$$

$$\frac{|\vec{k}_1|}{|\vec{p}_a|} = 1. \quad (5.5.30)$$

So, applying eq. (4.5.48) to eq. (5.5.20), we obtain:

$$\begin{aligned} \frac{d\sigma}{d(\cos \theta)} = & \frac{\pi\alpha^2}{s} \left[\frac{E_e + E_\gamma}{E_e + E_\gamma \cos \theta} + \frac{E_e + E_\gamma \cos \theta}{E_e + E_\gamma} + 2m^2 \left(\frac{\cos \theta - 1}{(E_e + E_\gamma)(E_e + E_\gamma \cos \theta)} \right) \right. \\ & \left. + m^4 \left(\frac{\cos \theta - 1}{(E_e + E_\gamma)(E_e + E_\gamma \cos \theta)} \right)^2 \right]. \end{aligned} \quad (5.5.31)$$

In a typical Compton scattering situation, the energies in the center-of-momentum frame are much larger than the electron's mass. So, consider the high-energy limit $E_\gamma \gg m$. Naively, we can set $E_e = E_\gamma$ and $m = 0$ in that limit. However, this requires some care for $\cos \theta \approx -1$, since then the denominator factor $E_e + E_\gamma \cos \theta$ can become large. This is most important for the first term in eq. (5.5.31). In fact, this term gives the dominant contribution to the total cross-section, coming from the $\cos \theta \approx -1$ (back-scattering) region. Integrating with respect to $\cos \theta$, we find:

$$\int_{-1}^1 \frac{E_e + E_\gamma}{E_e + E_\gamma \cos \theta} d(\cos \theta) = \frac{E_e + E_\gamma}{E_\gamma} \ln \left(\frac{E_e + E_\gamma}{E_e - E_\gamma} \right). \quad (5.5.32)$$

Now, expanding in the small mass of the electron,

$$E_e - E_\gamma = E_\gamma \sqrt{1 + m^2/E_\gamma^2} - E_\gamma = E_\gamma \left(1 + \frac{m^2}{2E_\gamma^2} + \dots - 1 \right) = \frac{m^2}{2E_\gamma} + \mathcal{O}(m^4), \quad (5.5.33)$$

$$E_e + E_\gamma = 2E_\gamma + \mathcal{O}(m^2). \quad (5.5.34)$$

Therefore,

$$\int_{-1}^1 \frac{E_e + E_\gamma}{E_e + E_\gamma \cos \theta} d(\cos \theta) = 2 \ln(4E_\gamma^2/m^2) + \mathcal{O}(m^2) = 2 \ln(s/m^2) + \mathcal{O}(m^2), \quad (5.5.35)$$

with the dominant contribution coming from $\cos\theta$ near -1 , where the denominator of the integrand becomes small. Integrating the second term in eq. (5.5.31), one finds:

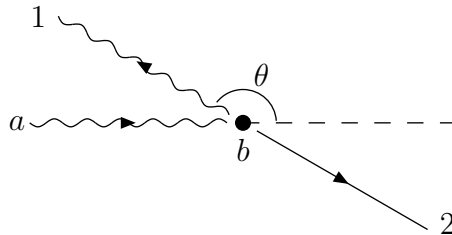
$$\int_{-1}^1 \frac{E_e + E_\gamma \cos\theta}{E_e + E_\gamma} d(\cos\theta) = \frac{2E_e}{E_e + E_\gamma} = 1 + \mathcal{O}(m^2). \quad (5.5.36)$$

The remaining two terms vanish as $m^2/s \rightarrow 0$. So, for $s \gg m^2$ we have:

$$\sigma = \int_{-1}^1 \frac{d\sigma}{d(\cos\theta)} d(\cos\theta) = \frac{\pi\alpha^2}{s} [2\ln(s/m^2) + 1] \quad (5.5.37)$$

plus terms that vanish like $(m^2/s^2)\ln(s/m^2)$ as $m^2/s \rightarrow 0$. The cross-section falls at high energy like $1/s$, but with a logarithmic enhancement coming from back-scattered photons with angles $\theta \approx \pi$. The origin of this enhancement can be traced to the u -channel propagator, which becomes large when $u - m^2 = 2p_b \cdot k_1 = 2E_\gamma(E_e + E_\gamma \cos\theta)$ becomes small. This corresponds to the virtual electron in the u -channel Feynman diagram going nearly on-shell. (Notice that $s - m^2$ can never become small when $s \gg m^2$.)

Just for fun, let us redo the analysis of Compton scattering, starting from eq. (5.5.20), but now working in the lab frame in which the initial state electron is at rest. Let us call the energy of the initial state photon ω and that of the final state photon ω' . (Recall that $\hbar = 1$ in our units, so the energy of a photon is equal to its angular frequency.)



Then, in terms of the lab photon scattering angle θ , the 4-momenta are:

$$p_a = (\omega, 0, 0, \omega), \quad (5.5.38)$$

$$p_b = (m, 0, 0, 0), \quad (5.5.39)$$

$$k_1 = (\omega', 0, \omega' \sin\theta, \omega' \cos\theta), \quad (5.5.40)$$

$$k_2 = (\omega + m - \omega', 0, -\omega' \sin\theta, \omega - \omega' \cos\theta). \quad (5.5.41)$$

Here we have used four-momentum conservation and the on-shell conditions $p_a^2 = k_1^2 = 0$ and $p_b^2 = m^2$. Applying the last on-shell condition $k_2^2 = m^2$ now leads to:

$$2m(\omega - \omega') + 2\omega\omega'(\cos\theta - 1) = 0. \quad (5.5.42)$$

This can be used to solve for ω' in terms of $\cos \theta$, or vice versa:

$$\omega' = \frac{\omega}{1 + \frac{\omega}{m}(1 - \cos \theta)}; \quad (5.5.43)$$

$$\cos \theta = 1 - \frac{m(\omega - \omega')}{\omega\omega'}. \quad (5.5.44)$$

In terms of lab-frame variables, one has:

$$p_a \cdot p_b = \omega m; \quad (5.5.45)$$

$$p_b \cdot k_1 = \omega' m, \quad (5.5.46)$$

so that, from eq. (5.5.20):

$$\frac{1}{4} \sum_{\text{spins}} |\mathcal{M}|^2 = 2e^4 \left[\frac{\omega}{\omega'} + \frac{\omega'}{\omega} + 2m \left(\frac{1}{\omega} - \frac{1}{\omega'} \right) + m^2 \left(\frac{1}{\omega} - \frac{1}{\omega'} \right)^2 \right]. \quad (5.5.47)$$

This can be simplified slightly by using

$$m \left(\frac{1}{\omega} - \frac{1}{\omega'} \right) = \cos \theta - 1, \quad (5.5.48)$$

which follows from eq. (5.5.42), so that

$$\frac{1}{4} \sum_{\text{spins}} |\mathcal{M}|^2 = 2e^4 \left[\frac{\omega}{\omega'} + \frac{\omega'}{\omega} - \sin^2 \theta \right]. \quad (5.5.49)$$

Now to find the differential cross-section, we must apply eq. (4.5.32):

$$d\sigma = \frac{1}{4E_a E_b |\vec{v}_a - \vec{v}_b|} \left(\frac{1}{4} |\mathcal{M}|^2 \right) d\Phi_2, \quad (5.5.50)$$

where $d\Phi_2$ is the two-body Lorentz-invariant phase space, as defined in eq. (4.5.33), for the final state particles in the lab frame. Evaluating the prefactors for the case at hand:

$$E_a = \omega, \quad (5.5.51)$$

$$E_b = m, \quad (5.5.52)$$

$$|\vec{v}_a - \vec{v}_b| = 1 - 0 = 1. \quad (5.5.53)$$

(Recall that the speed of the photon is $c = 1$.)

The two-body phase space in the lab frame is:

$$d\Phi_2 = (2\pi)^4 \delta^{(4)}(k_1 + k_2 - p_a - p_b) \frac{d^3 \vec{k}_1}{(2\pi)^3 2E_1} \frac{d^3 \vec{k}_2}{(2\pi)^3 2E_2} \quad (5.5.54)$$

$$= \delta^{(3)}(\vec{k}_1 + \vec{k}_2 - \omega \hat{z}) \delta(\omega' + E_2 - \omega - m) \frac{d^3 \vec{k}_1}{16\pi^2 \omega' E_2} d^3 \vec{k}_2, \quad (5.5.55)$$

where ω' is now defined to be equal to $E_1 = |\vec{k}_1|$ and E_2 is defined to be $\sqrt{|\vec{k}_2|^2 + m^2}$. Performing the \vec{k}_2 integral using the 3-momentum delta function just sets $\vec{k}_2 = \omega \hat{z} - \vec{k}_1$, resulting in:

$$d\Phi_2 = \delta(\omega' + E_2 - \omega - m) \frac{d^3\vec{k}_1}{16\pi^2\omega'E_2}, \quad (5.5.56)$$

where now

$$E_2 = \sqrt{\omega'^2 - 2\omega\omega'\cos\theta + \omega^2 + m^2}. \quad (5.5.57)$$

The phase space for the final state photon can be simplified by writing it in terms of angular coordinates and doing the integral $\int d\phi = 2\pi$:

$$d^3\vec{k}_1 = d\phi d(\cos\theta) \omega'^2 d\omega' = 2\pi d(\cos\theta) \omega'^2 d\omega'. \quad (5.5.58)$$

Therefore,

$$d\Phi_2 = \delta(\omega' + E_2 - \omega - m) \frac{d(\cos\theta) \omega' d\omega'}{8\pi E_2}. \quad (5.5.59)$$

In order to do the ω' integral, it is simplest, as usual, to make a change of integration variables to the argument of the delta function. So, defining

$$K = \omega' + E_2 - \omega - m, \quad (5.5.60)$$

we have

$$\frac{dK}{d\omega'} = 1 + \frac{\omega' - \omega \cos\theta}{E_2}. \quad (5.5.61)$$

Therefore,

$$\frac{\omega' d\omega'}{E_2} = \frac{\omega' dK}{E_2 + \omega' - \omega \cos\theta}. \quad (5.5.62)$$

Performing the dK integration sets $K = 0$, so $E_2 = \omega + m - \omega'$. Using eq. (5.5.62) in eq. (5.5.59) gives

$$d\Phi_2 = \frac{\omega'}{m + \omega(1 - \cos\theta)} \frac{d(\cos\theta)}{8\pi} = \frac{\omega'^2}{8\pi m\omega} d(\cos\theta), \quad (5.5.63)$$

where eq. (5.5.43) has been used to simplify the denominator. Finally using this in eq. (5.5.50) yields:

$$d\sigma = \left(\frac{1}{4} \sum_{\text{spins}} |\mathcal{M}|^2 \right) \frac{\omega'^2}{32\pi m\omega^2} d(\cos\theta), \quad (5.5.64)$$

so that, putting in eq. (5.5.49),

$$\frac{d\sigma}{d(\cos\theta)} = \frac{\pi\alpha^2}{m^2} \left(\frac{\omega'}{\omega}\right)^2 \left[\frac{\omega'}{\omega} + \frac{\omega}{\omega'} - \sin^2\theta\right]. \quad (5.5.65)$$

This result is the Klein-Nishina formula.

As in the center-of-momentum frame, the largest differential cross-section is found for back-scattered photons with $\cos\theta = -1$, which corresponds to the smallest possible final-state photon energy ω' . Notice that, according to eq. (5.5.43), when $\omega \gg m$, one gets very low energies ω' when the photon is back-scattered. One can now integrate the lab-frame differential cross-section $\int_{-1}^1 d(\cos\theta)$ to get the total cross-section, using the dependence of ω' on $\cos\theta$ as given in eq. (5.5.43). The result is:

$$\sigma = \pi\alpha^2 \left[\left(\frac{1}{\omega m} - \frac{2}{\omega^2} - \frac{2m}{\omega^3} \right) \ln \left(1 + \frac{2\omega}{m} \right) + \frac{4}{\omega^2} + \frac{2(m+\omega)}{m(m+2\omega)^2} \right]. \quad (5.5.66)$$

In the high-energy (small m) limit, this becomes:

$$\sigma = \pi\alpha^2 \left[\frac{1}{\omega m} \ln \left(\frac{2\omega}{m} \right) + \frac{1}{2\omega m} + \dots \right]. \quad (5.5.67)$$

We can re-express this in terms of the Mandelstam variable $s = (\omega + m)^2 - \omega^2 = 2\omega m + m^2 \approx 2\omega m$,

$$\sigma = \frac{\pi\alpha^2}{s} \left[2\ln(s/m^2) + 1 + \dots \right]. \quad (5.5.68)$$

Equation (5.5.68) is the same result that we found in the center-of-momentum frame, eq. (5.5.37). This is an example of a general fact: the total cross-section does not depend on the choice of reference frame, provided that one boosts along a direction parallel to the collision axis. To see why, one need only look at the definition of the total cross-section given in eq. (4.5.2). The numbers of particles N_S , N_a , and N_b can be simply counted, and so certainly do not depend on any choice of inertial reference frame, while the area A is invariant under Lorentz boosts along the collision axis.

The low-energy Thomson scattering limit is also interesting. In the lab frame, $\omega \ll m$ implies $\omega'/\omega = 1$, so that

$$\frac{d\sigma}{d(\cos\theta)} = \frac{\pi\alpha^2}{m^2} (1 + \cos^2\theta), \quad (5.5.69)$$

which is independent of energy. The total cross-section in this limit is then

$$\sigma = \frac{8\pi\alpha^2}{3m^2}. \quad (5.5.70)$$

Unlike the case of high-energy Compton scattering, Thomson scattering is symmetric under $\theta \rightarrow \pi - \theta$, with a factor of 2 enhancement in the forward ($\theta = 0$) and backward ($\theta = \pi$) directions compared to right-angle ($\theta = \pi/2$) scattering.

5.5.2 $e^+e^- \rightarrow \gamma\gamma$

As our final example of a QED process let us consider $e^+e^- \rightarrow \gamma\gamma$ in the high-energy limit. We could always compute the reduced matrix element starting from the Feynman rules. However, since we have already done Compton scattering, it is easier to use crossing. Labeling the physical momenta for Compton scattering now with primes, we can make the following comparison table:

$$\begin{array}{cc} \text{Compton} & e^+e^- \rightarrow \gamma\gamma \end{array} \quad (5.5.71)$$

$$\gamma \leftrightarrow p'_a \quad e^+ \leftrightarrow p_a \quad (5.5.72)$$

$$e^- \leftrightarrow p'_b \quad e^- \leftrightarrow p_b \quad (5.5.73)$$

$$\gamma \leftrightarrow k'_1 \quad \gamma \leftrightarrow k_1 \quad (5.5.74)$$

$$e^- \leftrightarrow k'_2 \quad \gamma \leftrightarrow k_2. \quad (5.5.75)$$

For convenience, we have chosen e^+ to be labeled by “ a ”, so that the initial-state e^- can have the same label “ b ” in both processes. Then according to the Crossing Symmetry Theorem, we can obtain $\sum_{\text{spins}} |\mathcal{M}_{e^+e^- \rightarrow \gamma\gamma}|^2$ by making the replacements

$$p'_a = -k_2; \quad p'_b = p_b; \quad k'_1 = k_1; \quad k'_2 = -p_a \quad (5.5.76)$$

in the Compton scattering result (for small m):

$$\sum_{\text{spins}} |\mathcal{M}_{\gamma e^- \rightarrow \gamma e^-}|^2 = 8e^4 \left(\frac{p'_a \cdot p'_b}{p'_b \cdot k'_1} + \frac{p'_b \cdot k'_1}{p'_a \cdot p'_b} \right), \quad (5.5.77)$$

obtained from eq. (5.5.20). Because the crossing involves one fermion (a final state electron changes into an initial state positron), there is also a factor of $(-1)^1 = -1$, according to eq. (5.3.7). So, the result is:

$$\sum_{\text{spins}} |\mathcal{M}_{e^+e^- \rightarrow \gamma\gamma}|^2 = (-1)8e^4 \left(\frac{-k_2 \cdot p_b}{p_b \cdot k_1} + \frac{p_b \cdot k_1}{-k_2 \cdot p_b} \right) \quad (5.5.78)$$

$$= 8e^4 \left(\frac{k_2 \cdot p_b}{p_b \cdot k_1} + \frac{p_b \cdot k_1}{k_2 \cdot p_b} \right). \quad (5.5.79)$$

The situation here is $2 \rightarrow 2$ massless particle scattering, so we can steal the kinematics information directly from eqs. (5.2.139)-(5.2.143). The relevant facts for the present case are:

$$p_b \cdot k_1 = -\frac{u}{2} = \frac{s}{4}(1 + \cos \theta), \quad (5.5.80)$$

$$p_b \cdot k_2 = -\frac{t}{2} = \frac{s}{4}(1 - \cos \theta). \quad (5.5.81)$$

Therefore,

$$\frac{1}{4} \sum_{\text{spins}} |\mathcal{M}_{e^+e^- \rightarrow \gamma\gamma}|^2 = 2e^4 \left(\frac{t}{u} + \frac{u}{t} \right) = 4e^4 \left(\frac{1 + \cos^2 \theta}{\sin^2 \theta} \right). \quad (5.5.82)$$

It is a useful check, and a vindication of the $(-1)^F$ factor in the Crossing Symmetry Theorem, that this is positive! Now plugging this into the formula eq. (4.5.49) for the differential cross-section, we get:

$$\frac{d\sigma}{d\cos(\theta)} = \frac{2\pi\alpha^2}{s} \left(\frac{1 + \cos^2 \theta}{\sin^2 \theta} \right). \quad (5.5.83)$$

This cross-section is symmetric as $\theta \rightarrow \pi - \theta$. That was inevitable, since the two final state photons are identical; the final state in which a photon is observed coming out at a (θ, ϕ) is actually the *same* as a state in which a photon is observed at an angle $(\pi - \theta, -\phi)$. When we find the total cross-section, we should therefore divide by 2 (or just integrate over half of the range for $\cos \theta$) to avoid overcounting. This is the same overcounting issue for identical final state particles that arose for Møller scattering at the end of section 5.3.2.

The integrand in eq. (5.5.83) diverges for $\sin \theta = 0$. This is because we have set $m = 0$ in the kinematics, which is not valid for scattering very close to the collision axis. If you put back non-zero m , you will find that instead of diverging, the total cross-section features a logarithmic enhancement $\ln(s/m^2)$ coming from small $\sin \theta$. In a real $e^-e^+ \rightarrow \gamma\gamma$ experiment, however, photons very close to the electron and positron beams will not be seen by any detector. The observable cross-section in one of these colliding beam experiments is something more like

$$\sigma_{\text{cut}} = \frac{1}{2} \int_{-\cos \theta_{\text{cut}}}^{\cos \theta_{\text{cut}}} \frac{d\sigma}{d(\cos \theta)} d(\cos \theta) \quad (5.5.84)$$

$$= \frac{2\pi\alpha^2}{s} \left[\ln \left(\frac{1 + \cos \theta_{\text{cut}}}{1 - \cos \theta_{\text{cut}}} \right) - \cos \theta_{\text{cut}} \right]. \quad (5.5.85)$$

(You can easily check that this is a positive and increasing function of $\cos \theta_{\text{cut}}$.) On the other hand, if you are interested in the total cross-section for electron-positron annihilation with no cuts applied on the angle, then you must take into account the non-zero electron mass. Redoing everything with $m \ll \sqrt{s}$ but non-zero, you can show:

$$\sigma = \frac{2\pi\alpha^2}{s} \left[\ln \left(\frac{s}{2m^2} \right) - 1 \right]. \quad (5.5.86)$$

The logarithmic enhancement at large s in this formula comes entirely from the $\sin \theta \approx 0$ region. Note that this formula is just what you would have gotten by plugging in

$$\cos \theta_{\text{cut}} = 1 - 4m^2/s \quad (5.5.87)$$

into eq. (5.5.85), for small m . In this sense, the finite mass of the electron “cuts off” the would-be logarithmic divergence of the cross-section for small $\sin \theta$.

6 Decay Processes

6.1 Decay rates and partial widths

So far, we have studied only $2 \rightarrow 2$ scattering processes. This is because in QED as a stand-alone theory, the fundamental particles are stable. Photons cannot decay into anything else (in any theory), because they are massless. The electron is the lightest particle that carries charge, so it cannot decay because of charge conservation. The photon interaction vertex with a fermion line does not change the type of fermion. So if there is only a muon in the initial state, you can easily convince yourself that there must be at least one muon in the final state. Going to the rest frame of the initial muon, the total energy of the process is simply m_μ , but the energy of the final state would have to be larger than this, so if only QED interactions are allowed, the muon must also be stable. The weak interactions get around this by allowing interaction vertices that change the fermion type. Moreover, bound states can decay even in QED.

For any type of unstable particle, the probability that a decay will occur in a very short interval of time Δt should be proportional to Δt . So we can define the decay rate Γ [also known as the decay width; it is equal to the resonance width in eq. (1.2.1)] as the constant of proportionality:

$$(\text{Probability of decay in time } \Delta t) = \Gamma \Delta t. \quad (6.1.1)$$

Suppose we observe the decays of a large sample of particles of this type, all at rest. If the number of particle at time t is denoted $N(t)$, then the number of particles remaining a short time later is therefore:

$$N(t + \Delta t) = (1 - \Gamma \Delta t) N(t). \quad (6.1.2)$$

It follows that

$$\frac{dN}{dt} = \lim_{\Delta t \rightarrow 0} \frac{N(t + \Delta t) - N(t)}{\Delta t} = -\Gamma N, \quad (6.1.3)$$

so that

$$N(t) = e^{-\Gamma t} N(0). \quad (6.1.4)$$

When one has computed or measured Γ for some particle, it is traditional and sensible to quote the result as measured in the rest frame of the particle. If the particle is moving with velocity β , then because of relativistic time dilation, the survival probability for a particular particle as a function of the laboratory time t is:

$$(\text{Probability of particle survival}) = e^{-\Gamma t \sqrt{1-\beta^2}}. \quad (6.1.5)$$

The quantity

$$\tau = 1/\Gamma \quad (6.1.6)$$

is also known as the mean lifetime of the particle at rest. [Putting in the units recovers eq. (1.2.2); see eq. (A.1.6).] There is often more than one final state available for a decaying particle. One can then compute or measure the decay rates into particular final states. The rate Γ for a particular final state or class of final states is called a partial width. The sum of all exclusive partial widths should add up to the total decay rate, of course.

Consider a process in which a particle at rest with 4-momentum

$$p^\mu = (M, 0, 0, 0) \quad (6.1.7)$$

decays to several particles with 4-momenta k_i and masses m_i . Given the reduced matrix element \mathcal{M} for this process, one can show by arguments similar to those in 4.5 for cross-sections that the differential decay rate is:

$$d\Gamma = \frac{1}{2M} |\mathcal{M}|^2 d\Phi_n, \quad (6.1.8)$$

where

$$d\Phi_n = (2\pi)^4 \delta^{(4)}(p - \sum_i k_i) \prod_{i=1}^n \left(\frac{d^3 \vec{k}_i}{(2\pi)^3 2E_i} \right) \quad (6.1.9)$$

is the n -body Lorentz-invariant phase space. [Compare this to eq. (4.5.33); you will see that the only difference is that the $p_a + p_b$ in the 4-momentum delta function for a scattering process has been replaced by p for a decay process.] To find the contribution to the decay rate for final-state particles with 3-momenta restricted to be in some ranges, we should integrate $d\Gamma$ over those ranges. To find the total decay rate Γ , we should integrate the 3-momenta over all available \vec{k}_i . The energies in this formula are defined by

$$E_i = \sqrt{\vec{k}_i^2 + m_i^2}. \quad (6.1.10)$$

6.2 Two-body decays

Most of the decay processes that one encounters in high-energy physics are two-particle or three-particle final states. As general rule, if the number of particles in the final state is larger, then the decay partial width for that final state tends to be smaller, so a particle will typically decay into few-particle states if it can. If a two-particle final state is available, it is usually a very good bet that three-particle final states will lose. However, there are some exceptions to this, including in the important case of the Higgs boson.

Let us simplify the formula eq. (6.1.8) for the case of two-particle final states with arbitrary masses. The evaluation of the two-particle final-state phase space is exactly the same as in eqs. (4.5.36)-(4.5.45), with the simple replacement $E_{\text{CM}} \rightarrow M$. Therefore,

$$d\Phi_2 = \frac{K}{16\pi^2 M} d\phi_1 d(\cos \theta_1), \quad (6.2.1)$$

and

$$d\Gamma = \frac{K}{32\pi^2 M^2} |\mathcal{M}|^2 d\phi_1 d(\cos \theta_1). \quad (6.2.2)$$

It remains to solve for K . Energy conservation requires that

$$E_1 + E_2 = \sqrt{K^2 + m_1^2} + \sqrt{K^2 + m_2^2} = M. \quad (6.2.3)$$

One can solve this by writing it as

$$E_1 - M = \sqrt{E_1^2 - m_1^2 + m_2^2} \quad (6.2.4)$$

and squaring both sides. The solution is:

$$E_1 = \frac{M^2 + m_1^2 - m_2^2}{2M}, \quad (6.2.5)$$

$$E_2 = \frac{M^2 + m_2^2 - m_1^2}{2M}, \quad (6.2.6)$$

$$K = \frac{\sqrt{\lambda(M^2, m_1^2, m_2^2)}}{2M}, \quad (6.2.7)$$

where

$$\lambda(x, y, z) \equiv x^2 + y^2 + z^2 - 2xy - 2xz - 2yz. \quad (6.2.8)$$

is known as the triangle function.[†] It is useful to tabulate results for some common special cases:

- If the final-state masses are equal, $m_1 = m_2 = m$, then the final state particles share the energy equally in the rest frame:

$$E_1 = E_2 = M/2, \quad (6.2.9)$$

$$K = \frac{M}{2} \sqrt{1 - 4m^2/M^2}, \quad (6.2.10)$$

and

$$d\Gamma = \frac{|\mathcal{M}|^2}{64\pi^2 M} \sqrt{1 - 4m^2/M^2} d\phi_1 d(\cos \theta_1). \quad (6.2.11)$$

[†]It is so-named because, if each of $\sqrt{x}, \sqrt{y}, \sqrt{z}$ is less than the sum of the other two, then $\lambda(x, y, z)$ is -16 times the square of the area of a triangle with sides $\sqrt{x}, \sqrt{y}, \sqrt{z}$. However, in the present context M, m_1, m_2 never form a triangle; if $M < m_1 + m_2$, then the decay is forbidden.

- If one of the final-state particle is massless, $m_2 = 0$, then:

$$E_1 = \frac{M^2 + m_1^2}{2M}, \quad (6.2.12)$$

$$E_2 = K = \frac{M^2 - m_1^2}{2M}. \quad (6.2.13)$$

This illustrates the general feature that since the final state particles have equal 3-momentum magnitudes, the heavier particle gets more energy. In this case,

$$d\Gamma = \frac{|\mathcal{M}|^2}{64\pi^2 M} (1 - m_1^2/M^2) d\phi_1 d(\cos \theta_1). \quad (6.2.14)$$

- If the decaying particle has spin 0, or if its spin is not measured, then there can be no special direction in the decay, so the final state particles must be distributed isotropically in the center-of-momentum frame. One then obtains the total decay rate from

$$d\phi_1 d(\cos \theta_1) \rightarrow 4\pi, \quad (6.2.15)$$

provided that the two final state particles are distinguishable. There is an extra factor of 1/2 if they are identical, to avoid counting each final state twice [see the discussions at the end of sections 5.3.2 and 5.5.2].

6.3 Scalar decays to fermion-antifermion pairs: Higgs decay

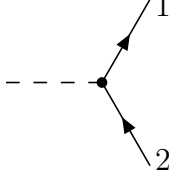
Let us now consider a simple and very important decay process, namely a scalar particle ϕ decaying to a fermion-antifermion pair. As a model, let us consider the Lagrangian already mentioned in section 4.7:

$$\mathcal{L}_{\text{int}} = -y\phi\bar{\Psi}\Psi. \quad (6.3.1)$$

This type of interaction is called a Yukawa interaction, and y is a Yukawa coupling. The corresponding Feynman rule was argued to be equal to $-iy$ times an identity matrix in Dirac spinor space, as shown in the picture immediately after eq. (4.7.10). Consider an initial state containing a single ϕ particle of mass M and 4-momentum p , and a final state containing a fermion and antifermion each with mass m and with 4-momenta and spins k_1, s_1 and k_2, s_2 respectively. Then the matrix element will be of the form

$${}_{\text{OUT}}\langle k_1, s_1; k_2, s_2 | p \rangle_{\text{OUT}} = -i\mathcal{M}(2\pi)^4 \delta^{(4)}(k_1 + k_2 - p). \quad (6.3.2)$$

The Feynman rules for fermion external states don't depend on the choice of interaction vertex, so they are the same as for QED. Therefore we can draw the Feynman diagram:



and immediately write down the reduced matrix element for the decay:

$$\mathcal{M} = -iy \bar{u}(k_1, s_1) v(k_2, s_2). \quad (6.3.3)$$

To turn \mathcal{M} into a physically observable decay rate, we need to compute the squared reduced matrix element summed over final state spins. From eq. (6.3.3),

$$\mathcal{M}^* = iy \bar{v}_2 u_1, \quad (6.3.4)$$

so

$$|\mathcal{M}|^2 = y^2 (\bar{u}_1 v_2) (\bar{v}_2 u_1). \quad (6.3.5)$$

Summing over s_2 , we have:

$$\sum_{s_2} |\mathcal{M}|^2 = y^2 \bar{u}_1 (\not{k}_2 - m) u_1 \quad (6.3.6)$$

$$= y^2 \text{Tr}[(\not{k}_2 - m) u_1 \bar{u}_1]. \quad (6.3.7)$$

Now summing over s_1 gives:

$$\sum_{s_1, s_2} |\mathcal{M}|^2 = y^2 \text{Tr}[(\not{k}_2 - m)(\not{k}_1 + m)] \quad (6.3.8)$$

$$= y^2 (\text{Tr}[\not{k}_2 \not{k}_1] - m^2 \text{Tr}[1]) \quad (6.3.9)$$

$$= 4y^2 (k_1 \cdot k_2 - m^2), \quad (6.3.10)$$

where we have used the fact that the trace of an odd number of gamma matrices vanishes, and eqs. (A.2.8) and (A.2.9). The fermion and antifermion have the same mass m , so

$$M^2 = (k_1 + k_2)^2 = k_1^2 + k_2^2 + 2k_1 \cdot k_2 = m^2 + m^2 + 2k_1 \cdot k_2 \quad (6.3.11)$$

implies that

$$k_1 \cdot k_2 - m^2 = \frac{M^2}{2} - 2m^2. \quad (6.3.12)$$

Therefore,

$$\sum_{\text{spins}} |\mathcal{M}|^2 = 2y^2 M^2 \left(1 - \frac{4m^2}{M^2}\right), \quad (6.3.13)$$

and, using eq. (6.2.11),

$$d\Gamma = \frac{y^2 M}{32\pi^2} \left(1 - \frac{4m^2}{M^2}\right)^{3/2} d\phi_1 d(\cos\theta_1). \quad (6.3.14)$$

Doing the (trivial) angular integrals finally gives the total decay rate:

$$\Gamma = \frac{y^2 M}{8\pi} \left(1 - \frac{4m^2}{M^2}\right)^{3/2}. \quad (6.3.15)$$

In the Standard Model, the Higgs boson h plays the role of ϕ , and couples to each fermion f with a Lagrangian that is exactly of the form given above:

$$\mathcal{L}_{\text{int}} = - \sum_f y_f h \bar{\Psi}_f \Psi_f. \quad (6.3.16)$$

The Yukawa coupling for each fermion is approximately proportional to its mass:

$$y_f \approx \frac{\bar{m}_f}{175 \text{ GeV}}. \quad (6.3.17)$$

(The reason for this will be explained below in section 11.3.) However, the \bar{m}_f appearing in this formula is not quite equal to the mass, because of higher-order corrections. For quarks, these corrections are quite large, and \bar{m}_f tends to come out considerably smaller than the masses of the quarks quoted in Table 1.3.

At the LHC, one of the major goals is to study the Higgs boson through its decay modes. The Higgs boson mass has been measured to be about 125 GeV. Since the top quark has a mass of about 173 GeV, the decay $h \rightarrow t\bar{t}$ is kinematically forbidden. The next-lightest fermions in the Standard Model are the bottom quark, charm quark, and tau lepton, so we expect decays $h \rightarrow b\bar{b}$ and $h \rightarrow \tau^-\tau^+$ and $h \rightarrow c\bar{c}$. For quarks, the sum in eq. (6.3.16) includes a summation over 3 colors, leading to an extra factor of $n_f = 3$ in the decay rate. Since the kinematic factor $(1 - 4m_f^2/M_h^2)^{3/2}$ is close to 1 for all allowed fermion-antifermion final states, the leading-order prediction for the decay rate to a particular fermion is approximately:

$$\Gamma(h \rightarrow f\bar{f}) = \frac{n_f y_f^2 M_h}{16\pi} \propto n_f \bar{m}_f^2. \quad (6.3.18)$$

Estimates of the \bar{m}_f from present experimental data are:

$$\bar{m}_b \approx 2.7 \text{ GeV} \quad \rightarrow \quad y_b \approx 0.0154, \quad (6.3.19)$$

$$\bar{m}_\tau \approx 1.77 \text{ GeV} \quad \rightarrow \quad y_\tau \approx 0.0101, \quad (6.3.20)$$

$$\bar{m}_c \approx 0.58 \text{ GeV} \quad \rightarrow \quad y_c \approx 0.0033, \quad (6.3.21)$$

for a Higgs with mass $M_h = 125$ GeV. (Notice that even though the charm quark is heavier than the tau lepton, it turns out that $\overline{m}_\tau > \overline{m}_c$ because of the large higher-order corrections for the charm quark.) Therefore, the prediction is that $b\bar{b}$ final states win, with, very roughly:

$$\Gamma(h \rightarrow b\bar{b}) : \Gamma(h \rightarrow \tau^-\tau^+) : \Gamma(h \rightarrow c\bar{c}) \quad :: \quad 3(\overline{m}_b)^2 : (\overline{m}_\tau)^2 : 3(\overline{m}_c)^2 \quad (6.3.22)$$

$$:: \quad 1 : 0.143 : 0.046. \quad (6.3.23)$$

A more accurate accounting of the Higgs boson width and branching ratios must take into account many important corrections beyond our scope here. For example, higher-order Feynman diagram are important, and increase the partial widths into quarks substantially. Second, there are other final states that can appear in h decays, notably gluon-gluon (gg) and $\gamma\gamma$, which both occur due to Feynman diagrams with loops, and W^+W^- and Z^0Z^0 . Naively, the last two are not kinematically allowed, since $2m_W$ and $2m_Z$ are both greater than m_h . However, they can still contribute if one or both of the weak vector bosons is off-shell (virtual). These decays are often written as $h \rightarrow WW^{(*)}$ and $h \rightarrow ZZ^{(*)}$, with the $(*)$ indicating an off-shell particle. Normally, such decays would be negligible compared to 2-body decays to on-shell particles, but they are competitive because the bottom quark squared Yukawa coupling $y_b^2 \approx 0.00024$ is so small.

Taking into account these effects,[†] it turns out that the total width of the Higgs boson is approximately 4.2 MeV, assuming $m_h = 125$ GeV. This is an extremely small decay width for such a heavy particle. One can define the branching ratio to be the partial decay rate into a particular final state, divided by the total decay rate, so for example

$$\text{BR}(h \rightarrow b\bar{b}) = \Gamma(h \rightarrow b\bar{b})/\Gamma_{\text{total}}. \quad (6.3.24)$$

In the Standard Model with $m_h = 125$ GeV, the predicted branching fractions into b , τ , and c pairs, taking into account all known effects, are:

$$\text{BR}(h \rightarrow b\bar{b}) \approx 0.577, \quad (6.3.25)$$

$$\text{BR}(h \rightarrow \tau^-\tau^+) \approx 0.063, \quad (6.3.26)$$

$$\text{BR}(h \rightarrow c\bar{c}) \approx 0.029. \quad (6.3.27)$$

Some other branching ratios that turn out to be extremely important for the Higgs boson at the Large Hadron collider, but rely on more involved calculations, are:

$$\text{BR}(h \rightarrow WW^{(*)}) \approx 0.215, \quad (6.3.28)$$

$$\text{BR}(h \rightarrow ZZ^{(*)}) \approx 0.0264, \quad (6.3.29)$$

$$\text{BR}(h \rightarrow gg) \approx 0.0857, \quad (6.3.30)$$

$$\text{BR}(h \rightarrow \gamma\gamma) \approx 0.00228. \quad (6.3.31)$$

[†]For the results quoted in this paragraph, see <https://arxiv.org/abs/1307.1347> S. Heinemeyer et al., “Handbook of LHC Higgs Cross Sections: 3. Higgs Properties”.

We will return to the subject of the Higgs boson branching ratios in section 11.5.

Finally, consider the helicities for the process $h \rightarrow f\bar{f}$. If we demanded that the final states have particular helicities, then we would have obtained for the matrix element, using P_R, P_L projection matrices:

$$\text{R-fermion, R-antifermion:} \quad \mathcal{M} = -iy \bar{u}_2 P_L P_L v_1 = -iy \bar{u}_2 P_L v_1 \neq 0 \quad (6.3.32)$$

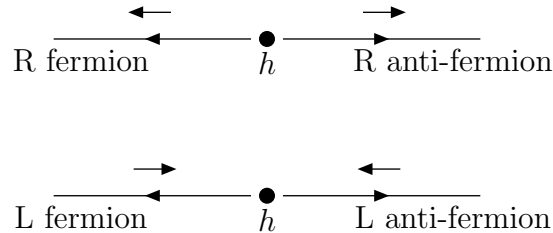
$$\text{L-fermion, L-antifermion:} \quad \mathcal{M} = -iy \bar{u}_2 P_R P_R v_1 = -iy \bar{u}_2 P_R v_1 \neq 0 \quad (6.3.33)$$

$$\text{R-fermion, L-antifermion:} \quad \mathcal{M} = -iy \bar{u}_2 P_L P_R v_1 = 0 \quad (6.3.34)$$

$$\text{L-fermion, R-antifermion:} \quad \mathcal{M} = -iy \bar{u}_2 P_R P_L v_1 = 0 \quad (6.3.35)$$

[Recall, from eqs. (5.2.63)-(5.2.66), that to get a L fermion or antifermion in the final state, one puts in a P_R next to the spinor, while to get a R fermion or antifermion in the final state, one puts in a P_L .] So, the rule here is that helicity is always violated by the scalar-fermion-antifermion vertex, since the scalar must decay to a state with equal helicities.

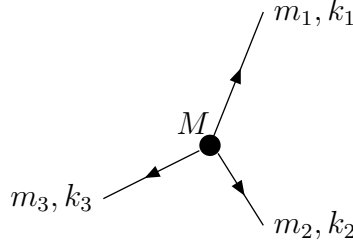
One may understand this result from angular momentum conservation. The initial state had no spin and no orbital angular momentum. In the final state, the spins of the outgoing particles must therefore have opposite directions. Since they have momentum in opposite directions, this means they must also have the same helicity. Drawing a short arrow to represent the spin, the allowed cases of RR helicities and LL helicities look like:



The helicities of tau leptons can be (statistically) measured from the angular distributions of their decay products, so this effect may eventually be measured with a sample of $h \rightarrow \tau^- \tau^+$ decay events.

6.4 Three-body decays

Let us consider a generic three-body decay process in which a particle of mass M decays to three lighter particles with masses m_1, m_2 , and m_3 . We will work in the rest frame of the decaying particle, so its four-vector is $p^\mu = (M, 0, 0, 0)$, and the four-vectors of the remaining particles are k_1, k_2 , and k_3 respectively:



In general, the formula for a three-body differential decay rate is

$$d\Gamma = \frac{1}{2M} |\mathcal{M}|^2 d\Phi_3, \quad (6.4.1)$$

where

$$d\Phi_3 = (2\pi)^4 \delta^{(4)}(p - k_1 - k_2 - k_3) \frac{d^3\vec{k}_1}{(2\pi)^3 2E_1} \frac{d^3\vec{k}_2}{(2\pi)^3 2E_2} \frac{d^3\vec{k}_3}{(2\pi)^3 2E_3} \quad (6.4.2)$$

is the Lorentz-invariant phase space. Since there are 9 integrals to do, and 4 delta functions, the result for $d\Gamma$ is a differential with respect to 5 remaining variables. The best choice of 5 variables depends on the problem at hand, so there are several ways to present the result. Two of the 5 variables can be chosen to be the energies E_1 and E_2 of two of the final-state particles; then the energy of the third particle $E_3 = M - E_1 - E_2$ is also known from energy conservation. In the rest frame of the decaying particle, the three final-state particle 3-momenta must lie in a plane, because of momentum conservation. Specifying E_1 and E_2 also uniquely fixes the angles between the three particle momenta within this decay plane. The remaining 3 variables just correspond to the orientation of the decay plane with respect to some fixed coordinate axis. If we think of the three 3-momenta within the decay plane as describing a rigid body, then the relative orientation can be described using three Euler angles. These can be chosen to be the spherical coordinate angles ϕ_1 and θ_1 for particle 1, and an angle α_2 that measures the rotation of the 3-momentum direction of particle 2 as measured about the axis of the momentum vector of particle 1. Then one can show:

$$d\Phi_3 = \frac{1}{256\pi^5} dE_1 dE_2 d\phi_1 d(\cos\theta_1) d\alpha_2. \quad (6.4.3)$$

The choice of which particles to label as 1 and 2 is arbitrary, and should be made to maximize convenience.

If the initial state particle spin is averaged over, or if it is spinless, then there is no special direction to measure the orientation of the final state decay plane with respect to. In that case, for particular E_1 and E_2 , the reduced matrix element cannot depend on the angles ϕ_1 , θ_1 , or α_2 , and one can do the integrals

$$\int_0^{2\pi} d\phi_1 \int_{-1}^1 d(\cos\theta_1) \int_0^{2\pi} d\alpha_2 = (2\pi)(2)(2\pi) = 8\pi^2. \quad (6.4.4)$$

Then,

$$d\Phi_3 = \frac{1}{32\pi^3} dE_1 dE_2, \quad (6.4.5)$$

and so, for spinless or spin-averaged initial states,

$$d\Gamma = \frac{1}{64\pi^3 M} |\mathcal{M}|^2 dE_1 dE_2. \quad (6.4.6)$$

To do the remaining energy integrals, one must find the limits of integration. If one decides to do the E_2 integral first, then by doing the kinematics one can show for any particular E_1 that

$$E_2^{\text{max,min}} = \frac{1}{2m_{23}^2} \left[(M - E_1)(m_{23}^2 + m_2^2 - m_3^2) \pm \sqrt{(E_1^2 - m_1^2) \lambda(m_{23}^2, m_2^2, m_3^2)} \right], \quad (6.4.7)$$

where the triangle function $\lambda(x, y, z)$ was defined by eq. (6.2.8), and

$$m_{23}^2 = (k_2 + k_3)^2 = (p - k_1)^2 = M^2 - 2E_1 M + m_1^2 \quad (6.4.8)$$

is the invariant (mass)² of the combination of particles 2 and 3. Then the limits of integration for the final E_1 integral are:

$$m_1 < E_1 < \frac{M^2 + m_1^2 - (m_2 + m_3)^2}{2M}. \quad (6.4.9)$$

A good strategy is usually to choose the label “1” for the particle whose energy we care the most about. Then after doing the dE_2 integral, we will be left with an expression for $d\Gamma/dE_1$.

In the special case that all final state particles are massless (or small enough to neglect) $m_1 = m_2 = m_3 = 0$, then these limits of integration simplify to:

$$\frac{M}{2} - E_1 < E_2 < \frac{M}{2}, \quad (6.4.10)$$

$$0 < E_1 < \frac{M}{2}. \quad (6.4.11)$$

7 Fermi Theory of Weak Interactions

7.1 Weak nuclear decays

In nuclear physics, the weak interactions are responsible for decays of long-lived isotopes. A nucleus with Z protons and $A - Z$ neutrons, so A nucleons in all, is denoted by AZ . If kinematically allowed, one can observe decays:

$${}^AZ \rightarrow {}^A(Z+1) + e^- \bar{\nu}_e. \quad (7.1.1)$$

The existence of the antineutrino $\bar{\nu}_e$ was inferred by Pauli as a “desperate remedy” to save the principle of energy conservation. The simplest example of this is the decay of the neutron into a proton, electron, and antineutrino:

$$n \rightarrow p^+ e^- \bar{\nu}_e \quad (7.1.2)$$

with a mean lifetime of[†]

$$\tau = 881.5 \pm 1.5 \text{ sec.} \quad (7.1.3)$$

Decays of heavier nuclei can be thought of as involving the subprocess:

$$“n” \rightarrow “p^+” e^- \bar{\nu}_e, \quad (7.1.4)$$

where the quotes indicated that the neutron and proton are really not separate entities, but part of the nuclear bound states. So for example, tritium decays according to

$${}^3\text{H} \rightarrow {}^3\text{He} + e^- \bar{\nu}_e \quad (\tau = 5.6 \times 10^8 \text{ sec} = 17.7 \text{ years}), \quad (7.1.5)$$

and carbon-14 decays according to

$${}^{14}\text{C} \rightarrow {}^{14}\text{N} + e^- \bar{\nu}_e \quad (\tau = 1.8 \times 10^{11} \text{ sec} = 8280 \text{ years}). \quad (7.1.6)$$

Nuclear physicists usually quote the half life $t_{1/2}$ rather than the mean lifetime τ . They are related by

$$t_{1/2} = \tau \ln(2), \quad (7.1.7)$$

so that $t_{1/2} = 5730$ years for Carbon-14, making it ideal for dating dead organisms. In the upper atmosphere, cosmic rays produce energetic neutrons, which in turn constantly convert ${}^{14}\text{N}$ nuclei

[†]The lifetime of the neutron is an infamous example of an experimental measurement that has shifted dramatically over time. As recently as the late 1960’s, it was thought that $\tau_n = 1010 \pm 30$ seconds, and as recently as 2010, the official value was 885.7 ± 0.8 seconds. Even today the systematic uncertainties are a source of concern.

into ^{14}C . Carbon-dioxide-breathing organisms, or those that eat them, maintain an equilibrium with the carbon content of the atmosphere, at a level of roughly $^{14}\text{C}/^{12}\text{C} \approx 10^{-12}$. However, a complication is the fact that this ratio is not constant; it dropped in the early 20th century as more ordinary ^{12}C entered the atmosphere because of the burning of fossil fuels containing the carbon of organisms that have been dead for a very long time. The relative abundance $^{14}\text{C}/^{12}\text{C} \approx 10^{-12}$ then doubled after 1954 because of nuclear weapons testing, reaching a peak in the mid 1960's from which it has since declined. In any case, dead organisms lose half of their ^{14}C every 5730 ± 30 years, and certainly do not regain it by breathing or eating. So, by measuring the rate of e^- beta rays consistent with ^{14}C decay produced by a sample, and determining the historic atmospheric $^{14}\text{C}/^{12}\text{C}$ ratio as a function of time with control samples or by other means, one can date the death of a sample of organic matter.

One can also have decays that release a positron and neutrino:

$$^AZ \rightarrow ^A(Z-1) + e^+ \nu_e. \quad (7.1.8)$$

These can be thought of as coming from the subprocess

$$“p^+” \rightarrow “n” e^+ \nu_e. \quad (7.1.9)$$

In free space, the proton cannot decay, simply because $m_p < m_n$, but under the right circumstances it is kinematically allowed when the proton and neutron are parts of nuclear bound states. An example is

$$^{14}\text{O} \rightarrow ^{14}\text{N} + e^+ \nu_e \quad (\tau = 71 \text{ sec}). \quad (7.1.10)$$

The long lifetimes of such decays are what originally gave rise to the name “weak” interactions.

Charged pions also decay through the weak interactions, with a mean lifetime of

$$\tau_{\pi^\pm} = 2.6 \times 10^{-8} \text{ sec}. \quad (7.1.11)$$

This is still a very long lifetime by particle physics standards, and corresponds to a proper decay length of $c\tau = 7.8$ meters. The probability that a charged pion with velocity β will travel a distance L in empty space before decaying is therefore

$$P = e^{-(L/7.8 \text{ m})\sqrt{1-\beta^2}/\beta}. \quad (7.1.12)$$

This means that a relativistic charged pion will typically travel several meters before decaying, unless it interacts (which it usually will in a collider detector). The main decay mode is

$$\pi^- \rightarrow \mu^- \bar{\nu}_\mu \quad (7.1.13)$$

with a branching ratio of 0.99988. (This includes submodes in which an additional photon is radiated away.) The only other significant decay mode is

$$\pi^- \rightarrow e^- \bar{\nu}_e. \quad (7.1.14)$$

with a branching ratio 1.2×10^{-4} . This presents a puzzle: since the electron is lighter, there is more kinematic phase space available for the second decay, yet the first decay dominates by almost a factor of 10^4 . We will calculate the reason for this later, in section 7.6.

7.2 Muon decay

The muon decays according to

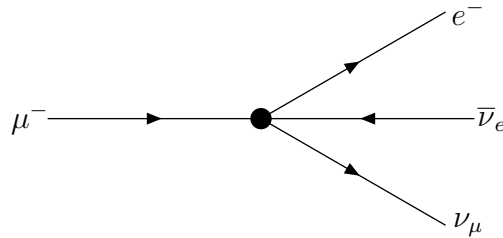
$$\mu^- \rightarrow e^- \bar{\nu}_e \nu_\mu \quad (\tau = 2.2 \times 10^{-6} \text{ sec}). \quad (7.2.1)$$

This corresponds to a decay width of

$$\Gamma = 3.0 \times 10^{-19} \text{ GeV}, \quad (7.2.2)$$

implying a proper decay length of $c\tau = 659$ meters. Muons do not undergo hadronic interactions like pions do, so that relativistic muons will usually penetrate at least the inner layers of particle detectors with a very high probability.

The Feynman diagram for muon decay can be drawn as:



This involves a 4-fermion interaction vertex.[†] Because of the correspondence between interactions and terms in the Lagrangian, we therefore expect that the Lagrangian should contain terms schematically of the form

$$\mathcal{L}_{\text{int}} = (\bar{\nu}_\mu \dots \mu) (\bar{e} \dots \nu_e) \quad \text{or} \quad (\bar{\nu}_\mu \dots \nu_e) (\bar{e} \dots \mu), \quad (7.2.3)$$

where the symbols μ, ν_μ, e, ν_e mean the Dirac spinor fields for the muon, muon neutrino, electron, and electron neutrino, and the ellipses mean matrices in Dirac spinor space. To be more precise about the interaction Lagrangian, one needs clues from experiment.

[†]We will later find out that this is not a true fundamental interaction of the theory, but rather an “effective” interaction that is derived from the low-energy effects of the W^- boson.

One clue is the fact that there are three quantum numbers, called lepton numbers, that are additively conserved to a high accuracy in most experiments. (The only confirmed exceptions are neutrino oscillation experiments.) They are assigned as:

$$L_e = \begin{cases} +1 & \text{for } e^-, \nu_e \\ -1 & \text{for } e^+, \bar{\nu}_e \\ 0 & \text{for all other particles} \end{cases} \quad (7.2.4)$$

$$L_\mu = \begin{cases} +1 & \text{for } \mu^-, \nu_\mu \\ -1 & \text{for } \mu^+, \bar{\nu}_\mu \\ 0 & \text{for all other particles} \end{cases} \quad (7.2.5)$$

$$L_\tau = \begin{cases} +1 & \text{for } \tau^-, \nu_\tau \\ -1 & \text{for } \tau^+, \bar{\nu}_\tau \\ 0 & \text{for all other particles} \end{cases} \quad (7.2.6)$$

So, for example, in the nuclear decay examples above, one always has $L_e = 0$ in the initial state, and $L_e = 1 - 1 = 0$ in the final state, with $L_\mu = L_\tau = 0$ trivially in each case. The muon decay mode in eq. (7.2.1) has $(L_e, L_\mu) = (0, 1)$ in both the initial and final states. If lepton numbers were not conserved, then one might expect that decays like

$$\mu^- \rightarrow e^- \gamma \quad (7.2.7)$$

would be allowed. However, these decays have never been observed, and the most recent limit from the MEG experiment at the Paul Scherrer Institute is

$$\text{BR}(\mu^- \rightarrow e^- \gamma) < 4.2 \times 10^{-13}. \quad (7.2.8)$$

(Actually, the MEG experiment searches for the decay $\mu^+ \rightarrow e^+ \gamma$, but the branching ratio should be the same with all particles replaced by their anti-particles.) This is a remarkably strong constraint, since this decay only has to compete with the already weak mode in eq. (7.2.1). It implies that

$$\Gamma(\mu^- \rightarrow e^- \gamma) < 1.3 \times 10^{-31} \text{ GeV}. \quad (7.2.9)$$

The BaBar and Belle experiments have put similar (but not as stringent) bounds on tau lepton number non-conservation:

$$\text{BR}(\tau^- \rightarrow e^- \gamma) < 3.3 \times 10^{-8} \quad \text{BaBar}, \quad (7.2.10)$$

$$\text{BR}(\tau^- \rightarrow \mu^- \gamma) < 4.4 \times 10^{-8} \quad \text{BaBar}, \quad (7.2.11)$$

$$\text{BR}(\tau^- \rightarrow e^- \pi^0) < 8.0 \times 10^{-8} \quad \text{Belle}. \quad (7.2.12)$$

Since 1998, experimental results from neutrinos produced in the Sun, the atmosphere, by accelerators, and in reactors have given strong evidence for oscillations of neutrinos that are

caused by them having small non-zero masses that violate the individual lepton numbers. (It is still an open question whether they also violate the total lepton number

$$L \equiv L_e + L_\mu + L_\tau; \quad (7.2.13)$$

for more on this, see section 11.4.) However, these are very small effects for colliding beam experiments, and can be ignored for almost all conceivable processes at the Tevatron and the LHC.

The (near) conservation of lepton numbers suggests that the interaction Lagrangian for the weak interactions can always be written in terms of fermion bilinears involving one barred and one unbarred Dirac spinor from each lepton family. So, we will write the weak interactions for leptons in terms of building blocks with net $L_e = L_\mu = L_\tau = 0$, for example, like the first term in eq. (7.2.3) but not the second. More generally, we will want to use building blocks:

$$(\bar{\ell} \dots \nu_\ell) \quad \text{or} \quad (\bar{\nu}_\ell \dots \ell), \quad (7.2.14)$$

where ℓ is any of e, μ, τ . Now, since each Dirac spinor has 4 components, a basis for fermion bilinears involving any two fields Ψ_1 and Ψ_2 will have $4 \times 4 = 16$ elements. These can be classified by their transformation properties under the proper Lorentz group and the parity transformation $\vec{x} \rightarrow -\vec{x}$, as follows:

Term	Number	Parity ($\vec{x} \rightarrow -\vec{x}$)	Type
$\bar{\Psi}_1 \Psi_2$	1	+1	Scalar = S
$\bar{\Psi}_1 \gamma_5 \Psi_2$	1	-1	Pseudo-scalar = P
$\bar{\Psi}_1 \gamma^\mu \Psi_2$	4	$(-1)^\mu$	Vector = V
$\bar{\Psi}_1 \gamma^\mu \gamma_5 \Psi_2$	4	$-(-1)^\mu$	Axial-vector = A
$\frac{i}{2} \bar{\Psi}_1 [\gamma^\mu, \gamma^\nu] \Psi_2$	6	$(-1)^\mu (-1)^\nu$	Tensor = T .

The entry under Parity indicates the multiplicative factor under which each of these terms transforms when $\vec{x} \rightarrow -\vec{x}$, with

$$(-1)^\mu = \begin{cases} +1 & \text{for } \mu = 0 \\ -1 & \text{for } \mu = 1, 2, 3. \end{cases} \quad (7.2.15)$$

The weak interaction Lagrangian for leptons could be formed out of any product of such terms with $\Psi_1, \Psi_2 = \ell, \nu_\ell$. Fermi originally proposed that the weak interaction fermion building blocks were of the type V , so that muon decays would be described by

$$\mathcal{L}_{\text{int}}^V = -G(\bar{\nu}_\mu \gamma^\rho \mu)(\bar{e} \gamma_\rho \nu_e) + \text{c.c.} \quad (7.2.16)$$

Here “c.c.” means complex conjugate; this is necessary since the Dirac spinor fields are complex. Some other possibilities could have been that the building blocks were of type A :

$$\mathcal{L}_{\text{int}}^A = -G(\bar{\nu}_\mu \gamma^\rho \gamma_5 \mu)(\bar{e} \gamma_\rho \gamma_5 \nu_e) + \text{c.c.} \quad (7.2.17)$$

or some combination of V and A , or some combination of S and P , or perhaps even T .

Fermi's original proposal of V for the weak interactions turned out to be wrong. The most important clue for determining the correct answer for the proper Lorentz and parity structure of the weak interaction building blocks came from an experiment on polarized ^{60}Co decay by Wu in 1957. The ^{60}Co nucleus has spin $J = 5$, so that when cooled and placed in a magnetic field, the nuclear spins align with \vec{B} . Wu then measured the angular dependence of the electron spin from the decay



The nucleus ^{60}Ni has spin $J = 4$, so the net angular momentum carried away by the electron and antineutrino is 1. The observation was that the electron is emitted preferentially in the direction opposite to the original spin of the ^{60}Co nucleus. This can be explained consistently with angular momentum conservation if the electron produced in the decay is always polarized left-handed and the antineutrino is always right-handed. Using short arrows to designate spin directions, the most favored configuration is:



The importance of this experiment and others was that right-handed electrons and left-handed antineutrinos do not seem to participate in the weak interactions. This means that when writing the interaction Lagrangian for weak interactions, we can always put a P_L to the left of the electron's Dirac field, and a P_R to the right of a $\bar{\nu}_e$ field. This helped establish that the correct form for the fermion bilinear in the Lagrangian is $V - A$:

$$\bar{e} P_R \gamma^\rho \nu_e = \bar{e} \gamma^\rho P_L \nu_e = \frac{1}{2} \bar{e} \gamma^\rho (1 - \gamma_5) \nu_e. \quad (7.2.19)$$

Since this is a complex quantity, and the Lagrangian density must be real, one must also have terms involving the complex conjugate of eq. (7.2.19):

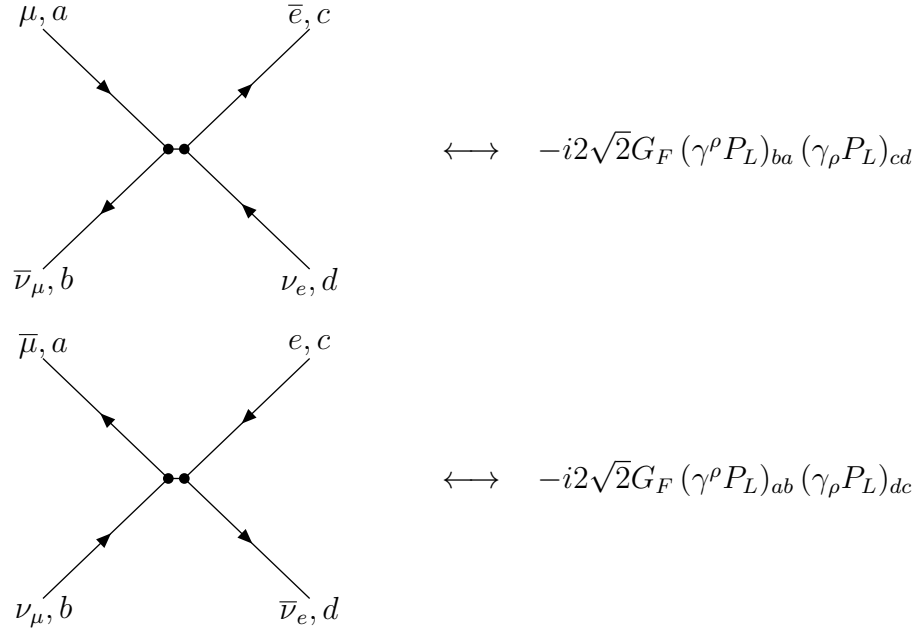
$$\bar{\nu}_e P_R \gamma^\rho e = \bar{\nu}_e \gamma^\rho P_L e. \quad (7.2.20)$$

The feature that was considered most surprising at the time was that right-handed Dirac fermion fields $P_R e$, $P_R \nu_e$, and left-handed Dirac barred fermion fields $\bar{e} P_L$, and $\bar{\nu}_e P_L$ never appear in any part of the weak interaction Lagrangian.

For muon decay, the relevant four-fermion interaction Lagrangian is:

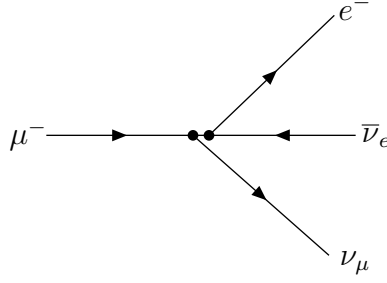
$$\mathcal{L}_{\text{int}} = -2\sqrt{2}G_F(\bar{\nu}_\mu\gamma^\rho P_L\mu)(\bar{e}\gamma_\rho P_L\nu_e) + \text{c.c.} \quad (7.2.21)$$

Here G_F is a coupling constant with dimensions of $[\text{mass}]^{-2}$, known as the Fermi constant. Its numerical value is most precisely determined from muon decay. The factor of $2\sqrt{2}$ is a historical convention. Using the correspondence between terms in the Lagrangian and particle interactions, we therefore have two Feynman rules:



These are related by reversing of all arrows, corresponding to the complex conjugate in eq. (7.2.21). The slightly separated dots in the Feynman rule picture are meant to indicate the Dirac spinor structure. The Feynman rules for external state fermions and antifermions are exactly the same as in QED, with neutrinos treated as fermions and antineutrinos as antifermions. This weak interaction Lagrangian for muon decay violates parity maximally, since it treats left-handed fermions differently from right-handed fermions. However, helicity is conserved by this interaction Lagrangian, just as in QED, because of the presence of one gamma matrix in each fermion bilinear.

We can now derive the reduced matrix element for muon decay, and use it to compute the differential decay rate of the muon. Comparing this to the experimentally measured result will allow us to find the numerical value of G_F , and determine the energy spectrum of the final state electron. At lowest order, the only Feynman diagram for $\mu^- \rightarrow e^- \bar{\nu}_e \nu_\mu$ is:



using the first of the two Feynman rules above. Let us label the momenta and spins of the particles as follows:

Particle	Momentum	Spin	Spinor
μ^-	p_a	s_a	$u(p_a, s_a) = u_a$
e^-	k_1	s_1	$\bar{u}(k_1, s_1) = \bar{u}_1$
$\bar{\nu}_e$	k_2	s_2	$v(k_2, s_2) = v_2$
ν_μ	k_3	s_3	$\bar{u}(k_3, s_3) = \bar{u}_3$

(7.2.22)

The reduced matrix element is obtained by starting at the end of each fermion line with a barred spinor and following it back (moving opposite the arrow direction) to the beginning. In this case, that means starting with the muon neutrino and electron barred spinors. The result is:

$$\mathcal{M} = -i2\sqrt{2}G_F(\bar{u}_3\gamma^\rho P_L u_a)(\bar{u}_1\gamma_\rho P_L v_2). \quad (7.2.23)$$

This illustrates a general feature; in the weak interactions, there should be a P_L next to each unbarred spinor in a matrix element, or equivalently a P_R next to each barred spinor. (The presence of the gamma matrix ensures the equivalence of these two statements, since $P_L \leftrightarrow P_R$ when moved through a gamma matrix.) Taking the complex conjugate, we have:

$$\mathcal{M}^* = i2\sqrt{2}G_F(\bar{u}_a P_R \gamma^\sigma u_3)(\bar{v}_2 P_R \gamma_\sigma u_1). \quad (7.2.24)$$

Therefore,

$$|\mathcal{M}|^2 = 8G_F^2 (\bar{u}_3\gamma^\rho P_L u_a)(\bar{u}_a P_R \gamma^\sigma u_3) (\bar{u}_1\gamma_\rho P_L v_2)(\bar{v}_2 P_R \gamma_\sigma u_1). \quad (7.2.25)$$

In the following, we can neglect the mass of the electron m_e , since $m_e/m_\mu < 0.005$. Now we can average over the initial-state spin s_a and sum over the final-state spins s_1, s_2, s_3 using the usual tricks:

$$\frac{1}{2} \sum_{s_a} u_a \bar{u}_a = \frac{1}{2} (\not{p}_a + m_\mu), \quad (7.2.26)$$

$$\sum_{s_1} u_1 \bar{u}_1 = \not{k}_1, \quad (7.2.27)$$

$$\sum_{s_2} v_2 \bar{v}_2 = \not{k}_2, \quad (7.2.28)$$

$$\sum_{s_3} u_3 \bar{u}_3 = \not{k}_3, \quad (7.2.29)$$

to turn the result into a product of traces:

$$\frac{1}{2} \sum_{\text{spins}} |\mathcal{M}|^2 = 4G_F^2 \text{Tr}[\gamma^\rho P_L (\not{p}_a + m_\mu) P_R \gamma^\sigma \not{k}_3] \text{Tr}[\gamma_\rho P_L \not{k}_2 P_R \gamma_\sigma \not{k}_1] \quad (7.2.30)$$

$$= 4G_F^2 \text{Tr}[\gamma^\rho \not{p}_a P_R \gamma^\sigma \not{k}_3] \text{Tr}[\gamma_\rho \not{k}_2 P_R \gamma_\sigma \not{k}_1] \quad (7.2.31)$$

Fortunately, we have already seen a product of traces just like this one, in eq. (5.2.100), so that by substituting in the appropriate 4-momenta, we immediately get:

$$\frac{1}{2} \sum_{\text{spins}} |\mathcal{M}|^2 = 64G_F^2 (p_a \cdot k_2)(k_1 \cdot k_3). \quad (7.2.32)$$

Our next task is to turn this reduced matrix element into a differential decay rate.

Applying the results of subsection 6.4 to the example of muon decay, with $M = m_\mu$ and $m_1 = m_2 = m_3 = 0$. According to our result of eq. (7.2.32), we need to evaluate the dot products $p_a \cdot k_2$ and $k_1 \cdot k_3$. Since these are Lorentz scalars, we can evaluate them in a frame where \vec{k}_2 is along the z -axis. Then

$$p_a = (m_\mu, 0, 0, 0), \quad (7.2.33)$$

$$k_2 = (E_{\bar{\nu}_e}, 0, 0, E_{\bar{\nu}_e}). \quad (7.2.34)$$

Therefore,

$$p_a \cdot k_2 = m_\mu E_{\bar{\nu}_e}. \quad (7.2.35)$$

Also, $k_1 \cdot k_3 = \frac{1}{2}[(k_1 + k_3)^2 - k_1^2 - k_3^2] = \frac{1}{2}[(p_a - k_2)^2 - 0 - 0] = \frac{1}{2}[p_a^2 + k_2^2 - 2p_a \cdot k_2]$, so

$$k_1 \cdot k_3 = \frac{1}{2}(m_\mu^2 - 2m_\mu E_{\bar{\nu}_e}). \quad (7.2.36)$$

Therefore, from eq. (7.2.32),

$$\frac{1}{2} \sum_{\text{spins}} |\mathcal{M}|^2 = 32G_F^2 (m_\mu^3 E_{\bar{\nu}_e} - 2m_\mu^2 E_{\bar{\nu}_e}^2). \quad (7.2.37)$$

Plugging this into eq. (6.4.6) with $M = m_\mu$, and choosing $E_1 = E_e$ and $E_2 = E_{\bar{\nu}_e}$, we get:

$$d\Gamma = dE_e dE_{\bar{\nu}_e} \frac{G_F^2}{2\pi^3} (m_\mu^2 E_{\bar{\nu}_e} - 2m_\mu E_{\bar{\nu}_e}^2). \quad (7.2.38)$$

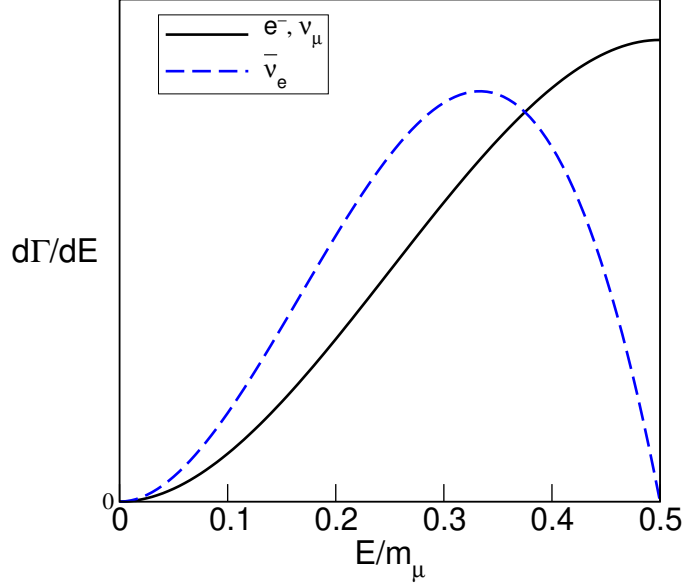
Doing the $dE_{\bar{\nu}_e}$ integral using the limits of integration of eq. (6.4.10), we obtain:

$$d\Gamma = dE_e \int_{\frac{m_\mu}{2} - E_e}^{\frac{m_\mu}{2}} dE_{\bar{\nu}_e} \frac{G_F^2}{2\pi^3} (m_\mu^2 E_{\bar{\nu}_e} - 2m_\mu E_{\bar{\nu}_e}^2) = dE_e \frac{G_F^2}{\pi^3} \left(\frac{m_\mu^2 E_e^2}{4} - \frac{m_\mu E_e^3}{3} \right). \quad (7.2.39)$$

We have obtained the differential decay rate for the energy of the final state electron:

$$\frac{d\Gamma}{dE_e} = \frac{G_F^2 m_\mu^2}{4\pi^3} E_e^2 \left(1 - \frac{4E_e}{3m_\mu} \right). \quad (7.2.40)$$

The shape of this distribution is shown below as the solid line:



We see that the electron energy is peaked near its maximum value of $m_\mu/2$. This corresponds to the situation where the electron is recoiling directly against both the neutrino and antineutrino, which are collinear; for example, $k_1 = (m_\mu/2, 0, 0, -m_\mu/2)$, and $k_2^\mu = k_3^\mu = (m_\mu/4, 0, 0, m_\mu/4)$:



The helicity of the initial state is undefined, since the muon is at rest. However, we know that the final state e^- , ν_μ , and $\bar{\nu}_e$ have well-defined L, L, and R helicities respectively, as shown above by the short arrows pointing in the spin directions, since this is dictated by the weak interactions. In the case of maximum E_e , therefore, the spins of ν_μ and $\bar{\nu}_e$ must be in opposite directions. The helicity of the electron is L, so its spin must be opposite to its 3-momentum direction. By momentum conservation, this tells us that the electron must move in the opposite direction to the initial muon spin in the limit that E_e is near the maximum.

The smallest possible electron energies are near 0, which occurs when the neutrino and antineutrino move in nearly opposite directions, so that the 3-momentum of the electron recoiling against them is very small.

We have done the most practically sensible thing by plotting the differential decay rate in terms of the electron energy, since that is what is directly observable in an experiment. Just for fun, however, let us pretend that we could directly measure the ν_μ and $\bar{\nu}_e$ energies, and compute the distributions for them. To find $d\Gamma/dE_{\nu_\mu}$, we can take $E_2 = E_{\bar{\nu}_e}$ and $E_1 = E_{\nu_\mu}$ in eqs. (6.4.6) and (6.4.10)-(6.4.11), with the reduced matrix element from eq. (7.2.37). Then

$$d\Gamma = dE_{\nu_\mu} dE_{\bar{\nu}_e} \frac{G_F^2}{2\pi^3} (m_\mu^2 E_{\bar{\nu}_e} - 2m_\mu E_{\bar{\nu}_e}^2), \quad (7.2.41)$$

and the range of integration for $E_{\bar{\nu}_e}$ is now:

$$\frac{m_\mu}{2} - E_{\nu_\mu} < E_{\bar{\nu}_e} < \frac{m_\mu}{2}, \quad (7.2.42)$$

so that

$$d\Gamma = dE_{\nu_\mu} \int_{\frac{m_\mu}{2} - E_{\nu_\mu}}^{\frac{m_\mu}{2}} dE_{\bar{\nu}_e} \frac{G_F^2}{2\pi^3} (m_\mu^2 E_{\bar{\nu}_e} - 2m_\mu E_{\bar{\nu}_e}^2) = dE_e \frac{G_F^2}{\pi^3} \left(\frac{m_\mu^2 E_{\nu_\mu}^2}{4} - \frac{m_\mu E_{\nu_\mu}^3}{3} \right). \quad (7.2.43)$$

Therefore, the E_{ν_μ} distribution of final states has the same shape as the E_e distribution:

$$\frac{d\Gamma}{dE_{\nu_\mu}} = \frac{G_F^2 m_\mu^2}{4\pi^3} E_{\nu_\mu}^2 \left(1 - \frac{4E_{\nu_\mu}}{m_\mu} \right). \quad (7.2.44)$$

Finally, we can find $d\Gamma/dE_{\bar{\nu}_e}$, by choosing $E_2 = E_e$ and $E_1 = E_{\bar{\nu}_e}$ in eqs. (6.4.6) and (6.4.10)-(6.4.11) with eq. (7.2.37). Then:

$$d\Gamma = dE_{\bar{\nu}_e} \int_{\frac{m_\mu}{2} - E_{\bar{\nu}_e}}^{\frac{m_\mu}{2}} dE_e \frac{G_F^2}{2\pi^3} (m_\mu^2 E_{\bar{\nu}_e} - 2m_\mu E_{\bar{\nu}_e}^2) = dE_{\bar{\nu}_e} \frac{G_F^2}{2\pi^3} (m_\mu^2 E_{\bar{\nu}_e}^2 - 2m_\mu E_{\bar{\nu}_e}^3), \quad (7.2.45)$$

so that

$$\frac{d\Gamma}{dE_{\bar{\nu}_e}} = \frac{G_F^2 m_\mu^2}{2\pi^3} E_{\bar{\nu}_e}^2 \left(1 - \frac{2E_{\bar{\nu}_e}}{m_\mu} \right). \quad (7.2.46)$$

This distribution is plotted as the dashed line in the previous graph. Unlike the distributions for E_e and E_{ν} , we see that $d\Gamma/dE_{\bar{\nu}_e}$ vanishes when $E_{\bar{\nu}_e}$ approaches its maximum value of $\frac{m_\mu}{2}$. We can understand this by noting that when $E_{\bar{\nu}_e}$ is maximum, the $\bar{\nu}_e$ must be recoiling against both e and ν_e moving in the opposite direction, so the L, L, R helicities of e , ν_μ , and $\bar{\nu}_e$ tell us that the total spin of the final state is 3/2:



Since the initial-state muon only had spin 1/2, the quantum states have 0 overlap, and the rate must vanish in that limit of maximal $E_{\bar{\nu}_e}$.

The total decay rate for the muon is found by integrating either eq. (7.2.40) with respect to E_e , or eq. (7.2.44) with respect to E_{ν_μ} , or eq. (7.2.46) with respect to $E_{\bar{\nu}_e}$. In each case, we get:

$$\Gamma = \int_0^{m_\mu/2} \left(\frac{d\Gamma}{dE_e} \right) dE_e = \int_0^{m_\mu/2} \left(\frac{d\Gamma}{dE_{\nu_\mu}} \right) dE_{\nu_\mu} = \int_0^{m_\mu/2} \left(\frac{d\Gamma}{dE_{\bar{\nu}_e}} \right) dE_{\bar{\nu}_e} \quad (7.2.47)$$

$$= \frac{G_F^2 m_\mu^5}{192\pi^3}. \quad (7.2.48)$$

It is a good check that the final result does not depend on the choice of the final energy integration variable. It is also good to check units: G_F^2 has units of $[\text{mass}]^{-4}$ or $[\text{time}]^4$, while m_μ^5 has units of $[\text{mass}]^5$ or $[\text{time}]^{-5}$, so Γ indeed has units of $[\text{mass}]$ or $[\text{time}]^{-1}$.

Experiments tell us that

$$\Gamma(\mu^- \rightarrow e^- \nu_\mu \bar{\nu}_e) = 2.99591(3) \times 10^{-19} \text{ GeV}, \quad m_\mu = 0.1056584 \text{ GeV}, \quad (7.2.49)$$

so we obtain the numerical value of Fermi's constant from eq. (7.2.48):

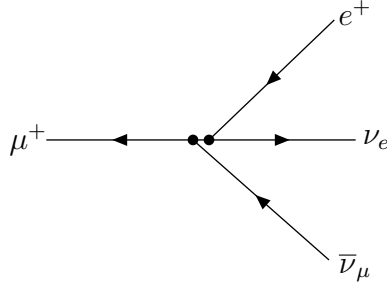
$$G_F = 1.166364(5) \times 10^{-5} \text{ GeV}^{-2}. \quad (7.2.50)$$

(This determination also includes some small and delicate corrections reviewed below in section 7.3.)

The 4-fermion weak interaction Lagrangian of eq. (7.2.21) describes several other processes besides the decay $\mu^- \rightarrow e^- \bar{\nu}_e \nu_\mu$ that we studied in subsection 7.2. As the simplest example, we can just replace each particle in the process by its anti-particle:

$$\mu^+ \rightarrow e^+ \nu_e \bar{\nu}_\mu, \quad (7.2.51)$$

for which the Feynman diagram is just obtained by changing all of the arrow directions:



The evaluations of the reduced matrix element and the differential and total decay rates for this decay are very similar to those for the $\mu^- \rightarrow e^- \bar{\nu}_e \nu_\mu$. For future reference, let us label the 4-momenta for this process as follows:

Particle	Momentum	Spinor
μ^+	p'_a	\bar{v}_a
e^+	k'_1	v_1
ν_e	k'_2	\bar{u}_2
$\bar{\nu}_\mu$	k'_3	v_3

(7.2.52)

The reduced matrix element, following from the “+c.c.” term in eq. (7.2.21), is then

$$\mathcal{M} = -i2\sqrt{2}G_F(\bar{v}_a\gamma^\rho P_L v_3)(\bar{u}_2\gamma_\rho P_L v_1). \quad (7.2.53)$$

As one might expect, the result for the spin-summed squared matrix element,

$$\sum_{\text{spins}} |\mathcal{M}|^2 = 128 G_F^2 (p'_a \cdot k'_2)(k'_1 \cdot k'_3), \quad (7.2.54)$$

is exactly the same as obtained in eq. (7.2.32), with the obvious substitution of primed 4-momenta. The differential and total decay rates that follow from this are, of course, exactly the same as for μ^- decay.

This is actually a special case of a general symmetry relation between particles and anti-particles, which holds true in any local quantum field theory, and is known as the CPT Theorem. The statement of the theorem is that the laws of physics, as specified by the Lagrangian, are left unchanged after one performs the *combined* operations of:

- charge conjugation (C): replacing each particle by its antiparticle,
- parity (P): replacing $\vec{x} \rightarrow -\vec{x}$,
- time reversal (T): replacing $t \rightarrow -t$.

It turns out to be impossible to write down any theory that fails to obey this rule, as long as the Lagrangian is invariant under proper Lorentz transformations and contains a finite number of spacetime derivatives and obeys some other technical assumptions. Among other things, the CPT Theorem implies that the mass and the total decay rate of a particle must each be equal to the same quantities for the corresponding anti-particle. (It does not say that the differential decay rate to a particular final state configuration necessarily has to be equal to the anti-particle differential decay rate to the same configuration of final-state anti-particles; that stronger result holds only if the theory is invariant under T. The four-fermion Fermi interaction for leptons does respect invariance under T, but it is violated by a tiny amount in the weak interactions of quarks.) We will study some other processes implied by the Fermi weak interaction Lagrangians in subsections 7.4, 7.5, and 7.6 below.

7.3 Corrections to muon decay

In the previous subsection, we derived the μ^- decay rate in terms of Fermi's four-fermion weak interaction coupling constant G_F . Since this decay process is actually the one that is used to experimentally determine G_F most accurately, it is worthwhile to note the leading corrections to it.

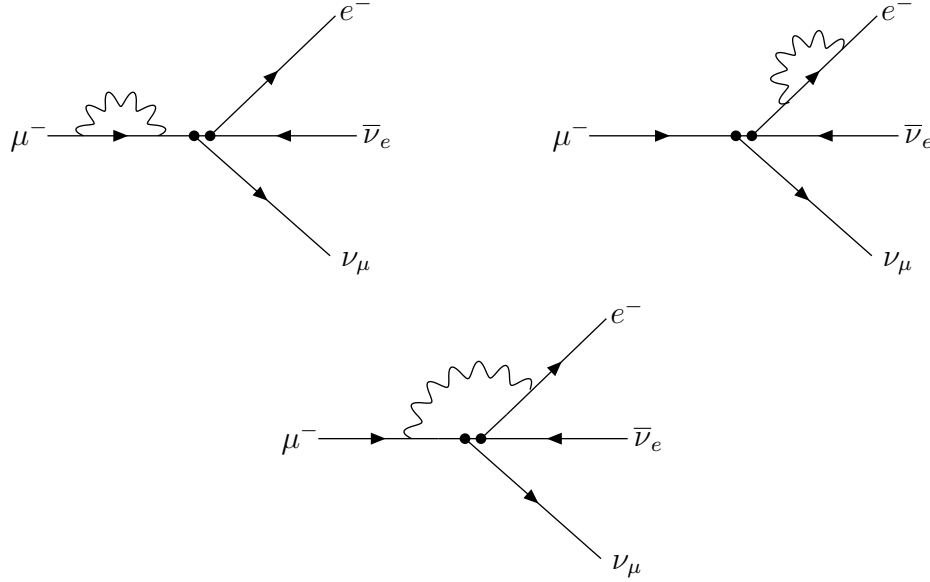
First, there is the dependence on m_e , which we neglected, but could have included at the cost of a more complicated phase space integration. Taking this into account using correct

kinematics for $m_e \neq 0$ and the limits of integration in eq. (6.4.7)-(6.4.9), one finds that the decay rate must be multiplied by a correction factor $F_{\text{kin}}(m_e^2/m_\mu^2)$, where

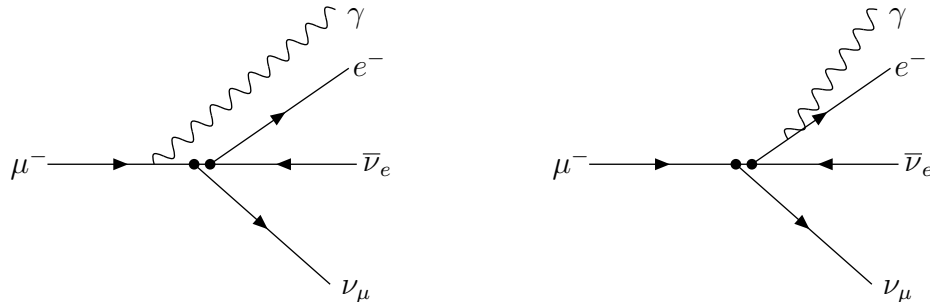
$$F_{\text{kin}}(x) = 1 - 8x + 8x^3 - x^4 - 12x^2 \ln x. \quad (7.3.1)$$

Numerically, $F_{\text{kin}}(m_e^2/m_\mu^2) = 0.999813$.

There are also corrections coming from two types of QED effects. First, there are loop diagrams involving virtual photons:



Evaluating these diagrams is beyond the scope of this course. However, it should be clear that they give contributions to the reduced matrix element proportional to $e^2 G_F$, since each contains two photon interaction vertices. These contributions to the reduced matrix element actually involve divergent loop integrals, which must be “regularized” by using a high-energy cutoff. There is then a logarithmic dependence on the cutoff energy, which can then be absorbed into a redefinition of the mass and coupling parameters of the model, by the systematic process of renormalization. The interference of the loop diagrams with the original lowest-order diagram then gives a contribution to the decay rate proportional to αG_F^2 . There are also QED contributions from diagrams with additional photons in the final state:



The QED diagrams involving an additional photon contribute to a 4-body final state, with a reduced matrix element proportional to eG_F . After squaring, summing over final spins, and averaging over the initial spin, and integrating over the 4-body phase space, the contribution to the decay rate is again proportional to αG_F^2 . Much of this contribution actually comes from very soft (low-energy) photons, which are difficult or impossible to resolve experimentally. Therefore, one usually just combines the two types of QED contributions into a total inclusive decay rate with one or more extra photons in the final state. After a heroic calculation, one finds that the QED effect on the total decay rate is to multiply by a correction factor

$$F_{\text{QED}}(\alpha) = 1 + \frac{\alpha}{\pi} \left(\frac{25}{8} - \frac{\pi^2}{2} - \frac{m_e^2}{m_\mu^2} \left[9 + 4\pi^2 + 24 \ln\left(\frac{m_e}{m_\mu}\right) \right] \right) + \left(\frac{\alpha}{\pi} \right)^2 C_2 + \dots \quad (7.3.2)$$

where the C_2 contribution refers to even higher-order corrections from: the interference between Feynman diagrams with two virtual photons and the original Feynman diagram; the interference between Feynman diagrams with one virtual photons plus one final state photon and the original Feynman diagram; the square of the reduced matrix element for a Feynman diagram involving one virtual photon; and two photons in the final state. A complicated calculation shows that $C_2 \approx 6.68$. Because of the renormalization procedure, the QED coupling α actually is dependent on the energy scale, and should be evaluated at the energy scale of interest for this problem, which is naturally m_μ . At that scale, $\alpha \approx 1/135.9$, so numerically

$$F_{\text{QED}}(\alpha) \approx 0.995802. \quad (7.3.3)$$

Finally, there are corrections involving the fact that the point-like four-fermion interaction is actually due to the effect of a virtual W^- boson. This gives a correction factor

$$F_W = 1 + \frac{3m_\mu^2}{5M_W^2} \approx 1.000001, \quad (7.3.4)$$

using $M_W = 80.4$ GeV. The predicted decay rate defining G_F experimentally including all these higher-order effects is

$$\Gamma_{\mu^-} = \frac{G_F^2 m_\mu^5}{192\pi^3} F_{\text{kin}} F_{\text{QED}} F_W. \quad (7.3.5)$$

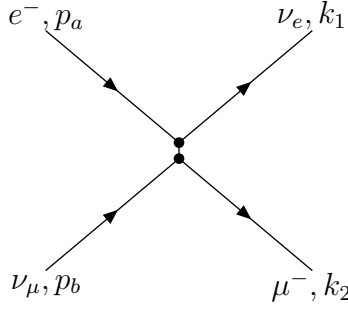
The dominant remaining uncertainty in G_F quoted in eq. (7.2.50) comes from the experimental input of the muon lifetime.

7.4 Inverse muon decay ($e^- \nu_\mu \rightarrow \nu_e \mu^-$)

Consider the process of muon-neutrino scattering on an electron:

$$e^- \nu_\mu \rightarrow \nu_e \mu^-. \quad (7.4.1)$$

The Feynman diagram for this process is:



in which we see that the following particles have been crossed from the previous diagram for μ^+ decay:

$$\text{initial } \mu^+ \rightarrow \text{final } \mu^- \quad (7.4.2)$$

$$\text{final } e^+ \rightarrow \text{initial } e^- \quad (7.4.3)$$

$$\text{final } \bar{\nu}_\mu \rightarrow \text{initial } \nu_\mu. \quad (7.4.4)$$

In fact, this scattering process is often known as inverse muon decay. To apply the Crossing Symmetry Theorem stated in section 5.3, we can assign momentum labels p_a, p_b, k_1, k_2 to $e^-, \nu_\mu, \nu_e, \mu^-$ respectively, as shown in the figure, and then make the following comparison table:

$\mu^+ \rightarrow e^+ \nu_e \bar{\nu}_\mu$	$e^- \nu_\mu \rightarrow \nu_e \mu^-$	
μ^+, p'_a	μ^-, k_2	
e^+, k'_1	e^-, p_a	
ν_e, k'_2	ν_e, k_1	
$\bar{\nu}_\mu, k'_3$	ν_μ, p_b	(7.4.5)

Therefore, we obtain the spin-summed, squared matrix element for $e^- \nu_\mu \rightarrow \nu_e \mu^-$ by making the replacements

$$p'_a = -k_2; \quad k'_1 = -p_a; \quad k'_2 = k_1; \quad k'_3 = -p_b \quad (7.4.6)$$

in eq. (7.2.54), and then multiplying by $(-1)^3$ for three crossed fermions, resulting in:

$$\sum_{\text{spins}} |\mathcal{M}_{e^- \nu_\mu \rightarrow \nu_e \mu^-}|^2 = 128 G_F^2 (k_2 \cdot k_1) (p_a \cdot p_b). \quad (7.4.7)$$

Let us evaluate this result in the limit of high-energy scattering, so that m_μ can be neglected, and in the center-of-momentum frame. In that case, all four particles being treated as massless, we can take the kinematics results from eqs. (5.2.139)-(5.2.143), so that $p_a \cdot p_b = k_1 \cdot k_2 = s/2$, and

$$\sum_{\text{spins}} |\mathcal{M}_{e^- \nu_\mu \rightarrow \nu_e \mu^-}|^2 = 32 G_F^2 s^2. \quad (7.4.8)$$

Including a factor of $1/2$ for the average over the initial-state electron spin,[†] and using eq. (4.5.49),

$$\frac{d\sigma}{d(\cos\theta)} = \frac{G_F^2 s}{2\pi}. \quad (7.4.9)$$

This differential cross-section is isotropic (independent of θ), so it is trivial to integrate $\int_{-1}^1 d(\cos\theta) = 2$ to get the total cross-section:

$$\sigma_{e^-\nu_\mu \rightarrow \nu_e \mu^-} = \frac{G_F^2 s}{\pi}. \quad (7.4.10)$$

Numerically, we can evaluate this using eq. (7.2.50):

$$\sigma_{e^-\nu_\mu \rightarrow \nu_e \mu^-} = 16.9 \text{ fb} \left(\frac{\sqrt{s}}{\text{GeV}} \right)^2. \quad (7.4.11)$$

In a typical experimental setup, the electrons will be contained in a target of ordinary material at rest in the lab frame. The muon neutrinos might be produced from a beam of decaying μ^- , which are in turn produced by decaying pions, as discussed later. If we call the ν_μ energy in the lab frame E_{ν_μ} , then the center-of-momentum energy is given by

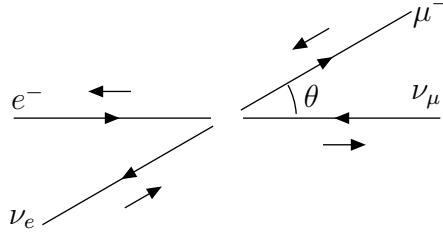
$$\sqrt{s} = E_{\text{CM}} = \sqrt{2E_{\nu_\mu}m_e + m_e^2} \approx \sqrt{2E_{\nu_\mu}m_e}. \quad (7.4.12)$$

Substituting this into eq. (7.4.11) gives:

$$\sigma_{e^-\nu_\mu \rightarrow \nu_e \mu^-} = 1.7 \times 10^{-2} \text{ fb} \left(\frac{E_{\nu_\mu}}{\text{GeV}} \right). \quad (7.4.13)$$

This is a very small cross-section for typical neutrino energies encountered in present experiments, but it does grow with E_{ν_μ} .

The isotropy of $e^-\nu_\mu \rightarrow \nu_e \mu^-$ scattering in the center-of-momentum frame can be understood from considering what the helicities dictated by the weak interactions tell us about the angular momentum. Since this is a weak interaction process involving only fermions and not anti-fermions, they are all L helicity.



We therefore see that the initial and final states both have total spin 0, so that the process is s -wave, and therefore necessarily isotropic.

[†]In the Standard Model with neutrino masses neglected, *all* neutrinos are left-handed, and *all* antineutrinos are right-handed. Since there is only one possible ν_μ helicity, namely L , it would be incorrect to average over the ν_μ spin. This is a general feature; one should never average over initial-state neutrino or antineutrino spins, as long as they are being treated as massless.

7.5 $e^- \bar{\nu}_e \rightarrow \mu^- \bar{\nu}_\mu$

As another example, consider the process of antineutrino-electron scattering:

$$e^- \bar{\nu}_e \rightarrow \mu^- \bar{\nu}_\mu. \quad (7.5.1)$$

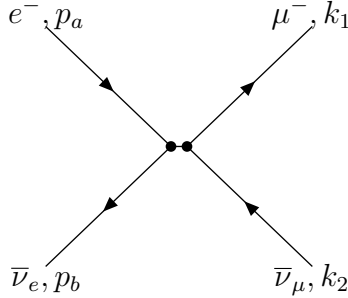
This process can again be obtained by crossing $\mu^+ \rightarrow e^+ \nu_e \bar{\nu}_\mu$ according to

$$\text{initial } \mu^+ \rightarrow \text{final } \mu^- \quad (7.5.2)$$

$$\text{final } e^+ \rightarrow \text{initial } e^- \quad (7.5.3)$$

$$\text{final } \nu_e \rightarrow \text{initial } \bar{\nu}_e, \quad (7.5.4)$$

as can be seen from the Feynman diagram:



Therefore, we obtain the spin-summed squared matrix element for $e^- \bar{\nu}_e \rightarrow \mu^- \bar{\nu}_\mu$ by making the substitutions

$$p'_a = -k_1; \quad k'_1 = -p_a; \quad k'_2 = -p_b; \quad k'_3 = k_2 \quad (7.5.5)$$

in eq. (7.2.54), and multiplying again by $(-1)^3$ because of the three crossed fermions. The result this time is:

$$\sum_{\text{spins}} |\mathcal{M}|^2 = 128 G_F^2 (k_1 \cdot p_b) (p_a \cdot k_2) = 32 G_F^2 u^2 = 8 G_F^2 s^2 (1 + \cos \theta)^2, \quad (7.5.6)$$

where eqs. (5.2.141) and (5.2.143) for 2→2 massless kinematics have been used. Here θ is the angle between the incoming e^- and the outgoing μ^- 3-momenta.

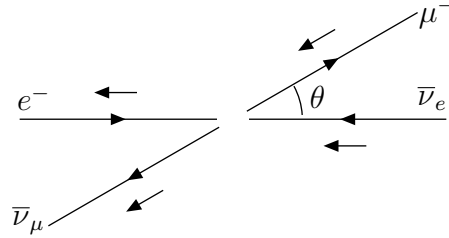
Substituting this result into eq. (4.5.49), with a factor of 1/2 to account for averaging over the initial e^- spin, we obtain:

$$\frac{d\sigma_{e^- \bar{\nu}_e \rightarrow \mu^- \bar{\nu}_\mu}}{d(\cos \theta)} = \frac{G_F^2 s}{8\pi} (1 + \cos \theta)^2. \quad (7.5.7)$$

Performing the $d(\cos \theta)$ integration gives a total cross-section of:

$$\sigma_{e^- \bar{\nu}_e \rightarrow \mu^- \bar{\nu}_\mu} = \frac{G_F^2 s}{3\pi}. \quad (7.5.8)$$

This calculation shows that in the center-of-momentum frame, the μ^- tends to keep going in the same direction as the original e^- . This can be understood from the helicity-spin-momentum diagram:



Since the helicities of e^- , $\bar{\nu}_e$, μ^- , $\bar{\nu}_\mu$ are respectively L, R, L, R, the total spin of the initial state must be pointing in the direction opposite to the e^- 3-momentum, and the total spin of the final state must be pointing opposite to the μ^- direction. The overlap between these two states is therefore maximized when the e^- and μ^- momenta are parallel, and vanishes when the μ^- tries to come out in the opposite direction to the e^- . Of course, this reaction usually occurs in a laboratory frame in which the initial e^- was at rest, so one must correct for this when interpreting the distribution in the lab frame.

The total cross-section for this reaction is $1/3$ of that for the reaction $e^- \nu_e \rightarrow \mu^- \nu_\mu$. This is because the former reaction is an isotropic s -wave (angular momentum 0), while the latter is a p -wave (angular momentum 1), which can only use one of the three possible $J = 1$ final states, namely, the one with \vec{J} pointing along the $\bar{\nu}_\mu$ direction.

7.6 Charged currents and π^\pm decay

The interaction Lagrangian term responsible for muon decay and for the cross-sections discussed above is just one term in the weak-interaction Lagrangian. More generally, we can write the Lagrangian as a product of a weak-interaction charged current J_ρ^- and its complex conjugate J_ρ^+ :

$$\mathcal{L}_{\text{int}} = -2\sqrt{2}G_F J_\rho^+ J^{-\rho}. \quad (7.6.1)$$

The weak-interaction charged current is obtained by adding together terms for pairs of fermions, with the constraint that the total charge of the current is -1 , and all Dirac fermion fields involved in the current are left-handed, and all barred fields are right-handed:

$$J_\rho^- = \bar{\nu}_e \gamma_\rho P_L e + \bar{\nu}_\mu \gamma_\rho P_L \mu + \bar{\nu}_\tau \gamma_\rho P_L \tau + \bar{u} \gamma_\rho P_L d' + \bar{c} \gamma_\rho P_L s' + \bar{t} \gamma_\rho P_L b'. \quad (7.6.2)$$

Notice that we have included contributions for the quarks. The quark fields d' , s' , and b' appearing here are actually not quite mass eigenstates, because of mixing; this is the reason for

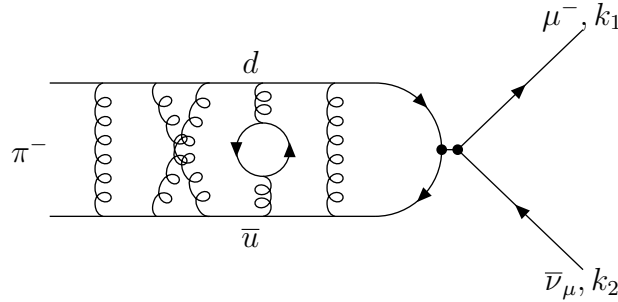
the primes. The complex conjugate of J_ρ^- has charge +1, and is given by:

$$J_\rho^+ = (J_\rho^-)^* = \bar{e}\gamma_\rho P_L \nu_e + \bar{\mu}\gamma_\rho P_L \nu_\mu + \bar{\tau}\gamma_\rho P_L \nu_\tau + \bar{d}'\gamma^\rho P_L u + \bar{s}'\gamma^\rho P_L c + \bar{b}'\gamma^\rho P_L t. \quad (7.6.3)$$

Both $J^{-\rho}$ and $J^{+\rho}$ transform under proper Lorentz transformations as four-vectors, and are $V - A$ fermion bilinears.

Unfortunately, there is an obstacle to a detailed, direct testing of the $(V - A)(V - A)$ form of the weak interaction Lagrangian for quarks. This is because the quarks are bound into hadrons by strong interactions, so that cross-sections and decays involving the weak interactions are subject to very large and very complicated corrections. However, one can still do a quantitative analysis of some aspects of weak decays involving hadrons, by a method of parameterizing our ignorance.

To see how this works, consider the process of charged pion decay. A π^- consists of a bound state made from a valence d quark and \bar{u} antiquark, together with many virtual gluons and quark-antiquark pairs. A Feynman diagram for $\pi^- \rightarrow \mu^- \bar{\nu}_\mu$ decay following from the current-current Lagrangian might therefore look like:



Unfortunately, the left-part of this Feynman diagram, involving the complications of the π^- bound state, is just a cartoon for the strong interactions, which are not amenable to perturbative calculation. The \bar{u} antiquark and d quark do not even have fixed momenta in this diagram, since they exchange energy and momentum with each other and with the virtual gluons and quark-anti-quark pairs. In principle, one can find some distribution for the \bar{u} and d momenta, and try to average over that distribution, but the strong interactions are very complicated so this is not very easy to do from the theoretical side. However, by considering what we do know about the current-current Lagrangian, we can write down the general form of the reduced matrix element. First, we know that the external state spinors for the fermions are:

Particle	Momentum	Spinor	
μ^-	k_1	\bar{u}_1	(7.6.4)
$\bar{\nu}_\mu$	k_2	v_2	

In terms of these spinors, we can write:

$$\mathcal{M} = -i\sqrt{2}G_F f_\pi p_\rho (\bar{u}_1 \gamma^\rho P_L v_2). \quad (7.6.5)$$

In this formula, the factor $(\bar{u}_1 \gamma^\rho P_L v_2)$ just reflects the fact that leptons are immune from the complications of the strong interactions. The factor $f_\pi p_\rho$ takes into account the part of the reduced matrix element involving the π^- ; here p^ρ is the 4-momentum of the pion. The point is that whatever the pion factor in the reduced matrix element is, we know that it is a four-vector in order to contract with the lepton part, and it must be proportional to p^ρ , since there is no other vector quantity in the problem that it can depend on. (Recall that pions are spinless, so there is no spin dependence.) So we are simply parameterizing all of our ignorance of the bound-state properties of the pion in terms of a single constant f_π , called the pion decay constant. It is a quantity with dimensions of mass. In principle we could compute it if we had perfect ability to calculate with the strong interactions. In practice, f_π is an experimentally measured quantity, with its value following most accurately from the π^- lifetime that we will compute below. The factor $\sqrt{2}G_F$ is another historical convention; it could have been absorbed into the definition of f_π . But it is useful to have the G_F appear explicitly as a sign that this is a weak interaction; then f_π is entirely a strong-interaction parameter.

Let us now compute the decay rate for $\pi^- \rightarrow \mu^- \bar{\nu}_\mu$. Taking the complex square of the reduced matrix element eq. (7.6.5), we have:

$$|\mathcal{M}|^2 = 2G_F^2 f_\pi^2 p_\rho p_\sigma (\bar{u}_1 \gamma^\rho P_L v_2) (\bar{v}_2 P_R \gamma^\sigma u_1). \quad (7.6.6)$$

Now summing over final state spins in the usual way gives:

$$\sum_{\text{spins}} |\mathcal{M}|^2 = 2G_F^2 f_\pi^2 p_\rho p_\sigma \text{Tr}[\gamma^\rho P_L \not{k}_2 P_R \gamma^\sigma (\not{k}_1 + m_\mu)] = 2G_F^2 f_\pi^2 \text{Tr}[\not{p} \not{k}_2 P_R \not{p} \not{k}_1]. \quad (7.6.7)$$

Note that we do not neglect the mass of the muon, since $m_\mu/m_{\pi^\pm} = 0.1056 \text{ GeV}/0.1396 \text{ GeV} = 0.756$ is not a small number. However, the term in eq. (7.6.7) that explicitly involves m_μ does not contribute, since the trace of 3 gamma matrices (with or without a P_R) vanishes. Evaluating the trace, we have:

$$\text{Tr}[\not{p} \not{k}_2 P_R \not{p} \not{k}_1] = 4(p \cdot k_1)(p \cdot k_2) - 2p^2(k_1 \cdot k_2). \quad (7.6.8)$$

The decay kinematics tells us that:

$$p^2 = m_{\pi^\pm}^2; \quad k_1^2 = m_\mu^2; \quad k_2^2 = m_{\bar{\nu}_\mu}^2 = 0; \quad (7.6.9)$$

$$p \cdot k_1 = \frac{1}{2}[-(p - k_1)^2 + p^2 + k_1^2] = \frac{1}{2}(m_{\pi^\pm}^2 + m_\mu^2); \quad (7.6.10)$$

$$p \cdot k_2 = \frac{1}{2}[-(p - k_2)^2 + p^2 + k_2^2] = \frac{1}{2}(-m_\mu^2 + m_{\pi^\pm}^2); \quad (7.6.11)$$

$$k_1 \cdot k_2 = \frac{1}{2}[(k_1 + k_2)^2 - k_1^2 - k_2^2] = \frac{1}{2}(m_{\pi^\pm}^2 - m_\mu^2). \quad (7.6.12)$$

Therefore, $\text{Tr}[\not{p}_2 P_R \not{p}_1] = m_\mu^2(m_{\pi^\pm}^2 - m_\mu^2)$, and

$$\sum_{\text{spins}} |\mathcal{M}|^2 = 2G_F^2 f_\pi^2 m_{\pi^\pm}^2 m_\mu^2 \left(1 - \frac{m_\mu^2}{m_{\pi^\pm}^2}\right), \quad (7.6.13)$$

so that using eq. (6.2.14), we get:

$$d\Gamma = \frac{G_F^2 f_\pi^2 m_{\pi^\pm}^2 m_\mu^2}{32\pi^2} \left(1 - \frac{m_\mu^2}{m_{\pi^\pm}^2}\right)^2 d\phi d(\cos\theta), \quad (7.6.14)$$

where (θ, ϕ) are the angles for the μ^- three-momentum. Of course, since the pion is spinless, the differential decay rate is isotropic, so the angular integration trivially gives $d\phi d(\cos\theta) \rightarrow 4\pi$, and:

$$\Gamma(\pi^- \rightarrow \mu^- \bar{\nu}_\mu) = \frac{G_F^2 f_\pi^2 m_{\pi^\pm}^2 m_\mu^2}{8\pi} \left(1 - \frac{m_\mu^2}{m_{\pi^\pm}^2}\right)^2. \quad (7.6.15)$$

The charged pion can also decay according to $\pi^- \rightarrow e^- \bar{\nu}_e$. The calculation of this decay rate is identical to the one just given, except that m_e is substituted everywhere for m_μ . Therefore, we have:

$$\Gamma(\pi^- \rightarrow e^- \bar{\nu}_e) = \frac{G_F^2 f_\pi^2 m_{\pi^\pm}^2 m_e^2}{8\pi} \left(1 - \frac{m_e^2}{m_{\pi^\pm}^2}\right)^2, \quad (7.6.16)$$

and the ratio of branching ratios is predicted to be:

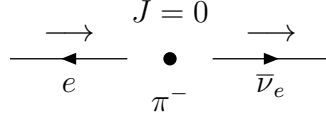
$$\frac{\text{BR}(\pi^- \rightarrow e^- \bar{\nu}_e)}{\text{BR}(\pi^- \rightarrow \mu^- \bar{\nu}_\mu)} = \frac{\Gamma(\pi^- \rightarrow e^- \bar{\nu}_e)}{\Gamma(\pi^- \rightarrow \mu^- \bar{\nu}_\mu)} = \left(\frac{m_e^2}{m_\mu^2}\right) \left(\frac{m_{\pi^\pm}^2 - m_e^2}{m_{\pi^\pm}^2 - m_\mu^2}\right)^2 = 1.2 \times 10^{-4}. \quad (7.6.17)$$

The ratio eq. (7.6.17) is a robust prediction of the theory, because the dependence on f_π has canceled out. Since there are no other kinematically-possible two-body decay channels open to π^- , it should decay to $\mu^- \bar{\nu}_\mu$ almost always, with a rare decay to $e^- \bar{\nu}_e$ occurring 0.012% of the time. This has been confirmed experimentally. We can also use the measurement of the total lifetime of the π^- to find f_π numerically, using eq. (7.6.15). The result is:

$$f_\pi = 0.128 \text{ GeV}. \quad (7.6.18)$$

It is not surprising that this value is of the same order-of-magnitude as the mass of the pion.

The most striking feature of the π^- decay rate is that it is proportional to m_μ^2 , with \mathcal{M} proportional to m_μ . This is what leads to the strong suppression of decays to $e^- \bar{\nu}_e$ (already mentioned at the end of section 7.1). We found this result just by calculating. To understand it better, we can draw a momentum-helicity-spin diagram, using the fact that the ℓ^- and $\bar{\nu}_\ell$ produced in the weak interactions are L and R respectively:



The π^- has spin 0, but the final state predicted by the weak interaction helicities unambiguously has spin 1. Therefore, if helicity were exactly conserved, the π^- could not decay at all! However, helicity conservation only holds in the high-energy limit in which we can treat all fermions as massless. This decay is said to be helicity-suppressed, since the only reason it can occur is because m_μ and m_e are non-zero. In the limit $m_\ell \rightarrow 0$, we recover exact helicity conservation and the reduced matrix element and the decay lifetime vanish. This explains why they should be proportional to m_ℓ and m_ℓ^2 respectively. The helicity suppression of this decay is therefore a good prediction of the rule that the weak interactions affect only L fermions and R antifermions. In the final state, the charged lepton μ^- or e^- is said to undergo a helicity flip, meaning that the L-helicity fermion produced by the weak interactions has an amplitude to appear in the final state as a R-fermion. In general, a helicity flip for a fermion entails a suppression in the reduced matrix element proportional to the mass of the fermion divided by its energy.

Having computed the decay rate following from eq. (7.6.5), let us find a Lagrangian that would give rise to it involving a quantum field for the pion. Although the pion is a composite, bound-state particle, we can still invent a quantum field for it, in an approximate, “effective” description. The π^- corresponds to a charged spin-0 field. Previously, we studied spin-0 particles described by a real scalar field. However, the particle and antiparticle created by a real scalar field turned out to be the same thing. Here we want something different; since the π^- is charged, its antiparticle π^+ is clearly a different particle. This means that the π^- particle should be described by a complex scalar field.

Let us therefore define $\pi^-(x)$ to be a complex scalar field, with its complex conjugate given by

$$\pi^+(x) \equiv (\pi^-(x))^*. \quad (7.6.19)$$

We can construct a real free Lagrangian density from these complex fields as follows:

$$\mathcal{L} = \partial_\mu \pi^+ \partial^\mu \pi^- - m_{\pi^\pm}^2 \pi^+ \pi^-. \quad (7.6.20)$$

[Compare to the Lagrangian density for a real scalar field, eq. (4.1.18).] This Lagrangian density describes free pion fields with mass m_{π^\pm} . At any fixed time $t = 0$, the π^+ and π^- fields can be

expanded in creation and annihilation operators as:

$$\pi^-(\vec{x}) = \int d\vec{p} (e^{i\vec{p}\cdot\vec{x}} a_{\vec{p},-} + e^{-i\vec{p}\cdot\vec{x}} a_{\vec{p},+}^\dagger); \quad (7.6.21)$$

$$\pi^+(\vec{x}) = \int d\vec{p} (e^{i\vec{p}\cdot\vec{x}} a_{\vec{p},+} + e^{-i\vec{p}\cdot\vec{x}} a_{\vec{p},-}^\dagger). \quad (7.6.22)$$

Note that these fields are indeed complex conjugates of each other, and that they are each complex since $a_{\vec{p},-}$ and $a_{\vec{p},+}$ are taken to be independent. The operators $a_{\vec{p},-}$ and $a_{\vec{p},-}^\dagger$ act on states by destroying and creating a π^- particle with 3-momentum \vec{p} . Likewise, the operators $a_{\vec{p},+}$ and $a_{\vec{p},+}^\dagger$ act on states by destroying and creating a π^+ particle with 3-momentum \vec{p} . In particular, the single particle states are:

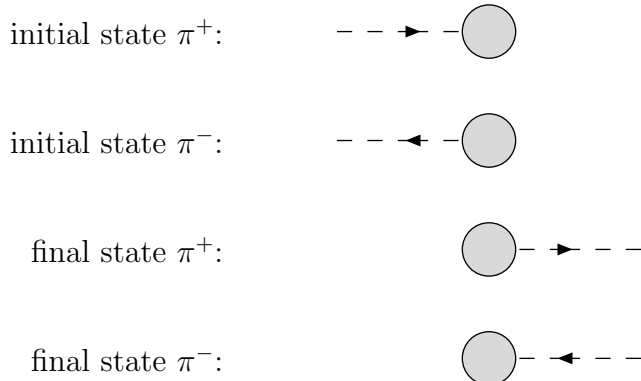
$$a_{\vec{p},-}^\dagger |0\rangle = |\pi^-; \vec{p}\rangle, \quad (7.6.23)$$

$$a_{\vec{p},+}^\dagger |0\rangle = |\pi^+; \vec{p}\rangle. \quad (7.6.24)$$

One can now carry through canonical quantization as usual. Given an interaction Lagrangian, one can derive the corresponding Feynman rules for the propagator and interaction vertices. Since a π^- moving forward in time is a π^+ moving backwards in time, and vice versa, there is only one propagator for π^\pm fields. It differs from the propagator for an ordinary scalar in that it carries an arrow indicating the direction of the flow of charge:

$$- - - \blacktriangleright - - - \quad \longleftrightarrow \quad \frac{i}{p^2 - m_{\pi^\pm}^2 + i\epsilon}$$

The external state pion lines also carry an arrow direction telling us whether it is a π^- or a π^+ particle. A pion line entering from the left with an arrow pointing to the right means a π^+ particle in the initial state, while a line entering from the left with an arrow pointing back to the left means a π^- particle in the initial state. Similarly, if a pion line leaves the diagram to the right, it represents a final state pion, with an arrow to the right meaning a π^+ and an arrow to the left meaning a π^- . We can summarize this with the following mnemonic figures:



In each case the Feynman rule factor associated with the initial- or final-state pion is just 1.

Returning to the reduced matrix element of eq. (7.6.5), we can interpret this as coming from a pion-lepton-antineutrino interaction vertex. When we computed the decay matrix element, the pion was on-shell, but in general this need not be the case. The pion decay constant f_π must therefore be generalized to a function $f(p^2)$, with

$$f(p^2)|_{p^2=m_{\pi\pm}^2} = f_\pi \quad (7.6.25)$$

when the pion is on-shell. The momentum-space factor $f(p^2)p_\rho$ can be interpreted by identifying the 4-momentum as a differential operator acting on the pion field, using:

$$p_\rho \leftrightarrow i\partial_\rho. \quad (7.6.26)$$

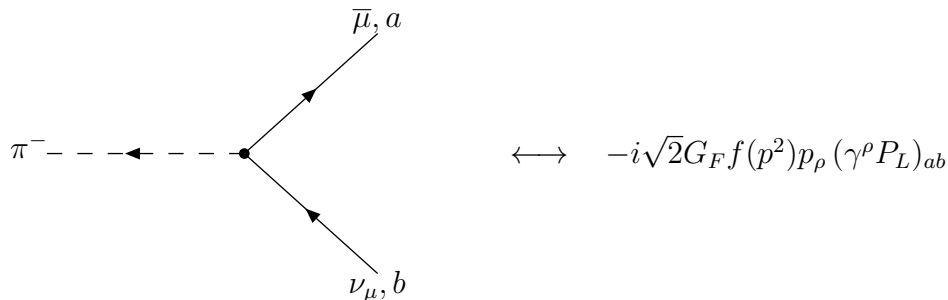
Then, reversing the usual procedure of inferring the Feynman rule from a term in the interaction Lagrangian, we conclude that the effective interaction describing π^- decay is:

$$\mathcal{L}_{\text{int}, \pi^- \bar{\mu} \nu_\mu} = -\sqrt{2} G_F (\bar{\mu} \gamma^\rho P_L \nu_\mu) f (-\partial^2) \partial_\rho \pi^-. \quad (7.6.27)$$

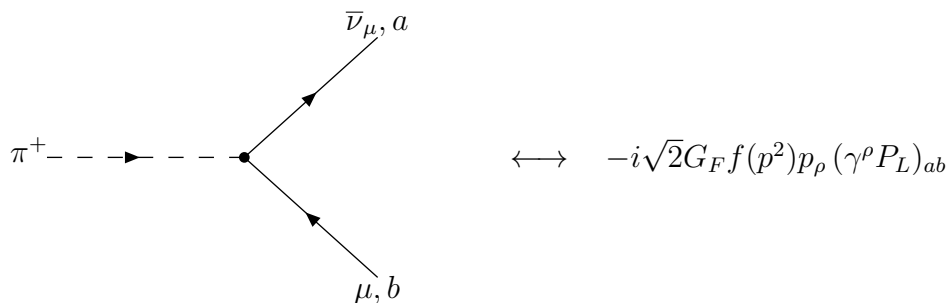
Here $f(-\partial^2)$ can in principle be defined in terms of its power-series expansion in the differential operator $-\partial^2 = \vec{\nabla}^2 - \partial_t^2$ acting on the pion field. In practice, one usually just works in momentum space where it is $f(p^2)$. Since the Lagrangian must be real, we must also include the complex conjugate of this term:

$$\mathcal{L}_{\text{int}, \pi^+ \mu \bar{\nu}_\mu} = -\sqrt{2} G_F (\bar{\nu}_\mu \gamma^\rho P_L \mu) f(-\partial^2) \partial_\rho \pi^+. \quad (7.6.28)$$

The Feynman rules for these effective interactions are:



and



In each Feynman diagram, the arrow on the pion line describes the direction of flow of charge, and the 4-momentum p^ρ is taken to be flowing in to the vertex. When the pion is on-shell, one can replace $f(p^2)$ by the pion decay constant f_π .

Other charged mesons made out of a quark and antiquark, like the K^\pm , D^\pm , and D_s^\pm , have their own decay constants f_K , f_D , and f_{D_s} , and their decays can be treated in a similar way.

7.7 Unitarity, renormalizability, and the W boson

An important feature of weak-interaction $2 \rightarrow 2$ cross-sections following from Fermi's four-fermion interaction is that they grow proportional to s for very large s ; see eqs. (7.4.10) and (7.5.8). This had to be true on general grounds just from dimensional analysis. Any reduced matrix element that contains one four-fermion interaction will be proportional to G_F , so the cross-section will have to be proportional to G_F^2 . Since this has units of $[\text{mass}]^{-4}$, and cross-sections must have dimensions of $[\text{mass}]^{-2}$, it must be that the cross-section scales like the square of the characteristic energy of the process, s , in the high-energy limit in which all other kinematic mass scales are comparatively unimportant. This behavior of $\sigma \propto s$ is not acceptable for arbitrarily large s , since the cross-section is bounded by the fact that the probability for any two particles to scatter cannot exceed 1. In quantum mechanical language, the constraint is on the unitarity of the time-evolution operator e^{-iHt} . If the cross-section grows too large, then our perturbative approximation $e^{-iHt} = 1 - iHt$ represented by the lowest-order Feynman diagram must break down. The reduced matrix element found from just including this Feynman diagram will have to be compensated somehow by higher-order diagrams, or by changing the physics of the weak interactions at some higher energy scale.

Let us develop the dimensional analysis of fields and couplings further. We know that the Lagrangian must have the same units as energy. In the standard system in which $c = \hbar = 1$, this is equal to units of $[\text{mass}]$. Since $d^3\vec{x}$ has units of $[\text{length}]^3$, or $[\text{mass}]^{-3}$, and

$$L = \int d^3\vec{x} \mathcal{L}, \quad (7.7.1)$$

it must be that \mathcal{L} has units of $[\text{mass}]^4$. This fact allows us to evaluate the units of all fields and couplings in a theory. For example, a spacetime derivative has units of inverse length, or $[\text{mass}]$. Therefore, from the kinetic terms for scalars, fermions, and vector fields found for example in eqs. (4.1.18), (4.1.26), and (4.1.34), we find that these types of fields must have dimensions of $[\text{mass}]$, $[\text{mass}]^{3/2}$, and $[\text{mass}]$ respectively. This allows us to evaluate the units of various possible interaction couplings that appear in the Lagrangian density. For example, a coupling of n scalar fields,

$$\mathcal{L}_{\text{int}} = -\frac{\lambda_n}{n!} \phi^n \quad (7.7.2)$$

implies that λ_n has units of $[\text{mass}]^{4-n}$. A vector-fermion-fermion coupling, like e in QED, is dimensionless. The effective coupling f_π for on-shell pions has dimensions of $[\text{mass}]$, because of the presence of a spacetime derivative together with a scalar field and two fermion fields in the Lagrangian. Summarizing this information for the known types of fields and couplings that we have encountered so far:

<i>Object</i>	<i>Dimension</i>	<i>Role</i>	(7.7.3)
\mathcal{L}	$[\text{mass}]^4$	Lagrangian density	
∂_μ	$[\text{mass}]$	derivative	
ϕ	$[\text{mass}]$	scalar field	
Ψ	$[\text{mass}]^{3/2}$	fermion field	
A^μ	$[\text{mass}]$	vector field	
λ_3	$[\text{mass}]$	scalar ³ coupling	
λ_4	$[\text{mass}]^0$	scalar ⁴ coupling	
y	$[\text{mass}]^0$	scalar-fermion-fermion (Yukawa) coupling	
e	$[\text{mass}]^0$	photon-fermion-fermion coupling	
G_F	$[\text{mass}]^{-2}$	fermion ⁴ coupling	
f_π	$[\text{mass}]$	fermion ² -scalar-derivative coupling	
u, v, \bar{u}, \bar{v}	$[\text{mass}]^{1/2}$	external-state spinors	
$\mathcal{M}_{N_i \rightarrow N_f}$	$[\text{mass}]^{4-N_i-N_f}$	reduced matrix element for $N_i \rightarrow N_f$ particles	
σ	$[\text{mass}]^{-2}$	cross-section	
Γ	$[\text{mass}]$	decay rate.	

It is a general fact that theories with couplings with negative mass dimension, like G_F , or λ_n for $n \geq 5$, always suffer from a problem known as non-renormalizability.[†] In a renormalizable theory, the divergences that occur in loop diagrams due to integrating over arbitrarily large 4-momenta for virtual particles can be regularized by introducing a high momentum cutoff, and then the resulting dependence on the unknown cutoff can be absorbed into a redefinition of the masses and coupling constants of the theory. In contrast, in a non-renormalizable theory, one finds that this process requires introducing an infinite number of different couplings, each of which must be redefined in order to absorb the momentum-cutoff dependence. This dependence on an infinite number of different coupling constants makes non-renormalizable theories non-predictive, although only in principle. We can always use non-renormalizable theories as effective theories at low energies, as we have done in the case of the four-fermion theory of the weak

[†]The converse is not true; just because a theory has only couplings with positive or zero mass dimension does not guarantee that it is renormalizable. It is a necessary, but not sufficient, condition.

In the limit of low energies and momenta, $|p_\rho| \ll m_W$, this propagator just becomes a constant:

$$\frac{i}{p^2 - m_W^2 + i\epsilon} \left[-g_{\rho\sigma} + \frac{p_\rho p_\sigma}{m_W^2} \right] \longrightarrow i \frac{g_{\rho\sigma}}{m_W^2}. \quad (7.7.4)$$

In order to complete the correspondence between the effective four-fermion interaction and the more fundamental version involving the vector boson, we need W -fermion-antifermion vertex Feynman rules of the form:

$$\begin{aligned} & \begin{array}{c} \bar{\ell}, a \\ \nearrow \\ W, \rho \\ \searrow \\ \nu_\ell, b \end{array} \longleftrightarrow -i \frac{g}{\sqrt{2}} (\gamma^\rho P_L)_{ab} \\ & \begin{array}{c} \bar{\nu}_\ell, a \\ \nearrow \\ W, \rho \\ \searrow \\ \ell, b \end{array} \longleftrightarrow -i \frac{g}{\sqrt{2}} (\gamma^\rho P_L)_{ab} \end{aligned}$$

Here g is a fundamental coupling of the weak interactions, and the $1/\sqrt{2}$ is a standard convention. These are the Feynman rules involving W^\pm interactions with leptons; there are similar rules for interactions with the quarks in the charged currents J_ρ^+ and J_ρ^- given earlier in eqs. (7.6.2) and (7.6.3). The interaction Lagrangian for W bosons with standard model fermions corresponding to these Feynman rules is:

$$\mathcal{L}_{\text{int}} = -\frac{g}{\sqrt{2}} (W^{+\rho} J_\rho^- + W^{-\rho} J_\rho^+). \quad (7.7.5)$$

Comparing the four-fermion vertex to the reduced matrix element from W -boson exchange, we find that we must have:

$$-i2\sqrt{2}G_F = \left(\frac{-ig}{\sqrt{2}} \right)^2 \left(\frac{i}{m_W^2} \right), \quad (7.7.6)$$

so that

$$G_F = \frac{g^2}{4\sqrt{2}m_W^2}. \quad (7.7.7)$$

The W^\pm boson has been discovered, with a mass $m_W = 80.4$ GeV, so we conclude that

$$g \approx 0.65. \quad (7.7.8)$$

Since this is a dimensionless coupling, there is at least a chance to make this into a renormalizable theory that is unitary in perturbation theory. At very high energies, the W^\pm propagator will

behave like $1/p^2$, rather than the $1/m_W^2$ that is encoded in G_F in the four-fermion approximation. This “softens” the weak interactions at high energies, leading to cross-sections that fall, rather than rise, at very high \sqrt{s} .

When a massive vector boson appears in a final state, it has a Feynman rule given by a polarization vector $\epsilon^\mu(p, \lambda)$, just like the photon did. The difference is that a massive vector particle V has three physical polarization states $\lambda = 1, 2, 3$, satisfying

$$p^\rho \epsilon_\rho(p, \lambda) = 0 \quad (\lambda = 1, 2, 3). \quad (7.7.9)$$

One can sum over these polarizations for an initial or final state in a squared reduced matrix element, with the result:

$$\sum_{\lambda=1}^3 \epsilon_{\rho}(p, \lambda) \epsilon_{\sigma}^*(p, \lambda) = -g_{\rho\sigma} + \frac{p_{\rho} p_{\sigma}}{m_V^2}. \quad (7.7.10)$$

Summarizing the propagator and external state Feynman rules for a generic massive vector boson for future reference:

$$\begin{array}{lcl}
\rho \text{---}\text{---}\sigma & \longleftrightarrow & \frac{i}{p^2 - m_V^2 + i\epsilon} \left[-g_{\rho\sigma} + \frac{p_\rho p_\sigma}{m_V^2} \right] \\
\text{initial state vector: } \mu \text{---}\text{---}\text{[blob]} & \longleftrightarrow & \epsilon_\mu(p, \lambda) \\
\text{final state vector: } \text{[blob]} \text{---}\text{---}\mu & \longleftrightarrow & \epsilon_\mu^*(p, \lambda)
\end{array}$$

If the massive vector is charged, like the W^\pm bosons, then an arrow is added to each line to show the direction of flow of charge.

The weak interactions and the strong interactions are invariant under non-Abelian gauge transformations, which involve a generalization of the type of gauge invariance we have already encountered in the case of QED. This means that the gauge transformations not only multiply fields by phases, but can mix the fields. In the next section we will begin to study the properties of field theories, known as Yang-Mills theories, which have a non-Abelian gauge invariance. This will enable us to get a complete theory of the weak interactions.

8 Gauge theories

8.1 Groups and representations

In this section, we will generalize the idea of gauge invariance found in electrodynamics. Recall that in QED the Lagrangian is defined in terms of a covariant derivative

$$D_\mu = \partial_\mu + iQeA_\mu \quad (8.1.1)$$

and a field strength

$$F_{\mu\nu} = \partial_\mu A_\nu - \partial_\nu A_\mu \quad (8.1.2)$$

as

$$\mathcal{L} = -\frac{1}{4}F^{\mu\nu}F_{\mu\nu} + i\bar{\Psi}\not{D}\Psi - m\bar{\Psi}\Psi. \quad (8.1.3)$$

This Lagrangian is invariant under the local gauge transformation

$$A_\mu \rightarrow A'_\mu = A_\mu - \frac{1}{e}\partial_\mu\theta, \quad (8.1.4)$$

$$\Psi \rightarrow \Psi' = e^{iQ\theta}\Psi, \quad (8.1.5)$$

where $\theta(x)$ is any function of spacetime, called a gauge parameter. Now, the result of doing one gauge transformation θ_1 followed by another gauge transformation θ_2 is always a third gauge transformation parameterized by the function $\theta_1 + \theta_2$:

$$A_\mu \rightarrow (A_\mu - \frac{1}{e}\partial_\mu\theta_1) - \frac{1}{e}\partial_\mu\theta_2 = A_\mu - \frac{1}{e}\partial_\mu(\theta_1 + \theta_2), \quad (8.1.6)$$

$$\Psi \rightarrow e^{iQ\theta_2}(e^{iQ\theta_1}\Psi) = e^{iQ(\theta_1+\theta_2)}\Psi. \quad (8.1.7)$$

Mathematically, these gauge transformations are an example of a group.

A group is a set of elements $G = \{g_i\}$ and a rule for multiplying them, with the properties:

- 1) *Closure*: If g_i and g_j are elements of the group G , then the product $g_i g_j$ is also an element of G .
- 2) *Associativity*: $g_i(g_j g_k) = (g_i g_j)g_k$.
- 3) *Existence of an Identity*: There is a unique element $I = g_1$ of the group, such that for all g_i in G , $I g_i = g_i I = g_i$.
- 4) *Inversion*: For each g_i , there is a unique inverse element $(g_i)^{-1}$ satisfying $(g_i)^{-1} g_i = g_i (g_i)^{-1} = I$.

It may or may not be also true that the group also satisfies the commutativity property:

$$g_i g_j = g_j g_i. \quad (8.1.8)$$

If this is satisfied, then the group is called commutative or Abelian. Otherwise it is non-commutative or non-Abelian.

In generalizing the QED Lagrangian, we will be interested in continuous Lie groups. A continuous group has an uncountably infinite number of elements labeled by one or more continuously varying parameters, which turn out to be nothing other than the generalizations of the gauge parameter θ in QED. A Lie group is a continuous group that also has the desirable property of being differentiable with respect to the gauge parameters.

The action of group elements on physics states or fields can be represented by a set of complex $n \times n$ matrices acting on n -dimensional complex vectors. This association of group elements with $n \times n$ matrices and the states or fields that they act on is said to form a representation of the group. The matrices obey the same rules as the group elements themselves.

For example, the group of QED gauge transformations is the Abelian Lie group $U(1)$. According to eq. (8.1.5), the group is represented on Dirac fermion fields by complex 1×1 matrices:

$$U_Q(\theta) = e^{iQ\theta}. \quad (8.1.9)$$

Here θ labels the group elements, and the charge Q labels the representation of the group. So we can say that the electron, muon, and tau Dirac fields each live in a representation of the group $U(1)$ with charge $Q = -1$; the Dirac fields for up, charm, and top quarks each live in a representation with charge $Q = 2/3$; and the Dirac fields for down, strange and bottom quarks each live in a representation with $Q = -1/3$. We can read off the charge of any field if we know how it transforms under the gauge group. A barred Dirac field transforms with the opposite phase from the original Dirac field of charge Q , and therefore has charge $-Q$.

Objects that transform into themselves with no change are said to be in the singlet representation. In general, the Lagrangian should be invariant under gauge transformations, and therefore must be in the singlet representation. For example, each term of the QED Lagrangian carries no charge, and so is a singlet of $U(1)$. The photon field A_μ has charge 0, and is therefore usually said (by a slight abuse of language) to transform as a singlet representation of $U(1)$. [Technically, it does not really transform under gauge transformations as any representation of the group $U(1)$, because of the derivative term in eq. (8.1.4), unless θ is a constant function so that one is making the same transformation everywhere in spacetime.]

Let us now generalize to non-Abelian groups, which always involve representations containing more than one field or state. Let φ_i be a set of objects that together transform in some

representation R of the group G . The number of components of φ_i is called the dimension of the representation, d_R , so that $i = 1, \dots, d_R$. Under a group transformation,

$$\varphi_i \rightarrow \varphi'_i = U_i^j \varphi_j \quad (8.1.10)$$

where U_i^j is a representation matrix. We are especially interested in transformations that are represented by unitary matrices, so that their action can be realized on the quantum Hilbert space by a unitary operator. Consider the subset of group elements that are infinitesimally close to the identity element. We can write these in the form:

$$U(\epsilon)_i^j = (1 + i\epsilon^a T^a)_i^j. \quad (8.1.11)$$

Here the T_i^{aj} are a basis for all the possible infinitesimal group transformations. The number of matrices T^a is called the dimension of the group, d_G , and there is an implicit sum over $a = 1, \dots, d_G$. The ϵ^a are a set of d_G infinitesimal gauge parameters (analogous to θ in QED) that tell us how much of each is included in the transformation represented by $U(\epsilon)$. Since $U(\epsilon)$ is unitary,

$$U(\epsilon)^\dagger = U(\epsilon)^{-1} = 1 - i\epsilon^a T^a, \quad (8.1.12)$$

from which it follows that the matrices T^a must be Hermitian.

Consider two group transformations g_ϵ and g_δ parameterized by ϵ^a and δ^a . By the closure property we can then form a new group element

$$g_\epsilon g_\delta g_\epsilon^{-1} g_\delta^{-1}. \quad (8.1.13)$$

Working with some particular representation, this corresponds to

$$U(\epsilon)U(\delta)U(\epsilon)^{-1}U(\delta)^{-1} = (1 + i\epsilon^a T^a)(1 + i\delta^b T^b)(1 - i\epsilon^c T^c)(1 - i\delta^d T^d) \quad (8.1.14)$$

$$= 1 - \epsilon^a \delta^b [T^a, T^b] + \dots \quad (8.1.15)$$

The closure property requires that this is a representation of the group element in eq. (8.1.13), which must also be close to the identity. It follows that

$$[T^a, T^b] = if^{abc} T^c \quad (8.1.16)$$

for some set of numbers f^{abc} , called the structure constants of the group. In practice, one often picks a particular representation of matrices T^a as the defining or fundamental representation. This determines the structure constants f^{abc} once and for all. The set of matrices T^a for all other representations are then required to reproduce eq. (8.1.16), which fixes their overall

normalization. Equation (8.1.16) defines the Lie algebra corresponding to the Lie group, and the hermitian matrices T^a are said to be generators of the Lie algebra for the corresponding representation. Many physicists have a bad habit of using the words “Lie group” and “Lie algebra” interchangeably, because we often only care about the subset of gauge transformations that are close to the identity.

For any given representation R , one can always choose the generators so that:

$$\text{Tr}(T_R^a T_R^b) = I(R) \delta^{ab}. \quad (8.1.17)$$

The number $I(R)$ is called the index of the representation. A standard choice is that the index of the fundamental representation of a non-Abelian Lie algebra is $1/2$. (This can always be achieved by rescaling the T^a , if necessary.) From eqs. (8.1.16) and (8.1.17), one obtains for any representation R :

$$iI(R)f^{abc} = \text{Tr}([T_R^a, T_R^b]T_R^c). \quad (8.1.18)$$

It follows, from the cyclic property of the trace, that f^{abc} is totally antisymmetric under interchange of any two of a, b, c . By using the Jacobi identity,

$$[T^a, [T^b, T^c]] + [T^b, [T^c, T^a]] + [T^c, [T^a, T^b]] = 0, \quad (8.1.19)$$

which holds for any three matrices, one also finds the useful result:

$$f^{ade}f^{bce} + f^{cde}f^{abe} + f^{bde}f^{cae} = 0. \quad (8.1.20)$$

Two representations R and R' are said to be equivalent if there exists some fixed matrix X such that:

$$XT_R^a X^{-1} = T_{R'}^a, \quad (8.1.21)$$

for all a . Obviously, this requires that R and R' have the same dimension. From a physical point of view, equivalent representations are indistinguishable from each other.

A representation R of a Lie algebra is said to be reducible if it is equivalent to a representation in block-diagonal form; in other words, if there is some matrix X that can be used to put all of the T_R^a simultaneously in a block-diagonal form:

$$XT_R^a X^{-1} = \begin{pmatrix} T_{r_1}^a & 0 & \cdots & 0 \\ 0 & T_{r_2}^a & \cdots & 0 \\ \vdots & \vdots & \ddots & \vdots \\ 0 & 0 & \cdots & T_{r_n}^a \end{pmatrix} \quad \text{for all } a. \quad (8.1.22)$$

Here the $T_{r_i}^a$ are representation matrices for smaller representations r_i . One calls this a direct sum, and writes it as

$$R = r_1 \oplus r_2 \oplus \dots \oplus r_n. \quad (8.1.23)$$

A representation that is not equivalent to a direct sum of smaller representations in this way is said to be irreducible. Heuristically, reducible representations are those that can be chopped up into smaller pieces that can be consistently treated individually.

With the above conventions on the Lie algebra generators, one can show that for each irreducible representation R :

$$(T_R^a T_R^a)_i^j = C(R) \delta_i^j \quad (8.1.24)$$

(with an implicit sum over $a = 1, \dots, d_G$), where $C(R)$ is another characteristic number of the representation R , called the quadratic Casimir invariant. If we take the sum over a of eq. (8.1.17), it is equal to the trace of eq. (8.1.24). It follows that for each irreducible representation R , the dimension, the index, and the Casimir invariant are related to the dimension of the group by:

$$d_G I(R) = d_R C(R). \quad (8.1.25)$$

The simplest irreducible representation of any Lie algebra is just:

$$T_i^{aj} = 0. \quad (8.1.26)$$

This is called the singlet representation.

Suppose that we have some representation with matrices T_i^{aj} . Then one can show that the matrices $-(T_i^{aj})^*$ also form a representation of the algebra eq. (8.1.16). This is called the complex conjugate of the representation R , and is often denoted \bar{R} :

$$T_{\bar{R}}^a = -T_R^{a*}. \quad (8.1.27)$$

If $T_{\bar{R}}^a$ is equivalent to T_R^a , so that there is some fixed matrix X such that

$$X T_{\bar{R}}^a X^{-1} = T_R^a, \quad (8.1.28)$$

then the representation R is said to be a real representation,[†] and otherwise R is said to be complex.

[†]Real representations can be divided into two sub-cases, “positive-real” and “pseudo-real”, depending on whether the matrix X can or cannot be chosen to be symmetric. In a pseudo-real representation, the T^a cannot all be made antisymmetric and imaginary; in a positive-real representation, they can.

One can also form the tensor product of any two representations R, R' of the Lie algebra to get another representation:

$$(T_{R \otimes R'}^a)_{i,x}^{j,y} \equiv (T_R^a)_i^j \delta_x^y + \delta_i^j (T_{R'}^a)_x^y. \quad (8.1.29)$$

The representation $R \otimes R'$ has dimension $d_R d_{R'}$, and is typically reducible:

$$R \otimes R' = R_1 \oplus \dots \oplus R_n \quad (8.1.30)$$

with

$$d_{R \otimes R'} = d_R d_{R'} = d_{R_1} + \dots + d_{R_n}. \quad (8.1.31)$$

This is a way to make larger representations ($R_1 \dots R_n$ out of smaller ones (R, R').

One can check from the identity eq. (8.1.20) that the matrices

$$(T^a)_b^c = -if^{abc} \quad (8.1.32)$$

form a representation, called the adjoint representation, with the same dimension as the group G . As a matter of terminology, the quadratic Casimir invariant of the adjoint representation is also called the Casimir invariant of the group, and given the symbol $C(G)$. Note that, from eq. (8.1.25), the index of the adjoint representation is equal to its quadratic Casimir invariant:

$$C(G) \equiv C(\text{adjoint}) = I(\text{adjoint}). \quad (8.1.33)$$

We now list, without proof, some further group theory facts regarding Lie algebra representations:

- The number of inequivalent irreducible representations of a Lie group is always infinite.
- Unlike group element multiplication, the tensor product multiplication of representations is both associative and commutative:

$$(R_1 \otimes R_2) \otimes R_3 = R_1 \otimes (R_2 \otimes R_3), \quad (8.1.34)$$

$$R_1 \otimes R_2 = R_2 \otimes R_1. \quad (8.1.35)$$

- The tensor product of any representation with the singlet representation just gives the original representation back:

$$1 \otimes R = R \otimes 1 = R. \quad (8.1.36)$$

- The tensor product of two real representations R_1 and R_2 is always a direct sum of representations that are either real or appear in complex conjugate pairs.

- The adjoint representation is always real.
- The tensor product of two irreducible representations contains the singlet representation if and only if they are complex conjugates of each other:

$$R_1 \otimes R_2 = 1 \oplus \dots \quad \longleftrightarrow \quad R_2 = \overline{R}_1. \quad (8.1.37)$$

It follows that if R is real, then $R \otimes R$ contains a singlet.

- The tensor product of a representation and its complex conjugate always contains both the singlet and adjoint representations:

$$R \otimes \overline{R} = 1 \oplus \text{Adjoint} \oplus \dots \quad (8.1.38)$$

- As a corollary of the preceding rules, the tensor product of the adjoint representation with itself always contains both the singlet and the adjoint:

$$\text{Adjoint} \otimes \text{Adjoint} = 1_S \oplus \text{Adjoint}_A \oplus \dots \quad (8.1.39)$$

Here the S and A mean that the indices of the two adjoints on the left are combined symmetrically and antisymmetrically respectively.

- If the tensor product of two representations contains a third, then the tensor product of the first representation with the conjugate of the third representation contains the conjugate of the second representation:

$$R_1 \otimes R_2 = R_3 \oplus \dots, \quad \longleftrightarrow \quad R_1 \otimes \overline{R}_3 = \overline{R}_2 \oplus \dots, \quad (8.1.40)$$

$$R_1 \otimes R_2 \otimes R_3 = 1 \oplus \dots, \quad \longleftrightarrow \quad R_1 \otimes R_2 = \overline{R}_3 \oplus \dots \quad (8.1.41)$$

- If $R_1 \otimes R_2 = r_1 \oplus \dots \oplus r_n$, then the indices satisfy the following rule:

$$I(R_1)d_{R_2} + I(R_2)d_{R_1} = \sum_{i=1}^n I(r_i). \quad (8.1.42)$$

Let us recall how Lie algebra representations work in the example of $SU(2)$, the group of unitary 2×2 matrices (that's the "U(2)" part of the name) with determinant 1 (that's the "S", for special, part of the name). This group is familiar from the study of angular momentum in quantum mechanics, and the defining or fundamental representation is the familiar spin-1/2 one with φ_i with $i = 1, 2$ or up,down. The Lie algebra generators in the fundamental representation are:

$$T^a = \frac{\sigma^a}{2} \quad (a = 1, 2, 3), \quad (8.1.43)$$

where the σ^a are the three Pauli matrices [see, for example, eq. (3.1.23)]. One finds that the structure constants are

$$f^{abc} = \epsilon^{abc} = \begin{cases} +1 & \text{if } a, b, c = 1, 2, 3 \text{ or } 2, 3, 1 \text{ or } 3, 1, 2 \\ -1 & \text{if } a, b, c = 1, 3, 2 \text{ or } 3, 2, 1 \text{ or } 2, 1, 3 \\ 0 & \text{otherwise.} \end{cases} \quad (8.1.44)$$

Irreducible representations exist for any “spin” $j = n/2$, where n is an integer, and have dimension $2j + 1$. The representation matrices J^a in the spin- j representation satisfy the $SU(2)$ Lie algebra:

$$[J^a, J^b] = i\epsilon^{abc} J^c. \quad (8.1.45)$$

These representation matrices can be chosen to act on states $\varphi_m = |j, m\rangle$, according to:

$$J^3 |j, m\rangle = m |j, m\rangle, \quad (8.1.46)$$

$$J^a J^a |j, m\rangle = j(j+1) |j, m\rangle, \quad (8.1.47)$$

or, in matrix-vector notation:

$$J_m^{3m'} \varphi_{m'} = m \varphi_m, \quad (8.1.48)$$

$$(J^a J^a)_m^{m'} \varphi_{m'} = j(j+1) \varphi_m. \quad (8.1.49)$$

We therefore recognize from eq. (8.1.24) that the quadratic Casimir invariant of the spin- j representation of $SU(2)$ is $C(R_j) = j(j+1)$. It follows from eq. (8.1.25) that the index of the spin- j representation is $I(R_j) = j(j+1)(2j+1)/3$. The $j = 1/2$ representation is real, because

$$X(-\frac{\sigma^{a*}}{2})X^{-1} = \frac{\sigma^a}{2}, \quad (8.1.50)$$

where

$$X = \begin{pmatrix} 0 & i \\ -i & 0 \end{pmatrix}. \quad (8.1.51)$$

More generally, one can show that all representations of $SU(2)$ are real. Making a table of the representations of $SU(2)$:

	spin	dimension	$I(R)$	$C(R)$	real?	
singlet	0	1	0	0	yes	
fundamental	1/2	2	1/2	3/4	yes	
adjoint	1	3	2	2	yes	
	3/2	4	5	15/4	yes	
...	
	j	$2j+1$	$j(j+1)(2j+1)/3$	$j(j+1)$	yes	(8.1.52)

The tensor product of any two representations of $SU(2)$ is reducible to a direct sum, as:

$$j_1 \otimes j_2 = |j_1 - j_2| \oplus (|j_1 - j_2| + 1) \oplus \dots \oplus (j_1 + j_2) \quad (8.1.53)$$

in which j is used to represent the representation of spin j .

The group $SU(2)$ has many applications in physics. First, it serves as the Lie algebra of angular momentum operators. The strong force (but not the electromagnetic or weak forces, or mass terms) is invariant under a different $SU(2)$ isospin symmetry, under which the up and down quarks transform as a $j = 1/2$ doublet. Isospin is a global symmetry, meaning that the same symmetry transformation must be made simultaneously everywhere:

$$\begin{pmatrix} u \\ d \end{pmatrix} \rightarrow \exp(i\theta^a \sigma^a / 2) \begin{pmatrix} u \\ d \end{pmatrix}, \quad (8.1.54)$$

with a constant θ^a that does not depend on position in spacetime. The weak interactions involve a still different $SU(2)$, known as weak isospin or $SU(2)_L$. Weak isospin is a gauge symmetry that acts only on left-handed fermion fields. The irreducible $j = 1/2$ representations of $SU(2)_L$ are composed of the pairs of fermions that couple to a W^\pm boson, namely:

$$\begin{pmatrix} \nu_{eL} \\ e_L \end{pmatrix}; \quad \begin{pmatrix} \nu_{\mu L} \\ \mu_L \end{pmatrix}; \quad \begin{pmatrix} \nu_{\tau L} \\ \tau_L \end{pmatrix}; \quad (8.1.55)$$

$$\begin{pmatrix} u_L \\ d'_L \end{pmatrix}; \quad \begin{pmatrix} c_L \\ s'_L \end{pmatrix}; \quad \begin{pmatrix} t_L \\ b'_L \end{pmatrix}. \quad (8.1.56)$$

Here e_L means $P_L e$, etc., and the primes mean that these are not quark mass eigenstates. When one makes an $SU(2)_L$ gauge transformation, the transformation can be different at each point in spacetime. However, one must make the same transformation simultaneously on each of these representations. We will come back to study the $SU(2)_L$ symmetry in more detail later, and see more precisely how it ties into the weak interactions and QED.

One can generalize the $SU(2)$ group to non-Abelian groups $SU(N)$ for any integer $N \geq 2$. The Lie algebra generators of $SU(N)$ in the fundamental representation are Hermitian traceless $N \times N$ matrices. In general, a basis for the complex $N \times N$ matrices is $2N^2$ dimensional, since each matrix has N^2 entries with a real and imaginary part. The condition that the matrices are Hermitian removes half of these, since each entry in the matrix is required to be the complex conjugate of another entry. Finally, the single condition of tracelessness removes one from the basis. That leaves $d_{SU(N)} = N^2 - 1$ as the dimension of the group and of the adjoint representation. For all $N \geq 3$, the fundamental representation is complex.

For example, Quantum Chromo-Dynamics (QCD), the theory of the strong interactions, is a gauge theory based on the group $SU(3)$, which has dimension $d_G = 8$. In the fundamental representation, the generators of the Lie algebra are given by:

$$T^a = \frac{1}{2} \lambda^a \quad (a = 1, \dots, 8), \quad (8.1.57)$$

where the λ^a are known as the Gell-Mann matrices:

$$\begin{aligned}\lambda^1 &= \begin{pmatrix} 0 & 1 & 0 \\ 1 & 0 & 0 \\ 0 & 0 & 0 \end{pmatrix}; & \lambda^2 &= \begin{pmatrix} 0 & -i & 0 \\ i & 0 & 0 \\ 0 & 0 & 0 \end{pmatrix}; & \lambda^3 &= \begin{pmatrix} 1 & 0 & 0 \\ 0 & -1 & 0 \\ 0 & 0 & 0 \end{pmatrix}; \\ \lambda^4 &= \begin{pmatrix} 0 & 0 & 1 \\ 0 & 0 & 0 \\ 1 & 0 & 0 \end{pmatrix}; & \lambda^5 &= \begin{pmatrix} 0 & 0 & -i \\ 0 & 0 & 0 \\ i & 0 & 0 \end{pmatrix}; & \lambda^6 &= \begin{pmatrix} 0 & 0 & 0 \\ 0 & 0 & 1 \\ 0 & 1 & 0 \end{pmatrix}; \\ \lambda^7 &= \begin{pmatrix} 0 & 0 & 0 \\ 0 & 0 & -i \\ 0 & i & 0 \end{pmatrix}; & \lambda^8 &= \frac{1}{\sqrt{3}} \begin{pmatrix} 1 & 0 & 0 \\ 0 & 1 & 0 \\ 0 & 0 & -2 \end{pmatrix}.\end{aligned}\tag{8.1.58}$$

Note that each of these matrices is Hermitian and traceless, as required. They have also been engineered to satisfy $\text{Tr}(\lambda^a \lambda^b) = 2\delta^{ab}$, so that

$$\text{Tr}(T^a T^b) = \frac{1}{2} \delta^{ab},\tag{8.1.59}$$

and therefore the index of the fundamental representation is

$$I(F) = 1/2.\tag{8.1.60}$$

One can also check that

$$(T^a T^a)_i^j = \frac{4}{3} \delta_i^j,\tag{8.1.61}$$

so that the quadratic Casimir invariant of the fundamental representation is

$$C(F) = 4/3.\tag{8.1.62}$$

By taking commutators of each pair of generators, one finds that the non-zero structure constants of $SU(3)$ are:

$$f^{123} = 1;\tag{8.1.63}$$

$$f^{147} = -f^{156} = f^{246} = f^{257} = f^{345} = -f^{367} = 1/2;\tag{8.1.64}$$

$$f^{458} = f^{678} = \sqrt{3}/2.\tag{8.1.65}$$

and those related to the above by permutations of indices, following from the condition that the f^{abc} are totally antisymmetric. From these one can find the adjoint representation matrices using eq. (8.1.32), with, for example:

$$T_{\text{adjoint}}^1 = -i \begin{pmatrix} 0 & 0 & 0 & 0 & 0 & 0 & 0 & 0 \\ 0 & 0 & 1 & 0 & 0 & 0 & 0 & 0 \\ 0 & -1 & 0 & 0 & 0 & 0 & 0 & 0 \\ 0 & 0 & 0 & 0 & 0 & 0 & 1/2 & 0 \\ 0 & 0 & 0 & 0 & 0 & -1/2 & 0 & 0 \\ 0 & 0 & 0 & 0 & 1/2 & 0 & 0 & 0 \\ 0 & 0 & 0 & -1/2 & 0 & 0 & 0 & 0 \\ 0 & 0 & 0 & 0 & 0 & 0 & 0 & 0 \end{pmatrix},\tag{8.1.66}$$

etc. However, it is almost never necessary to actually use the explicit form of any matrix representation larger than the fundamental. Instead, one relies on group-theoretic identities. For example, calculations of Feynman diagrams often involve the index or Casimir invariant of the fundamental representation, and the Casimir invariant of the group. One can easily compute the latter by using eq. (8.1.24) and (8.1.32):

$$f^{abc}f^{abd} = C(G)\delta^{cd}, \quad (8.1.67)$$

with the result $C(G) = 3$.

Following is a table of the smallest few irreducible representations of $SU(3)$:

	dimension	$I(R)$	$C(R)$	real?	
singlet	1	0	0	yes	
fundamental	3	1/2	4/3	no	
anti-fundamental	$\bar{\mathbf{3}}$	1/2	4/3	no	
	6	5/2	10/3	no	(8.1.68)
	$\bar{\mathbf{6}}$	5/2	10/3	no	
adjoint	8	3	3	yes	
	10	15/2	6	no	
	$\bar{\mathbf{10}}$	15/2	6	no	
	...				(8.1.69)

It is usual to refer to each representation by its dimension in boldface. In general, the representations can be classified by two non-negative integers α and β . The dimension of the representation labeled by α, β is

$$d_{\alpha,\beta} = (\alpha + 1)(\beta + 1)(\alpha + \beta + 2)/2. \quad (8.1.70)$$

Some tensor products involving these representations are:

$$\mathbf{3} \otimes \bar{\mathbf{3}} = \mathbf{1} \oplus \mathbf{8} \quad (8.1.71)$$

$$\mathbf{3} \otimes \mathbf{3} = \bar{\mathbf{3}}_A \oplus \mathbf{6}_S \quad (8.1.72)$$

$$\bar{\mathbf{3}} \otimes \bar{\mathbf{3}} = \mathbf{3}_A \oplus \bar{\mathbf{6}}_S \quad (8.1.73)$$

$$\mathbf{3} \otimes \mathbf{3} \otimes \mathbf{3} = \mathbf{1}_A \oplus \mathbf{8}_M \oplus \mathbf{8}_M \oplus \mathbf{10}_S \quad (8.1.74)$$

$$\mathbf{8} \otimes \mathbf{8} = \mathbf{1}_S \oplus \mathbf{8}_A \oplus \mathbf{8}_S \oplus \mathbf{10}_A \oplus \bar{\mathbf{10}}_A \oplus \mathbf{27}_S. \quad (8.1.75)$$

Here, when we take the tensor product of two or more identical representations, the irreducible representations on the right side are labeled as A , S , or M depending on whether they involve an antisymmetric, symmetric, or mixed symmetry combination of the indices of the original representations on the left side.

In $SU(N)$, one can build any representation out of objects that carry only indices transforming under the fundamental \mathbf{N} and anti-fundamental $\overline{\mathbf{N}}$ representations. It is useful to employ lowered indices for the fundamental, and raised indices for the antifundamental. Then an object carrying n lowered and m raised indices:

$$\varphi_{i_1 \dots i_n}^{j_1 \dots j_m} \quad (8.1.76)$$

transforms under the tensor product representation

$$\underbrace{\mathbf{N} \otimes \dots \otimes \mathbf{N}}_{n \text{ times}} \otimes \underbrace{\overline{\mathbf{N}} \otimes \dots \otimes \overline{\mathbf{N}}}_{m \text{ times}}. \quad (8.1.77)$$

This is always reducible. To reduce it, one can decompose φ into parts that have different symmetry and trace properties. So, for example, we can take an object that transforms under $SU(3)$ as $\mathbf{N} \times \overline{\mathbf{N}}$, and write it as:

$$\varphi_i^j = \left(\varphi_i^j - \frac{1}{N} \delta_i^j \varphi_k^k \right) + \left(\frac{1}{N} \delta_i^j \varphi_k^k \right). \quad (8.1.78)$$

The first term in parentheses transforms as an adjoint representation, and the second as a singlet, under $SU(N)$. For $SU(3)$, this corresponds to the rule of eq. (8.1.71).

Similarly, an object that transforms under $SU(N)$ as $\mathbf{N} \times \mathbf{N}$ can be decomposed as

$$\varphi_{ij} = \frac{1}{2}(\varphi_{ij} + \varphi_{ji}) + \frac{1}{2}(\varphi_{ij} - \varphi_{ji}). \quad (8.1.79)$$

The two terms on the right-hand side correspond to an $N(N+1)/2$ -dimensional symmetric tensor, and an $N(N-1)/2$ -dimensional antisymmetric tensor, irreducible representations. For $N=3$, these are the $\mathbf{6}$ and $\overline{\mathbf{3}}$ representations, respectively, and this decomposition corresponds to eq. (8.1.72). By using this process of taking symmetric and anti-symmetric parts and removing traces, one can find all necessary tensor-product representation rules for any $SU(N)$ group.

8.2 The Yang-Mills Lagrangian and Feynman rules

In this subsection, we will construct the Lagrangian and Feynman rules for a theory of Dirac fermions and gauge bosons transforming under a non-Abelian gauge group, called a Yang-Mills theory.

Let the Dirac fermion fields be given by Ψ_i , where i is an index in some representation of the gauge group with generators T_i^{aj} . Here $i = 1, \dots, d_R$ and $a = 1, \dots, d_G$. Under a gauge transformation, we have:

$$\Psi_i \rightarrow U_i^j \Psi_j \quad (8.2.1)$$

where

$$U = \exp(i\theta^a T^a). \quad (8.2.2)$$

Specializing to the case of an infinitesimal gauge transformation $\theta^a = \epsilon^a$, we have

$$\Psi_i \rightarrow (1 + i\epsilon^a T^a)_i^j \Psi_j. \quad (8.2.3)$$

Our goal is to build a Lagrangian that is invariant under this transformation.

First let us consider how barred spinors transform. Taking the Hermitian conjugate of eq. (8.2.3), we find

$$\Psi^{\dagger i} \rightarrow \Psi^{\dagger j} (1 - i\epsilon^a T^a)_j^i, \quad (8.2.4)$$

where we have used the fact that T^a are Hermitian matrices. (Notice that taking the Hermitian conjugate changes the heights of the representation indices, and in the case of matrices, reverses their order. So the Dirac spinor carries a lowered representation index, while the Hermitian conjugate spinor carries a raised index.) Now we can multiply on the right by γ^0 . The Dirac gamma matrices are completely separate from the gauge group representation indices, so we get the transformation rule for the barred Dirac spinors:

$$\bar{\Psi}^i \rightarrow \bar{\Psi}^j (1 - i\epsilon^a T^a)_j^i. \quad (8.2.5)$$

We can rewrite this in a slightly different way by noting that

$$T_j^{ai} = (T_j^{ai})^\dagger = (T^{ai}_j)^*, \quad (8.2.6)$$

so that

$$\bar{\Psi}^i \rightarrow (1 + i\epsilon^a [-T^{a*}])^i_j \bar{\Psi}^j. \quad (8.2.7)$$

Comparing with eq. (8.1.27), this establishes that $\bar{\Psi}^i$ transforms in the complex conjugate of the representation carried by Ψ_i .

Since $\bar{\Psi}^i$ and Ψ_i transform as complex conjugate representations of each other, their tensor product must be a direct sum of representations that includes a singlet. The singlet is obtained by summing over the index i :

$$\bar{\Psi}^i \Psi_i. \quad (8.2.8)$$

As a check of this, under an infinitesimal gauge transformation, this term becomes:

$$\bar{\Psi}^i \Psi_i \rightarrow \bar{\Psi}^j (1 - i\epsilon^a T^a)_j^i (1 + i\epsilon^b T^b)_i^k \Psi_k \quad (8.2.9)$$

$$= \bar{\Psi}^i \Psi_i + \mathcal{O}(\epsilon^2), \quad (8.2.10)$$

where the terms linear in ϵ^a have indeed canceled. Therefore, we can include a fermion mass term in the Lagrangian:

$$\mathcal{L}_m = -m\bar{\Psi}^i\Psi_i. \quad (8.2.11)$$

This shows that each component of the field Ψ_i must have the same mass.

Next we would like to include a derivative kinetic term for the fermions. Just as in QED, the term

$$i\bar{\Psi}^i\gamma^\mu\partial_\mu\Psi_i \quad (8.2.12)$$

is not acceptable by itself, because $\partial_\mu\Psi_i$ does not gauge transform in the same way that Ψ_i does. The problem is that the derivative can act on the gauge-parameter function ϵ^a , giving an extra term:

$$\partial_\mu\Psi_i \rightarrow (1 + i\epsilon^a T^a)_i^j \partial_\mu\Psi_j + i(\partial_\mu\epsilon^a)T_i^{aj}\Psi_j. \quad (8.2.13)$$

By analogy with QED, we can fix this by writing a covariant derivative involving vectors fields, which will also transform in such a way as to cancel the last term in eq. (8.2.13):

$$D_\mu\Psi_i = \partial_\mu\Psi_i + igA_\mu^a T_i^{aj}\Psi_j. \quad (8.2.14)$$

The vector boson fields A_μ^a are known as gauge fields. They carry an adjoint representation index a in addition to their spacetime vector index μ . The number of such fields is equal to the number of generator matrices T^a , which we recall is the dimension of the gauge group d_G . The quantity g is a coupling, known as a gauge coupling. It is dimensionless, and is the direct analog of the coupling e in QED. The entries of the matrix T_i^{aj} take the role played by the charges q in QED. Notice that the definition of the covariant derivative depends on the representation matrices for the fermions, so there is really a different covariant derivative depending on which fermion representation one is acting on.

Now one can check that the Lagrangian

$$\mathcal{L}_{\text{fermions}} = i\bar{\Psi}^i\gamma^\mu D_\mu\Psi_i - m\bar{\Psi}^i\Psi_i \quad (8.2.15)$$

is invariant under infinitesimal gauge transformations, provided that the gauge field is taken to transform as:

$$A_\mu^a \rightarrow A_\mu^a - \frac{1}{g}\partial_\mu\epsilon^a - f^{abc}\epsilon^b A_\mu^c. \quad (8.2.16)$$

The term with a derivative acting on ϵ^a is the direct analog of a corresponding term in QED, see eq. (8.1.4). The last term vanishes for Abelian groups like QED, but it is necessary to ensure that the covariant derivative of a Dirac field transforms in the same way as the field itself:

$$D_\mu\Psi_i \rightarrow (1 + i\epsilon^a T^a)_i^j D_\mu\Psi_j. \quad (8.2.17)$$

If we limit ourselves to constant gauge parameters $\partial_\mu \epsilon^a = 0$, then the transformation in eq. (8.2.16) is of the correct form for a field in the adjoint representation.

Having introduced a gauge field for each Lie algebra generator, we must now include kinetic terms for them. By analogy with QED, the gauge field Lagrangian has the form:

$$\mathcal{L}_{\text{gauge}} = -\frac{1}{4} F^{\mu\nu a} F_{\mu\nu}^a, \quad (8.2.18)$$

with an implied sum on a , where $F_{\mu\nu}^a$ is an antisymmetric field strength tensor for each Lie algebra generator. However, we must also require that this Lagrangian is invariant under gauge transformations. This is accomplished if we choose:

$$F_{\mu\nu}^a = \partial_\mu A_\nu^a - \partial_\nu A_\mu^a - g f^{abc} A_\mu^b A_\nu^c. \quad (8.2.19)$$

Then one can check, using eq. (8.2.16), that

$$F_{\mu\nu}^a \rightarrow F_{\mu\nu}^a - f^{abc} \epsilon^b F_{\mu\nu}^c. \quad (8.2.20)$$

From this it follows that $\mathcal{L}_{\text{gauge}}$ transforms as:

$$-\frac{1}{4} F^{\mu\nu a} F_{\mu\nu}^a \rightarrow -\frac{1}{4} F^{\mu\nu a} F_{\mu\nu}^a - \frac{1}{2} F^{\mu\nu a} f^{abc} \epsilon^b F_{\mu\nu}^c + \mathcal{O}(\epsilon^2). \quad (8.2.21)$$

The extra term linear in ϵ vanishes, because the part $F^{\mu\nu a} F_{\mu\nu}^c$ is symmetric under interchange of $a \leftrightarrow c$, but its gauge indices are contracted with f^{abc} , which is antisymmetric under the same interchange. Therefore, eq. (8.2.18) is a gauge singlet.

Putting the above results together, we have found a gauge-invariant Lagrangian for Dirac fermions coupled to a non-Abelian gauge field:

$$\mathcal{L}_{\text{Yang-Mills}} = \mathcal{L}_{\text{gauge}} + \mathcal{L}_{\text{fermions}}. \quad (8.2.22)$$

Now we can find the Feynman rules for this theory in the usual way. First we identify the kinetic terms that are quadratic in the fields. That part of $\mathcal{L}_{\text{Yang-Mills}}$ is:

$$\mathcal{L}_{\text{kinetic}} = -\frac{1}{4} (\partial_\mu A_\nu^a - \partial_\nu A_\mu^a) (\partial^\mu A^{\nu\mu} - \partial^\nu A^{\mu\mu}) + i \bar{\Psi}^i \not{\partial} \Psi_i - m \bar{\Psi}^i \Psi_i. \quad (8.2.23)$$

These terms have exactly the same form as in the QED Lagrangian, but with a sum over d_G copies of the vector fields, labeled by a , and over d_R copies of the fermion field, labeled by i . Therefore we can obtain the Feynman rules for vector and fermion propagators in the same way. For the gauge fields, we need to include a gauge-fixing term, just as in QED [compare eq. (5.1.32) and the surrounding discussion], in order to have a well-defined propagator:

$$\mathcal{L}_{\text{gauge-fixing}} = -\frac{1}{2\xi} (\partial^\mu A_\mu^a)^2 \quad (8.2.24)$$

with the index a summed over. This leads to:

$$\begin{array}{c} \mu, a \\ \text{~~~~~} \nearrow \quad \searrow \text{~~~~~} \\ \text{~~~~~} \end{array} \longleftrightarrow \delta^{ab} \frac{i}{p^2 + i\epsilon} \left[-g_{\mu\nu} + (1-\xi) \frac{p_\mu p_\nu}{p^2} \right]$$

where p^μ is the 4-momentum along either direction in the wavy line, and one can take $\xi = 1$ for Feynman gauge and $\xi = 0$ for Landau gauge. The δ^{ab} in the Feynman rule just means that a gauge field does not change to a different type as it propagates. Likewise, the Dirac fermion propagator is:


$$\begin{array}{c} j \qquad \qquad i \\ \hline \longrightarrow \end{array} \quad \longleftrightarrow \quad \delta_i^j \frac{i(\not{p} + m)}{p^2 - m^2 + i\epsilon}$$

with 4-momentum p^μ along the arrow direction, and m the mass of the Dirac fermion. Again the factor of δ_i^j means the fermion does not change its identity as it propagates.

The interaction Feynman rules follow from the remaining terms in $\mathcal{L}_{\text{Yang-Mills}}$. First, there is a fermion-fermion-vector interaction coming from the covariant derivative in \mathcal{L}_Ψ . Identifying the Feynman rule as i times the term in the Lagrangian [recall the discussion surrounding eq. (4.7.8)], from

$$\mathcal{L}_{A\bar{\Psi}\Psi} = -g A_\mu^a \bar{\Psi} \gamma^\mu T^a \Psi \quad (8.2.25)$$

we get:

μ, a

 i
 j

\longleftrightarrow
 $-igT_i^{aj}\gamma^\mu$

This rule says that the coupling of a gauge field to a fermion line is proportional to the corresponding Lie algebra generator matrix. Since the matrices T^a are not diagonal for non-Abelian groups, this interaction can change one fermion into another. The Lagrangian density $\mathcal{L}_{\text{gauge}}$ contains three-gauge-field and four-gauge-field couplings, proportional to g and g^2 respectively. After combining some terms using the antisymmetry of the f^{abc} symbol, they can be written as

$$\mathcal{L}_{AAA} = gf^{abc}(\partial_\mu A_\nu^a)A^{\mu b}A^{\nu c}, \quad (8.2.26)$$

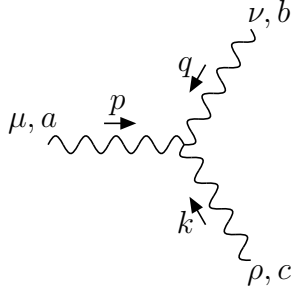
$$\mathcal{L}_{AAAA} = -\frac{g^2}{4} f^{abe} f^{cde} A_\mu^a A_\nu^b A^{\mu c} A^{\nu d}. \quad (8.2.27)$$

The three-gauge-field couplings involve a spacetime derivative, which we can treat according to the rule of eq. (7.6.26), as i times the momentum of the field it acts on (in the direction going into the vertex). Then the Feynman rule for the interaction of three gauge bosons with (spacetime

vector, gauge) indices μ, a and ν, b and ρ, c is obtained by taking functional derivatives of the Lagrangian density with respect to the corresponding fields:

$$i \frac{\delta^3}{\delta A_\mu^a \delta A_\nu^b \delta A_\rho^c} \mathcal{L}_{AAA}, \quad (8.2.28)$$

resulting in:

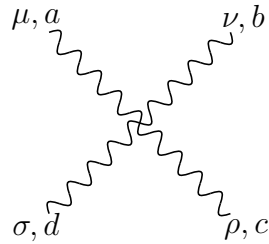


$$\longleftrightarrow -g f^{abc} [g^{\mu\nu}(p-q)^\rho + g^{\nu\rho}(q-k)^\mu + g^{\rho\mu}(k-p)^\nu]$$

where p^μ , q^μ , and k^μ are the gauge boson 4-momenta flowing into the vertex. Likewise, the Feynman rule for the coupling of four gauge bosons with indices μ, a and ν, b and ρ, c and σ, d is:

$$i \frac{\delta^4}{\delta A_\mu^a \delta A_\nu^b \delta A_\rho^c \delta A_\sigma^d} \mathcal{L}_{AAAA}, \quad (8.2.29)$$

leading to:



$$\longleftrightarrow -ig^2 [f^{abe} f^{cde} (g^{\mu\rho} g^{\nu\sigma} - g^{\mu\sigma} g^{\nu\rho}) + f^{ace} f^{bde} (g^{\mu\nu} g^{\rho\sigma} - g^{\mu\sigma} g^{\nu\rho}) + f^{ade} f^{bce} (g^{\mu\nu} g^{\rho\sigma} - g^{\mu\rho} g^{\nu\sigma})]$$

There are more terms in these Feynman rules than in the corresponding Lagrangian, since the functional derivatives have a choice of several fields on which to act. Notice that these fields are invariant under the simultaneous interchange of all the indices and momenta for any two vector bosons, for example $(\mu, a, p) \leftrightarrow (\nu, b, q)$. The above Feynman rules are all that is needed to calculate tree-level Feynman diagrams in a Yang-Mills theory with Dirac fermions. External state fermions and gauge bosons are assigned exactly the same rules as for fermions and photons in QED. The external state particles carry a representation or gauge index determined by the interaction vertex to which that line is attached.

[However, this is not quite the end of the story if one needs to compute loop diagrams. In that case, one must take into account that not all of the gauge fields that can propagate in loops are actually physical. One way to fix this problem is by introducing “ghost” fields that

only appear in loops, never in initial or final states. The ghost fields do not create and destroy real particles; they are really just book-keeping devices that exist only to cancel the unphysical contributions of gauge fields in loops. We will not do any loop calculations in this course, so we will not go into more detail on that issue.]

The Yang-Mills theory we have constructed makes several interesting predictions. One is that the gauge fields are necessarily massless. If one tries to get around this by introducing a mass term for the vector gauge fields, like:

$$\mathcal{L}_{A\text{-mass}} = m_V^2 A_\mu^a A^{a\mu}, \quad (8.2.30)$$

then one finds that this term is not invariant under the gauge transformation of eq. (8.2.16). Therefore, if we put in such a term, we necessarily violate the gauge invariance of the Lagrangian, and the gauge symmetry will not be a symmetry of the theory. This sounds like a serious problem, because there is only one known freely-propagating, non-composite, massless vector field, the photon. In particular, the massive W^\pm boson cannot be described by the Yang-Mills theory that we have so far. One way to proceed would be to simply keep the term in eq. (8.2.30), and accept that the theory is not fully invariant under the gauge symmetry. The only problem with this is that the theory would be non-renormalizable in that case; as a related problem, unitarity would be violated in scattering at very high energies. Instead, we can explain the non-zero mass of the W^\pm boson by enlarging the theory to include scalar fields, leading to a spontaneous breakdown in the gauge symmetry.

Another nice feature of the Yang-Mills theory is that several different couplings are predicted to be related to each other. Once we have picked a gauge group G , a set of irreducible representations for the fermions, and the gauge coupling g , then the interaction terms are all fixed. In particular, if we know the coupling of one type of fermion to the gauge fields, then we know g . This in turn allows us to predict, as a consequence of the gauge invariance, what the couplings of other fermions to the gauge fields should be (as long as we know their representations), and what the three-gauge-boson and four-gauge-boson vertices should be.

9 Quantum Chromo-Dynamics (QCD)

9.1 QCD Lagrangian and Feynman rules

The strong interactions are based on a Yang-Mills theory with gauge group $SU(3)_c$, with quarks transforming in the fundamental $\mathbf{3}$ representation. The subscript c is to distinguish this as the group of invariances under transformations of the color degrees of freedom. As far as we can tell, this is an exact symmetry of nature. (There is also an approximate $SU(3)_{\text{flavor}}$ symmetry under which the quark flavors u, d, s transform into each other; isospin is an $SU(2)$ subgroup of this symmetry.) Each of the quark Dirac fields u, d, s, c, b, t transforms separately as a $\mathbf{3}$ of $SU(3)_c$, and each barred Dirac field $\bar{u}, \bar{d}, \bar{s}, \bar{c}, \bar{b}, \bar{t}$ therefore transforms as a $\bar{\mathbf{3}}$, as we saw on general grounds in subsection 8.2.

For example, an up quark is created in an initial state by any one of the three color component fields:

$$u = \begin{pmatrix} u_{\text{red}} \\ u_{\text{blue}} \\ u_{\text{green}} \end{pmatrix} = \begin{pmatrix} u_1 \\ u_2 \\ u_3 \end{pmatrix}, \quad (9.1.1)$$

while an anti-up quark is created in an initial state by any of the fields:

$$\bar{u} = (\bar{u}_{\text{red}} \quad \bar{u}_{\text{blue}} \quad \bar{u}_{\text{green}}) = (\bar{u}_1 \quad \bar{u}_2 \quad \bar{u}_3). \quad (9.1.2)$$

Since $SU(3)_c$ is an exact symmetry, no experiment can tell the difference between a red quark and a blue quark, so the labels are intrinsically arbitrary. In fact, we can do a different $SU(3)_c$ transformation at each point in spacetime, but simultaneously on each quark flavor, so that:

$$u \rightarrow e^{i\theta^a(x)T^a} u, \quad d \rightarrow e^{i\theta^a(x)T^a} d, \quad s \rightarrow e^{i\theta^a(x)T^a} s, \quad \text{etc.}, \quad (9.1.3)$$

where $T^a = \frac{\lambda^a}{2}$ with $a = 1, \dots, 8$, and the $\theta^a(x)$ are any gauge parameter functions of our choosing. This symmetry is in addition to the $U(1)_{\text{EM}}$ gauge transformations:

$$u \rightarrow e^{i\theta(x)Q_u} u, \quad d \rightarrow e^{i\theta(x)Q_d} d, \quad s \rightarrow e^{i\theta(x)Q_s} s, \quad \text{etc.}, \quad (9.1.4)$$

where $Q_u = Q_c = Q_t = 2/3$ and $Q_d = Q_s = Q_b = -1/3$. For each of the 8 generator matrices T^a of $SU(3)_c$, there is a corresponding gauge vector boson called a gluon, represented by a field G_μ^a carrying both a spacetime vector index and an $SU(3)_c$ adjoint representation index.

One says that the unbroken gauge group of the Standard Model is $SU(3)_c \times U(1)_{\text{EM}}$, with the fermions and gauge bosons transforming as:



The spacetime- and gauge-index structure are just as given in section 8.2 in the general case, with $g \rightarrow g_3$.

9.2 Scattering of quarks and gluons

9.2.1 Quark-quark scattering ($qq \rightarrow qq$)

To see how the Feynman rules for QCD work in practice, let us consider the example of quark-quark scattering. This is not a directly observable process, because the quarks in both the initial state and final state are parts of bound states. However, it does form the microscopic part of a calculation for the observable process hadron+hadron \rightarrow jet+jet. We will see how to use the microscopic cross-section result to obtain the observable cross-section later, in subsection 9.4. To be specific, let us consider the process of an up-quark and down-quark scattering from each other:

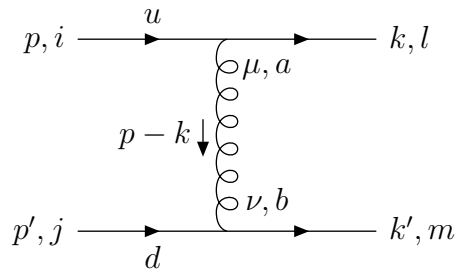
$$ud \rightarrow ud. \quad (9.2.1)$$

Let us assign momenta, spin, and color to the quarks as follows:

Particle	Momentum	Spin	Spinor	Color
initial u	p	s_1	$u(p, s_1) = u_1$	i
initial d	p'	s_2	$u(p', s_2) = u_2$	j
final u	k	s_3	$\bar{u}(k, s_3) = \bar{u}_3$	l
final d	k'	s_4	$\bar{u}(k', s_4) = \bar{u}_4$	m

(9.2.2)

At leading order in an expansion in g_3 , there is only one Feynman diagram:



The reduced matrix element can now be written down by the same procedure as in QED. One obtains, using Feynman gauge ($\xi = 1$):

$$\mathcal{M} = [\bar{u}_3(-ig_3\gamma_\mu T_l^{ai})u_1] [\bar{u}_4(-ig_3\gamma_\nu T_m^{bj})u_2] \left[\frac{-ig^{\mu\nu}\delta^{ab}}{(p-k)^2} \right] \quad (9.2.3)$$

$$= ig_3^2 T_l^{ai} T_m^{aj} [\bar{u}_3\gamma_\mu u_1] [\bar{u}_4\gamma^\mu u_2] / t \quad (9.2.4)$$

where $t = (p-k)^2$. This matrix element is exactly what one finds in QED for $e^-\mu^- \rightarrow e^-\mu^-$, but with the QED squared coupling replaced by a product of matrices depending on the color combination:

$$e^2 \rightarrow g_3^2 T_l^{ai} T_m^{aj}. \quad (9.2.5)$$

This illustrates that the “color charge matrix” $g_3 T_l^{ai}$ is analogous to the electric charge eQ_f . There are $3^4 = 81$ color combinations for quark-quark scattering.

In order to find the differential cross-section, we continue as usual by taking the complex square of the reduced matrix element:

$$|\mathcal{M}|^2 = g_3^4 (T_l^{ai} T_m^{aj})(T_l^{bi} T_m^{bj})^* |\widehat{\mathcal{M}}|^2, \quad (9.2.6)$$

for each i, j, l, m (with no implied sum yet), and

$$\widehat{\mathcal{M}} = [\bar{u}_3\gamma_\mu u_1] [\bar{u}_4\gamma^\mu u_2] / t. \quad (9.2.7)$$

It is not possible, even in principle, to distinguish between colors. However, one can always imagine fixing, by an arbitrary choice, that the incoming u -quark has color red=1; then the colors of the other quarks can be distinguished up to $SU(3)_c$ rotations that leave the red component fixed. In practice, one does not measure the colors of quarks in an experiment, even with respect to some arbitrary choice, so we will sum over the colors of the final state quarks and average over the colors of the initial state quarks:

$$\frac{1}{3} \sum_i \frac{1}{3} \sum_j \sum_l \sum_m |\mathcal{M}|^2. \quad (9.2.8)$$

To do the color sum/average most easily, we note that, because the gauge group generator matrices are Hermitian,

$$(T_l^{bi} T_m^{bj})^* = (T_i^{bl} T_j^{bm}). \quad (9.2.9)$$

Therefore, the color factor is

$$\frac{1}{3} \sum_i \frac{1}{3} \sum_j \sum_l \sum_m (T_l^{ai} T_m^{aj})(T_l^{bi} T_m^{bj})^* = \frac{1}{9} \sum_{i,j,l,m} (T_l^{ai} T_i^{bl})(T_m^{aj} T_j^{bm}) \quad (9.2.10)$$

$$= \frac{1}{9} \text{Tr}(T^a T^b) \text{Tr}(T^a T^b) \quad (9.2.11)$$

$$= \frac{1}{9} I(\mathbf{3}) \delta^{ab} I(\mathbf{3}) \delta^{ab} \quad (9.2.12)$$

$$= \frac{1}{9} \left(\frac{1}{2}\right)^2 d_G \quad (9.2.13)$$

$$= \frac{2}{9} \quad (9.2.14)$$

In doing this, we have used the definition of the index of a representation eq. (8.1.17); the fact that the index of the fundamental representation is $1/2$; and the fact that the sum over a, b of $\delta^{ab} \delta^{ab}$ just counts the number of generators of the Lie algebra d_G , which is 8 for $SU(3)_c$.

Meanwhile, the rest of $|\mathcal{M}|^2$, including a sum over final state spins and an average over initial state spins, can be taken directly from the corresponding result for $e^- \mu^- \rightarrow e^- \mu^-$ in QED, which we found by crossing symmetry in eq. (5.3.23). Stripping off the factor e^4 associated with the QED charges, we find in the high energy limit of negligible quark masses,

$$\frac{1}{2} \sum_{s_1} \frac{1}{2} \sum_{s_2} \sum_{s_3} \sum_{s_4} |\widehat{\mathcal{M}}|^2 = 2 \left(\frac{s^2 + u^2}{t^2} \right). \quad (9.2.15)$$

Putting this together with the factor of g_3^4 and the color factor above, we have

$$\overline{|\mathcal{M}|^2} \equiv \frac{1}{9} \sum_{\text{colors}} \frac{1}{4} \sum_{\text{spins}} |\mathcal{M}|^2 = \frac{4g_3^4}{9} \left(\frac{s^2 + u^2}{t^2} \right). \quad (9.2.16)$$

The notation $\overline{|\mathcal{M}|^2}$ is a standard notation, which for a general process implies the appropriate sum/average over spin and color. The differential cross-section for this process is therefore:

$$\frac{d\sigma}{d(\cos \theta)} = \frac{1}{32\pi s} \overline{|\mathcal{M}|^2} = \frac{2\pi\alpha_s^2}{9s} \left(\frac{s^2 + u^2}{t^2} \right), \quad (9.2.17)$$

where

$$\alpha_s = \frac{g_3^2}{4\pi} \quad (9.2.18)$$

is the strong-interaction analog of the fine structure constant. Since we are neglecting quark masses, the kinematics for this process is the same as in any massless $2 \rightarrow 2$ process, for example as found in eqs. (5.2.139)-(5.2.143). Therefore, one can replace $\cos \theta$ in favor of the Mandelstam variable t , using

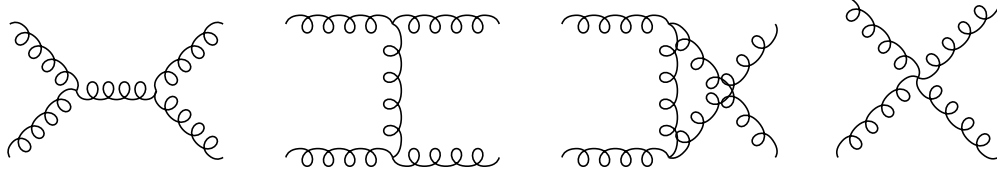
$$d(\cos \theta) = \frac{2dt}{s}, \quad (9.2.19)$$

so

$$\frac{d\sigma}{dt} = \frac{4\pi\alpha_s^2}{9s^2} \left(\frac{s^2 + u^2}{t^2} \right). \quad (9.2.20)$$

9.2.2 Gluon-gluon scattering ($gg \rightarrow gg$)

Let us now turn to QCD scattering of gluons. Because there are three-gluon and four-gluon interaction vertices, one has the interesting process $gg \rightarrow gg$ even at tree-level. (It is traditional to represent the gluon particle name, but not its quantum field, by g .) The corresponding QED process of $\gamma\gamma \rightarrow \gamma\gamma$ does not happen at tree-level, but does occur at one loop. In QCD, because of the three-gluon and four-gluon vertices, there are four distinct Feynman diagrams that contribute at tree-level:



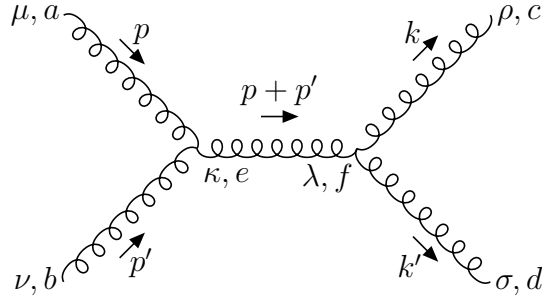
The calculation of the differential cross-section from these diagrams is an important, but quite tedious, one. Just to get an idea of how this proceeds, let us write down the reduced matrix element for the first (“ s -channel”) diagram, and then skip directly to the final answer.

Choosing polarization vectors and color indices for the gluons, we have:

Particle	Polarization vector	Color
initial gluon	$\epsilon_1^\mu = \epsilon^\mu(p, \lambda_1)$	a
initial gluon	$\epsilon_2^\nu = \epsilon^\nu(p', \lambda_2)$	b
final gluon	$\epsilon_3^{\rho*} = \epsilon^{\rho*}(k, \lambda_3)$	c
final gluon	$\epsilon_4^{\sigma*} = \epsilon^{\sigma*}(k', \lambda_4)$	d

(9.2.21)

Let the internal gluon line carry (vector,gauge) indices (κ, e) on the left and (λ, f) on the right. Labeling the Feynman diagram in detail:



The momenta flowing into the leftmost 3-gluon vertex are, starting from the upper-left incoming gluon and going clockwise, $(p, -p-p', p')$. Also, the momenta flowing into the rightmost 3-gluon vertex are, starting from the upper-right final-state gluon and going clockwise, $(-k, -k', k+k')$. So we can use the Feynman rules of section 8.2 to obtain:

$$\begin{aligned}
 \mathcal{M}_{gg \rightarrow gg, s\text{-channel}} = & \epsilon_1^\mu \epsilon_2^\nu \epsilon_3^{\rho*} \epsilon_4^{\sigma*} \left[-gf^{aeb} \{ g_{\mu\kappa} (2p+p')_\nu + g_{\kappa\nu} (-p-2p')_\mu + g_{\nu\mu} (p'-p)_\kappa \} \right. \\
 & \left[-gf^{cdf} \{ g_{\rho\sigma} (k'-k)_\lambda + g_{\sigma\lambda} (-2k'-k)_\rho + g_{\lambda\rho} (2k+k')_\sigma \} \right] \\
 & \left. \left[\frac{-ig^{\kappa\lambda} \delta^{ef}}{(p+p')^2} \right] \right].
 \end{aligned}
 \tag{9.2.22}$$

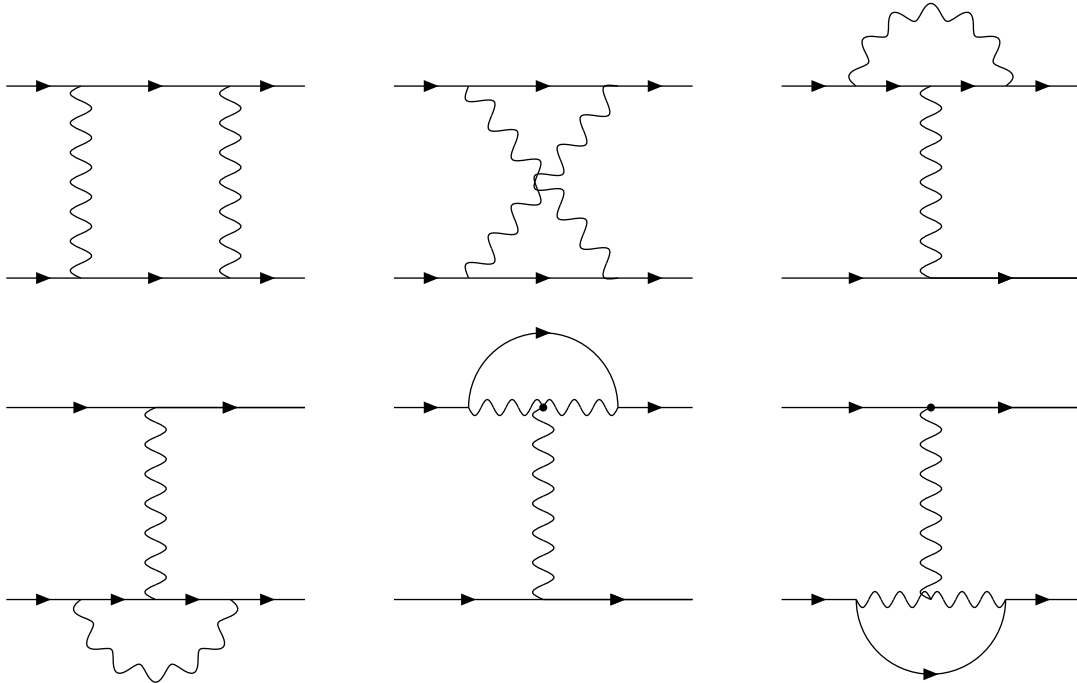
After writing down the reduced matrix elements for the other three diagrams, adding them together, taking the complex square, summing over final state polarizations and averaging over initial state polarizations, summing over final-state gluon colors and averaging over initial-state gluon colors according to $\frac{1}{8} \sum_a \frac{1}{8} \sum_b \sum_c \sum_d$ one finds:

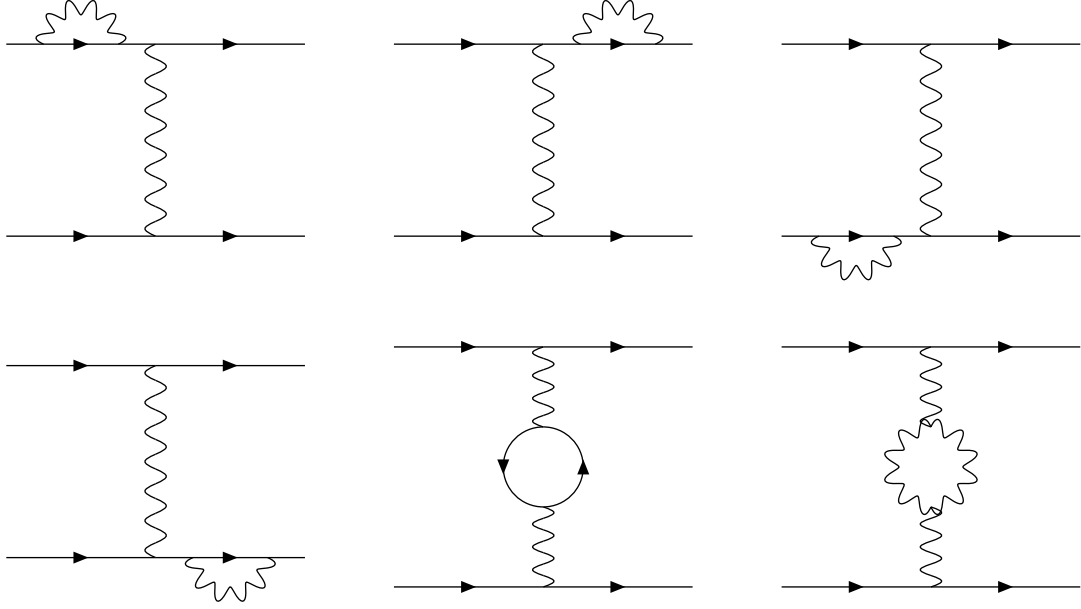
$$\frac{d\sigma_{gg \rightarrow gg}}{dt} = \frac{9\pi\alpha_s^2}{4s^2} \left[\frac{u^2 + t^2}{s^2} + \frac{s^2 + u^2}{t^2} + \frac{s^2 + t^2}{u^2} + 3 \right]. \quad (9.2.23)$$

When we collide a proton with another proton or an antiproton, this process, and the process $ud \rightarrow ud$, are just two of many possible subprocesses that can occur. There is no way to separate the proton into simpler parts, so one must deal with all of these possible subprocesses. We will consider the subprocesses of proton-(anti)proton scattering more systematically in the next subsection.

9.3 Renormalization

Since the strong interactions involve a coupling g_3 that is not small, we should worry about higher-order corrections to the treatment of quark-quark scattering in the previous subsection. Let us discuss this issue in a more general framework than just QCD. In a general gauge theory, the Feynman diagrams contributing to the reduced matrix element at one-loop order in fermion+fermion' \rightarrow fermion+fermion' scattering are the following:





In each of these diagrams, there is a loop momentum ℓ^μ that is unfixed by the external 4-momenta, and must be integrated over. Only the first two diagrams give a finite answer when one naively integrates $d^4\ell$. This is not surprising; we do not really know what physics is like at very high energy and momentum scales, so we have no business in integrating over them. Therefore, one must introduce a very high cutoff mass scale M , and replace the loop-momentum integral by one that kills the contributions to the reduced matrix element from $|\ell^\mu| \geq M$. Physically, M should be the mass scale at which some as-yet-unknown new physics enters in to alter the theory. It is generally thought that the highest this cutoff is likely to be is about $M_{\text{Planck}} = 2.4 \times 10^{18}$ GeV (give or take an order of magnitude), but it could very easily be much lower.

As an example of what can happen, consider the next-to-last Feynman diagram given above. Let us call $q^\mu = p^\mu - k^\mu$ the 4-momentum flowing through either of the vector-boson propagators. Then the part of the reduced matrix element associated with the fermion loop is:

$$\sum_f (-1) \int_{|\ell^\mu| \leq M} d^4\ell \, \text{Tr} \left\{ \left[-i\hat{g}(T_f)_i^{aj} \gamma^\mu \right] \left[\frac{i(\ell + \not{q} + \hat{m}_f)}{(\ell + q)^2 - \hat{m}_f^2 + i\epsilon} \right] \left[-i\hat{g}(T_f)_j^{bi} \gamma^\nu \right] \left[\frac{i(\ell + \hat{m}_f)}{\ell^2 - \hat{m}_f^2 + i\epsilon} \right] \right\}. \quad (9.3.1)$$

This involves a sum over all fermions that can propagate in the loop, and a trace over the spinor indices of the fermion loop. For reasons that will become clear shortly, we are calling the gauge coupling of the theory \hat{g} and the mass of each fermion species \hat{m}_f . We are being purposefully vague about what $\int_{|\ell^\mu| \leq M} d^4\ell$ means, in part because there are actually several different ways to cutoff the integral at large M . (A straightforward step-function cutoff will work, but is clumsy to carry out and even clumsier to interpret.)

The $d^4\ell$ factor can be written as an angular part times a radial part $|\ell|^3 d|\ell|$. Now there are up to five powers of $|\ell|$ in the numerator (three from the $d^4\ell$, and two from the propagators), and four powers of $|\ell|$ in the denominator from the propagators. So naively, one might expect that the result of doing the integral will scale like M^2 for a large cutoff M . However, there is a conspiratorial cancellation, so that the large- M behavior is only logarithmic. The result is proportional to:

$$\hat{g}^2(q^2 g^{\mu\nu} - q^\mu q^\nu) \sum_f \text{Tr}(T_f^a T_f^b) [\ln(M/\bar{m}) + \dots] \quad (9.3.2)$$

where the \dots represents a contribution that does not get large as M gets large. The \bar{m} is a characteristic mass scale of the problem; it is something with dimensions of mass built out of q^μ and the \hat{m}_f . It must appear in the formula in the way it does in order to make the argument of the logarithm dimensionless. The arbitrariness in the precise definition of \bar{m} can be absorbed into the “ \dots ”.

When one uses eq. (9.3.2) in the rest of the Feynman diagram, it is clear that the entire contribution must be proportional to:

$$\mathcal{M}_{\text{fermion loop in gauge propagator}} \propto \hat{g}^4 \sum_f I(R_f) \ln(M/\bar{m}) + \dots \quad (9.3.3)$$

What we are trying to keep track of here is just the number of powers of \hat{g} , the group-theory factor, and the large- M dependence on $\ln(M/\bar{m})$.

A similar sort of calculation applies to the last diagram involving a gauge vector boson loop. Each of the three-vector couplings involves a factor of f^{abc} , with two of the indices contracted because of the propagators. So it must be that the loop part of the diagram make a contribution proportional to $f^{acd} f^{bcd} = C(G) \delta^{ab}$. It is again logarithmically divergent, so that

$$\mathcal{M}_{\text{gauge loop in gauge propagator}} \propto \hat{g}^4 C(G) \ln(M/\bar{m}) + \dots \quad (9.3.4)$$

Doing everything carefully, one finds that the contributions to the differential cross-section is given by:

$$d\sigma = d\sigma_{\text{tree}}(\hat{g}) \left\{ 1 + \frac{\hat{g}^2}{4\pi^2} \left[\frac{11}{3} C(G) - \frac{4}{3} \sum_f I(R_f) \right] \ln(M/\bar{m}) + \dots \right\}, \quad (9.3.5)$$

where $d\sigma_{\text{tree}}(\hat{g})$ is the tree-level result (which we have already worked out in the special case of QCD), considered to be a function of \hat{g} . To be specific, it is proportional to \hat{g}^4 . Let us ignore all the other diagrams for now; the justification for this will be revealed soon.

The cutoff M may be quite large. Furthermore, we typically do not know what it is, or what the specific very-high-energy physics associated with it is. (If we did, we could just redo the

calculation with that physics included, and a higher cutoff.) Therefore, it is convenient to absorb our ignorance of M into a redefinition of the coupling. Specifically, inspired by eq. (9.3.5), one defines a renormalized or running coupling $g(\mu)$ by writing:

$$\hat{g} = g(\mu) \left\{ 1 - \frac{(g(\mu))^2}{16\pi^2} \left[\frac{11}{3}C(G) - \frac{4}{3} \sum_f I(R_f) \right] \ln(M/\mu) \right\}, \quad (9.3.6)$$

Here μ is a new mass scale, called the renormalization scale, that we get to pick. (It is not uncommon to see the renormalization scale denoted by Q instead of μ .) The original coupling \hat{g} is called the bare coupling. One can invert this relation to write the renormalized coupling in terms of the bare coupling:

$$g(\mu) = \hat{g} \left\{ 1 + \frac{\hat{g}^2}{16\pi^2} \left[\frac{11}{3}C(G) - \frac{4}{3} \sum_f I(R_f) \right] \ln(M/\mu) + \dots \right\}, \quad (9.3.7)$$

where we are treating $g(\mu)$ as an expansion in \hat{g} , dropping terms of order \hat{g}^5 everywhere.

The reason for this strategic definition is that, since we know that $d\sigma_{\text{tree}}(\hat{g})$ is proportional to \hat{g}^4 , we can now write, using eqs. (9.3.5) and (9.3.6):

$$d\sigma = d\sigma_{\text{tree}}(g) (\hat{g}/g)^4 \left\{ 1 + \frac{\hat{g}^2}{4\pi^2} \left[\frac{11}{3}C(G) - \frac{4}{3} \sum_f I(R_f) \right] \ln(M/\bar{m}) + \dots \right\} \quad (9.3.8)$$

$$= d\sigma_{\text{tree}}(g) \left\{ 1 + \frac{g^2}{4\pi^2} \left[\frac{11}{3}C(G) - \frac{4}{3} \sum_f I(R_f) \right] \ln(\mu/\bar{m}) + \dots \right\}. \quad (9.3.9)$$

Here we are again dropping terms that go like g^4 ; these are comparable to 2-loop contributions that we are neglecting anyway. The factor $d\sigma_{\text{tree}}(g)$ is the tree-level differential cross-section, but with $g(\mu)$ in place of \hat{g} . This formula looks very much like eq. (9.3.5), but with the crucial difference that the unknown cutoff M has disappeared, and is replaced by the scale μ that we know, because we get to pick it.

What should we pick μ to be? In principle we could pick it to be the cutoff M , except that we do not know what that is. Besides, the logarithm could then be very large, and perturbation theory would converge very slowly or not at all. For example, suppose that $M = M_{\text{Planck}}$, and the characteristic energy scale of the experiment we are doing is, say, $\bar{m} = 0.511$ MeV or $\bar{m} = 1000$ GeV. These choice might be appropriate for experiments involving a non-relativistic electron and a TeV-scale collider, respectively. Then

$$\ln(M/\bar{m}) \approx 50 \text{ or } 35. \quad (9.3.10)$$

This logarithm typically gets multiplied by $1/16\pi^2$ times g^2 times a group-theory quantity, but is still large. This suggests that a really good choice for μ is to make the logarithm $\ln(\mu/\bar{m})$

as small as possible, so that the correction term in eq. (9.3.9) is small. Therefore, one should choose

$$\mu \approx \overline{m}. \quad (9.3.11)$$

Then, to a first approximation, one can calculate using the tree-level approximation using a renormalized coupling $g(\mu)$, knowing that the one-loop correction from these diagrams is small. The choice of renormalization scale eq. (9.3.11) allows us to write:

$$d\sigma \approx d\sigma_{\text{tree}}(g(\mu)). \quad (9.3.12)$$

Of course, this is only good enough to get rid of the large logarithmic one-loop corrections. If you really want *all* one-loop corrections, there is no way around calculating all the one-loop diagrams, keeping all the pieces, not just the ones that get large as $M \rightarrow \infty$.

What about the remaining diagrams? If we isolate the $M \rightarrow \infty$ behavior, they fall into three classes. First, there are diagrams that are not divergent at all (the first two diagrams). Second, there are diagrams (the third through sixth diagrams) that are individually divergent like $\ln(M/\overline{m})$, but sum up to a total that is not divergent. Finally, the seventh through tenth diagrams have a logarithmic divergence, but it can be absorbed into a similar redefinition of the mass. A clue to this is that they all involve sub-diagrams:



The one-loop renormalized or running mass $m_f(\mu)$ is defined in terms of the bare mass \hat{m}_f by

$$\hat{m}_f = m_f(\mu) \left(1 - \frac{g^2}{2\pi^2} C(R_f) \ln(M/\mu) \right), \quad (9.3.13)$$

or

$$m_f(\mu) = \hat{m}_f \left(1 + \frac{g^2}{2\pi^2} C(R_f) \ln(M/\mu) + \dots \right), \quad (9.3.14)$$

where $C(R_f)$ is the quadratic Casimir invariant of the representation carried by the fermion f . It is an amazing fact that the two redefinitions eqs. (9.3.6) and (9.3.13) are enough to remove the cutoff dependence of *all* cross-sections in the theory up to and including one-loop order. In other words, one can calculate $d\sigma$ for any process, and express it in terms of the renormalized mass $m(\mu)$ and the renormalized coupling $g(\mu)$, with no M -dependence. This is what it means for a theory to be renormalizable at one loop order.

In Yang-Mills theories, one can show that by doing some redefinitions of the form:

$$\hat{g} = g(\mu) \left[1 + \sum_{n=1}^L b_n g^{2n} p_n(\ln(M/\mu)) \right], \quad (9.3.15)$$

$$\hat{m}_f = m_f(\mu) \left[1 + \sum_{n=1}^L c_n g^{2n} q_n(\ln(M/\mu)) \right], \quad (9.3.16)$$

one can simultaneously eliminate all dependence on the cutoff in any process up to L -loop order. Here $p_n(x)$ and $q_n(x)$ are polynomials of degree n , and b_n, c_n are some constants that depend on group theory invariants like the Casimir invariants of the group and the representations, and the index. At any finite loop order, what is left in the expression for any cross-section after writing it in terms of the renormalized mass $m(\mu)$ and renormalized coupling $g(\mu)$ is a polynomial in $\ln(\mu/\overline{m})$; these are to be made small by choosing[†] $\mu \approx \overline{m}$. This is what it means for a theory to be renormalizable at all loop orders. Typically, the specifics of these redefinitions is only known at 2- or 3- or occasionally 4- loop order, except in some special theories. If a theory is non-renormalizable, it does not necessarily mean that the theory is useless; we saw that the four-fermion theory of the weak interactions makes reliable predictions, and we still have no more predictive theory for gravity than Einstein's relativity. It does mean that we expect the theory to have trouble making predictions about processes at high energy scales.

We have seen that we can eliminate the dependence on the unknown cutoff of a theory by defining a renormalized running coupling $g(\mu)$ and mass $m_f(\mu)$. When one does an experiment in high energy physics, the results are first expressed in terms of observable quantities like cross-sections, decay rates, and physical masses of particles. Using this data, one extracts the value of the running couplings and running masses at some appropriately-chosen renormalization scale μ , using a theoretical prediction like eq. (9.3.9), but with the non-logarithmic corrections included too. (The running mass is not quite the same thing as the physical mass. The physical mass can be determined from the experiment by kinematics, the running mass is related to it by various corrections.) The running parameters can then be used to make predictions for other experiments. This tests both the theoretical framework, and the specific values of the running parameters.

The bare coupling and the bare mass never enter into this process of comparing theory to experiment. If we measure $d\sigma$ in an experiment, we see from eq. (9.3.5) that in order to determine the bare coupling \hat{g} from the data, we would also need to know the cutoff M . However, we do not know what M is. We could guess at it, but this would usually be a wild guess, devoid of practical significance.

A situation that arises quite often is that one extracts running parameters from an experiment with a characteristic energy scale μ_0 , and one wants to compare with data from some other experiment that has a completely different characteristic energy scale μ . Here μ_0 and μ each might be the mass of some particle that is decaying, or the momentum exchanged between particles in a collision, or some suitable average of particle masses and exchanged momenta. It

[†]Of course, there might be more than one characteristic energy scale in a given problem, rather than a single \overline{m} . If so, and if they are very different from each other, then one may be stuck with some large logarithms, no matter what μ is chosen. This has to be dealt with by fancier methods.

would be unwise to use the same renormalization scale when computing the theoretical expectations for both experiments, because the loop corrections involved in at least one of the two cases will be unnecessarily large. What we need is a way of taking a running coupling as determined in the first experiment at a renormalization scale μ_0 , and getting from it the running coupling at any other scale μ . The change of the choice of scale μ is known as the renormalization group.[‡]

As an example, let us consider how $g(\mu)$ changes in a Yang-Mills gauge theory. Since the differential cross-section $d\sigma$ for fermion+fermion' \rightarrow fermion+fermion' is an observable, in principle it should not depend on the choice of μ , which is an arbitrary one made by us. Therefore, we can require that eq. (9.3.9) is independent of μ . Remembering that $d\sigma_{\text{tree}} \propto g^4$, we find:

$$0 = \frac{d}{d\mu}(d\sigma) = (d\sigma_{\text{tree}}) \left\{ \frac{4}{g} \frac{dg}{d\mu} + \frac{g^2}{4\pi^2} \left[\frac{11}{3}C(G) - \frac{4}{3} \sum_f I(R_f) \right] \frac{1}{\mu} + \dots \right\}, \quad (9.3.17)$$

where we are dropping all higher-loop-order terms that are proportional to $(d\sigma_{\text{tree}})g^4$. The first term in eq. (9.3.17) comes from the derivative acting on the g^4 inside $d\sigma_{\text{tree}}$. The second term comes from the derivative acting on the $\ln\mu$ one-loop correction term. The contribution from the derivative acting on the g^2 in the one-loop correction term can be self-consistently judged, from the equation we are about to write down, as proportional to $(d\sigma_{\text{tree}})g^5$, so it is neglected as a higher-loop-order effect in the expansion in g^2 . So, it must be true that:

$$\mu \frac{dg}{d\mu} = \frac{g^3}{16\pi^2} \left[-\frac{11}{3}C(G) + \frac{4}{3} \sum_f I(R_f) \right] + \dots \quad (9.3.18)$$

This differential equation, called the renormalization group equation or RG equation, tells us how to change the coupling $g(\mu)$ when we change the renormalization scale. An experimental result will provide a boundary condition at some scale μ_0 , and then we can solve the RG equation to find $g(\mu)$ at some other scale. Other experiments then test the whole framework. The right-hand side of the RG equation is known as the beta function for the running coupling $g(\mu)$, and is written $\beta(g)$, so that:

$$\mu \frac{dg}{d\mu} = \beta(g). \quad (9.3.19)$$

In a Yang-Mills gauge theory, including the effects of Feynman diagrams with more loops,

$$\beta(g) = \frac{g^3}{16\pi^2} b_0 + \frac{g^5}{(16\pi^2)^2} b_1 + \frac{g^7}{(16\pi^2)^3} b_2 + \dots \quad (9.3.20)$$

where we already know that

$$b_0 = -\frac{11}{3}C(G) + \frac{4}{3} \sum_f I(R_f), \quad (9.3.21)$$

[‡]The use of the word “group” is historical; this is not a group in the mathematical sense defined earlier.

and, just to give you an idea of how it goes,

$$b_1 = -\frac{34}{3}C(G)^2 + \frac{20}{3}C(G)\sum_f I(R_f) + 4\sum_f C(R_f)I(R_f), \quad (9.3.22)$$

etc. In QCD, the coefficients up to b_3 (four-loop order) have been calculated. In practical applications, it is usually best to work within an effective theory in which fermions much heavier than the scales μ of interest are ignored. The sum over fermions then includes only those satisfying $m_f \lesssim \mu$. The difference between this effective theory and the more complete theory with all known fermions included can be absorbed into a redefinition of running parameters. The advantage of doing this is that perturbation theory will converge more quickly and reliably if heavy fermions (that are, after all, irrelevant to the process under study) are not included.

In the one-loop order approximation, one can solve the RG equation explicitly. Writing

$$\frac{dg^2}{d\ln\mu} = \frac{b_0}{8\pi^2}g^4, \quad (9.3.23)$$

you can check that

$$g^2(\mu) = \frac{g^2(\mu_0)}{1 - \frac{b_0 g^2(\mu_0)}{8\pi^2} \ln(\mu/\mu_0)}. \quad (9.3.24)$$

To see how this works in QCD, let us examine the one-loop beta function. In $SU(3)$, $C(G) = 3$, and each quark flavor is in a fundamental $\mathbf{3}$ representation with $I(\mathbf{3}) = 1/2$. Therefore,

$$b_{0,QCD} = -11 + \frac{2}{3}n_f \quad (9.3.25)$$

where n_f is the number of “active” quarks in the effective theory, usually those with mass $\lesssim \mu$. The crucial fact is that since there are only 6 quark flavors known, $b_{0,QCD}$ is definitely negative for all accessible scales μ , and so the beta function is definitely negative. For an effective theory with $n_f = (3, 4, 5, 6)$ quark flavors, $b_0 = (-9, -25/3, -23/3, -7)$. Writing the solution to the RG equation, eq. (9.3.24), in terms of the running α_s , we have:

$$\alpha_s(\mu) = \frac{\alpha_s(\mu_0)}{1 - \frac{b_0 \alpha_s(\mu_0)}{2\pi} \ln(\mu/\mu_0)}. \quad (9.3.26)$$

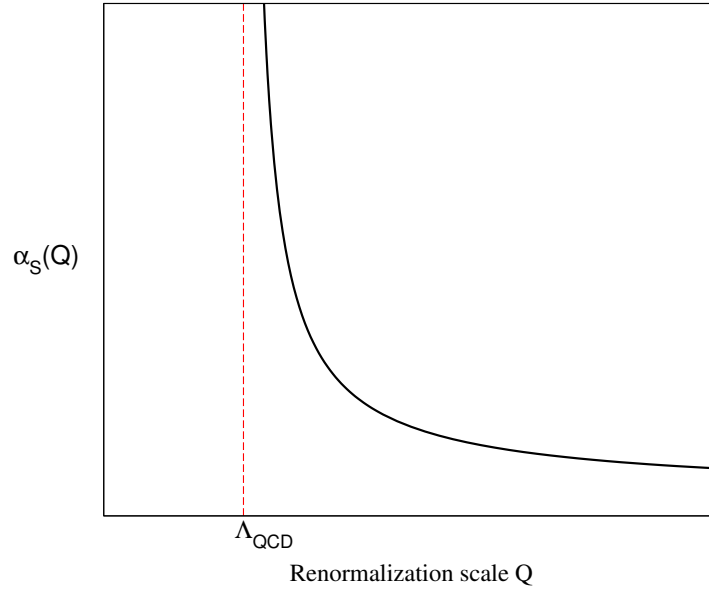
Since b_0 is negative, we can make α_s blow up by choosing μ small enough. To make this more explicit, we can define a quantity

$$\Lambda_{QCD} = \mu_0 e^{2\pi/b_0 \alpha_s(\mu_0)}, \quad (9.3.27)$$

with dimensions of [mass], implying that

$$\alpha_s(\mu) = \frac{2\pi}{b_0 \ln(\Lambda_{QCD}/\mu)}. \quad (9.3.28)$$

This shows that at the scale $\mu = \Lambda_{\text{QCD}}$, the QCD gauge coupling is predicted to blow up, according to the 1-loop RG equation. A qualitative graph of the running of $\alpha_s(\mu)$ as a function of renormalization scale μ is shown below:



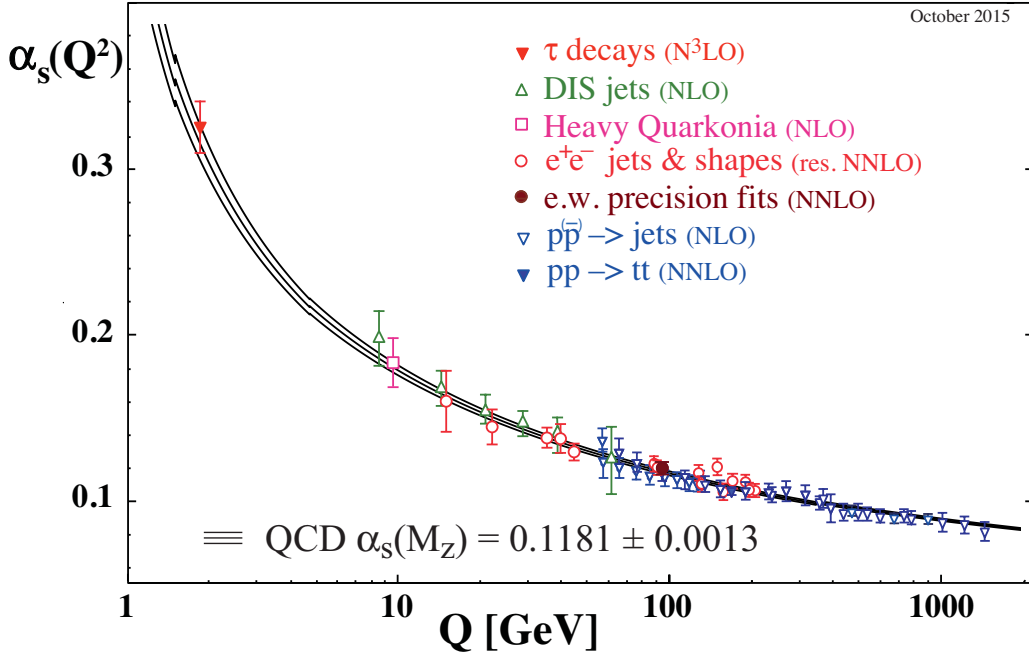
Of course, once $\alpha_s(\mu)$ starts to get big, we should no longer trust the one-loop approximation, since two-loop effects are definitely big. The whole analysis has been extended to four-loop order, with significant numerical changes, but the qualitative effect remains: at any finite loop order, there is some scale Λ_{QCD} at which the gauge coupling is predicted to blow up in a theory with a negative beta function. This is *not* a sign that QCD is wrong. Instead, it is a sign that perturbation theory is not going to be able to make good predictions when we do experiments near $\mu = \Lambda_{\text{QCD}}$ or lower energy scales. One can draw Feynman diagrams and make rough qualitative guesses, but the numbers cannot be trusted. On the other hand, we see that for experiments conducted at characteristic energies much larger than Λ_{QCD} , the gauge coupling is not large, and is getting smaller as μ gets larger. This means that perturbation theory becomes more and more trustworthy at higher and higher energies. This nice property of theories with negative β functions is known as asymptotic freedom. The name refers to the fact that quarks in QCD are becoming free (since the coupling is becoming small) as we probe them at larger energy scales.

Conversely, the fact that the QCD gauge coupling becomes non-perturbative in the infrared means that we cannot expect to describe free quarks at low energies using perturbation theory. This theoretical prediction goes by the name of infrared slavery. It agrees well with the fact that one does not observe free quarks outside of bound states. While it has not been proved mathematically that the infrared slavery of QCD necessarily requires the absence of free quarks, the two ideas are certainly compatible, and more complicated calculations show that they are

plausibly linked. Heuristically, the growth of the QCD coupling means that at very small energies or large distances, the force between two free color charges is large and constant as the distance increases. In the early universe, after the temperature dropped below Λ_{QCD} , all quarks and antiquarks and gluons arranged themselves into color-singlet bound states, and have remained that way ever since.

An important feature of the renormalization of QCD is that we can actually trade the gauge coupling as a parameter of the theory for the scale Λ_{QCD} . This is remarkable, since g_3 (or equivalently α_s) is a dimensionless coupling, while Λ_{QCD} is a mass scale. If we want, we can specify how strong the QCD interactions are either by quoting what $\alpha_s(\mu_0)$ is at some specified μ_0 , or by quoting what Λ_{QCD} is. This trade of a dimensionless parameter for a mass scale in a gauge theory is known as dimensional transmutation. Working in a theory with five “active” quarks u, d, s, c, b (the top quark is treated as part of the unknown theory above the cutoff), one finds Λ_{QCD} is about 210 MeV. One can also work in an effective theory with only four active quarks u, d, s, c , in which case Λ_{QCD} is about 290 MeV, or in an effective theory with only three active quarks u, d, s , in which case Λ_{QCD} is about 330 MeV. Alternatively, $\alpha_s(m_Z) = 0.1181 \pm 0.0013$. Recently, it has become standard to use this second way of specifying the QCD coupling strength. These results hold when the details of the cutoff and the renormalization are treated in the most popular way, called the $\overline{\text{MS}}$ scheme.[§] A summary of the experimental data on the QCD coupling is shown in the figure below (from the 2015 update of the Review of Particle Properties).

[§]In this scheme, one cuts off loop momentum integrals by a process known as dimensional regularization, which continuously varies the number of spacetime dimensions infinitesimally away from 4, rather than putting in a particular cutoff M . Although bizarre physically, this scheme is consistent with gauge invariance and relatively easy to calculate in.



The data determine $\alpha_s(\mu)$ at a variety of renormalization scales μ from 1.78 GeV up to more than 1000 GeV. (In the figure, Q was used as the name of the renormalization scale instead of μ .) The most accurate determinations come from lattice QCD calculations of the mass splittings in the Υ bottomonium system and from the hadronic branching ratio in τ decays, but other inputs to the average come from production of jets and $t\bar{t}$ pairs at hadron colliders, deep inelastic scattering at the HERA proton-electron collider, and jet production data in e^+e^- collisions. The four-loop renormalization group running of $\alpha_s(\mu)$ with inputs from various widely different μ are then used to determine the reference value $\alpha_s(m_Z)$.

We can contrast this situation with the case of QED. For a $U(1)$ group, there is no non-zero structure constant, so $C(G) = 0$. Also, since the generator of the group in a representation of charge Q_f is just the 1×1 matrix Q_f , the index for a fermion with charge Q_f is $I(R_f) = Q_f^2$. Therefore,

$$b_{0,\text{QED}} = \frac{4}{3} \left[3n_u(2/3)^2 + 3n_d(-1/3)^2 + n_\ell(-1)^2 \right] = \frac{16}{9}n_u + \frac{4}{9}n_d + \frac{4}{3}n_\ell, \quad (9.3.29)$$

where n_u is the number of up-type quark flavors (u, c, t), and n_d is the number of down-type quark flavors (d, s, b), and n_ℓ is the number of charged leptons (e, μ, τ) included in the chosen effective theory. If we do experiments with a characteristic energy scale $m_e \lesssim \mu \lesssim m_\mu$, then only the electron itself contributes, and $b_{0,\text{EM}} = 4/3$, so:

$$\frac{de}{d\ln\mu} = \beta_e = \frac{e^3}{16\pi^2} \left(\frac{4}{3} \right) \quad (m_e \lesssim \mu \lesssim m_\mu). \quad (9.3.30)$$

This corresponds to a very slow running. (Notice that the smaller a gauge coupling is, the slower it will run.) If we do experiments at characteristic energies that are much less than

the electron mass, then the relativistic electron is not included in the effective theory (virtual electron-positron pairs are less and less important at low energies), so $b_{0,\text{EM}} = 0$, and the electron charge does not run at all:

$$\frac{de}{d\ln\mu} = 0 \quad (\mu \ll m_e). \quad (9.3.31)$$

This means that QED is not quite “infrared free”, since the effective electromagnetic coupling is perturbative, but does not get arbitrarily small, at very large distance scales. At extremely high energies, the coupling e could in principle become very large, because the QED beta function is always positive. Fortunately, this is predicted to occur only at energy scales far beyond what we can probe, because e runs very slowly. Furthermore, QED is embedded in a larger, more complete theory anyway at energy scales in the hundreds of GeV range, so the apparent blowing up of $\alpha = e^2/4\pi$ much farther in the ultraviolet is just an illusion.

9.4 Parton distribution functions and hadron-hadron scattering

In general, a hadron is a QCD bound state of quarks, anti-quarks, and gluons. The characteristic size of a hadron, like the proton or antiproton, is always roughly $1/\Lambda_{\text{QCD}} \approx 10^{-13}$ cm, since this is the scale at which the strongly-interacting particles are confined. In general, the point-like quark, antiquark, and gluon parts of a hadron are called partons, and the description of hadrons in terms of them is called the parton model.

Suppose we scatter a hadron off of another particle (which might be another hadron or a lepton or photon) with a total momentum exchange much larger than Λ_{QCD} . The scattering can be thought of as factored into a “hard scattering” of one of the point-like partons, with the remaining partons as spectators, and “soft” QCD processes that involve exchanges and radiation of low energy virtual gluons. The hard scattering subprocess takes place on a time scale much shorter than $1/\Lambda_{\text{QCD}}$ expressed in seconds. Because of asymptotic freedom, at higher scattering energies it becomes a better and better approximation to think of the partons as individual entities that move collectively before and after the scattering, but are free particles at the moment of scattering. As a first approximation, we can consider only the hard scattering processes, and later worry about adding on the various soft processes as part of the higher-order corrections. This way of thinking about things allows us to compute cross-sections for hadron scattering by first calculating the partonic cross-sections leading to a desired final state, and then combining them with information about the multiplicity and momentum distributions of partons within the hadronic bound states.

For example, suppose we want to calculate the scattering of a proton and antiproton. This

involves the following 2→2 partonic subprocesses:

$$qq \rightarrow qq, \quad qq' \rightarrow qq', \quad \bar{q}\bar{q} \rightarrow \bar{q}\bar{q}, \quad \bar{q}\bar{q}' \rightarrow \bar{q}\bar{q}', \quad (9.4.1)$$

$$q\bar{q} \rightarrow gg, \quad q\bar{q} \rightarrow q\bar{q}, \quad q\bar{q} \rightarrow q'\bar{q}', \quad q\bar{q}' \rightarrow q\bar{q}', \quad (9.4.2)$$

$$gg \rightarrow qq, \quad \bar{q}g \rightarrow \bar{q}g, \quad gg \rightarrow gg, \quad gg \rightarrow q\bar{q}. \quad (9.4.3)$$

where g is a gluon and q is any fixed quark flavor and q' is any quark flavor that is definitely different from q . Let the center-of-mass energy of the proton and antiproton be called \sqrt{s} . Each parton only carries a fraction of the energy of the energy of the proton it belongs to, so the partonic center-of-mass energy, call it $\sqrt{\hat{s}}$, will be significantly less than \sqrt{s} . One often uses hatted Mandelstam variables \hat{s} , \hat{t} and \hat{u} for the partonic scattering event. If $\sqrt{\hat{s}} \gg \Lambda_{\text{QCD}}$, then the two partons in the final state will be sufficiently energetic that they can usually escape from most or all of the spectator quarks and gluons before hadronizing (forming bound states). However, before traveling a distance $1/\Lambda_{\text{QCD}}$, they must rearrange themselves into color-singlet combinations, possibly by creating quark-antiquark or gluon-antigluon pairs out of the vacuum. This hadronization process can be quite complicated, but will usually result in a jet of hadronic particles moving with roughly the same 4-momentum as the parton that was produced. So, all of the partonic process cross-sections in eq. (9.4.3) contribute to the observable cross-section for the process:

$$p\bar{p} \rightarrow jj + X, \quad (9.4.4)$$

where j stands for a jet. The X stands for “anything”, and includes stray hadronic junk left over from the original proton and antiproton. Similarly, partonic hard scatterings like:

$$q\bar{q} \rightarrow q'\bar{q}'g, \quad qq \rightarrow qgg, \quad \bar{q}g \rightarrow \bar{q}gg, \quad gg \rightarrow ggg, \quad (9.4.5)$$

and so on, will contribute to an observable cross-section for

$$p\bar{p} \rightarrow jjj + X. \quad (9.4.6)$$

The 2×2 hard scattering processes can also contribute to this process if one of the final state partons hadronizes by splitting into two jets, or if there is an additional jet from the initial state.

In order to use the calculation of cross-sections for partonic processes like eq. (9.4.3) to obtain measurable cross-sections, we need to know how likely it is to have a given parton inside the initial-state hadron with a given 4-momentum. Since we are mostly interested in high-energy scattering problems, we can make things simple, and treat the hadron and all of its constituents as nearly massless. (For the proton, this means that we are assuming that $\sqrt{s} \gg m_p \approx 1 \text{ GeV}$.)

Suppose we therefore take the total 4-momentum of the hadron h in an appropriate Lorentz frame to be:

$$p_h^\mu = (E, 0, 0, E). \quad (9.4.7)$$

This is sometimes called the “infinite momentum frame”, even though E is finite, since $E \gg m_p$. Consider a parton constituent A (a quark, antiquark, or gluon) that carries a fraction x of the hadron’s momentum:

$$p_A^\mu = x(E, 0, 0, E). \quad (9.4.8)$$

The variable x is a standard notation, and is called the (longitudinal) momentum fraction for the parton, or Feynman’s x . It is older than QCD, dating back to a time when the proton was suspected to contain point-like partons with properties that were then obscure. In order to describe the partonic content of a hadron, one defines:

$$\left(\begin{array}{c} \text{Probability of finding a parton of type } A \text{ with} \\ \text{4-momentum between } xp^\mu \text{ and } (x + dx)p^\mu \\ \text{inside a hadron } h \text{ with 4-momentum } p^\mu \end{array} \right) = f_A^h(x) dx. \quad (9.4.9)$$

The function $f_A^h(x)$ is called the parton distribution function or PDF for the parton A in the hadron h . The parton can be either one of the two or three valence quarks or antiquarks that are the nominal constituents of the hadron, or one of an indeterminate number of virtual sea quarks and gluons. Either type of parton can participate in a scattering event.

Hadronic collisions studied in laboratories usually involve protons or antiprotons, so the PDFs of the proton and antiproton are especially interesting. The proton is nominally a bound state of three valence quarks, namely two up quarks and one down quark, so we are certainly interested in the up-quark and down-quark distribution functions

$$f_u^p(x) \quad \text{and} \quad f_d^p(x).$$

The proton also contains virtual gluons, implying a gluon distribution function:

$$f_g^p(x). \quad (9.4.10)$$

Furthermore, there are always virtual quark-antiquark pairs within the proton. This adds additional contributions to $f_u^p(x)$ and $f_d^p(x)$, and also means that there is a non-zero probability of finding antiup, antidown, or strange or antistrange quarks:

$$f_{\bar{u}}^p(x), \quad f_{\bar{d}}^p(x), \quad f_s^p(x), \quad f_{\bar{s}}^p(x). \quad (9.4.11)$$

These parton distribution functions are implicitly summed over color and spin. So $f_u^p(x)$ tells us the probability of finding an up quark with the given momentum fraction x and any color and

spin. Since the gluon is its own antiparticle (it lives in the adjoint representation of the gauge group, which is always a real representation), there is not a separate $f_g^p(x)$.

Although the charm, bottom and top quarks are heavier than the proton, virtual charm-anticharm, bottom-antibottom, and top-antitop pairs can exist as long as their total energy does not exceed m_p . This can happen because, as virtual particles, they need not be on-shell. So, one can even talk about the parton distribution functions $f_c^p(x)$, $f_{\bar{c}}^p(x)$, $f_b^p(x)$, $f_{\bar{b}}^p(x)$, $f_t^p(x)$, $f_{\bar{t}}^p(x)$. Fortunately, these are small so one can often neglect them, although they can be important for processes involving charm or bottom quarks in the final state.

Given the PDFs for the proton, the PDFs for the antiproton follow immediately from the fact that it is the proton's antiparticle. The probability of finding a given parton in the proton with a given x is the same as the probability of finding the corresponding antiparton in the antiproton with the same x . Therefore, if we know the PDFs for the proton, there is no new information in the PDFs for the antiproton. We can just describe everything having to do with proton and antiproton collisions in terms of the proton PDFs. To simplify the notation, it is traditional to write the proton and antiproton PDFs as:

$$g(x) = f_g^p(x) = f_g^{\bar{p}}(x), \quad (9.4.12)$$

$$u(x) = f_u^p(x) = f_u^{\bar{p}}(x), \quad (9.4.13)$$

$$d(x) = f_d^p(x) = f_d^{\bar{p}}(x), \quad (9.4.14)$$

$$\bar{u}(x) = f_{\bar{u}}^p(x) = f_{\bar{u}}^{\bar{p}}(x), \quad (9.4.15)$$

$$\bar{d}(x) = f_{\bar{d}}^p(x) = f_{\bar{d}}^{\bar{p}}(x), \quad (9.4.16)$$

$$s(x) = f_s^p(x) = f_s^{\bar{p}}(x), \quad (9.4.17)$$

$$\bar{s}(x) = f_{\bar{s}}^p(x) = f_{\bar{s}}^{\bar{p}}(x). \quad (9.4.18)$$

The PDFs are also functions of another parameter Q (sometimes denoted μ or μ_F), known as the factorization scale. The factorization scale can be thought of as the energy scale that serves as the boundary between what is treated as the short-distance hard partonic process and what is taken to be part of the long-distance physics associated with hadronization. The choice of the factorization scale is an arbitrary one, and in principle the final result should not depend on it, just like the choice of renormalization scale discussed in section 9.3 is arbitrary. It is very common to choose the factorization scale equal to the renormalization scale, although this is not mandatory. (When they are distinguished in the literature, some authors use Q for the renormalization scale and μ for the factorization scale, and some use the reverse as we have here. Some use the same letter for both, especially when choosing them to be the same numerically.) The PDFs have a mild logarithmic dependence on the choice of factorization scale Q , which can be computed in perturbation theory by a set of equations known as the DGLAP

(Dokshitzer–Gribov–Lipatov–Altarelli–Parisi) equations. So they are really functions $g(x, Q^2)$ etc., although the Q -dependence is often left implicit for brevity, as we will mostly do below.

It is usual to choose the factorization scale Q to be comparable to some energy scale relevant to the physical process of interest. For example, in deeply inelastic scattering of leptons off of protons, with momentum transfer to the scattered quark q^μ , the factorization scale is typically chosen as $Q^2 = -q^2$. This Q^2 is positive, since q^μ is a spacelike vector. When producing a pair of heavy particles with some mass m , it is common to choose $Q = m$ or some fraction thereof. After having completed a calculation, one often varies the renormalization and factorization scales (either together or independently) over a range (say, from $Q = m/4$ to $Q = 2m$ in the case just mentioned) to see how the cross-section or other observables that resulted from the calculation vary. This is a test of the accuracy of the perturbation theory calculation, since in principle if one could calculate exactly rather than to some low order in perturbation theory, the results should not depend on either scale choice at all.

In the proton, antiquarks are always virtual, and so must be accompanied by a quark with the same flavor. This implies that if we add up all the up quarks found in the proton, and subtract all the anti-ups, we must find a total of 2 quarks:

$$\int_0^1 dx \left[u(x, Q^2) - \bar{u}(x, Q^2) \right] = 2. \quad (9.4.19)$$

Similarly, summing over all x the probability of finding a down quark with a given x , and subtracting the same thing for anti-downs, one has:

$$\int_0^1 dx \left[d(x, Q^2) - \bar{d}(x, Q^2) \right] = 1. \quad (9.4.20)$$

Most of the strange quarks in the proton come from the process of a virtual gluon splitting into a strange and anti-strange pair. Since the virtual gluon treats quarks and antiquarks on an equal footing, for every strange quark with a given x , there should be[†] an equal probability of finding an antistrange with the same x :

$$s(x, Q^2) = \bar{s}(x, Q^2). \quad (9.4.21)$$

The up-quark PDF can be thought of as divided into a contribution $u_v(x)$ from the two valence quarks, and a contribution $u_s(x)$ from the sea (non-valence) quarks that are accompanied by an anti-up. (Here and below the factorization scale dependence is left implicit, for brevity.) So we have:

$$u(x) = u_v(x) + u_s(x), \quad u_s(x) = \bar{u}(x); \quad (9.4.22)$$

$$d(x) = d_v(x) + d_s(x), \quad d_s(x) = \bar{d}(x). \quad (9.4.23)$$

[†]Although QCD interactions do not change quark flavors, there is a small strangeness violation in the weak interactions, so the following rule is not quite exact.

There is also a constraint that the total 4-momentum of all partons found in the proton must be equal to the 4-momentum of the proton that they form. This rule takes the form:

$$\int_0^1 dx x [g(x) + u(x) + \bar{u}(x) + d(x) + \bar{d}(x) + s(x) + \bar{s}(x) + \dots] = 1, \quad (9.4.24)$$

or more generally, for any hadron h made out of parton species A ,

$$\sum_A \int_0^1 dx x f_A^h(x) = 1. \quad (9.4.25)$$

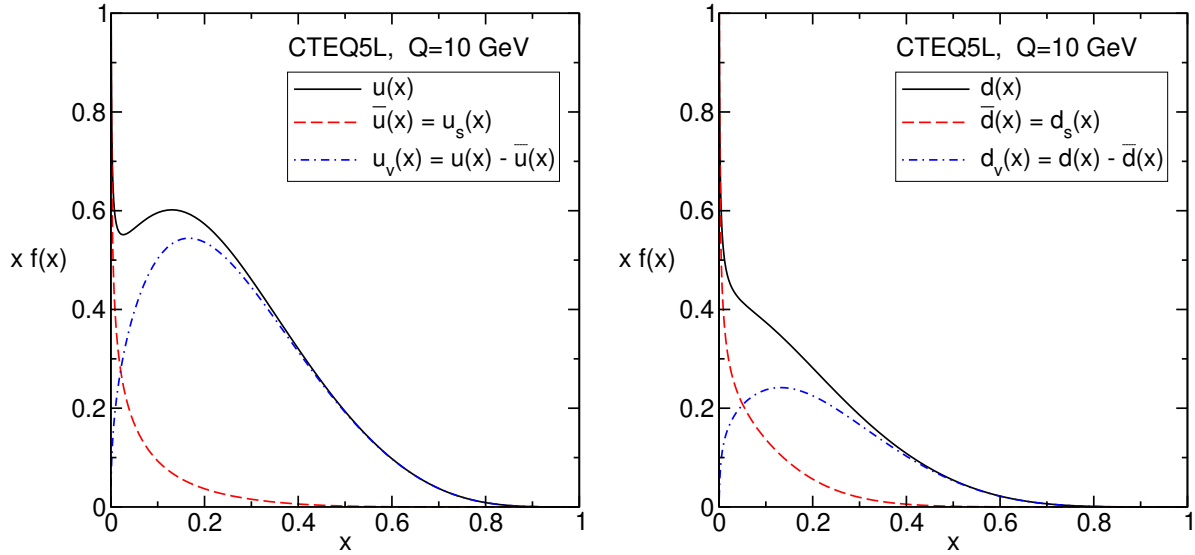
Each term $x f_A^h(x)$ represents the probability that a parton is found with a given momentum fraction x , multiplied by that momentum fraction. One of the first compelling pieces of evidence that the gluons are actual particles carrying real momentum and energy, and not just abstract group-theoretic constructs, was that if one excludes them from the sum rule eq. (9.4.24), only about half of the proton's 4-momentum is accounted for:

$$\int_0^1 dx x [u(x) + \bar{u}(x) + d(x) + \bar{d}(x) + s(x) + \bar{s}(x) + \dots] \approx 0.5. \quad (9.4.26)$$

If we could solve the bound state problem for the proton in QCD, like one can solve the hydrogen atom in quantum mechanics, then we could derive the PDFs directly from the Hamiltonian. However, we saw in section 9.3 why this is not practical; perturbation theory in QCD is not accurate for studying low-energy problems like bound-state problems, because the gauge coupling becomes very large at low energies. Instead, the proton PDFs are measured by experiments including those in which charged leptons and neutrinos probe the proton, like $\ell^- p \rightarrow \ell^- + X$ and $\nu p \rightarrow \ell^- + X$. Several collaborations perform fits of available data to determine the PDFs, and periodically publish updated result both in print and as computer code. Two such collaborations are CTEQ (Coordinated Theoretical-Experimental Project on QCD) and MSTW (Martin, Stirling, Thorne, Watt), formerly MRST (Martin, Roberts, Stirling, Thorne). In each case, the PDFs are given in the form of computer codes obtained by fitting to experimental data. Because of different techniques and weighting of the data, the PDFs from different groups are always somewhat different.

As an example, let us consider the CTEQ5L PDF set. Here, the “5” says which update of the PDFs is being provided, this one from the year 2000, and the “L” stands for “lowest order”, which means it is the set appropriate when one only has the lowest-order calculation of the partonic cross-section. This set is somewhat old; we use it only because it is relatively easy to evaluate, since it is given in parameterized function form rather than interpolation table form. There are more recent sets CTEQ6 and CT10 and CT14 from CTEQ, and MSTW2008 from MSTW. Each of these has a version appropriate for lowest-order work, and other versions appropriate when one has the next-to-leading order (NLO) or next-next-leading order (NNLO)

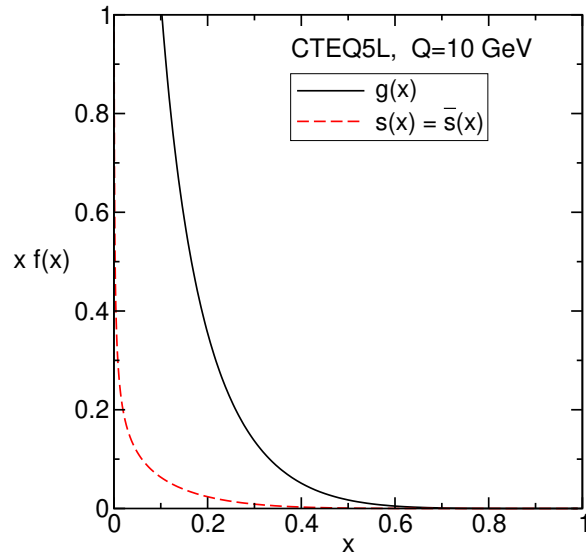
formulas for the hard scattering process of interest. At $Q = 10$ GeV, the CTEQ5L PDFs for $u(x)$, $\bar{u}(x)$, and the valence contribution $u_v(x) \equiv u(x) - \bar{u}(x)$ are shown below, together with a similar graph for the down quark and antiquark distributions:



Here I follow tradition by graphing x times the PDF in each case, since they all tend to get large near $x = 0$.

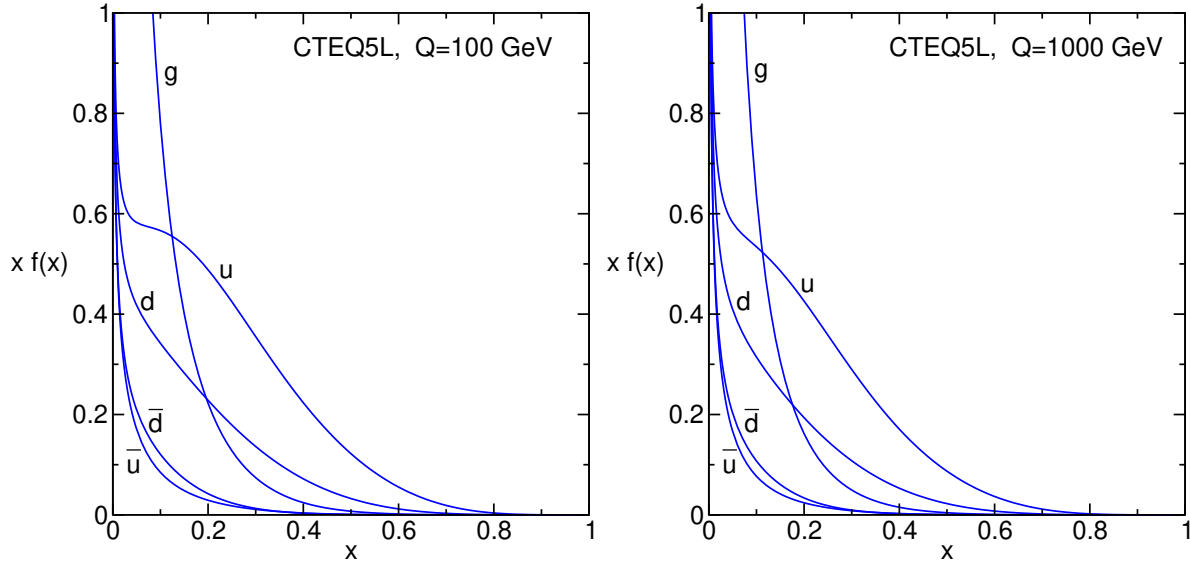
We see from the first graph that the valence up-quark distribution is peaked below $x = 0.2$, with a long tail for larger x (where an up-quark is found to have a larger fraction of the proton's energy). There is even a significant chance of finding that an up quark has more than half of the proton's 4-momentum. In contrast, the sea quark distribution $\bar{u}(x)$ is strongly peaked near $x = 0$. This is a general feature of sea partons; the chance that a virtual particle can appear is greater when it carries a smaller energy, and thus a smaller fraction x of the proton's total momentum. The solid curve shows the total up-quark PDF for this value of Q . The sea distribution $\bar{d}(x)$ is not very different from that of the anti-up, but the distribution $d_v(x)$ is of course only about half as big as $u_v(x)$, since there is only one valence down quark to find in the proton.

Next, let us look at the strange and gluon PDFs:



The parton distribution function for gluons grows very quickly as one moves towards $x = 0$. This is because there are 8 gluon color combinations available, and each virtual gluon can give rise to more virtual gluons because of the 3-gluon and 4-gluon vertex. This means that the chance of finding a gluon gets very large if one requires that it only have a small fraction of the total 4-momentum of the proton. The PDFs $s(x) = \bar{s}(x)$ are suppressed by the non-zero strange quark mass, since this imposes a penalty on making virtual strange and antistrange quarks. This explains why $s(x) < \bar{d}(x)$.

The value of the factorization scale $Q = 10$ GeV corresponds roughly to the appropriate energy scale for many of the experiments that were actually used to fit for the PDFs. However, at the Tevatron and LHC, one will often be studying events with a much larger characteristic energy scale, like $Q \sim m_t$ for top events and perhaps $Q \sim 1000$ GeV for supersymmetry events at the LHC. Larger Q is appropriate for probing the proton at larger energy scales, or shorter distance scales. The next two graphs show the CTEQ5L PDFs for $Q = 100$ and 1000 GeV:



As Q increases from $Q = 100$ to 1000 GeV, the PDFs become larger at very small x (although this is hard to see from the graphs), but smaller for $x \gtrsim 0.015$ for gluons and $x \gtrsim 0.04$ for quarks. More generally, the variation with Q can be made quantitative using the DGLAP equations, which are built into the computer codes that provide the parton distributions as a function of x and Q .

Now suppose we have available a set of PDFs, and let us see how to use them to get a cross-section. Consider scattering two hadrons h and h' , and let the partonic differential cross-sections for the desired final state X be

$$d\hat{\sigma}(ab \rightarrow X) \quad (9.4.27)$$

for any two partons a (to be taken from h) and b (from h'). The hat is used as a reminder that this is a partonic process. If X has two particles 1,2 in it, then one defines partonic Mandelstam variables:

$$\hat{s} = (p_a + p_b)^2, \quad (9.4.28)$$

$$\hat{t} = (p_a - k_1)^2, \quad (9.4.29)$$

$$\hat{u} = (p_a - k_2)^2. \quad (9.4.30)$$

Let us work in the center-of-momentum frame, with approximately massless hadrons and partons, so that

$$p_h^\mu = (E, 0, 0, E), \quad (9.4.31)$$

$$p_{h'}^\mu = (E, 0, 0, -E). \quad (9.4.32)$$

Then we can define a Feynman x for each of the initial-state partons, x_a and x_b , so:

$$p_a^\mu = x_a(E, 0, 0, E), \quad (9.4.33)$$

$$p_b^\mu = x_b(E, 0, 0, -E). \quad (9.4.34)$$

It follows that, with $s = (p_h + p_{h'})^2$ for the whole hadronic event,

$$\hat{s} = (x_a + x_b)^2 E^2 - (x_a - x_b)^2 E^2 = 4x_a x_b E^2 = s x_a x_b. \quad (9.4.35)$$

Here s is determined by the collider [(1960 GeV)² at the Tevatron and (13 TeV)² presently at the LHC], while \hat{s} is different for each event. Now, to find the total cross-section to produce the final state X in h, h' collisions, we should multiply the partonic cross-section by the probabilities of finding in h a parton a with momentum fraction in the range x_a to $x_a + dx_a$ and the same probability for parton b in h' ; then integrate over all possible x_a and x_b , and then sum over all the different parton species a and b . The result is:

$$d\sigma(hh' \rightarrow X) = \sum_{a,b} \int_0^1 dx_a \int_0^1 dx_b d\hat{\sigma}(ab \rightarrow X) f_a^h(x_a) f_b^{h'}(x_b). \quad (9.4.36)$$

This integration is done by computer, using PDFs with Q chosen equal to some energy characteristic of the event. The partonic differential cross-section $d\hat{\sigma}(ab \rightarrow X)$ depends on the momentum fractions x_a and x_b through $p_a^\mu = x_a p_h^\mu$ and $p_b^\mu = x_b p_{h'}^\mu$, with p_h^μ and $p_{h'}^\mu$ controlled or known by the experimenter.

9.5 Top-antitop production in $p\bar{p}$ and pp collisions

As an example, let us consider top-antitop production, first at the Tevatron. The parton-level processes that can contribute to this are, with the first parton taken to be from the proton and the second from the antiproton:

$$u\bar{u} \rightarrow t\bar{t}, \quad d\bar{d} \rightarrow t\bar{t}, \quad gg \rightarrow t\bar{t}, \quad \bar{d}d \rightarrow t\bar{t}, \quad \bar{u}u \rightarrow t\bar{t}, \quad s\bar{s} \rightarrow t\bar{t}, \quad \bar{s}s \rightarrow t\bar{t}. \quad (9.5.1)$$

These are listed in the order of their numerical importance in contributing to the total cross-section for $t\bar{t}$ at the Tevatron. Notice that the most likely thing is to find a quark in the proton and an antiquark in the anti-proton, but there is also a small but non-zero probability of finding an anti-quark in the proton, and a quark in the anti-proton. All of the processes involving quark and antiquark in the initial state involve the same parton-level cross-section

$$\frac{d\hat{\sigma}(q\bar{q} \rightarrow t\bar{t})}{d\hat{t}}. \quad (9.5.2)$$

The gluon-gluon process has a partonic cross-section that is somewhat more difficult to obtain:

$$\begin{aligned} \frac{d\hat{\sigma}(gg \rightarrow t\bar{t})}{d\hat{t}} = & \frac{\pi\alpha_s^2}{8\hat{s}^2} \left[\frac{6(m^2 - \hat{t})(m^2 - \hat{u})}{\hat{s}^2} - \frac{m^2(\hat{s} - 4m^2)}{3(m^2 - \hat{t})(m^2 - \hat{u})} \right. \\ & + \frac{4[(m^2 - \hat{t})(m^2 - \hat{u}) - 2m^2(m^2 + \hat{t})]}{3(m^2 - \hat{t})^2} + \frac{4[(m^2 - \hat{t})(m^2 - \hat{u}) - 2m^2(m^2 + \hat{u})]}{3(m^2 - \hat{u})^2} \\ & \left. - \frac{3[(m^2 - \hat{t})(m^2 - \hat{u}) + m^2(\hat{u} - \hat{t})]}{\hat{s}(m^2 - \hat{t})} - \frac{3[(m^2 - \hat{t})(m^2 - \hat{u}) + m^2(\hat{t} - \hat{u})]}{\hat{s}(m^2 - \hat{u})} \right], \end{aligned} \quad (9.5.3)$$

where m is the mass of the top quark. Even these leading-order partonic differential cross-sections depend implicitly on the renormalization scale μ , through the renormalized coupling $\alpha_s(\mu)$.

In order to find the total cross-section, one can first integrate the partonic cross-sections with respect to \hat{t} ; this is equivalent to integrating over the final-state top quark angle $\hat{\theta}$ in the partonic COM frame, since they are related linearly by

$$\hat{t} = m_t^2 + \frac{\hat{s}}{2} \left(-1 + \cos \hat{\theta} \sqrt{1 - 4m_t^2/\hat{s}} \right). \quad (9.5.4)$$

Therefore, for each partonic process one has

$$\hat{\sigma} = \int_{\hat{t}_{\min}}^{\hat{t}_{\max}} \frac{d\hat{\sigma}}{d\hat{t}} d\hat{t}, \quad (9.5.5)$$

where

$$\hat{t}_{\max, \min} = m_t^2 + \frac{\hat{s}}{2} \left(-1 \pm \sqrt{1 - 4m_t^2/\hat{s}} \right). \quad (9.5.6)$$

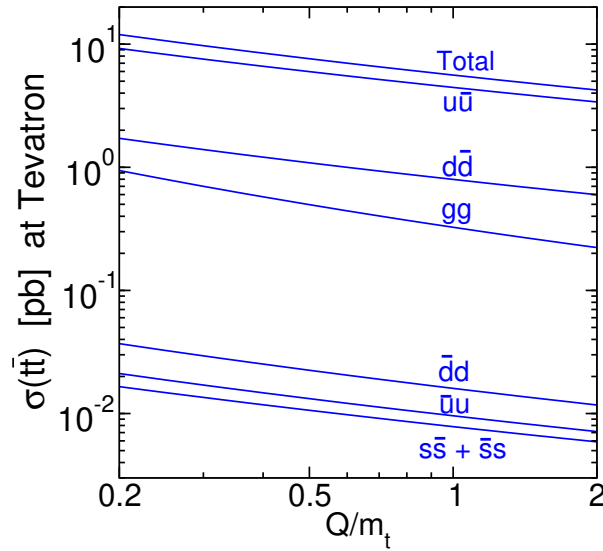
It is also useful to note that eq. (9.4.35) implies

$$x_b = \frac{\hat{s}}{x_a s}; \quad dx_b = \frac{d\hat{s}}{x_a s}. \quad (9.5.7)$$

So instead of integrating over x_b , we can integrate over \hat{s} . The limits of integration on \hat{s} are from $\hat{s}_{\min} = 4m_t^2$ (the minimum required to make a top-antitop pair) to $\hat{s}_{\max} = s$ (the maximum available from the proton and antiproton, corresponding to $x_a = x_b = 1$). For a given \hat{s} , the range of x_a is from \hat{s}/s to 1. Relabeling x_a as just x , we therefore have:

$$\begin{aligned} \sigma(p\bar{p} \rightarrow t\bar{t}) = & \int_{4m_t^2}^s d\hat{s} \int_{\hat{s}/s}^1 dx \frac{1}{xs} \left\{ \hat{\sigma}(q\bar{q} \rightarrow t\bar{t}) \left[u(x)u(\hat{s}/xs) + d(x)d(\hat{s}/xs) + \bar{u}(x)\bar{u}(\hat{s}/xs) \right. \right. \\ & \left. \left. + \bar{d}(x)\bar{d}(\hat{s}/xs) + 2s(x)s(\hat{s}/xs) \right] + \hat{\sigma}(gg \rightarrow t\bar{t})g(x)g(\hat{s}/xs) \right\}. \end{aligned} \quad (9.5.8)$$

Using the CTEQ5L PDFs and $m_t = 173$ GeV, with $\sqrt{s} = 1960$ GeV, and computing $\alpha_s(\mu)$ using eq. (9.3.26) starting from $\alpha_s(m_t) = 0.1082$, and working with the leading-order partonic cross-sections, the results as a function of the common factorization and renormalization scale $Q = \mu$ look like:



Unfortunately, the accuracy of the above results, obtained with only leading order partonic cross-sections and PDFs, is clearly not very high. Ideally, the lines should be flat, but there is instead a strong dependence of the leading-order prediction on $Q = \mu$. The higher-order corrections to the quark-antiquark processes turn out to be of order 10 to 20%, while the gluon-gluon process gets about a 70% correction from its leading-order value at $Q = \mu = m_t$. Accurate comparisons with experiment require a much more detailed and sophisticated treatment of the higher-order effects, including at least a next-to-leading order calculation of the partonic cross-sections. Still, some useful information can be gleaned. Experience has shown that evaluating the leading-order result at $Q \sim m_t/2$ gives a decent estimate of the total cross-section, although a principled justification for this scale choice is hard to make. Also, the relative sizes of the parton-level contributions can be understood qualitatively from the PDFs as follows. To produce a top-antitop pair, we must have $\hat{s} > 4m_t^2$, so according to eq. (9.4.35),

$$x_a x_b > 4m_t^2/s = 4(173)^2/(1960)^2 = 0.0312. \quad (9.5.9)$$

So at least one of the momentum fraction x 's must be larger than 0.1765 for $m_t = 173$ GeV. This means that the largest contributions come from the valence quarks. Since there are roughly twice as many valence up quarks as down quarks in the proton for a given x , and twice as many antiups as antidowns in the antiproton, the ratio of top-antitop events produced from up-antiup should be about 4 times that from down-antidown. The gluon-gluon contribution is suppressed in this case because most of the gluons are at small x and do not have enough energy to make a top-antitop pair. Finally, the contributions from sea partons ($\bar{u}, \bar{d}, s, \bar{s}$ in the proton, and u, d, s, \bar{s} in the antiproton) are highly suppressed for the same reason.

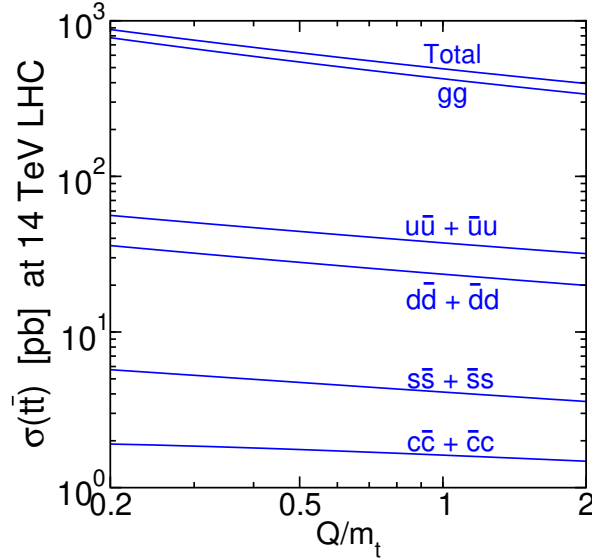
Let us now consider $t\bar{t}$ production for the Large Hadron Collider, a pp collider, by taking into account the larger \sqrt{s} and the different parton distribution function roles. Since both of

the initial-state hadrons are protons, the formula for the total cross-section is now:

$$\begin{aligned} \sigma(pp \rightarrow t\bar{t}) = & \int_{4m_t^2}^s d\hat{s} \int_{\hat{s}/s}^1 dx \frac{1}{xs} \left\{ \hat{\sigma}(q\bar{q} \rightarrow t\bar{t}) \left[2u(x)\bar{u}(\hat{s}/xs) + 2d(x)\bar{d}(\hat{s}/xs) + 2s(x)\bar{s}(\hat{s}/xs) \right] \right. \\ & \left. + \hat{\sigma}(gg \rightarrow t\bar{t}) g(x)g(\hat{s}/xs) \right\}. \end{aligned} \quad (9.5.10)$$

The factors of 2 are present because each proton can contribute either the quark, or the antiquark; then the contribution of the other proton is fixed. The gluon-gluon contribution has the same form as in $p\bar{p}$ collisions, because the gluon distribution is identical in protons and in antiprotons.

Numerically integrating the above formula with a computer using the CTEQ5L PDFs, one finds the leading order results shown below, as a function of the common factorization and renormalization scale $Q = \mu$, for the case of $\sqrt{s} = 14$ TeV:



Again these leading-order results are highly dependent on $Q = \mu$, and subject to large corrections at next-to-leading order and beyond. The most striking feature of the LHC result is that in contrast to the Tevatron situation, the gluon-gluon partonic contribution is dominant over the quark-antiquark contributions for the LHC. This is partly because all of the quark-antiquark contributions now require a sea antiquark PDF, but that is not the main reason. The really important effect is that at very high energies like at the LHC, the top quark can be considered light (!) and so one can make them using partons with much lower x . For example, with $\sqrt{s} = 14$ TeV, the kinematic constraint on the longitudinal momentum fractions becomes

$$x_a x_b > 4(173)^2 / (14000)^2 = 0.000611, \quad (9.5.11)$$

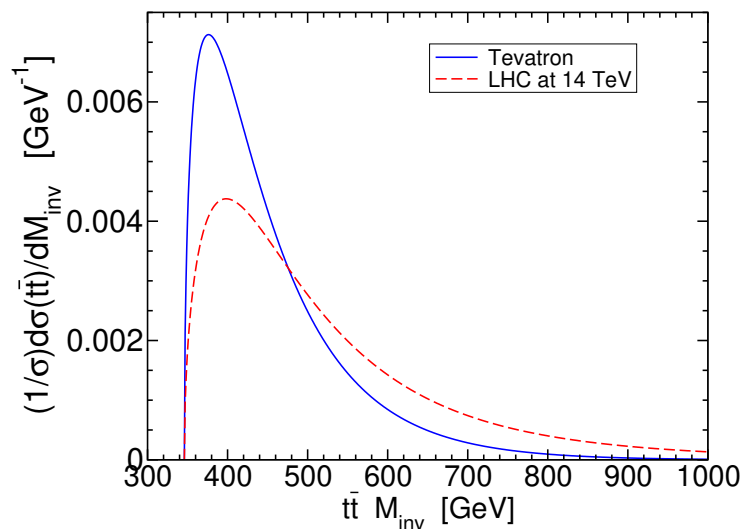
so that now the smaller one can be as low as 0.0247. At low x , we saw above that the gluon distribution function is very large; one has plenty of gluons available with less than 1/10 of the

protons' total energy, and they dominate over the quark and antiquark PDFs. This is actually a common feature, and is why you sometimes hear people somewhat whimsically call the LHC a “gluon collider”; with so much energy available for the protons, many processes are dominated by the large gluon PDF at low x . There are some processes that do not rely on gluons at all, however. We will see one example in subsection 9.7. Those processes are dominated by sea quarks at the LHC. Also, many processes get a large contribution from gluon-squark scattering as well, for example gluon-squark production in supersymmetry.

One can also look at the distribution of $t\bar{t}$ production as a function of the total invariant mass $M_{\text{inv}} = \sqrt{\hat{s}}$ of the hard scattering process, by leaving the \hat{s} integration in eqs. (9.5.8) and (9.5.10) unperformed. The resulting shape of the distribution normalized by the total cross-section,

$$\frac{1}{\sigma(t\bar{t})} \frac{d\sigma(t\bar{t})}{dM_{\text{inv}}} = \frac{2\sqrt{s}}{\sigma(t\bar{t})} \frac{d\sigma(t\bar{t})}{d\hat{s}}, \quad (9.5.12)$$

is shown below for the Tevatron and the LHC with $\sqrt{s} = 14$ TeV:



The invariant mass distribution of the $t\bar{t}$ system is peaked not far above $2m_t$ in both cases, indicating that the top and antitop usually have only semi-relativistic velocities. This is because the PDFs fall rapidly with increasing x , so the most important contributions to the production cross-section occur when both x 's are not very far above their minimum allowed values. At the LHC, the top and antitop are likelier to be produced with higher energy than at the Tevatron, with a more substantial tail at high mass.

9.6 Kinematics in hadron-hadron scattering

Let us now consider the general problem of kinematics associated with hadron-hadron collisions with underlying $2 \rightarrow 2$ parton scattering. To make things simple, we will suppose all of the

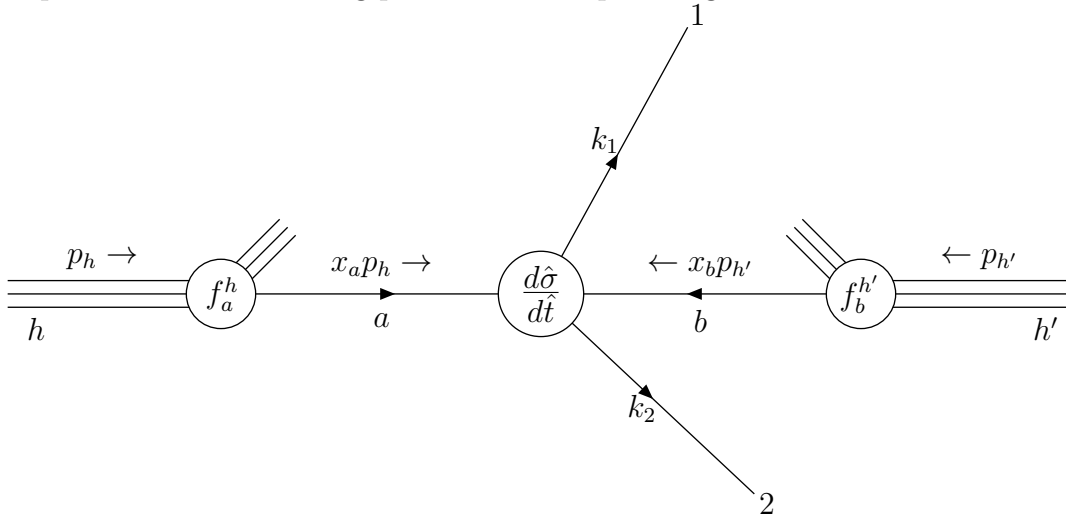
particles are essentially massless, so what we are about to do does not work for $t\bar{t}$ in the final state (but could be generalized to do so). After doing a sum/average over spins, colors, and any other unobserved degrees of freedom, we should be able to compute the differential cross-section for the partonic event from its Feynman diagrams as:

$$\frac{d\hat{\sigma}(ab \rightarrow 12)}{d\hat{t}}. \quad (9.6.1)$$

As we learned in subsection 9.4, we can then write:

$$d\sigma(hh' \rightarrow 12 + X) = \sum_{a,b} f_a^h(x_a) f_b^{h'}(x_b) \frac{d\hat{\sigma}(ab \rightarrow 12)}{d\hat{t}} d\hat{t} dx_a dx_b. \quad (9.6.2)$$

A cartoon picture of the scattering process in real space might look like:



There are several different ways to choose the kinematic variables describing the final state. There are three significant degrees of freedom: two angles at which the final-state particles emerge with respect to the collision axis, and one overall momentum scale. (Once the magnitude of the momentum transverse to the beam for one particle is specified, the other is determined.) The angular dependence about the collision axis is trivial, so we can ignore it.

For example, we can use the following three variables: momentum of particle 1 transverse to the collision axis, p_T ; the total center-of-momentum energy of the final state partons, $\sqrt{\hat{s}}$; and the longitudinal rapidity of the two-parton system in the lab frame, defined by

$$Y = \frac{1}{2} \ln(x_a/x_b). \quad (9.6.3)$$

This may look like an obscure definition, but it is the rapidity (see section 2) needed to boost along the collision axis to get to the center-of-momentum frame for the two-parton system. It is equal to 0 if the final-state particles are back-to-back, which would occur in the special case

that the initial-state partons have the same energy in the lab frame. Instead of the variables (x_a, x_b, \hat{t}) , we can use the more directly observable variables (\hat{s}, p_T^2, Y) , or perhaps some subset of these with the others integrated over. Working in the center-of-momentum frame of the partons, we can write:

$$p_a^\mu = (\hat{E}, 0, 0, \hat{E}), \quad (9.6.4)$$

$$p_b^\mu = (\hat{E}, 0, 0, -\hat{E}), \quad (9.6.5)$$

$$k_1^\mu = (\hat{E}, 0, p_T, \sqrt{\hat{E}^2 - p_T^2}), \quad (9.6.6)$$

$$k_2^\mu = (\hat{E}, 0, -p_T, -\sqrt{\hat{E}^2 - p_T^2}), \quad (9.6.7)$$

with

$$\hat{s} = 4\hat{E}^2 = x_a x_b s, \quad (9.6.8)$$

from which it follows that

$$\hat{t} = (p_a - k_1)^2 = \frac{\hat{s}}{2} \left(1 + \sqrt{1 - 4p_T^2/\hat{s}} \right), \quad (9.6.9)$$

$$\hat{u} = (p_a - k_2)^2 = \frac{\hat{s}}{2} \left(1 - \sqrt{1 - 4p_T^2/\hat{s}} \right), \quad (9.6.10)$$

and so

$$p_T^2 = \frac{\hat{t}\hat{u}}{\hat{s}} = -\frac{\hat{t}(sx_a x_b + \hat{t})}{sx_a x_b}, \quad (9.6.11)$$

where the last equality uses $\hat{u} = -\hat{s} - \hat{t} = -sx_a x_b - \hat{t}$ for massless particles. Making the change of variables (x_a, x_b, \hat{t}) to (\hat{s}, p_T^2, Y) for a differential cross-section requires

$$d\hat{t} dx_a dx_b = J d\hat{s} d(p_T^2) dY, \quad (9.6.12)$$

where J is the determinant of the Jacobian matrix of the transformation. Evaluating it, by taking the inverse of the determinant of its inverse, one finds:

$$J = \left| \frac{\partial(\hat{s}, p_T^2, Y)}{\partial(\hat{t}, x_a, x_b)} \right|^{-1} = \frac{x_a x_b}{\hat{s} + 2\hat{t}}. \quad (9.6.13)$$

Therefore, eq. (9.6.2) becomes:

$$\frac{d\sigma(hh' \rightarrow 12 + X)}{d\hat{s} d(p_T^2) dY} = \frac{x_a x_b}{\hat{s} + 2\hat{t}} \sum_{a,b} f_a^h(x_a) f_b^{h'}(x_b) \frac{d\hat{\sigma}(ab \rightarrow 12)}{d\hat{t}}, \quad (9.6.14)$$

where the variables x_a, x_b, \hat{t} on the right-hand side are understood to be determined in terms of \hat{s}, p_T^2 and Y by eqs. (9.6.8), (9.6.11), and (9.6.3).

9.7 Drell-Yan scattering ($\ell^+\ell^-$ production in hadron collisions)

As an example, let us consider the process of Drell-Yan scattering, which is the production of lepton pairs in hadron-hadron collisions through a virtual photon:

$$hh' \rightarrow \ell^+\ell^-. \quad (9.7.1)$$

This does not involve QCD as the hard partonic scattering, since the leptons $\ell = e, \mu$, or τ are singlets under $SU(3)_c$ color. However, it still depends on QCD, because to evaluate it we need to know the PDFs for the quarks inside the hadrons. Since gluons have no electric charge and do not couple to photons, the underlying partonic process is always:

$$q\bar{q} \rightarrow \ell^+\ell^-. \quad (9.7.2)$$

with the q coming from either h or h' . The cross-section for this, for $\sqrt{s} \ll m_Z$ and not near a resonance, can be obtained by exactly the same methods as in 5.2.1 for $e^+e^- \rightarrow \mu^+\mu^-$; we just need to remember to use the charge of the quark Q_q instead of the charge of the electron, and to average over initial-state colors. The latter effect leads to a suppression of $1/3$; there is no reaction if the colors do not match. One finds that the differential partonic cross-section is:

$$\frac{d\hat{\sigma}(q\bar{q} \rightarrow \ell^+\ell^-)}{d\hat{t}} = \frac{2\pi\alpha^2 Q_q^2 (\hat{t}^2 + \hat{u}^2)}{3\hat{s}^4}. \quad (9.7.3)$$

Therefore, using $\hat{u} = -\hat{s} - \hat{t}$ for massless scattering, and writing separate contributions from finding the quark, and the antiquark, in h :

$$\frac{d\sigma(hh' \rightarrow \ell^+\ell^-)}{d\hat{s} dp_T^2 dY} = \frac{2\pi\alpha^2}{3} \frac{\hat{t}^2 + (\hat{s} + \hat{t})^2}{\hat{s}^4(\hat{s} + 2\hat{t})} x_a x_b \sum_q Q_q^2 \left[f_q^h(x_a) f_{\bar{q}}^{h'}(x_b) + f_{\bar{q}}^h(x_a) f_q^{h'}(x_b) \right]. \quad (9.7.4)$$

This can be used to make a prediction for the experimental distribution of events with respect to each of \hat{s} , p_T , and Y .

Alternatively, we can choose to integrate the partonic differential cross-section with respect to \hat{t} first. Since \hat{t} determines the scattering angle with respect to the collision axis, this will eliminate the integration over p_T^2 . The total partonic cross-section obtained by integrating eq. (9.7.3) is:

$$\hat{\sigma}(q\bar{q} \rightarrow \ell^+\ell^-) = \frac{4\pi\alpha^2 Q_q^2}{9\hat{s}}. \quad (9.7.5)$$

Therefore we get:

$$d\sigma(hh' \rightarrow \ell^+\ell^-) = dx_a dx_b \frac{4\pi\alpha^2}{9\hat{s}} \sum_q Q_q^2 \left[f_q^h(x_a) f_{\bar{q}}^{h'}(x_b) + f_{\bar{q}}^h(x_a) f_q^{h'}(x_b) \right]. \quad (9.7.6)$$

Now making the change of variables from (x_a, x_b) to (\hat{s}, Y) requires:

$$dx_a dx_b = \left| \frac{\partial(\hat{s}, Y)}{\partial(x_a, x_b)} \right|^{-1} d\hat{s} dY = \frac{d\hat{s} dY}{s}, \quad (9.7.7)$$

we therefore have:

$$\frac{d\sigma(hh' \rightarrow \ell^+ \ell^-)}{d\hat{s} dY} = \frac{4\pi\alpha^2}{9s\hat{s}} \sum_q Q_q^2 \left[f_q^h(x_a) f_q^{h'}(x_b) + f_q^h(x_a) f_q^{h'}(x_b) \right]. \quad (9.7.8)$$

Still another way to present the result is to leave only \hat{s} unintegrated, by again first integrating the partonic differential cross-section with respect to \hat{t} , and then trading one of the Feynman- x variables for \hat{s} , and do the remaining x -integration. This is how we wrote the top-antitop total cross-section. The Jacobian factor in the change of variables from $(x_a, x_b) \rightarrow (x_a, \hat{s})$ is now:

$$dx_a dx_b = \left| \frac{\partial\hat{s}}{\partial x_b} \right|^{-1} dx_a d\hat{s} = \frac{dx_a d\hat{s}}{x_a s}. \quad (9.7.9)$$

Using this in eq. (9.7.6) now gives, after replacing x_a by x and integrating:

$$\frac{d\sigma(hh' \rightarrow \ell^+ \ell^-)}{d\hat{s}} = \frac{4\pi\alpha^2}{9\hat{s}^2} \sum_q Q_q^2 \int_{\hat{s}/s}^1 dx \frac{\hat{s}}{xs} \left[f_q^h(x) f_q^{h'}(\hat{s}/xs) + f_q^h(x) f_q^{h'}(\hat{s}/xs) \right]. \quad (9.7.10)$$

This version makes a nice prediction that is (almost) independent of the actual parton distribution functions. The right-hand side could have depended on both \hat{s} and s in an arbitrary way, but to the extent that the PDFs are independent of Q , we see that it is predicted to scale like $1/\hat{s}^2$ times some function of the ratio \hat{s}/s . Since the PDFs run slowly with Q , this is a reasonably good prediction. Drell-Yan scattering has been studied in $hh' = p\bar{p}$, pp , $\pi^\pm p$, and $K^\pm p$ scattering experiments, and in each case the results indeed satisfy the scaling law:

$$\hat{s}^2 \frac{d\sigma(hh' \rightarrow \ell^+ \ell^-)}{d\hat{s}} = F_{hh'}(\hat{s}/s) \quad (9.7.11)$$

to a very good approximation, for low \hat{s} not near a resonance. Furthermore, the functions $F_{hh'}$ gives information about the PDFs.

Because of the relatively clean signals of muons in particle detectors, the Drell-Yan process

$$p\bar{p} \rightarrow \mu^- \mu^+ + X \quad \text{or} \quad pp \rightarrow \mu^- \mu^+ + X \quad (9.7.12)$$

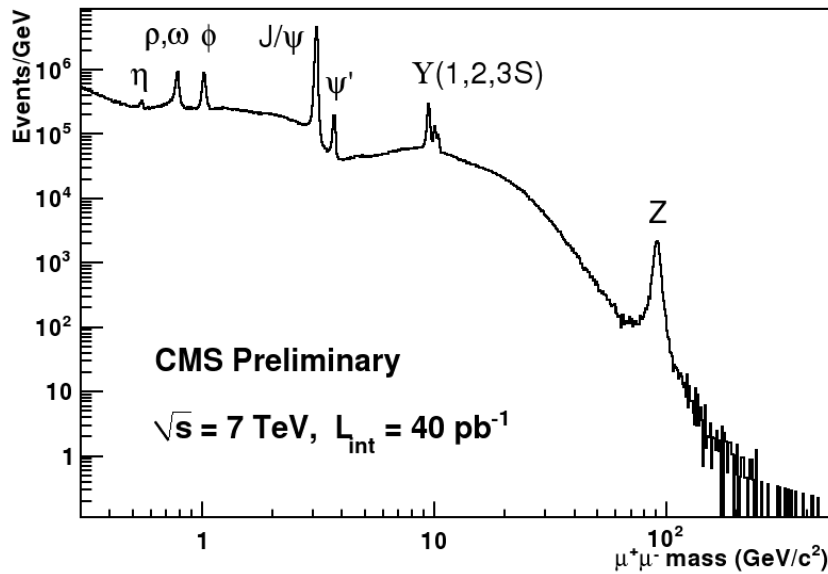
is often one of the first things one studies at a hadron collider to make sure everything is working correctly and understood. It also provides a test of the PDFs, especially at small x .

For larger \sqrt{s} , one must take into account the s -channel Feynman diagram with a Z boson in place of the virtual photon. The resulting cross-section can be obtained from eq. (9.7.10) by replacing

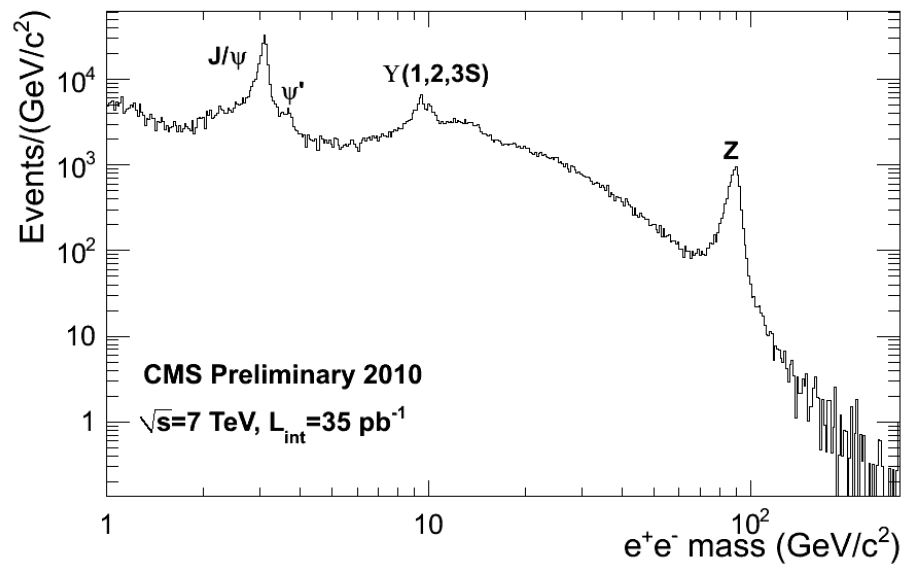
$$\frac{4\pi\alpha^2}{9\hat{s}^2} \sum_q Q_q^2 \rightarrow \frac{4\pi\alpha^2}{9} \sum_q \left[\frac{Q_q^2}{\hat{s}^2} + \frac{(V_q^2 + A_q^2)(V_\ell^2 + A_\ell^2)}{(\hat{s} - m_Z^2)^2 + m_Z^2 \Gamma_Z^2} - \frac{2Q_q V_q V_\ell (1 - m_Z^2/\hat{s})}{(\hat{s} - m_Z^2)^2 + m_Z^2 \Gamma_Z^2} \right], \quad (9.7.13)$$

where V_f and A_f are coupling coefficients associated with the Z -fermion-antifermion interaction vertex, and will be specified explicitly at the end of section 11.1. The first term is from the virtual photon contribution to the matrix element, while the second comes from the virtual Z boson contribution, and features a Breit-Wigner resonance denominator from the Z boson propagator, which depends on the mass and width $m_Z = 91.188$ GeV and $\Gamma_Z = 2.495$ GeV. The last term is due to the interference between these two amplitudes.

At the end of 2010, the CMS and ATLAS LHC detector collaborations released their measurements of the $\mu^-\mu^+$ and e^-e^+ invariant mass distributions. The dimuon plot from CMS is shown below:



Clearly visible are the effects of the η , ρ , ω , ϕ , J/ψ , ψ' , and Υ 1S, 2S, and 3S meson resonances, the Z boson resonance, and the general decrease of the cross-section with $\sqrt{\hat{s}}$ (the invariant mass of the final state). The distribution includes the effects of the intrinsic widths of the resonances as well as detector resolution effects and trigger and detector efficiencies. A similar plot is shown below for the e^-e^+ final state. Note that the detector resolution and the trigger efficiency are evidently worse for electrons than for muons.



10 Spontaneous Symmetry Breaking

10.1 Global symmetry breaking

Not all of the symmetries of the laws of physics are evident in the state that describes a physical system, or even in the vacuum state with no particles. For example, in condensed matter physics, the ground state of a ferromagnetic system involves a magnetization vector that points in some particular direction, even though Maxwell's equations in matter do not contain any special direction. This is because it is energetically favorable for the magnetic moments in the material to line up, rather than remaining randomized. The state with randomized magnetic moments is unstable to small perturbations, like a stick balanced on one end, and will settle in the more energetically-favored magnetized state.

The situation in which the laws of physics are invariant under some symmetry transformations, but the vacuum state is not, is called spontaneous symmetry breaking. In this section we will study how this works in quantum field theory. There are two types of continuous symmetry transformations; global, in which the transformation does not depend on position in spacetime, and local (or gauge) in which the transformation can be different at each point. We will work out how spontaneous symmetry breaking works in each of these cases, using the example of a $U(1)$ symmetry, and then guess the generalizations to non-Abelian symmetries.

Consider a complex scalar field $\phi(x)$ with a Lagrangian density:

$$\mathcal{L} = \partial^\mu \phi^* \partial_\mu \phi - V(\phi, \phi^*), \quad (10.1.1)$$

with potential energy

$$V(\phi, \phi^*) = m^2 \phi^* \phi + \lambda (\phi^* \phi)^2, \quad (10.1.2)$$

where m^2 and λ are parameters of the theory. This Lagrangian is invariant under the global $U(1)$ transformations:

$$\phi(x) \rightarrow \phi'(x) = e^{i\alpha} \phi(x) \quad (10.1.3)$$

where α is any constant. The classical equations of motion for ϕ and ϕ^* following from \mathcal{L} are [see eq. (4.1.25)]:

$$\partial^\mu \partial_\mu \phi + \frac{\delta V}{\delta \phi^*} = 0, \quad (10.1.4)$$

$$\partial^\mu \partial_\mu \phi^* + \frac{\delta V}{\delta \phi} = 0. \quad (10.1.5)$$

Clearly, there is a solution with $\partial_\mu \phi = \partial_\mu \phi^* = 0$, where $\phi(x)$ is just equal to any constant that minimizes the potential.

If $m^2 > 0$ and $\lambda > 0$, then the minimum of the potential is at $\phi = 0$. The quantum mechanical counterpart of this statement is that the ground state of the system will be one in which the expectation value of $\phi(x)$ vanishes:

$$\langle 0 | \phi(x) | 0 \rangle = 0. \quad (10.1.6)$$

The scalar particles created and destroyed by the field $\phi(x)$ correspond to quantized oscillations of $\phi(x)$ about the minimum of the potential. They have squared mass equal to m^2 , and interact with a four-scalar vertex proportional to λ .

Let us now consider what happens if the signs of the parameters m^2 and λ are different. If $\lambda < 0$, then the potential $V(\phi, \phi^*)$ is unbounded from below for arbitrarily large $|\phi|$. This cannot lead to an acceptable theory. Classically there would be runaway solutions in which $|\phi(x)| \rightarrow \infty$, gaining an infinite amount of kinetic energy. The quantum mechanical counterpart of this statement is that the expectation value of $\phi(x)$ will grow without bound.

However, there is nothing wrong with the theory if $m^2 < 0$ and $\lambda > 0$. (One should think of m^2 as simply a parameter that appears in the Lagrangian density, and not as the square of some mythical real number m .) In that case, the potential $V(\phi, \phi^*)$ has a “Mexican hat” shape, with a local maximum at $\phi = 0$, and a degenerate set of minima with

$$|\phi_{\min}|^2 = \frac{v^2}{2}, \quad (10.1.7)$$

where we have defined:

$$v = \sqrt{-m^2/\lambda}. \quad (10.1.8)$$

The potential V does not depend on the phase of $\phi(x)$ at all, so it is impossible to unambiguously determine the phase of $\phi(x)$ at the minimum. However, by an arbitrary choice, we can make $\text{Im}(\phi_{\min}) = 0$. In quantum mechanics, the system will have a ground state in which the expectation value of $\phi(x)$ is constant and equal to the classical minimum:

$$\langle 0 | \phi(x) | 0 \rangle = \frac{v}{\sqrt{2}}. \quad (10.1.9)$$

The quantity v is a measurable property of the vacuum state, known as the vacuum expectation value, or VEV, of $\phi(x)$. If we now ask what the VEV of ϕ is after performing a $U(1)$ transformation of the form eq. (10.1.3), we find:

$$\langle 0 | \phi'(x) | 0 \rangle = e^{i\alpha} \langle 0 | \phi(x) | 0 \rangle = e^{i\alpha} \frac{v}{\sqrt{2}} \neq \frac{v}{\sqrt{2}}. \quad (10.1.10)$$

The VEV is not invariant under the $U(1)$ symmetry operation acting on the fields of the theory; this reflects the fact that we had to make an arbitrary choice of phase. One cannot restore the

invariance by defining the symmetry operation to also multiply $|0\rangle$ by a phase, since $\langle 0|$ will rotate by the opposite phase, canceling out of eq. (10.1.10). Therefore, the vacuum state must not be invariant under the global $U(1)$ symmetry rotation, and the symmetry is spontaneously broken. The sign of the parameter m^2 is what determines whether or not spontaneous symmetry breaking takes place in the theory.

In order to further understand the behavior of this theory, it is convenient to rewrite the scalar field in terms of its deviation from its VEV. One way to do this is to write:

$$\phi(x) = \frac{1}{\sqrt{2}}[v + R(x) + iI(x)], \quad (10.1.11)$$

$$\phi^*(x) = \frac{1}{\sqrt{2}}[v + R(x) - iI(x)], \quad (10.1.12)$$

where R and I are each real scalar fields, representing the real and imaginary parts of ϕ . The derivative part of the Lagrangian can now be rewritten in terms of R and I , as:

$$\mathcal{L} = \frac{1}{2}\partial^\mu R\partial_\mu R + \frac{1}{2}\partial^\mu I\partial_\mu I. \quad (10.1.13)$$

The potential appearing in the Lagrangian can be found in terms of R and I most easily by noticing that it can be rewritten as

$$V(\phi, \phi^*) = \lambda(\phi^*\phi - v^2/2)^2 - \lambda v^4/4. \quad (10.1.14)$$

Dropping the last term that does not depend on the fields, and plugging in eqs. (10.1.11) and (10.1.12), this becomes:

$$V(R, I) = \frac{\lambda}{4}[(v + R)^2 + I^2 - v^2]^2 \quad (10.1.15)$$

$$= \lambda v^2 R^2 + \lambda v R(R^2 + I^2) + \frac{\lambda}{4}(R^2 + I^2)^2. \quad (10.1.16)$$

Comparing this expression with our previous discussion of real scalar fields in chapter 4, we can interpret the terms proportional to λv as RRR and RII interaction vertices, and the last term proportional to λ as $RRRR$, $RRII$, and $IIII$ interaction vertices. The first term proportional to λv^2 is a mass term for R , but there is no term quadratic in I , so it corresponds to a massless real scalar particle. Comparing to the Klein-Gordon Lagrangian density of eq. (4.1.18), we can identify the physical particle masses:

$$m_R^2 = 2\lambda v^2 = -2m^2, \quad (10.1.17)$$

$$m_I^2 = 0. \quad (10.1.18)$$

It is useful to redo this analysis in a slightly different way, by writing

$$\phi(x) = \frac{1}{\sqrt{2}}[v + h(x)]e^{iG(x)/v}, \quad (10.1.19)$$

$$\phi^*(x) = \frac{1}{\sqrt{2}}[v + h(x)]e^{-iG(x)/v}, \quad (10.1.20)$$

instead of eqs. (10.1.11), (10.1.12). Again $h(x)$ and $G(x)$ are two real scalar fields, related to $R(x)$ and $I(x)$ by a non-linear functional transformation. In terms of these fields, the potential is:

$$V(h) = \lambda v^2 h^2 + \lambda v h^3 + \frac{\lambda}{4} h^4. \quad (10.1.21)$$

Notice that the field G does not appear in V at all. This is because G just corresponds to the phase of ϕ , and the potential was chosen to be invariant under $U(1)$ phase transformations. However, G does have interactions coming from the part of the Lagrangian density containing derivatives. To find the derivative part of the Lagrangian, we compute:

$$\partial_\mu \phi = \frac{1}{\sqrt{2}} e^{iG/v} \left[\partial_\mu h + \frac{i(v+h)}{v} \partial_\mu G \right], \quad (10.1.22)$$

$$\partial_\mu \phi^* = \frac{1}{\sqrt{2}} e^{-iG/v} \left[\partial_\mu h - \frac{i(v+h)}{v} \partial_\mu G \right], \quad (10.1.23)$$

so that:

$$\mathcal{L}_{\text{derivatives}} = \frac{1}{2} \partial^\mu h \partial_\mu h + \frac{1}{2} \left(1 + \frac{h}{v} \right)^2 \partial^\mu G \partial_\mu G. \quad (10.1.24)$$

The quadratic part of the Lagrangian, which determines the propagators for h and G , is

$$\mathcal{L}_{\text{quadratic}} = \frac{1}{2} \partial^\mu h \partial_\mu h - \frac{1}{2} m_h^2 h^2 + \frac{1}{2} \partial^\mu G \partial_\mu G, \quad (10.1.25)$$

with

$$m_h^2 = 2\lambda v^2, \quad (10.1.26)$$

$$m_G^2 = 0. \quad (10.1.27)$$

This confirms the previous result that the spectrum of particles consists of a massive real scalar (h) and a massless one (G). The interaction part of the Lagrangian following from eqs. (10.1.21) and (10.1.24) is:

$$\mathcal{L}_{\text{int}} = \left(\frac{1}{v} h + \frac{1}{2v^2} h^2 \right) \partial^\mu G \partial_\mu G - \lambda v h^3 - \frac{\lambda}{4} h^4. \quad (10.1.28)$$

The field and particle represented by G is known as a Nambu-Goldstone boson (or sometimes just a Goldstone boson). The original $U(1)$ symmetry acts on G by shifting it by a constant that depends on the VEV:

$$G \rightarrow G' = G + \alpha v; \quad (10.1.29)$$

$$h \rightarrow h' = h. \quad (10.1.30)$$

This explains why G only appears in the Lagrangian with derivatives acting on it. In general, a broken global symmetry is always signaled by the presence of a massless Nambu-Goldstone boson with only derivative interactions. This is an example of Goldstone's theorem, which we will state in a more general framework in subsection 10.3.

10.2 Local symmetry breaking and the Higgs mechanism

Let us now consider how things change if the spontaneously broken symmetry is local, or gauged. As a simple example, consider a $U(1)$ gauge theory with a fermion ψ with charge Q and gauge coupling g and a vector field A^μ transforming according to:

$$\psi(x) \rightarrow e^{iQ\theta(x)}\psi(x), \quad (10.2.1)$$

$$\bar{\psi}(x) \rightarrow e^{-iQ\theta(x)}\bar{\psi}(x), \quad (10.2.2)$$

$$A_\mu(x) \rightarrow A_\mu(x) - \frac{1}{g}\partial_\mu\theta(x). \quad (10.2.3)$$

In order to make a gauge-invariant Lagrangian density, the ordinary derivative is replaced by the covariant derivative:

$$D_\mu\psi = (\partial_\mu + iQgA_\mu)\psi. \quad (10.2.4)$$

Now, in order to spontaneously break the gauge symmetry, we introduce a complex scalar field ϕ with charge $+1$. It transforms under a gauge transformation like

$$\phi(x) \rightarrow e^{i\theta(x)}\phi(x); \quad \phi^*(x) \rightarrow e^{-i\theta(x)}\phi^*(x). \quad (10.2.5)$$

To make a gauge-invariant Lagrangian, we again replace the ordinary derivative acting on ϕ, ϕ^* by covariant derivatives:

$$D_\mu\phi = (\partial_\mu + igA_\mu)\phi; \quad D_\mu\phi^* = (\partial_\mu - igA_\mu)\phi^*. \quad (10.2.6)$$

The Lagrangian density for the scalar and vector degrees of freedom of the theory is:

$$\mathcal{L} = D_\mu\phi^*D^\mu\phi - V(\phi, \phi^*) - \frac{1}{4}F^{\mu\nu}F_{\mu\nu}, \quad (10.2.7)$$

where $V(\phi, \phi^*)$ is as given before in eq. (10.1.2). Because the covariant derivative of the field transforms like

$$D_\mu\phi \rightarrow e^{i\theta}D_\mu\phi, \quad (10.2.8)$$

this Lagrangian is easily checked to be gauge-invariant. If $m^2 > 0$ and $\lambda > 0$, then this theory describes a massive scalar, with self-interactions with a coupling proportional to λ , and interaction with the massless vector field A_μ .

However, if $m^2 < 0$, then the minimum of the potential for the scalar field brings about a non-zero VEV $\langle 0|\phi|0\rangle = v/\sqrt{2} = \sqrt{-m^2/2\lambda}$, just as in the global symmetry case. Using the same decomposition of ϕ into real fields h and G as given in eq. (10.1.19), one finds:

$$D_\mu\phi = \frac{1}{\sqrt{2}} \left[\partial_\mu h + ig(A_\mu + \frac{1}{gv}\partial_\mu G)(v + h) \right] e^{iG/v}. \quad (10.2.9)$$

It is convenient to define a new vector field:

$$V_\mu = A_\mu + \frac{1}{gv} \partial_\mu G, \quad (10.2.10)$$

since this is the combination that appears in eq. (10.2.9). Then

$$D_\mu \phi = \frac{1}{\sqrt{2}} [\partial_\mu h + igV_\mu(v + h)] e^{iG/v}, \quad (10.2.11)$$

$$D_\mu \phi^* = \frac{1}{\sqrt{2}} [\partial_\mu h - igV_\mu(v + h)] e^{-iG/v}. \quad (10.2.12)$$

Note also that since

$$\partial_\mu A_\nu - \partial_\nu A_\mu = \partial_\mu V_\nu - \partial_\nu V_\mu, \quad (10.2.13)$$

the vector field strength part of the Lagrangian is the same written in terms of the new vector V_μ as it was in terms of the old vector A_μ :

$$-\frac{1}{4} F^{\mu\nu} F_{\mu\nu} = -\frac{1}{4} (\partial_\mu V_\nu - \partial_\nu V_\mu) (\partial^\mu V^\nu - \partial^\nu V^\mu). \quad (10.2.14)$$

The complete Lagrangian density of the vector and scalar degrees of freedom is now:

$$\mathcal{L} = \frac{1}{2} [\partial^\mu h \partial_\mu h + g^2 (v + h)^2 V^\mu V_\mu] - \frac{1}{4} F^{\mu\nu} F_{\mu\nu} - \lambda (vh + h^2/2)^2. \quad (10.2.15)$$

This Lagrangian has the very important property that the field G has completely disappeared! Reading off the part quadratic in h , we see that it has the same squared mass as in the global symmetry case, namely

$$m_h^2 = 2\lambda v^2. \quad (10.2.16)$$

There is also a term quadratic in the vector field:

$$\mathcal{L}_{VV} = -\frac{1}{4} F^{\mu\nu} F_{\mu\nu} + \frac{g^2 v^2}{2} V^\mu V_\mu. \quad (10.2.17)$$

This means that by spontaneously breaking the gauge symmetry, we have given a mass to the corresponding vector field:

$$m_V^2 = g^2 v^2. \quad (10.2.18)$$

We can understand why the disappearance of the field G goes along with the appearance of the vector boson mass as follows. A massless spin-1 vector boson (like the photon) has only two possible polarization states, each transverse to its direction of motion. In contrast, a massive spin-1 vector boson has three possible polarization states; the two transverse, and one

longitudinal (parallel) to its direction of motion. The additional polarization state degree of freedom had to come from somewhere, so one real scalar degree of freedom had to disappear. The words used to describe this are that the vector boson becomes massive by “eating” the would-be Nambu-Goldstone boson G , which becomes its longitudinal polarization degree of freedom. This is called the Higgs mechanism. The original field $\phi(x)$ is called a Higgs field, and the surviving real scalar degree of freedom $h(x)$ is called by the generic term Higgs boson. The Standard Model Higgs boson and the masses of the W^\pm and Z bosons result from a slightly more complicated version of this same idea, as we will see.

An alternative way to understand what has just happened to the would-be Nambu-Goldstone boson field $G(x)$ is that it has been “gauged away”. Recall that

$$\phi = \frac{1}{\sqrt{2}}(v+h)e^{iG/v} \quad (10.2.19)$$

behaves under a gauge transformation as:

$$\phi \rightarrow e^{i\theta} \phi. \quad (10.2.20)$$

Normally we think of θ in this equation as just some ordinary function of spacetime, but since this is true for any θ , we can choose it to be proportional to the Nambu-Goldstone field itself:

$$\theta(x) = -G(x)/v. \quad (10.2.21)$$

This choice, known as “unitary gauge”, eliminates $G(x)$ completely, just as we saw in eq. (10.2.15). In unitary gauge,

$$\phi(x) = \frac{1}{\sqrt{2}}[v + h(x)]. \quad (10.2.22)$$

Notice also that the gauge transformation eq. (10.2.21) gives exactly the term in eq. (10.2.10), so that V_μ is simply the unitary gauge version of A_μ . The advantage of unitary gauge is that the true physical particle content of the theory (a massive vector and real Higgs scalar) is more obvious than in the version of the Lagrangian written in terms of the original fields ϕ and A_μ . However, it turns out to be easier to prove that the theory is renormalizable if one works in a different gauge in which the would-be Nambu-Goldstone bosons are retained. The physical predictions of the theory do not depend on which gauge one chooses, but the ease with which one can compute those results depends on picking the right gauge for the problem at hand.

Let us catalog the propagators and interactions of this theory, in unitary gauge. The propagators of the Higgs scalar and the massive vector are:

$$\begin{array}{c} \mu \\ \text{~~~~~} \nu \end{array} \longleftrightarrow \frac{i}{p^2 - m_V^2 + i\epsilon} \left[-g_{\mu\nu} + \frac{p_\mu p_\nu}{m_V^2} \right]$$

$$- - - - - \longleftrightarrow \frac{i}{p^2 - m_h^2 + i\epsilon}$$

From eq. (10.2.15), there are also hVV and $hhVV$ interaction vertices:

$$\begin{array}{ccc} \begin{array}{c} \mu \\ \diagup \\ - - - - - \\ \diagdown \\ \nu \end{array} & \longleftrightarrow & 2ig^2vg^{\mu\nu} \end{array} \qquad \begin{array}{ccc} \begin{array}{c} \mu \\ \diagup \\ - - - - - \\ \diagdown \\ \nu \end{array} & \longleftrightarrow & 2ig^2g^{\mu\nu} \end{array}$$

and hhh and $hhhh$ self-interactions:

$$\begin{array}{ccc} \begin{array}{c} \diagup \\ - - - - - \\ \diagdown \end{array} & \longleftrightarrow & -6i\lambda v \end{array} \qquad \begin{array}{ccc} \begin{array}{c} \diagup \\ - - - - - \\ \diagdown \end{array} & \longleftrightarrow & -6i\lambda \end{array}$$

Finally, a fermion with charge Q inherits the same interactions with V_μ that it had with A_μ , coming from the covariant derivative:

$$\begin{array}{ccc} \begin{array}{c} \mu \\ \diagup \\ \text{---} \\ \diagdown \end{array} & \longleftrightarrow & -iQg\gamma^\mu \end{array}$$

This is a general way of making massive vector fields in gauge theories with interacting scalars and fermions, without ruining renormalizability.

10.3 Goldstone's Theorem and the Higgs mechanism in general

Let us now state, without proof, how all of the considerations above generalize to arbitrary groups. First, suppose we have scalar fields ϕ_i in some representation of a global symmetry group with generators T_i^{aj} . There is some potential

$$V(\phi_i, \phi_i^*), \tag{10.3.1}$$

which we presume has a minimum where at least some of the ϕ_i are non-zero. This of course depends on the parameters and couplings appearing in V . The fields ϕ_i will then have VEVs that can be written:

$$\langle 0|\phi_i|0\rangle = \frac{v_i}{\sqrt{2}}. \quad (10.3.2)$$

Any group generators that satisfy

$$T_i^{aj}v_j = 0 \quad (10.3.3)$$

correspond to unbroken symmetry transformations. In general, the unbroken global symmetry group is the one formed from the unbroken symmetry generators, and the vacuum state is invariant under this unbroken subgroup. The broken generators satisfy

$$T_i^{aj}v_j \neq 0. \quad (10.3.4)$$

Goldstone's Theorem states that for every spontaneously broken generator, labeled by a , of a global symmetry group, there must be a corresponding Nambu-Goldstone boson. [The group $U(1)$ has just one generator, so there was just one Nambu-Goldstone boson.]

In the case of a local or gauge symmetry, each of the would-be Nambu-Goldstone bosons is eaten by the vector field with the corresponding index a . The vector fields for the broken generators become massive, with squared masses that can be computed in terms of the VEV(s) and the gauge coupling(s) of the theory. There are also Higgs boson(s) for the uneaten components of the scalar fields that obtained VEVs.

One might also ask whether it is possible for fields other than scalars to obtain vacuum expectation values. If one could succeed in concocting a theory in which a fermion spinor field or a vector field has a VEV:

$$\langle 0|\Psi_\alpha|0\rangle \neq 0 \quad (?), \quad (10.3.5)$$

$$\langle 0|A_\mu|0\rangle \neq 0 \quad (?), \quad (10.3.6)$$

then Lorentz invariance will necessarily be broken, since the alleged VEV carries an uncontracted spinor or vector index, and therefore transforms non-trivially under the Lorentz group. This would imply that the broken generators would include Lorentz boosts and rotations, in contradiction with experiment. However, there *can* be vacuum expectation values for antifermion-fermion composite fields, since they can form a Lorentz scalar:

$$\langle 0|\bar{\Psi}\Psi|0\rangle \neq 0. \quad (10.3.7)$$

This is called a fermion-antifermion condensate. In fact, in QCD the quark-antiquark composite fields do have vacuum expectation values:

$$\langle 0 | \bar{u}u | 0 \rangle \approx \langle 0 | \bar{d}d | 0 \rangle \approx \langle 0 | \bar{s}s | 0 \rangle \approx \mu^3 \neq 0, \quad (10.3.8)$$

where μ is a quantity with dimensions of [mass] which is set by the scale Λ_{QCD} at which non-perturbative effects become important. This is known as chiral symmetry breaking. The chiral symmetry is a global, approximate symmetry by which left-handed u, d, s quarks are rotated into each other and right-handed u, d, s quarks are rotated into each other. (The objects $\bar{q}q$ are color singlets, so these antifermion-fermion VEVs do not break $SU(3)_c$ symmetry.) Chiral symmetry breaking is actually the mechanism that is responsible for most of the mass of the proton and the neutron, and therefore most of the mass of everyday objects. When the chiral symmetry is spontaneously broken, the Nambu-Goldstone bosons that arise include the pions π^\pm and π^0 . They are not exactly massless because the chiral symmetry was really only approximate to begin with, but the Goldstone theorem successfully explains why they are much lighter than the proton; $m_\pi^2 \ll m_p^2$. They are often called pseudo-Nambu-Goldstone bosons, or PNGBs, with the “pseudo” indicating that the associated spontaneously broken global symmetry was only an approximate symmetry. Extensions of the Standard Model that feature new approximate global symmetries that are spontaneously broken generally predict the existence of heavy exotic PNGBs. For example, these are a ubiquitous feature of technicolor models.

11 The Standard Electroweak Model

11.1 $SU(2)_L \times U(1)_Y$ representations and Lagrangian

In this section, we will study the Higgs mechanism of the Standard Model, which is responsible for the masses of W^\pm and Z bosons, and the masses of the leptons and most of the masses of the heavier quarks.

The electroweak interactions are mediated by three massive vector bosons W^\pm, Z and the massless photon γ . The gauge group before spontaneous symmetry breaking must therefore have four generators. After spontaneous symmetry breaking, the remaining unbroken gauge group is electromagnetic gauge invariance. A viable theory must explain the qualitative experimental facts that the W^\pm bosons couple only to L-fermions (and R-antifermions), that the Z boson couples differently to L-fermions and R-fermions, but γ couples with the same strength to L-fermions and R-fermions. Also, there are very stringent quantitative experimental tests involving the relative strengths of fermion-antifermion-vector couplings and the ratio of the W and Z masses. The Standard Model (SM) of electroweak interactions of Glashow, Weinberg and Salam successfully incorporates all of these features and tests into a spontaneously broken gauge theory. In the SM, the gauge symmetry breaking is:

$$SU(2)_L \times U(1)_Y \rightarrow U(1)_{\text{EM}}. \quad (11.1.1)$$

We will need to introduce a Higgs field to produce this pattern of symmetry breaking.

The $SU(2)_L$ subgroup is known as weak isospin. Left-handed SM fermions are known to be doublets under $SU(2)_L$:

$$\begin{pmatrix} \nu_e \\ e_L \end{pmatrix}, \quad \begin{pmatrix} \nu_\mu \\ \mu_L \end{pmatrix}, \quad \begin{pmatrix} \nu_\tau \\ \tau_L \end{pmatrix}, \quad \begin{pmatrix} u_L \\ d_L \end{pmatrix}, \quad \begin{pmatrix} c_L \\ s_L \end{pmatrix}, \quad \begin{pmatrix} t_L \\ b_L \end{pmatrix}. \quad (11.1.2)$$

Notice that the electric charge of the upper member of each doublet is always 1 greater than that of the lower member. The $SU(2)_L$ representation matrix generators acting on these fields are proportional to the Pauli matrices:

$$T^a = \sigma^a/2, \quad (a = 1, 2, 3) \quad (11.1.3)$$

with corresponding vector gauge boson fields:

$$W_\mu^a, \quad (a = 1, 2, 3) \quad (11.1.4)$$

and a coupling constant g . The right-handed fermions

$$e_R, \quad \mu_R, \quad \tau_R, \quad u_R, \quad c_R, \quad t_R, \quad d_R, \quad s_R, \quad b_R, \quad (11.1.5)$$

are all singlets under $SU(2)_L$.

Meanwhile, the $U(1)_Y$ subgroup is known as weak hypercharge and has a coupling constant g' and a vector boson B_μ , sometimes known as the hyperphoton. The weak hypercharge Y is a conserved charge just like electric charge q , but it is different for left-handed and right-handed fermions. Both members of an $SU(2)_L$ doublet must have the same weak hypercharge in order to satisfy $SU(2)_L$ gauge invariance.

Following the general discussion of Yang-Mills gauge theories in section 8.2 [see eqs. (8.2.18) and (8.2.19)], the pure-gauge part of the electroweak Lagrangian density is:

$$\mathcal{L}_{\text{gauge}} = -\frac{1}{4}W_{\mu\nu}^a W^{a\mu\nu} - \frac{1}{4}B_{\mu\nu}B^{\mu\nu}, \quad (11.1.6)$$

where:

$$W_{\mu\nu}^a = \partial_\mu W_\nu^a - \partial_\nu W_\mu^a - g\epsilon^{abc}W_\mu^b W_\nu^c, \quad (11.1.7)$$

$$B_{\mu\nu} = \partial_\mu B_\nu - \partial_\nu B_\mu \quad (11.1.8)$$

are the $SU(2)_L$ and $U(1)_Y$ field strengths. The totally antisymmetric ϵ^{abc} (with $\epsilon^{123} = +1$) are the structure constants for $SU(2)_L$. This $\mathcal{L}_{\text{gauge}}$ provides for kinetic terms of the vector fields, and W_μ^a self-interactions.

The interactions of the electroweak gauge bosons with fermions are determined by the covariant derivative. For example, the covariant derivatives acting on the lepton fields are:

$$D_\mu \begin{pmatrix} \nu_e \\ e_L \end{pmatrix} = \left[\partial_\mu + ig'B_\mu Y_{\ell_L} + igW_\mu^a T^a \right] \begin{pmatrix} \nu_e \\ e_L \end{pmatrix}, \quad (11.1.9)$$

$$D_\mu e_R = [\partial_\mu + ig'B_\mu Y_{\ell_R}] e_R. \quad (11.1.10)$$

where Y_{ℓ_L} and Y_{ℓ_R} are the weak hypercharges of left-handed leptons and right-handed leptons, and 2×2 unit matrices are understood to go with the ∂_μ and B_μ terms in eq. (11.1.9). A multiplicative factor can always be absorbed into the definition of the coupling g' , so without loss of generality, it is traditional[†] to set $Y_{\ell_R} = Q_\ell = -1$. The weak hypercharges of all other fermions are then fixed. Using the explicit form of the $SU(2)_L$ generators in terms of Pauli matrices in eq. (11.1.3), the covariant derivative of left-handed leptons is:

$$D_\mu \begin{pmatrix} \nu_e \\ e_L \end{pmatrix} = \partial_\mu \begin{pmatrix} \nu_e \\ e_L \end{pmatrix} + i \left[g'Y_{\ell_L} \begin{pmatrix} B_\mu & 0 \\ 0 & B_\mu \end{pmatrix} + \frac{g}{2} \begin{pmatrix} W_\mu^3 & W_\mu^1 - iW_\mu^2 \\ W_\mu^1 + iW_\mu^2 & -W_\mu^3 \end{pmatrix} \right] \begin{pmatrix} \nu_e \\ e_L \end{pmatrix}. \quad (11.1.11)$$

Therefore, the covariant derivatives of the lepton fields can be summarized as:

$$D_\mu \nu_e = \partial_\mu \nu_e + i \left(g'Y_{\ell_L} B_\mu + \frac{g}{2} W_\mu^3 \right) \nu_e + i \frac{g}{2} (W_\mu^1 - iW_\mu^2) e_L, \quad (11.1.12)$$

$$D_\mu e_L = \partial_\mu e_L + i \left(g'Y_{\ell_L} B_\mu - \frac{g}{2} W_\mu^3 \right) e_L + i \frac{g}{2} (W_\mu^1 + iW_\mu^2) \nu_e, \quad (11.1.13)$$

$$D_\mu e_R = \partial_\mu e_R - ig'B_\mu e_R. \quad (11.1.14)$$

[†]Some references define the weak hypercharge normalization so that Y is a factor of 2 larger than here, for each particle.

The covariant derivative of a field must carry the same electric charge as the field itself, in order for charge to be conserved. Evidently, then, $W_\mu^1 - iW_\mu^2$ must carry electric charge $+1$ and $W_\mu^1 + iW_\mu^2$ must carry electric charge -1 , so these must be identified with the W^\pm bosons of the weak interactions. Consider the interaction Lagrangian following from

$$\mathcal{L} = i(\bar{\nu}_e \quad \bar{e}_L) \gamma^\mu D_\mu \begin{pmatrix} \nu_e \\ e_L \end{pmatrix} \quad (11.1.15)$$

$$= -\frac{g}{2} \bar{\nu}_e \gamma^\mu e_L (W_\mu^1 - iW_\mu^2) - \frac{g}{2} \bar{e}_L \gamma^\mu \nu_e (W_\mu^1 + iW_\mu^2) + \dots \quad (11.1.16)$$

Comparing with eqs. (7.6.2), (7.6.3), and (7.7.5), we find that to reproduce the weak-interaction Lagrangian of muon decay, we must have:

$$W_\mu^+ \equiv \frac{1}{\sqrt{2}}(W_\mu^1 - iW_\mu^2), \quad (11.1.17)$$

$$W_\mu^- \equiv \frac{1}{\sqrt{2}}(W_\mu^1 + iW_\mu^2). \quad (11.1.18)$$

The $1/\sqrt{2}$ normalization agrees with our previous convention; the real reason for it is so that the kinetic terms for W^\pm have a standard normalization: $\mathcal{L} = -\frac{1}{2}(\partial_\mu W_\nu^+ - \partial_\nu W_\mu^+)(\partial^\mu W^{-\nu} - \partial^\nu W^{-\mu})$.

The vector bosons B_μ and W_μ^3 are both electrically neutral. As a result of spontaneous symmetry breaking, we will find that they mix. In other words, the fields with well-defined masses (“mass eigenstates” or “mass eigenfields”) are not B_μ and W_μ^3 , but are orthogonal linear combinations of these two gauge eigenstate fields. One of the mass eigenstates is the photon field A^μ , and the other is the massive Z boson vector field, Z_μ . One can write the relation between the gauge eigenstate and mass eigenstate fields as a rotation in field space by an angle θ_W , known as the weak mixing angle:

$$\begin{pmatrix} W_\mu^3 \\ B_\mu \end{pmatrix} = \begin{pmatrix} \cos \theta_W & \sin \theta_W \\ -\sin \theta_W & \cos \theta_W \end{pmatrix} \begin{pmatrix} Z_\mu \\ A_\mu \end{pmatrix}, \quad (11.1.19)$$

with the inverse relation:

$$\begin{pmatrix} Z_\mu \\ A_\mu \end{pmatrix} = \begin{pmatrix} \cos \theta_W & -\sin \theta_W \\ \sin \theta_W & \cos \theta_W \end{pmatrix} \begin{pmatrix} W_\mu^3 \\ B_\mu \end{pmatrix}. \quad (11.1.20)$$

We now require that the resulting theory has the correct photon coupling to fermions, by requiring that the field A^μ appears in the covariant derivatives in the way dictated by QED. The covariant derivative of the right-handed electron field eq. (11.1.14) can be written:

$$D_\mu e_R = \partial_\mu e_R - ig' \cos \theta_W A_\mu e_R + ig' \sin \theta_W Z_\mu e_R. \quad (11.1.21)$$

Comparing to $D_\mu e_R = \partial_\mu e_R - ie A_\mu e_R$ from QED, we conclude that:

$$g' \cos \theta_W = e. \quad (11.1.22)$$

Similarly, one finds using eq. (11.1.19) that:

$$D_\mu e_L = \partial_\mu e_L + i \left(g' Y_{\ell_L} \cos \theta_W - \frac{g}{2} \sin \theta_W \right) A_\mu e_L + \dots \quad (11.1.23)$$

Again comparing to the prediction of QED that $D_\mu e_L = \partial_\mu e_L - ie A_\mu e_L$, it must be that:

$$\frac{g}{2} \sin \theta_W - g' Y_{\ell_L} \cos \theta_W = e \quad (11.1.24)$$

is the electromagnetic coupling. In the same way:

$$D_\mu \nu_e = \partial_\mu \nu_e + i \left(g' Y_{\ell_L} \cos \theta_W + \frac{g}{2} \sin \theta_W \right) A_\mu \nu_e + \dots \quad (11.1.25)$$

where the \dots represent W and Z terms. However, we know that the neutrino has no electric charge, and therefore its covariant derivative cannot involve the photon. So, the coefficient of A_μ in eq. (11.1.25) must vanish:

$$\frac{g}{2} \sin \theta_W + g' Y_{\ell_L} \cos \theta_W = 0. \quad (11.1.26)$$

Now combining eqs. (11.1.22), (11.1.24), and (11.1.26), we learn that:

$$Y_{\ell_L} = -1/2, \quad (11.1.27)$$

$$e = \frac{gg'}{\sqrt{g^2 + g'^2}}, \quad (11.1.28)$$

$$\tan \theta_W = g'/g, \quad (11.1.29)$$

so that

$$\sin \theta_W = \frac{g'}{\sqrt{g^2 + g'^2}}, \quad \cos \theta_W = \frac{g}{\sqrt{g^2 + g'^2}}. \quad (11.1.30)$$

These are requirements that will have to be satisfied by the spontaneous symmetry breaking mechanism. The numerical values from experiment are approximately:

$$g = 0.652, \quad (11.1.31)$$

$$g' = 0.357, \quad (11.1.32)$$

$$e = 0.313, \quad (11.1.33)$$

$$\sin^2 \theta_W = 0.231. \quad (11.1.34)$$

These are all renormalized, running parameters, evaluated at a renormalization scale $\mu = m_Z = 91.1876$ GeV in the $\overline{\text{MS}}$ scheme.

In a similar way, one can work out what the weak hypercharges of all of the other SM quarks and leptons have to be, in order to reproduce the correct electric charges appearing in the

coupling to the photon field A_μ from the covariant derivative. The results can be summarized in terms of the $SU(3)_c \times SU(2)_L \times U(1)_Y$ representations:

$$\begin{aligned}
\begin{pmatrix} \nu_e \\ e_L \end{pmatrix}, \quad \begin{pmatrix} \nu_\mu \\ \mu_L \end{pmatrix}, \quad \begin{pmatrix} \nu_\tau \\ \tau_L \end{pmatrix}, & \longleftrightarrow (\mathbf{1}, \mathbf{2}, -\frac{1}{2}), \\
e_R, \quad \mu_R, \quad \tau_R, & \longleftrightarrow (\mathbf{1}, \mathbf{1}, -1), \\
\begin{pmatrix} u_L \\ d_L \end{pmatrix}, \quad \begin{pmatrix} c_L \\ s_L \end{pmatrix}, \quad \begin{pmatrix} t_L \\ b_L \end{pmatrix}, & \longleftrightarrow (\mathbf{3}, \mathbf{2}, \frac{1}{6}), \\
u_R, \quad c_R, \quad t_R, & \longleftrightarrow (\mathbf{3}, \mathbf{1}, \frac{2}{3}), \\
d_R, \quad s_R, \quad b_R, & \longleftrightarrow (\mathbf{3}, \mathbf{1}, -\frac{1}{3}).
\end{aligned} \tag{11.1.35}$$

In general, the electric charge of any field f is given in terms of the eigenvalue of the 3 component of weak isospin matrix, T^3 , and the weak hypercharge Y , as:

$$Q_f = T_f^3 + Y_f. \tag{11.1.36}$$

Here T_f^3 is $+1/2$ for the upper component of a doublet, $-1/2$ for the lower component of a doublet, and 0 for an $SU(2)_L$ singlet. The couplings of the SM fermions to the Z boson then follow as a prediction. One finds for each SM fermion f :

$$\mathcal{L}_{Zf\bar{f}} = -Z^\mu \bar{f} \gamma_\mu (g_L^f P_L + g_R^f P_R) f, \tag{11.1.37}$$

where

$$g_L^f = g \cos \theta_W T_{fL}^3 - g' \sin \theta_W Y_{fL} = \frac{g}{\cos \theta_W} (T_{fL}^3 - \sin^2 \theta_W Q_f), \tag{11.1.38}$$

$$g_R^f = -g' \sin \theta_W Y_{fR} = -\frac{g}{\cos \theta_W} (\sin^2 \theta_W Q_f), \tag{11.1.39}$$

with coefficients:

fermion	T_{fL}^3	Y_{fL}	Y_{fR}	Q_f
ν_e, ν_μ, ν_τ	$\frac{1}{2}$	$-\frac{1}{2}$	0	0
e, μ, τ	$-\frac{1}{2}$	$-\frac{1}{2}$	-1	-1
u, c, t	$\frac{1}{2}$	$\frac{1}{6}$	$\frac{2}{3}$	$\frac{2}{3}$
d, s, b	$-\frac{1}{2}$	$\frac{1}{6}$	$-\frac{1}{3}$	$-\frac{1}{3}$

Equation (11.1.37) can also be rewritten in terms of vector and axial-vector couplings to the Z boson:

$$\mathcal{L}_{Zf\bar{f}} = -Z^\mu \bar{f} \gamma_\mu (g_V^f - g_A^f \gamma_5) f, \tag{11.1.40}$$

with

$$g_V^f = \frac{1}{2} (g_L^f + g_R^f) = \frac{g}{2 \cos \theta_W} (T_{fL}^3 - 2 \sin^2 \theta_W Q_f), \tag{11.1.41}$$

$$g_A^f = \frac{1}{2} (g_L^f - g_R^f) = \frac{g}{2 \cos \theta_W} (T_{fL}^3). \tag{11.1.42}$$

The coupling parameters appearing in eq. (9.7.13) are $V_f = g_V^f/e$ and $A_f = g_A^f/e$.

The partial decay widths and branching ratios of the Z boson can be worked out from these couplings, and agree with the results from experiment:

$$\text{BR}(Z \rightarrow \ell^+ \ell^-) = 0.033658 \pm 0.000023 \quad (\text{for } \ell = e, \mu, \tau, \text{ each}) \quad (11.1.43)$$

$$\text{BR}(Z \rightarrow \text{invisible}) = 0.2000 \pm 0.0006 \quad (11.1.44)$$

$$\text{BR}(Z \rightarrow \text{hadrons}) = 0.6991 \pm 0.0006. \quad (11.1.45)$$

The “invisible” branching ratio matches up extremely well with the theoretical prediction for the sum over the three $\nu_\ell \bar{\nu}_\ell$ final states, while “hadrons” is due to quark-antiquark final states. It is an important fact that the Z branching ratio into charged leptons is small. This is unfortunate, since backgrounds for leptons are smaller than for hadrons or missing energy, and Z bosons can appear in many searches for new phenomena.

11.2 The Standard Model Higgs mechanism

Let us now turn to the question of how to spontaneously break the electroweak gauge symmetry in a way that satisfies the above conditions. There is actually more than one way to do this, but the Standard Model chooses the simplest possibility, which is to introduce a complex $SU(2)_L$ -doublet scalar Higgs field with weak hypercharge $Y_\Phi = +1/2$:

$$\Phi = \begin{pmatrix} \phi^+ \\ \phi^0 \end{pmatrix} \quad \longleftrightarrow \quad (\mathbf{1}, \mathbf{2}, \frac{1}{2}). \quad (11.2.1)$$

Each of the fields ϕ^+ and ϕ^0 is a complex scalar field; we know that they carry electric charges $+1$ and 0 respectively from eq. (11.1.36). Under gauge transformations, Φ transforms as:

$$SU(2)_L : \quad \Phi(x) \rightarrow \Phi'(x) = e^{i\theta^a(x)\sigma^a/2} \Phi(x), \quad (11.2.2)$$

$$U(1)_Y : \quad \Phi(x) \rightarrow \Phi'(x) = e^{i\theta(x)/2} \Phi(x). \quad (11.2.3)$$

The Hermitian conjugate field transforms as:

$$SU(2)_L : \quad \Phi^\dagger \rightarrow \Phi'^\dagger = \Phi^\dagger e^{-i\theta^a \sigma^a/2}, \quad (11.2.4)$$

$$U(1)_Y : \quad \Phi^\dagger \rightarrow \Phi'^\dagger = \Phi^\dagger e^{-i\theta/2}. \quad (11.2.5)$$

It follows that the combinations

$$\Phi^\dagger \Phi \quad \text{and} \quad D^\mu \Phi^\dagger D_\mu \Phi \quad (11.2.6)$$

are gauge singlets. We can therefore build a gauge-invariant potential:

$$V(\Phi, \Phi^\dagger) = m^2 \Phi^\dagger \Phi + \lambda (\Phi^\dagger \Phi)^2, \quad (11.2.7)$$

and the Lagrangian density for Φ is:

$$\mathcal{L} = D^\mu \Phi^\dagger D_\mu \Phi - V(\Phi, \Phi^\dagger). \quad (11.2.8)$$

Now, provided that $m^2 < 0$, then $\Phi = \begin{pmatrix} 0 \\ 0 \end{pmatrix}$ is a local maximum, rather than a minimum, of the potential. This will ensure the spontaneous symmetry breaking that we demand. There are degenerate minima of the potential with

$$\Phi^\dagger \Phi = v^2/2, \quad v = \sqrt{-m^2/\lambda}. \quad (11.2.9)$$

Without loss of generality, we can choose the VEV of Φ to be real, and entirely in the second (electrically neutral) component of the Higgs field:

$$\langle 0|\Phi|0\rangle = \begin{pmatrix} 0 \\ v/\sqrt{2} \end{pmatrix}. \quad (11.2.10)$$

This is a convention, which can always be achieved by doing an $SU(2)_L$ gauge transformation on the field Φ to make it so. By definition, the surviving $U(1)$ gauge symmetry is $U(1)_{\text{EM}}$, so the component of Φ obtaining a VEV must be the one assigned 0 electric charge. The $U(1)_{\text{EM}}$ gauge transformations acting on Φ are a combination of $SU(2)_L$ and $U(1)_Y$ transformations:

$$\Phi \rightarrow \Phi' = \exp \left[i\theta \begin{pmatrix} 1 & 0 \\ 0 & 0 \end{pmatrix} \right] \Phi, \quad (11.2.11)$$

or, in components,

$$\phi^+ \rightarrow e^{i\theta} \phi^+, \quad (11.2.12)$$

$$\phi^0 \rightarrow \phi^0. \quad (11.2.13)$$

Comparing with the QED gauge transformation rule of eq. (8.1.5), we see that indeed ϕ^+ and ϕ^0 have charges +1 and 0, respectively.

The Higgs field Φ has two complex, so four real, scalar field degrees of freedom. Therefore, following the example of section 10.2, we can write it as:

$$\Phi(x) = e^{iG^a(x)\sigma^a/2v} \begin{pmatrix} 0 \\ \frac{v+h(x)}{\sqrt{2}} \end{pmatrix}, \quad (11.2.14)$$

where $G^a(x)$ ($a = 1, 2, 3$) and $h(x)$ are each real scalar fields. The G^a are would-be Nambu-Goldstone bosons, corresponding to the three broken generators in $SU(2)_L \times U(1)_Y \rightarrow U(1)_{\text{EM}}$. The would-be Nambu-Goldstone fields can be removed by going to unitary gauge, which means performing an $SU(2)_L$ gauge transformation of the form of eq. (11.2.2), with $\theta^a = -G^a/v$. This completely eliminates the G^a from the Lagrangian, so that in the unitary gauge we have simply

$$\Phi(x) = \begin{pmatrix} 0 \\ \frac{v+h(x)}{\sqrt{2}} \end{pmatrix}. \quad (11.2.15)$$

The field h creates and destroys the physical Higgs particle, an electrically neutral real scalar boson that has yet to be discovered experimentally. We can now plug this into the Lagrangian density of eq. (11.2.8), to find interactions and mass terms for the remaining Higgs field h and the vector bosons. The covariant derivative of Φ in unitary gauge is:

$$D_\mu \Phi = \frac{1}{\sqrt{2}} \begin{pmatrix} 0 \\ \partial_\mu h \end{pmatrix} + \frac{i}{\sqrt{2}} \left[\frac{g'}{2} B_\mu + \frac{g}{2} W_\mu^a \sigma^a \right] \begin{pmatrix} 0 \\ v + h \end{pmatrix}, \quad (11.2.16)$$

and its Hermitian conjugate is:

$$D_\mu \Phi^\dagger = \frac{1}{\sqrt{2}} (0 \quad \partial_\mu h) - \frac{i}{\sqrt{2}} (0 \quad v + h) \left[\frac{g'}{2} B_\mu + \frac{g}{2} W_\mu^a \sigma^a \right]. \quad (11.2.17)$$

Therefore,

$$D^\mu \Phi^\dagger D_\mu \Phi = \frac{1}{2} \partial_\mu h \partial^\mu h + \frac{(v + h)^2}{8} \begin{pmatrix} 0 & 1 \end{pmatrix} \begin{pmatrix} g' B_\mu + g W_\mu^3 & \sqrt{2} g W_\mu^- \\ \sqrt{2} g W_\mu^+ & g' B_\mu - g W_\mu^3 \end{pmatrix} \begin{pmatrix} 0 \\ 1 \end{pmatrix} \\ + \begin{pmatrix} g' B^\mu + g W^{3\mu} & \sqrt{2} g W^{-\mu} \\ \sqrt{2} g W^{+\mu} & g' B^\mu - g W^{3\mu} \end{pmatrix} \begin{pmatrix} 0 \\ 1 \end{pmatrix}, \quad (11.2.18)$$

or, after simplifying,

$$D^\mu \Phi^\dagger D_\mu \Phi = \frac{1}{2} \partial_\mu h \partial^\mu h + \frac{(v + h)^2}{4} \left[g^2 W_\mu^+ W^{-\mu} + \frac{1}{2} (g W_\mu^3 - g' B_\mu) (g W^{3\mu} - g' B^\mu) \right]. \quad (11.2.19)$$

This can be further simplified using:

$$g W_\mu^3 - g' B_\mu = \sqrt{g^2 + g'^2} [\cos \theta_W W_\mu^3 - \sin \theta_W B_\mu] = \sqrt{g^2 + g'^2} Z_\mu, \quad (11.2.20)$$

where the first equality uses eq. (11.1.30) and the second uses eq. (11.1.20). So finally we have:

$$\mathcal{L}_{\Phi \text{ kinetic}} = D^\mu \Phi^\dagger D_\mu \Phi = \frac{1}{2} \partial_\mu h \partial^\mu h + \frac{(v + h)^2}{4} \left[g^2 W_\mu^+ W^{-\mu} + \frac{1}{2} (g^2 + g'^2) Z_\mu Z^\mu \right]. \quad (11.2.21)$$

The parts of this proportional to v^2 make up $(\text{mass})^2$ terms for the W^\pm and Z vector bosons, vindicating the earlier assumption of neutral vector boson mixing with the form that we took for the sine and cosine of the weak mixing angle. Since there is no such $(\text{mass})^2$ term for the photon field A^μ , we have successfully shown that the photon remains massless, in agreement with the fact that $U(1)_{\text{EM}}$ gauge invariance remains unbroken. The specific prediction is:

$$m_W^2 = \frac{g^2 v^2}{4}, \quad m_Z^2 = \frac{(g^2 + g'^2) v^2}{4}, \quad (11.2.22)$$

which agrees with the experimental values provided that the VEV is approximately:

$$v = \sqrt{2} \langle \phi^0 \rangle = 246 \text{ GeV} \quad (11.2.23)$$

in the conventions used here.[†] Note that, comparing eqs. (7.7.7) and (11.2.22), the Fermi constant is simply related to the VEV, by:

$$G_F = \frac{1}{\sqrt{2}v^2}. \quad (11.2.24)$$

A non-trivial prediction of the theory is that

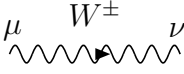
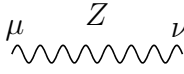
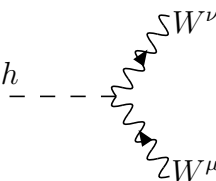
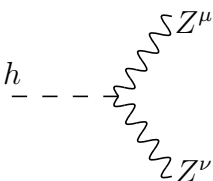
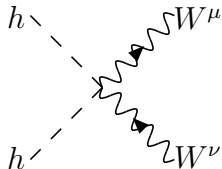
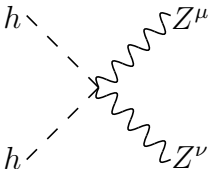
$$m_W/m_Z = \cos \theta_W. \quad (11.2.25)$$

All of the above predictions are subject to small, but measurable, loop corrections. For example, the present experimental values $m_W = 80.379 \pm 0.012$ GeV and $m_Z = 91.1876 \pm 0.0021$ GeV give:

$$\sin^2 \theta_W^{\text{on-shell}} \equiv 1 - m_W^2/m_Z^2 = 0.22301 \pm 0.00025, \quad (11.2.26)$$

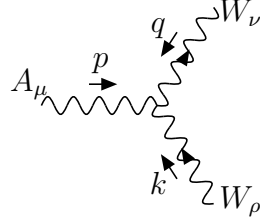
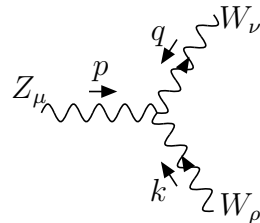
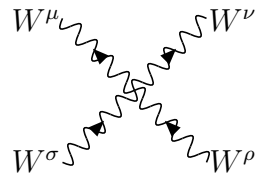
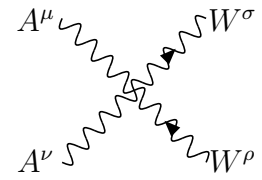
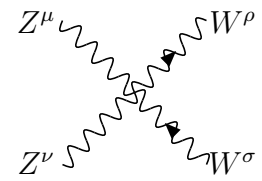
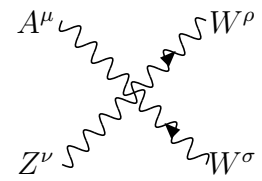
which is significantly lower than the $\overline{\text{MS}}$ -scheme running value in eq. (11.1.34).

The remaining terms in eq. (11.2.21) are Higgs-vector-vector and Higgs-Higgs-vector-vector couplings. This part of the Lagrangian density implies the following unitary gauge Feynman rules:

 $\frac{i}{p^2 - m_W^2 + i\epsilon} \left[-g_{\mu\nu} + \frac{p_\mu p_\nu}{m_W^2} \right]$	 $\frac{i}{p^2 - m_Z^2 + i\epsilon} \left[-g_{\mu\nu} + \frac{p_\mu p_\nu}{m_Z^2} \right]$
 $ig^{\mu\nu} g^2 v/2$	 $ig^{\mu\nu} (g^2 + g'^2) v/2$
 $ig^{\mu\nu} g^2/2$	 $ig^{\mu\nu} (g^2 + g'^2)/2$

[†]It should be noted that there is another extremely common convention in which v is defined to be a factor $1/\sqrt{2}$ smaller than here, so that $v = \langle \phi^0 \rangle = 174$ GeV in that convention.

with the arrow direction on W^\pm lines indicating the direction of the flow of positive charge. The field-strength Lagrangian terms of eq. (11.1.6) provides the momentum part of the W , Z propagators above, and also yields 3-gauge-boson and 4-gauge-boson interactions:

	$-ie[g^{\mu\nu}(p-q)^\rho + g^{\nu\rho}(q-k)^\mu + g^{\rho\mu}(k-p)^\nu]$
	$-ig \cos \theta_W [g^{\mu\nu}(p-q)^\rho + g^{\nu\rho}(q-k)^\mu + g^{\rho\mu}(k-p)^\nu]$
	$ig^2 X^{\mu\nu,\rho\sigma}$
	$-ie^2 X^{\mu\nu,\rho\sigma}$
	$-ig^2 \cos^2 \theta_W X^{\mu\nu,\rho\sigma}$
	$-ig^2 \sin \theta_W \cos \theta_W X^{\mu\nu,\rho\sigma}$

where:

$$X^{\mu\nu,\rho\sigma} = 2g^{\mu\nu}g^{\rho\sigma} - g^{\mu\rho}g^{\nu\sigma} - g^{\mu\sigma}g^{\nu\rho}. \quad (11.2.27)$$

Finally, the Higgs potential $V(\Phi, \Phi^\dagger)$ gives rise to a mass and self-interactions for h . In unitary gauge:

$$V(h) = \lambda v^2 h^2 + \lambda v h^3 + \frac{\lambda}{4} h^4, \quad (11.2.28)$$

just as in the toy model studied in 10.2. Therefore, the Higgs boson has self-interactions with Feynman rules:



and a mass

$$m_h = \sqrt{2\lambda}v, \quad (11.2.29)$$

It would be great if we could evaluate this numerically using present data. Unfortunately, while we know what the Higgs VEV v is, there is no present experiment that gives any direct measurement of λ . Indirectly we know what it needs to be from the Higgs boson mass, if the SM is the correct theory. Furthermore, there are indirect effects of the Higgs mass in loops of precision electroweak observables, such as the Z mass, W mass, $\sin^2 \theta_W$, etc. The experiments that measure these observables suggested well before the Higgs boson discovery that m_h should be less than 200 GeV. The self-consistency of these indirect constraints vs. physical mass was verified by the discovery of the Higgs boson at $m_h = 125$ GeV.

11.3 Fermion masses and Cabibbo-Kobayashi-Maskawa mixing

The gauge group representations for fermions in the Standard Model are chiral. This means that the left-handed fermions transform in a different representation than the right-handed fermions. Chiral fermions have the property that they cannot have masses without breaking the symmetry that makes them chiral.

For example, suppose we try to write down a mass term for the electron:

$$\mathcal{L}_{\text{electron mass}} = -m_e \bar{e}e. \quad (11.3.1)$$

The Dirac spinor for the electron can be separated into left- and right-handed pieces,

$$e = P_L e_L + P_R e_R, \quad (11.3.2)$$

and the corresponding barred spinor as:

$$\bar{e} = (e_L^\dagger P_L + e_R^\dagger P_R) \gamma^0 = e_L^\dagger \gamma^0 P_R + e_R^\dagger \gamma^0 P_L = \bar{e}_L P_R + \bar{e}_R P_L, \quad (11.3.3)$$

where, to avoid any confusion between $\overline{(e_L)}$ and $(\bar{e})P_L$, we explicitly define

$$\bar{e}_L \equiv e_L^\dagger \gamma^0, \quad \bar{e}_R \equiv e_R^\dagger \gamma^0. \quad (11.3.4)$$

Equation (11.3.1) can therefore be written:

$$\mathcal{L}_{\text{electron mass}} = -m_e(\bar{e}_L e_R + \bar{e}_R e_L). \quad (11.3.5)$$

The point is that this is clearly not a gauge singlet. In the first place, the e_L part of each term transforms as a doublet under $SU(2)_L$, and the e_R is a singlet, so each term is an $SU(2)_L$ doublet. Furthermore, the first term has $Y = Y_{e_R} - Y_{e_L} = -1/2$, while the second term has $Y = 1/2$. All terms in the Lagrangian must be gauge singlets in order not to violate the gauge symmetry, so the electron mass is disqualified from appearing in this form. More generally, for any Standard Model fermion f , the naive mass term

$$\mathcal{L}_{f \text{ mass}} = -m_f(\bar{f}_L f_R + \bar{f}_R f_L) \quad (11.3.6)$$

is not an $SU(2)_L$ singlet, and is not neutral under $U(1)_Y$, and so is not allowed.

Fortunately, fermion masses can still arise with the help of the Higgs field. For the electron, there is a gauge-invariant term:

$$\mathcal{L}_{\text{electron Yukawa}} = -y_e (\bar{\nu}_e \quad \bar{e}_L) \begin{pmatrix} \phi^+ \\ \phi^0 \end{pmatrix} e_R + \text{c.c.} \quad (11.3.7)$$

Here y_e is a Yukawa coupling of the type we studied in 6.3. The field $(\bar{\nu}_e \quad \bar{e}_L)$ carries weak hypercharge $+1/2$, as does the Higgs field, and e_R carries weak hypercharge -1 , so the whole term is a $U(1)_Y$ singlet, as required. Moreover, the doublets transform under $SU(2)_L$ as:

$$\begin{pmatrix} \phi^+ \\ \phi^0 \end{pmatrix} \rightarrow e^{-i\theta^a \sigma^a / 2} \begin{pmatrix} \phi^+ \\ \phi^0 \end{pmatrix}, \quad (11.3.8)$$

$$(\bar{\nu}_e \quad \bar{e}_L) \rightarrow (\bar{\nu}_e \quad \bar{e}_L) e^{+i\theta^a \sigma^a / 2}, \quad (11.3.9)$$

so eq. (11.3.7) is also an $SU(2)_L$ singlet. Going to the unitary gauge of eq. (11.2.15), it becomes:

$$\mathcal{L}_{\text{Yukawa}} = -\frac{y_e}{\sqrt{2}}(v+h)(\bar{e}_L e_R + \bar{e}_R e_L), \quad (11.3.10)$$

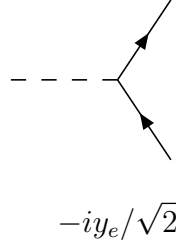
or, reassembling the Dirac spinors without projection matrices:

$$\mathcal{L}_{\text{Yukawa}} = -\frac{y_e}{\sqrt{2}}(v+h)\bar{e}e. \quad (11.3.11)$$

This can now be interpreted as an electron mass, equal to

$$m_e = \frac{y_e v}{\sqrt{2}}, \quad (11.3.12)$$

and, as a bonus, an electron-positron-Higgs interaction vertex, with Feynman rule:



Since we know the electron mass and the Higgs VEV already, we can compute the electron Yukawa coupling:

$$y_e = \sqrt{2} \left(\frac{0.511 \text{ MeV}}{246 \text{ GeV}} \right) = 2.94 \times 10^{-6}. \quad (11.3.13)$$

Unfortunately, this is so small that we can forget about ever observing the interactions of the Higgs particle h with an electron. Notice that although the neutrino participates in the Yukawa interaction, it disappears in unitary gauge from that term.

Masses for all of the other leptons, and the down-type quarks (d, s, b) in the Standard Model arise in exactly the same way. For example, the bottom quark mass comes from the gauge-invariant Yukawa coupling:

$$\mathcal{L} = -y_b (\bar{t}_L \quad \bar{b}_L) \begin{pmatrix} \phi^+ \\ \phi^0 \end{pmatrix} b_R + \text{c.c.}, \quad (11.3.14)$$

implying that, in unitary gauge, we have a b -quark mass and an $h\bar{b}b$ vertex:

$$\mathcal{L} = -\frac{y_b}{\sqrt{2}}(v + h)\bar{b}b. \quad (11.3.15)$$

The situation is slightly different for up-type quarks (u, c, t), because the complex conjugate of the field Φ must appear in order to preserve $U(1)_Y$ invariance. It is convenient to define

$$\tilde{\Phi} \equiv \begin{pmatrix} 0 & 1 \\ -1 & 0 \end{pmatrix} \Phi^* = \begin{pmatrix} \phi^{0*} \\ -\phi^{+*} \end{pmatrix}, \quad (11.3.16)$$

which transforms as an $SU(2)_L$ doublet in exactly the same way that Φ does:

$$\Phi \rightarrow e^{i\theta^a \sigma^a / 2} \Phi, \quad (11.3.17)$$

$$\tilde{\Phi} \rightarrow e^{i\theta^a \sigma^a / 2} \tilde{\Phi}. \quad (11.3.18)$$

Also, $\tilde{\Phi}$ has weak hypercharge $Y = -1/2$. (The field ϕ^{+*} has a negative electric charge.) Therefore, one can write a gauge-invariant Yukawa coupling for the top quark as:

$$\mathcal{L} = -y_t (\bar{t}_L \quad \bar{b}_L) \begin{pmatrix} \phi^{0*} \\ -\phi^{+*} \end{pmatrix} t_R + \text{c.c.} \quad (11.3.19)$$

Going to unitary gauge, one finds that the top quark has a mass:

$$\mathcal{L} = -\frac{y_t}{\sqrt{2}}(v+h)\bar{t}t. \quad (11.3.20)$$

In all cases, the unitary-gauge version of the gauge-invariant Yukawa interaction is

$$\mathcal{L} = -\frac{y_f}{\sqrt{2}}(v+h)\bar{f}f. \quad (11.3.21)$$

The mass and the h -fermion-antifermion coupling obtained by each Standard Model fermion in this way are both proportional to y_f . The Higgs mechanism not only explains the masses of the W^\pm and Z bosons, but also explains the masses of fermions. Notice that *all* of the particles in the Standard Model (except the photon and gluon, which must remain massless because of $SU(3)_c \times U(1)_{\text{EM}}$ gauge invariance) get a mass from spontaneous electroweak symmetry breaking of the form:

$$m_{\text{particle}} = kv, \quad (11.3.22)$$

where k is some combination of dimensionless couplings. For the fermions, it is proportional to a Yukawa coupling; for the W^\pm and Z bosons it depends on gauge couplings, and for the Higgs particle itself, it is the Higgs self-coupling λ .

There are two notable qualifications for quarks. First, gluon loops make a large modification to the tree-level prediction. For each quark, the physical mass measured from kinematics is

$$m_q = \frac{y_q v}{\sqrt{2}} \left[1 + \frac{4\alpha_s}{3\pi} + \dots \right], \quad (11.3.23)$$

where y_q is the running (renormalized) Yukawa coupling evaluated at a renormalization scale $\mu = m_q$. The QCD gluon-loop correction increases m_t by roughly 6%, and has an even larger effect on m_b because α_s is larger at the renormalization scale $\mu = m_b$ than at $\mu = m_t$. The two-loop and higher corrections (indicated by \dots) are smaller but still significant, and must be taken into account in precision work, for example when predicting the branching ratios of the Higgs boson decay. This was the reason for the notation \bar{m}_f (more nearly $y_f v/\sqrt{2}$ than m_f) that was used in 6.3.

A second qualification is that there is actually another source of quark masses, coming from non-perturbative QCD effects, as has already been mentioned at the end of section 10.3. If the Higgs field did not break $SU(2)_L \times U(1)_Y$, then these chiral symmetry breaking effects would do it anyway, using an antifermion-fermion VEV rather than a scalar VEV. This gives contributions to all quark masses that are roughly of order Λ_{QCD} . For the top, bottom, and even charm quarks, this is relatively insignificant. However, for the up and down quarks, it is actually the dominant effect. They get only a few MeV of their mass from the Higgs field. Therefore, the

most important source of mass in ordinary nuclear matter is really chiral symmetry breaking in QCD, *not* the Standard Model Higgs field.

The Standard Model fermions consist of three families with identical gauge interactions. Therefore, the most general form of the Yukawa interactions is actually:

$$\mathcal{L}_{e,\mu,\tau \text{ Yukawas}} = - \begin{pmatrix} \bar{\nu}^i & \bar{\ell}_L^i \end{pmatrix} \begin{pmatrix} \phi^+ \\ \phi^0 \end{pmatrix} \mathbf{y}_{\mathbf{e}i}^j \ell_{Rj} + \text{c.c.}, \quad (11.3.24)$$

$$\mathcal{L}_{d,s,b \text{ Yukawas}} = - \begin{pmatrix} \bar{u}_L^i & \bar{d}_L^i \end{pmatrix} \begin{pmatrix} \phi^+ \\ \phi^0 \end{pmatrix} \mathbf{y}_{\mathbf{d}i}^j d_{Rj} + \text{c.c.}, \quad (11.3.25)$$

$$\mathcal{L}_{u,c,t \text{ Yukawas}} = - \begin{pmatrix} \bar{u}_L^i & \bar{d}_L^i \end{pmatrix} \begin{pmatrix} \phi^{0*} \\ -\phi^{+*} \end{pmatrix} \mathbf{y}_{\mathbf{u}i}^j u_{Rj} + \text{c.c.} \quad (11.3.26)$$

Here i, j are indices that run over the three families, so that:

$$\ell_{Rj} = \begin{pmatrix} e_R \\ \mu_R \\ \tau_R \end{pmatrix}, \quad \ell_{Lj} = \begin{pmatrix} e_L \\ \mu_L \\ \tau_L \end{pmatrix}, \quad \nu_i = \begin{pmatrix} \nu_e \\ \nu_\mu \\ \nu_\tau \end{pmatrix}, \quad (11.3.27)$$

$$d_{Lj} = \begin{pmatrix} d_L \\ s_L \\ b_L \end{pmatrix}, \quad d_{Rj} = \begin{pmatrix} d_R \\ s_R \\ b_R \end{pmatrix}, \quad u_{Lj} = \begin{pmatrix} u_L \\ c_L \\ t_L \end{pmatrix}, \quad u_{Rj} = \begin{pmatrix} u_R \\ c_R \\ t_R \end{pmatrix}. \quad (11.3.28)$$

In a general basis, the Yukawa couplings

$$\mathbf{y}_{\mathbf{e}i}^j, \quad \mathbf{y}_{\mathbf{d}i}^j, \quad \mathbf{y}_{\mathbf{u}i}^j \quad (11.3.29)$$

are complex 3×3 matrices in family space. In unitary gauge, the Yukawa interaction Lagrangian can be written as:

$$\mathcal{L} = - \left(1 + \frac{h}{v} \right) \left\{ \bar{\ell}_L^i \mathbf{m}_{\mathbf{e}i}^j \ell'_{Rj} + \bar{d}_L^i \mathbf{m}_{\mathbf{d}i}^j d'_{Rj} + \bar{u}_L^i \mathbf{m}_{\mathbf{u}i}^j u'_{Rj} \right\} + \text{c.c.}, \quad (11.3.30)$$

where

$$\mathbf{m}_{\mathbf{f}i}^j = \frac{v}{\sqrt{2}} \mathbf{y}_{\mathbf{f}i}^j. \quad (11.3.31)$$

(The fermion fields are now labeled with a prime, to distinguish them from the basis we are about to introduce.) It therefore appears that the masses of Standard Model fermions are actually 3×3 complex matrices.

It is most convenient to work in a basis in which the fermion masses are real and positive, so that the Feynman propagators are simple. This can always be accomplished, thanks to the following:

Mass Diagonalization Theorem. Any complex matrix M can be diagonalized by a biunitary transformation:

$$U_L^\dagger M U_R = M_D \quad (11.3.32)$$

where M_D is diagonal with positive real entries, and U_L and U_R are unitary matrices.

To apply this in the present case, consider the following redefinition of the lepton fields:

$$\ell'_{Li} = L_{Li}{}^j \ell_{Lj}, \quad \ell'_{Ri} = L_{Ri}{}^j \ell_{Rj}. \quad (11.3.33)$$

where $L_{Li}{}^j$ and $L_{Ri}{}^j$ are unitary 3×3 matrices. The lepton mass term in the unitary gauge Lagrangian then becomes:

$$\mathcal{L} = - \left(1 + \frac{h}{v}\right) \bar{\ell}_L^i (L_L^\dagger \mathbf{m}_e L_R)_i{}^j \ell_{Rj}. \quad (11.3.34)$$

Now, the theorem just stated assures us that we can choose the matrices L_L and L_R so that:

$$L_L^\dagger \mathbf{m}_e L_R = \begin{pmatrix} m_e & 0 & 0 \\ 0 & m_\mu & 0 \\ 0 & 0 & m_\tau \end{pmatrix}. \quad (11.3.35)$$

So we can write in terms of the unprimed (mass eigenstate) fields:

$$\mathcal{L} = - \left(1 + \frac{h}{v}\right) (m_e \bar{e}e + m_\mu \bar{\mu}\mu + m_\tau \bar{\tau}\tau). \quad (11.3.36)$$

In the same way, one can do unitary-matrix redefinitions of the quark fields:

$$d'_{Li} = D_{Li}{}^j d_{Lj}, \quad d'_{Ri} = D_{Ri}{}^j d_{Rj}, \quad (11.3.37)$$

$$u'_{Li} = U_{Li}{}^j u_{Lj}, \quad u'_{Ri} = U_{Ri}{}^j u_{Rj}, \quad (11.3.38)$$

chosen in such a way that

$$D_L^\dagger \mathbf{m}_d D_R = \begin{pmatrix} m_d & 0 & 0 \\ 0 & m_s & 0 \\ 0 & 0 & m_b \end{pmatrix}, \quad (11.3.39)$$

$$U_L^\dagger \mathbf{m}_u U_R = \begin{pmatrix} m_u & 0 & 0 \\ 0 & m_c & 0 \\ 0 & 0 & m_t \end{pmatrix}, \quad (11.3.40)$$

with real and positive diagonal entries.

It might now seem that worrying about the possibility of non-diagonal 3×3 Yukawa matrices was just a waste of time, but one must now consider how these field redefinitions from primed (gauge eigenstate) to unprimed (mass eigenstate) fields affect the other terms in the Lagrangian. First, consider the derivative kinetic terms. For the leptons, \mathcal{L} contains

$$i \bar{\ell}_L^{j'} \not{\partial} \ell'_{Lj} = i (\bar{\ell}_L L_L^\dagger)^j \not{\partial} (L_L \ell_L)_j = i \bar{\ell}_L^j \not{\partial} \ell_{Lj}. \quad (11.3.41)$$

This relies on the fact that the (constant) field redefinition matrix L_L is unitary, $L_L^\dagger L_L = 1$. The same thing works for all of the other derivative kinetic terms, for example, for right-handed up-type quarks:

$$i \bar{u}_R^{j'} \not{\partial} u'_{Rj} = i (\bar{u}_R U_R^\dagger)^j \not{\partial} (U_R u_R)_j = i \bar{u}_R^j \not{\partial} u_{Rj}, \quad (11.3.42)$$

which relies on $U_R^\dagger U_R = 1$. So the redefinition has no effect at all here; the form of the derivative kinetic terms is exactly the same for unprimed fields as for primed fields.

There are also interactions of fermions with gauge bosons. For example, for the right-handed leptons, the QED Lagrangian contains a term

$$-eA_\mu \bar{\ell}_R^{j'} \gamma^\mu \ell'_{Rj} = -eA_\mu (\bar{\ell}_R L_R^\dagger)^j \gamma^\mu (L_R \ell_R)_j = -eA_\mu \bar{\ell}_R^j \gamma^\mu \ell_{Rj}. \quad (11.3.43)$$

Just as before, the unitary condition (this time $L_R^\dagger L_R = 1$) guarantees that the form of the Lagrangian term is exactly the same for unprimed fields as for primed fields. You can show quite easily that the same thing applies to interactions of all fermions with Z_μ and the gluon fields. The unitary redefinition matrices for quarks just commute with the $SU(3)_c$ generators, since they act on different indices.

But, there is one place in the Standard Model where the above argument does not work, namely the interactions of W^\pm vector bosons. This is because the W^\pm interactions involve two different types of fermions, with different unitary redefinition matrices. Consider first the interactions of the W^\pm with leptons. In terms of the original primed fields:

$$\mathcal{L} = -\frac{g}{\sqrt{2}} W_\mu^+ \bar{\nu}'^i \gamma^\mu \ell'_{Li} + \text{c.c.}, \quad (11.3.44)$$

so that

$$\mathcal{L} = -\frac{g}{\sqrt{2}} W_\mu^+ \bar{\nu}'^i \gamma^\mu (L_L \ell_L)_i + \text{c.c.} \quad (11.3.45)$$

Since we did not include a Yukawa coupling or mass term for the neutrinos, we did not have to make a unitary redefinition for them. But now we are free to do so; defining ν_i in the same way as the corresponding charged leptons, $\nu'_i = L_L \nu_j$, we get,

$$\bar{\nu}'^i = (\bar{\nu} L_L^\dagger)^i, \quad (11.3.46)$$

resulting in

$$\mathcal{L} = -\frac{g}{\sqrt{2}} W_\mu^+ \bar{\nu}^i \gamma^\mu \ell_{Li} + \text{c.c.} \quad (11.3.47)$$

So once again the interactions of W^\pm bosons have exactly the same form for mass-eigenstate leptons. However, consider the interactions of W^\pm bosons with quarks. In terms of the original primed fields,

$$\mathcal{L} = -\frac{g}{\sqrt{2}} W_\mu^+ \bar{u}'^i_L \gamma^\mu d'_{Li} + \text{c.c.}, \quad (11.3.48)$$

which becomes:

$$\mathcal{L} = -\frac{g}{\sqrt{2}} W_\mu^+ \bar{u}^i_L \gamma^\mu (U_L^\dagger D_L d_L)_i + \text{c.c.} \quad (11.3.49)$$

There is no reason why $U_L^\dagger D_L$ should be equal to the unit matrix, and in fact it is not. So we have finally encountered a consequence of going to the mass-eigenstate basis. The charged-current weak interactions contain a non-trivial matrix operating in quark family space,

$$V = U_L^\dagger D_L, \quad (11.3.50)$$

called the Cabibbo-Kobayashi-Maskawa matrix (or CKM matrix). The CKM matrix V is itself unitary, since $V^\dagger = (U_L^\dagger D_L)^\dagger = D_L^\dagger U_L$, implying that $V^\dagger V = V V^\dagger = 1$. But, it cannot be removed by going to some other basis using a further unitary matrix without ruining the diagonal quark masses. So we are stuck with it.

One can think of V as just a unitary rotation acting on the left-handed down quarks. From eq. (11.3.49), we can define

$$d'_{Li} = V_i^j d_{Lj}, \quad (11.3.51)$$

where the d_{Lj} are mass eigenstate quark fields, and the d'_{Li} are the quarks that interact in a simple way with W bosons:

$$\mathcal{L} = -\frac{g}{\sqrt{2}} W_\mu^+ \bar{u}_L^i \gamma^\mu d'_{Li} + \text{c.c.}, \quad (11.3.52)$$

and so in terms of mass eigenstate quark fields:

$$\mathcal{L} = -\frac{g}{\sqrt{2}} V_i^j W_\mu^+ \bar{u}_L^i \gamma^\mu d_{Lj} + \text{c.c.} \quad (11.3.53)$$

This is the entire effect of the non-diagonal Yukawa matrices.

The numerical entries of the CKM matrix are a subject of continuing experimental investigation. To a first approximation, it turns out that the CKM mixing is just a rotation of down and strange quarks:

$$V = \begin{pmatrix} \cos \theta_c & \sin \theta_c & 0 \\ -\sin \theta_c & \cos \theta_c & 0 \\ 0 & 0 & 1 \end{pmatrix} \quad (11.3.54)$$

where θ_c is called the Cabibbo angle. This implies that the interactions of W^+ with the mass-eigenstate quarks are very nearly:

$$\mathcal{L} = -\frac{g}{\sqrt{2}} W_\mu^+ \left(\cos \theta_c [\bar{u}_L \gamma^\mu d_L + \bar{c}_L \gamma^\mu s_L] + \sin \theta_c [\bar{u}_L \gamma^\mu s_L - \bar{c}_L \gamma^\mu d_L] + \bar{t}_L \gamma^\mu b_L \right). \quad (11.3.55)$$

The terms proportional to $\sin \theta_c$ are responsible for strangeness-changing decays. Numerically,

$$\cos \theta_c \approx 0.974, \quad \sin \theta_c \approx 0.23. \quad (11.3.56)$$

Strange hadrons have long lifetimes because they decay through the weak interactions, and with reduced matrix elements that are proportional to $\sin^2 \theta_c = 0.05$.

More precisely, the CKM matrix is:

$$V = \begin{pmatrix} V_{ud} & V_{us} & V_{ub} \\ V_{cd} & V_{cs} & V_{cb} \\ V_{td} & V_{ts} & V_{tb} \end{pmatrix} \approx \begin{pmatrix} 0.9743 & 0.2252 & 0.004 \\ 0.230 & 0.975 & 0.041 \\ 0.008 & 0.04 & 0.999 \end{pmatrix}, \quad (11.3.57)$$

where the numerical values given are estimates of the magnitude only (not the sign or phase). In fact, the CKM matrix contains one phase that cannot be removed by redefining phases of the fermion fields. This phase is the only source of CP violation in the Standard Model.

Weak decays of mesons involving the W bosons allow the entries of the CKM matrix to be probed experimentally. For example, decays

$$B \rightarrow \bar{D}\ell^+\nu_\ell, \quad (11.3.58)$$

where B is a meson containing a bottom quark and \bar{D} contains a charm quark, can be used to extract $|V_{cb}|$. The very long lifetimes of B mesons are explained by the fact that $|V_{ub}|$ and $|V_{cb}|$ are very small. One of the ways of testing the Standard Model is to check that the CKM matrix is indeed unitary:

$$V^\dagger V = 1, \quad (11.3.59)$$

which implies in particular that $V_{ud}V_{ub}^* + V_{cd}V_{cb}^* + V_{td}V_{tb}^* = 0$. This is an automatic consequence of the Standard Model, but if there is further unknown physics out there, then the weak interactions could appear to violate CKM unitarity.

The partial decay widths and branching ratios of the W boson can be worked out from eqs. (11.3.47) and (11.3.53), and agree well with the experimental results:

$$\text{BR}(W^+ \rightarrow \ell^+\nu_\ell) = 0.1086 \pm 0.0009 \quad (\text{for } \ell = e, \mu, \tau, \text{ each}) \quad (11.3.60)$$

$$\text{BR}(W^+ \rightarrow \text{hadrons}) = 0.6741 \pm 0.0027. \quad (11.3.61)$$

where the “hadrons” refers mostly to Cabibbo-allowed final states $u\bar{d}$ and $c\bar{s}$, with a much smaller contribution from the Cabibbo-suppressed final states $c\bar{d}$ and $u\bar{s}$. The $t\bar{b}$ final state is of course not available due to kinematics; this implies the useful fact that (up to a very small effect from CKM mixing) b quarks do not result from W decays in the Standard Model.

Also, the very small magnitudes of V_{td} and V_{ts} imply that top quarks decay to bottom quarks almost every time:

$$\text{BR}(t \rightarrow W^+b) \approx 1. \quad (11.3.62)$$

This greatly simplifies the experimental identification of top quarks.

11.4 Neutrino masses and the seesaw mechanism

Evidence from observation of neutrinos produced in the Sun, the atmosphere, accelerators, and reactors have now established that neutrinos do have mass. In the renormalizable version of the Standard Model given up to here, this cannot be explained. The basic reason for this is the absence of right-handed neutrinos from the list in eq. (11.1.35). To remedy the situation, we can add three right-handed fermions that are singlets under all three components of the gauge group $SU(3)_c \times SU(2)_L \times U(1)_Y$:

$$N_{R1}, N_{R2}, N_{R3} \longleftrightarrow (\mathbf{1}, \mathbf{1}, 0). \quad (11.4.1)$$

With these additional gauge-singlet right-handed neutrino degrees of freedom, it is now possible to write down a gauge-invariant Lagrangian interaction of the neutrinos with the Higgs field:

$$\mathcal{L}_{\nu \text{ neutrino Yukawas}} = - \begin{pmatrix} \bar{\nu}^i & \bar{\ell}_L^i \end{pmatrix} \begin{pmatrix} \phi^{0*} \\ -\phi^{+*} \end{pmatrix} \mathbf{y}_{\nu i}^j N_{Rj} + \text{c.c.} \quad (11.4.2)$$

Note the similarity of this with the up-type quark Yukawa couplings in eq. (11.3.26). Going to unitary gauge, one obtains a neutrino mass matrix

$$\mathbf{m}_{\nu i}^j = \frac{v}{\sqrt{2}} \mathbf{y}_{\nu i}^j. \quad (11.4.3)$$

just as in eq. (11.3.31) for the Standard Model charged fermions. This neutrino mass matrix can be diagonalized to obtain the physical neutrino masses as the absolute values of its eigenvalues. The neutrinos in this scenario are Dirac fermions, as the mass term couples together left-handed and right-handed degrees of freedom that are independent.

Although the magnitudes of the neutrino masses are not yet determined by experiment, there are strong upper bounds, as seen in Table 1.2 in the Introduction. Also, limits from the WMAP and Planck measurements of the cosmic background radiation, interpreted within the standard cosmological model, implies that the sum of the three Standard Model neutrinos should be at most 0.17 eV. Neutrino oscillation data do not constrain the individual neutrino masses, but imply that the largest differences between squared masses should be less than $3 \times 10^{-3} \text{ eV}^2$. So, several independent pieces of evidence indicate that neutrino masses are much smaller than any of the charged fermion masses. To accommodate this within the Dirac mass framework of eq. (11.4.3), the eigenvalues of the neutrino Yukawa matrix $\mathbf{y}_{\nu i}^j$ would have to be extremely small, no larger than about 10^{-9} . Such small dimensionless couplings appear slightly unnatural, in a purely subjective sense, and this suggests that neutrino masses may have a different origin than quark and leptons masses.

The seesaw mechanism is a way of addressing this problem, such that very small neutrino masses naturally occur, even if the corresponding Yukawa couplings are of order 1. One includes,

besides eq. (11.4.2), a new term in the Lagrangian:

$$\mathcal{L} = -\frac{1}{2}\mathbf{M}^{ij}\overline{N}_iN_j, \quad (11.4.4)$$

where N_i are the Majorana fermion fields (see section 3.4) that include N_{Ri} , and \mathbf{M}^{ij} is a symmetric mass matrix. If the neutrino fields carry lepton number 1, then this Majorana mass term necessarily violates the total lepton number $L = L_e + L_\mu + L_\tau$. Now the total mass matrix for the left-handed neutrino fields ν_{Li} and the right-handed neutrino fields N_{Ri} , including both eq. (11.4.3) and eq. (11.4.4), is:

$$\mathcal{M} = \begin{pmatrix} 0 & \frac{v}{\sqrt{2}}\mathbf{y}_\nu \\ \frac{v}{\sqrt{2}}\mathbf{y}_\nu^T & \mathbf{M} \end{pmatrix}. \quad (11.4.5)$$

The point of the seesaw mechanism is that if the eigenvalues of \mathbf{M} are much larger than those of the Dirac mass matrix $\frac{v}{\sqrt{2}}\mathbf{y}_\nu$, then the smaller set of mass eigenvalues of \mathcal{M} will be pushed down. Since \mathbf{M} does not arise from electroweak symmetry breaking, it can naturally be very large. For illustration, taking \mathbf{M} and \mathbf{y}_ν to be 1×1 matrices, the absolute values of the neutrino mass eigenvalues of \mathcal{M} are approximately:

$$\frac{v^2\mathbf{y}_\nu^2}{2\mathbf{M}}, \quad \text{and} \quad \mathbf{M} \quad (11.4.6)$$

in the limit $v\mathbf{y}_\nu \ll \mathbf{M}$. For example, to get a neutrino mass of order 0.1 eV, one could have $\mathbf{y}_\nu = 1.0$ and $\mathbf{M} = 3 \times 10^{14}$ GeV, or $\mathbf{y}_\nu = 0.1$ and $\mathbf{M} = 3 \times 10^{12}$ GeV. The light neutrino states (corresponding to the lighter eigenvectors of \mathcal{M}) are mostly the Standard Model ν_L and they are Majorana fermions. There are also three extremely heavy Majorana neutrino mass eigenstates, which decouple from present weak interaction experiments. The fact that the magnitude of \mathbf{M} necessary to make this work is not larger than the Planck scale, and is very roughly commensurate with other scales that occur in other theories such as supersymmetry, is encouraging. In any case, the ease with which the seesaw mechanism accommodates very small but non-zero neutrino masses has made it a favorite scenario of theorists.

In either of the two cases above, the left-handed parts of the neutrino mass eigenstates ν_1, ν_2, ν_3 (with masses $m_1 < m_2 < m_3$) can be related to the left-handed parts of the neutrino weak-interaction eigenstates ν_e, ν_μ, ν_τ (which each couple to the corresponding charged lepton only, and the W boson) by:

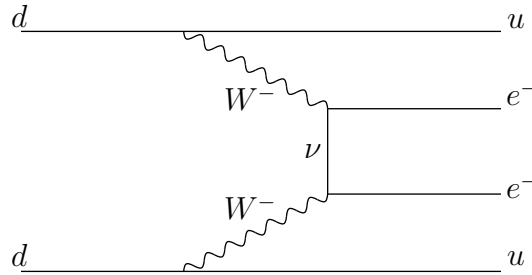
$$\begin{pmatrix} \nu_{eL} \\ \nu_{\mu L} \\ \nu_{\tau L} \end{pmatrix} = \mathcal{U} \begin{pmatrix} \nu_{1L} \\ \nu_{2L} \\ \nu_{3L} \end{pmatrix}, \quad (11.4.7)$$

where \mathcal{U} is a unitary matrix known as the Pontecorvo-Maki-Nakagawa-Sakata (PMNS) matrix. Neutrino oscillations are due to the fact that \mathcal{U} is not equal to the identity matrix.

To recap, by introducing right-handed gauge-singlet neutrino degrees of freedom, there are two distinct scenarios for neutrino masses. In the Dirac scenario, neutrinos and antineutrinos are distinct, and total lepton number is conserved although the individual lepton numbers are violated. In the Majorana scenario, neutrinos are their own antiparticles, and total lepton number is violated along with the individual lepton numbers. At this writing, both possibilities are consistent with the experimental data. To tell the difference between these two scenarios, one can look for neutrinoless double beta decay, i.e. a nuclear transition

$${}^AZ \rightarrow {}^A(Z+2) + e^-e^-, \quad (11.4.8)$$

(at the nucleon level $nn \rightarrow ppe^-e^-$), which can proceed via the quark-level Feynman diagram shown below.



Since this process requires a violation of total lepton number in the neutrino propagator, it can only occur in the case of Majorana neutrinos. It is the subject of continuing searches.

11.5 The Higgs boson discovery

One of the most momentous discoveries of the last half century was that of the Higgs boson. Before its discovery in 2012, its properties and even its existence were in doubt, despite the many successes of the Standard Model. Research publications on “Higgsless theories” had persisted to the very end. As discussed above, the simplest path to achieve masses for the W and Z bosons and the fermions of the Standard Model is to introduce a single scalar Higgs boson doublet that condenses, breaking electroweak symmetry down to the $U(1)_{\text{EM}}$. The fluctuation around this background value is the Higgs boson. However, when the theory was first formulated, there was little guidance as to what mass it should have. One only knew that it was controlled by the vacuum expectation value, which was known to be $v \simeq 246 \text{ GeV}$, and a dimensionless constant λ that was completely unknown, leading to an unknown mass $m_h = \sqrt{2\lambda}v$, as we saw in eq. (11.2.29).

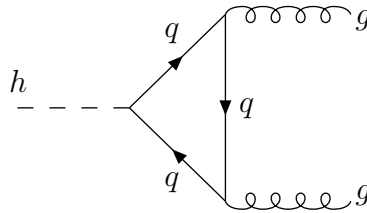
Experiments had been searching for the Higgs boson for decades without success. Just prior to its discovery, evidence from the sum of data collected from the Z pole experiments at CERN LEP and SLAC SLC, combined with the top quark and W mass measurements at Tevatron

and LEP2 at CERN, suggested that if the Standard Model is the underlying theory of the weak scale, then the Higgs boson mass needed to be in the range $114 \text{ GeV} < m_h \lesssim 180 \text{ GeV}$ at 95% confidence level. It should be emphasized that the lower bound of 114 GeV was derived directly by not seeing the Higgs boson produced and decay at LEP2, whereas the upper bound was derived indirectly, and thus less reliably, by a global analysis of compatibility to all data that is sensitive to the Higgs boson mass, via quantum loops. A problem with this kind of indirect bound is that it is always possible that some other unsuspected particle(s) also contribute in the loops, interfering with the Higgs boson contribution.

Below, we will review the physics of the Higgs boson discovery at the LHC, starting with a discussion of the decay modes.

11.5.1 Higgs boson decays revisited

In section 6.3, we have already calculated the leading-order decays of the Higgs boson into fermion-antifermion final states. However, there are other final states that are quite important besides $h \rightarrow f\bar{f}$. First, the Higgs boson can decay into two gluons, $h \rightarrow gg$, with the gluons eventually manifesting themselves in the detector as jets. This decay cannot happen at tree level, but does occur through the one-loop diagram below, where quarks go around the loop:



(One must also include the diagram with the gluons exchanged, or equivalently the diagram with the quarks running the other direction around the loop.) Even though one-loop graph amplitudes are usually not competitive with tree-level amplitudes, this is an exception because the gluons have strong couplings and because the top quark with its large y_t participates in the loop diagrams, while in the on-shell 2-body decays to fermions, only lighter fermions (with much smaller Yukawa couplings) can appear.

The resulting partial decay width for $h \rightarrow gg$ depends on the quark masses in two places. First, at the $hq\bar{q}$ vertex there is a Yukawa coupling, and second there needs to be a chirality flip in one of the propagators to enable a non-zero result. That is, the trace over the three fermion propagator numerators vanishes (due to an odd number of γ matrices) unless one of the propagators is traced over the mass term. These two facts explain why the top quark, being by far the most massive quark, gives a dominant contribution to this amplitude.

The spin-summed squared amplitude for the $h \rightarrow gg$ transition is

$$\sum |\mathcal{M}|^2 = \frac{m_h^4}{v^2} \left(\frac{\alpha_s}{\pi} \right)^2 \left| \sum_q A_{1/2}(\tau_q) \right|^2, \quad (11.5.1)$$

where the sum is over quark flavors $q = t, b, c, \dots$ with $\tau_q \equiv 4m_q^2/m_h^2$ and the kinematic function from doing the 1-loop integration is:

$$A_{1/2}(\tau) = \tau + \tau(1 - \tau)f(\tau) \quad (11.5.2)$$

where

$$f(\tau) = \begin{cases} \left[\sin^{-1}(1/\sqrt{\tau}) \right]^2, & (\text{for } \tau \geq 1), \\ -\frac{1}{4} \left[\ln \left(\frac{1+\sqrt{1-\tau}}{1-\sqrt{1-\tau}} \right) - i\pi \right]^2 & (\text{for } \tau \leq 1). \end{cases} \quad (11.5.3)$$

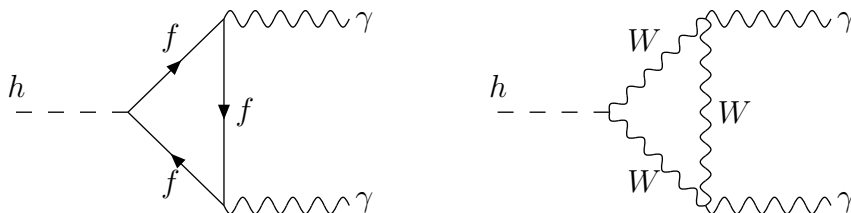
In the limit of small τ , the function $A_{1/2}(\tau)$ is proportional to τ and therefore to m_q^2/m_h^2 , so that to a very good approximation all quark contributions except for the top quark can indeed be neglected, consistent with the expectation explained in the previous paragraph. For large τ , appropriate for the top-quark contribution, the function $A_{1/2}(\tau)$ approaches a constant, with $A_{1/2}(\tau) = \frac{2}{3} + \frac{7}{45\tau} + \dots$

The partial width into gg can therefore be approximated as

$$\Gamma(h \rightarrow gg) = \frac{\sum |\mathcal{M}|^2}{32\pi m_h} = \frac{m_h^3}{32\pi v^2} \left(\frac{\alpha_s}{\pi} \right)^2 |A_{1/2}(\tau_t)|^2 \quad (11.5.4)$$

The first equality can be obtained from eqs. (6.2.14)-(6.2.15). Keep in mind that there is a factor of 1/2 from the indistinguishability of the gluons; otherwise each kinematic configuration of gluons would be double counted when the final state phase space is integrated over. Using $\alpha_s = 0.118$, $m_t = 173 \text{ GeV}$, $m_h = 125 \text{ GeV}$, and $v = 246 \text{ GeV}$, one finds $\Gamma(h \rightarrow gg) = 0.214 \text{ MeV}$. This is in contrast to a more complete and state-of-the-art computation, which instead gives $\Gamma(h \rightarrow gg + X) = 0.349 \text{ MeV}$, where X represents anything (including nothing). The reason for the discrepancy is that higher loop contributions and the radiation of additional soft gluons enhance the decay partial width.

The decay $h \rightarrow \gamma\gamma$ also is absent at tree-level, but does occur due to one-loop graphs where any charged particle goes around the loop. This again includes notably the top quark, but now the largest contribution is due to the W boson. The two most important Feynman diagrams are:



The resulting partial decay width is:

$$\Gamma(h \rightarrow \gamma\gamma) = \frac{m_h^3}{64\pi v^2} \left(\frac{\alpha}{\pi} \right)^2 \left| A_1(\tau_W) + \sum_f N_c^f Q_f^2 A_{1/2}(\tau_f) \right|^2 \quad (11.5.5)$$

where the sum is over $f = t, b, c, s, u, d$ and τ, μ, e , with $N_c^f = 3$ for quarks and $N_c^f = 1$ for leptons, with $Q_{t,c,u} = 2/3$ and $Q_{b,s,d} = -1/3$ and $Q_{\tau,\mu,e} = -1$, with $\tau_W = 4m_W^2/m_h^2$ and $\tau_f = 4m_f^2/m_h^2$, and

$$A_1(\tau) = 3\tau(\tau/2 - 1)f(\tau) - 3\tau/2 - 1, \quad (11.5.6)$$

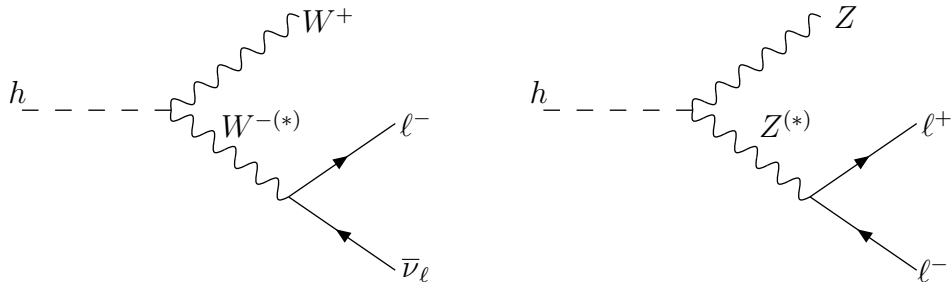
where $f(\tau)$ is the same function as appears in $A_{1/2}(\tau)$, and was given already in eq. (11.5.3). Although the resulting branching ratio to two photons is much smaller (about 2.3×10^{-3} in the Standard Model with $m_h = 125$ GeV, after taking into account higher-order corrections), it is still important because the corresponding backgrounds at colliders are also small.

The decay $h \rightarrow Z\gamma$ is also mediated by similar one-loop graphs, but it will not be reviewed here because it turns out to be quite small and not as useful, once the corresponding background rates are taken into account. It has still not been observed, but even this non-observation can constrain some non-minimal models.

Also significant are decays through two massive vector bosons, $h \rightarrow W^+W^-$ and $h \rightarrow ZZ$, corresponding to the Feynman rules found in section 11.2 [below eq. (11.2.26)] are important. In fact, these decays are important even if (as turns out to be true in the real world) $m_h < 2m_W$ and $m_h < 2m_Z$, despite the on-shell decays being forbidden so that one of the vector bosons must be virtual. One usually indicates this by writing

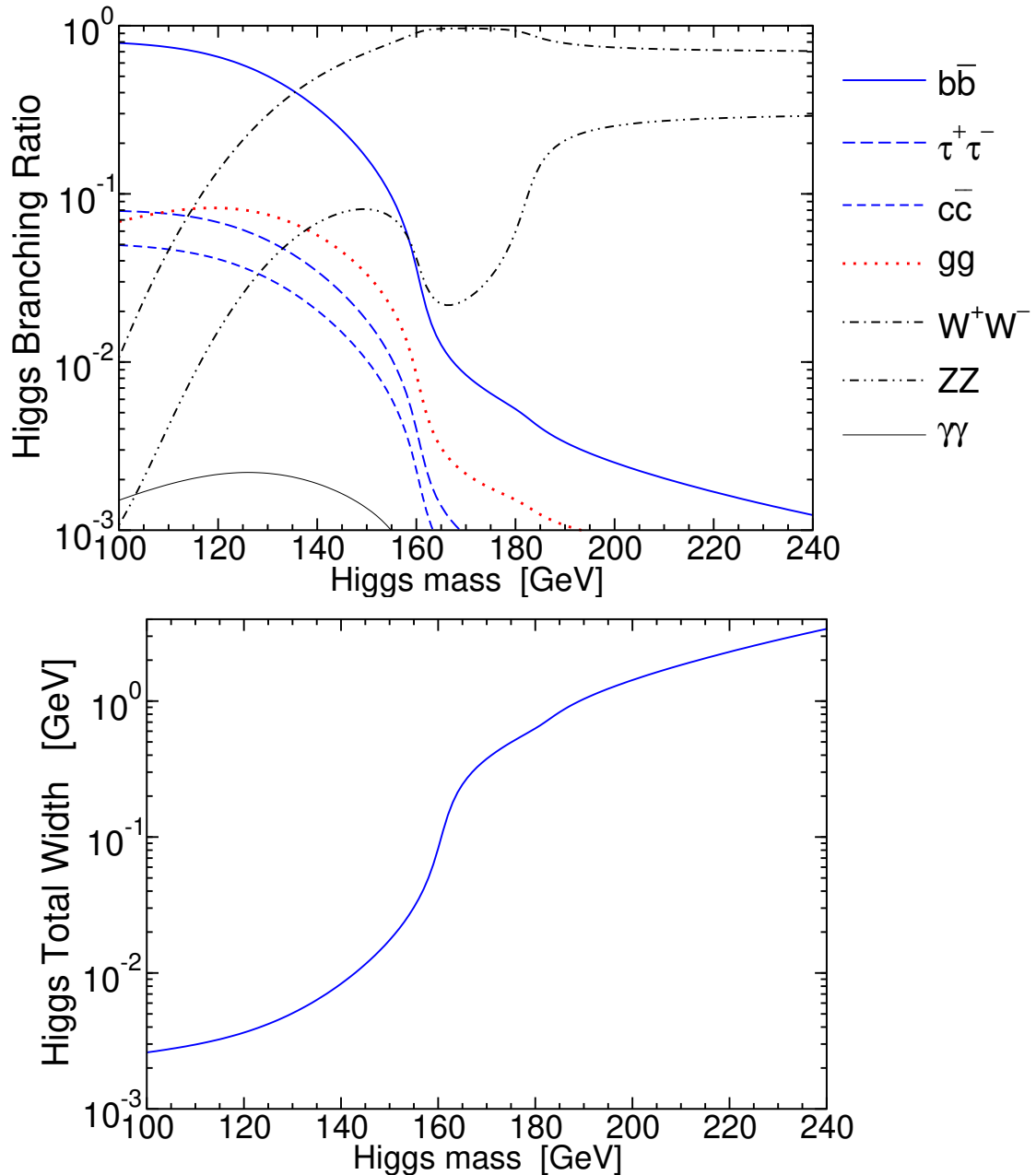
$$h \rightarrow WW^{(*)}, \quad h \rightarrow ZZ^{(*)}, \quad (11.5.7)$$

where the “(*)” means that the corresponding particle may be off-shell, depending on the kinematics. If one of the vector bosons is off-shell, then the decay can be thought of as really three-body. This means that the decay is really $h \rightarrow W^\pm f \bar{f}'$ or $h \rightarrow Z f \bar{f}$, where $f \bar{f}'$ is any final state that couples to the off-shell W^\pm , and $f \bar{f}$ is any fermion-antifermion final state that couples to the off-shell Z . For example, for leptonic final states of the off-shell vector boson:



Since the competing tree-level two-body decays $h \rightarrow f\bar{f}$ are suppressed by small Yukawa couplings, these three-body decays are competitive, despite their kinematic suppression. If we take m_h to be a free variable, as it was before the discovery, then the closer the vector bosons are to being on-shell, the larger the amplitude will be. The decays $h \rightarrow WW^{(*)}$ become increasingly important for larger m_h , and would actually dominate if $m_h \gtrsim 135$ GeV.

The results of a careful computation (using the program HDECAY by A. Djouadi, J. Kalinowski, and M. Spira, Comput. Phys. Commun. **108**, 56, (1998), hep-ph/9704448) including all these effects are shown in the two graphs below, which depict the state-of-the-art computations of the branching ratios and the total width Γ_{tot} for the Higgs boson, as a function of m_h for the range allowed before the discovery in 2012.



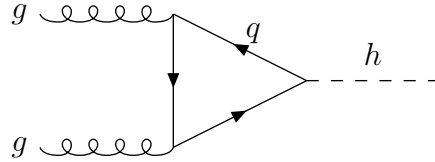
The largest decay modes were predicted to be $b\bar{b}$ and/or $WW^{(*)}$ over the entire range of m_h , with the total width dramatically increasing when both W bosons can be on shell. However, because it has very low backgrounds in colliders, the $\gamma\gamma$ final state was understood to be very important for the discovery of a light Higgs boson, despite its tiny branching ratio. The $ZZ^{(*)}$ final state is also important because it can lead to low-background signals if both of the Z bosons decay to leptons. Note that the gg final state is useless as a discovery mode because of huge QCD backgrounds to dijet production, but it is important to keep track of for two reasons. First, its presence reduces the branching ratios into the more useful final states. Second, it is related, by crossing symmetry, to the largest production cross-section mode, as we discuss next.

11.5.2 Higgs boson production at the LHC

At hadron colliders such as the LHC, the largest parton-level production processes for the Higgs boson is:

$$gg \rightarrow h, \quad (11.5.8)$$

This process cannot occur at tree-level, but it does occur due to the same one-loop diagram mentioned above in section 11.5.3 for the decay $h \rightarrow gg$. The roles of the initial state and the final state are simply exchanged, by crossing:



Although the amplitude is loop-suppressed, the large gluon PDFs at the LHC make it by far the most important production mode for a 125 GeV Higgs boson at the LHC, with a cross-section exceeding that of the next largest, the W -boson fusion process discussed below, by more than an order of magnitude. It was the process that figured most prominently in the initial discovery.

At leading order, the production cross-section for $gg \rightarrow h$ is directly proportional to the decay width $h \rightarrow gg$, by crossing symmetry. To see this connection, we begin with the generalized cross-section formula for initial state massless states with four-momentum p_a and p_b scattering to a single final state particle with four-momentum $k = (E, \vec{k})$, with $E = \sqrt{|\vec{k}|^2 + m_h^2}$ in the present case. From eqs. (4.5.32) and (4.5.33) with $n = 1$, and $|\vec{v}_a - \vec{v}_b| = 2$ and $4E_a E_b = \hat{s}$ in the center of momentum frame, we obtain:

$$d\hat{\sigma} = \frac{1}{2\hat{s}} \left(\frac{d^3\vec{k}}{(2\pi)^3} \frac{1}{2E} \right) \left(\frac{1}{4} \cdot \frac{1}{64} \cdot |\mathcal{M}|^2 \right) (2\pi)^4 \delta^{(4)}(p_a + p_b - k). \quad (11.5.9)$$

By crossing symmetry, $\sum |\mathcal{M}|^2$ is the same spin-summed and color-summed squared matrix element as in the decay calculation, but here it comes with the prefactor $\frac{1}{4} \cdot \frac{1}{64}$, since in this case we need to average (instead of sum) over initial state gluon spins (2 spins) and color factors (8 gluons $g^{a=1\dots 8}$). Since the cross-section is invariant under boosts along the beam direction we chose to work in the center-of-momentum frame where $\vec{p}_a + \vec{p}_b = 0$, so that the delta function vanishes except for $\vec{k} = 0$. For on-shell production of the Higgs boson, $E = \sqrt{\hat{s}} = m_h$.

Integrating Eq. (11.5.9) over the three-momentum \vec{k} and collecting terms we find that

$$\hat{\sigma} = \frac{\pi}{256m_h^2} \delta(\hat{s} - m_h^2) \sum |\mathcal{M}|^2 \quad (11.5.10)$$

Now, from eq. (11.5.4) we know that $\sum |\mathcal{M}|^2 = 32\pi m_h \Gamma$ and so the cross-section of $gg \rightarrow h$ can be obtained by knowing the partial decay width $h \rightarrow gg$:

$$\hat{\sigma}(gg \rightarrow h) = \frac{\pi^2}{8m_h} \Gamma(h \rightarrow gg) \delta(\hat{s} - m_h^2). \quad (11.5.11)$$

The δ function dependence of the cross-section corresponds to the fact that free, on-shell asymptotic states cannot scatter 2-to-1 unless the four-momenta of the first two particles $p_{a,b}^\mu$ are precisely arranged to construct the final momentum $k = p_1 + p_2$ such that $k^2 = m_h^2$. Unlike 2-to-2 scattering not just any sufficiently large incoming momenta will do. In the center of mass frame this requires that $E = m_h$ and $\vec{k} = 0$.

More generally, there is no way to allow $AB \rightarrow C$ particle scattering unless $m_A + m_B \leq m_C$. However, if that is allowed, then $C \rightarrow AB$ decays are allowed with the same amplitude, giving C a decay width. The decay width means that there is a finite spread of k^2 around m_C^2 (with the finite spread being determined by Γ_C) such that $AB \rightarrow C$ is allowed. The finite spread is the Breit-Wigner width, which is characterized by replacing the δ -function with

$$\delta(\hat{s} - m_h^2) \rightarrow \frac{1}{\pi} \frac{m_h \Gamma_h}{(\hat{s} - m_h^2)^2 + m_h^2 \Gamma_h^2}. \quad (11.5.12)$$

This is the correct physical and non-singular interpretation of the δ -function in Eq. (11.5.10), as one can show by treating the Higgs boson as a virtual intermediate state with a Feynman propagator. In practice, if the width is much less than the mass $\Gamma_h \ll m_h$, which is certainly the case for the Standard Model Higgs boson at 125 GeV (for which the total width is $\Gamma_h = 4.2$ MeV, so $\Gamma_h/m_h \simeq 3.4 \times 10^{-5}$), then the δ function is a good approximation. In general, replacing the Breit-Wigner peak with a δ -function is called the “narrow width approximation.”

In our case the narrow width approximation is useful and appropriate because we need to integrate over gluon-gluon luminosity in the very close neighborhood of $\sqrt{\hat{s}_{gg}} = m_h$, and the integrand hardly varies over the narrow width of the Higgs Breit-Wigner function. Writing $g(x)$ for the pdf of gluons at momentum fraction x , the total cross section in pp collisions is

$$\sigma(pp \rightarrow h) = \int_0^1 dx_a \int_0^1 dx_b g(x_a) g(x_b) \hat{\sigma}(gg \rightarrow h) \quad (11.5.13)$$

Recall that the partonic center of mass energy is $\hat{s} = x_a x_b s$. It is convenient to define a different set of variables,

$$\tau = x_a x_b \quad \text{and} \quad x = x_a. \quad (11.5.14)$$

The Jacobian of this variable change is $J = 1/x$, so that

$$\sigma(pp \rightarrow h) = \int_0^1 d\tau \int_\tau^1 \frac{dx}{x} g(x) g(\tau/x) \hat{\sigma}(\tau s). \quad (11.5.15)$$

With these integration variables, the parton-level cross-section $\hat{\sigma}$ is a function of $\hat{s} = \tau s$ only, and not x , so we can perform the x integral over the gluon PDFs separately. It is convenient to define a function of τ only, called the gluon-gluon luminosity function:

$$\frac{d\mathcal{L}(\tau)}{d\tau} = \int_\tau^1 \frac{dx}{x} g(x) g(\tau/x), \quad (11.5.16)$$

This leaves us with

$$\sigma(pp \rightarrow h) = \int_0^1 d\tau \frac{d\mathcal{L}(\tau)}{d\tau} \hat{\sigma}(\tau s). \quad (11.5.17)$$

For a given fixed value of m_h , the total leading-order cross-section for $pp \rightarrow h$ due to the $gg \rightarrow h$ parton-level process is therefore a simple function of s and m_h , and can be obtained by using the δ -function in $\hat{\sigma}$ to integrate over τ , with the result:

$$\sigma(pp \rightarrow h) = F_{gg}(\tau_h) \sigma_0 \quad (11.5.18)$$

where

$$\sigma_0 = \frac{\pi^2}{8m_h^3} \Gamma(h \rightarrow gg), \quad (11.5.19)$$

and

$$F_{gg}(\tau_h) = \tau_h \int_{\tau_h}^1 \frac{dx}{x} g(x) g(\tau_h/x) \quad (11.5.20)$$

is simply a dimensionless number dependent only on the ratio

$$\tau_h = m_h^2/s, \quad (11.5.21)$$

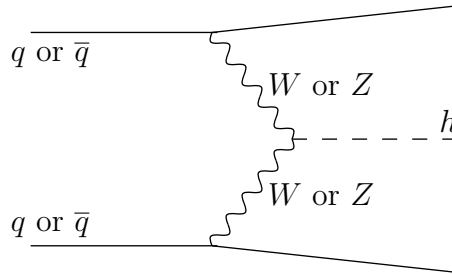
which in turn depends on the Higgs boson mass and the proton beam energy.

The numerical value of σ_0 , using the leading-order width $\Gamma(h \rightarrow gg) = 0.214$ MeV obtained above, is:

$$\sigma_0 = \frac{\pi^2}{8m_H^3} \Gamma(H \rightarrow gg) \simeq 53 \text{ fb} \quad (11.5.22)$$

Using the MSTW2008NLO parton distribution functions for gluons gives $F_{gg}(\tau_h) = 99, 127,$ and 292 for $\sqrt{s} = 7, 8,$ and 13 TeV, respectively, with $m_h = 125$ GeV (and the factorization scale in the gluon PDFs set equal to m_h). Thus, we get leading-order estimates of $\sigma(pp \rightarrow h) = 5.2$ pb, 6.7 pb, and 15.4 pb, for $\sqrt{s} = 7, 8,$ and 13 TeV, respectively. These simple estimates are considerably smaller than the results of state-of-the-art computations of $\sigma(pp \rightarrow h + X)$ coming from the CERN Higgs cross-section working group, which gives approximately 17 pb, 21 pb, and 49 pb, respectively. This increase of more than a factor of 3 compared to our results above is because of the large effects of higher-order loop corrections, the emission of additional soft gluons, and a more sophisticated use of PDFs, all of which we have not included in our simple analysis. This demonstrates the great importance of the heroic efforts that have been made to calculate such higher order effects. In addition, more sophisticated calculations provide crucial kinematic information about the kinematics of Higgs boson events, including the distribution of the transverse momenta of the Higgs boson, and the numbers and momenta of the additional jets that may be produced in the event.

Other parton-level processes that produce the Higgs boson at the LHC have smaller cross-sections, but are important because they involve additional final state particles whose presence can be used to control backgrounds. Furthermore, these processes involve different couplings, allowing tests of the proposition that the new scalar particle is really behaving as expected for the Standard Model Higgs. First, there are the weak vector boson fusion modes, which refers to the parton-level processes $qq \rightarrow qqh$, $q\bar{q} \rightarrow q\bar{q}h$, and $\bar{q}q \rightarrow \bar{q}qh$ through Feynman diagrams like this:



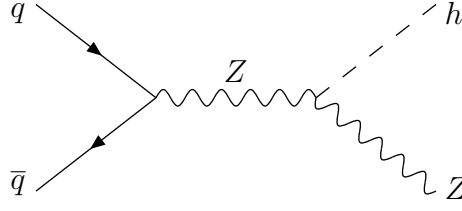
Here, the quark jets in the final state are usually found at small angles with respect to the beam. Tagging events with these forward jets is a way to reduce backgrounds.

Another type of channel features Higgs bosons that are radiated off of weak vector bosons:

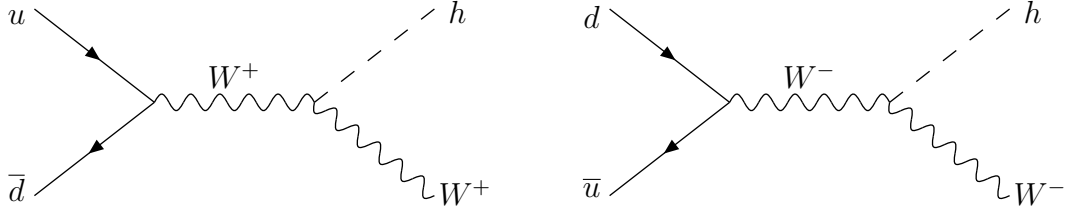
$$q\bar{q} \rightarrow Zh, \quad (11.5.23)$$

$$q\bar{q}' \rightarrow W^\pm h. \quad (11.5.24)$$

These channels provide useful modes for confirmation and study, because the presence of the extra weak boson reduces backgrounds. The process $q\bar{q} \rightarrow Zh$ occurs due to this Feynman diagram:

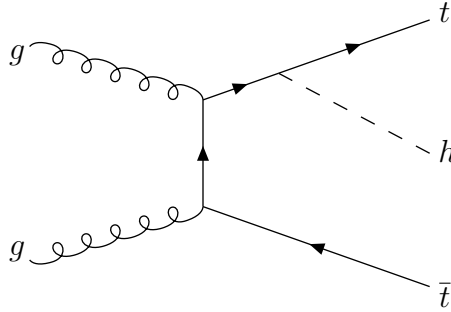


while the process $q\bar{q}' \rightarrow W^\pm h$ is due to parton-level Feynman diagrams like the ones below:



as well as others related by $d \rightarrow s$ and/or $u \rightarrow c$.

Another important process, long anticipated but only very recently observed, is $pp \rightarrow t\bar{t}h$, which is due to Feynman diagrams including the one below:



This is particularly useful as a direct test of the Higgs boson interaction with the top quark.

11.5.3 The Higgs boson discovery

The pp Large Hadron Collider experiments at CERN, ATLAS and CMS, were both designed to be able to cover the entire range of Higgs boson mass suggested by the indirect constraints on it. For much of the allowed mass region, the primary target for discovery was the decay to $\gamma\gamma$, manifested as a narrow mass peak of two photons centered on $m_h = m_{\gamma\gamma}^{\text{signal}}$. The main background, largely created by $q\bar{q} \rightarrow \gamma\gamma$, consists of a diffuse spectrum of $m_{\gamma\gamma}^{\text{bkgd}}$. There are also important contributions to the background from $gg \rightarrow \gamma\gamma$ and from fake photons.

Indeed, the diphoton signal is half of how the Higgs boson discovery was established – a peak of $\gamma\gamma$ events that ultimately could be identified with m_h . The left panel of Fig. 11.1 shows an ATLAS collaboration plot of this $\gamma\gamma$ peak after data collection at $\sqrt{s} = 7\text{ TeV}$ and 8 TeV . A similar result was obtained by CMS.

The other half of the Higgs discovery came about via $h \rightarrow ZZ^{(*)} \rightarrow 4\ell$ decays of the Higgs boson, where the $(*)$ indicates an off-shell Z boson, and 4ℓ indicates any one of the following

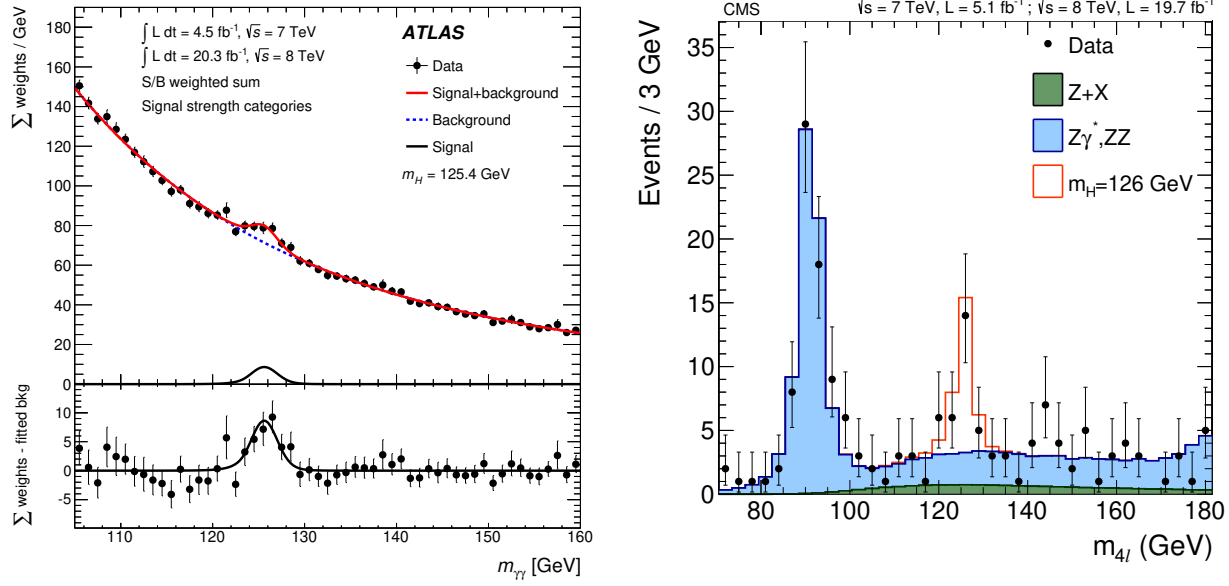


Figure 11.1: **Left panel:** The diphoton invariant mass spectrum from ATLAS data (Aad, G. *et al.* 2014 [ATLAS Collaboration], “Measurement of Higgs production in the diphoton decay channel in pp collisions at center-of-mass energies of 7 and 8 TeV with the ATLAS detector”, arXiv:1408.7084.). The upper red line is signal (from $h \rightarrow \gamma\gamma$) plus background (mostly $q\bar{q} \rightarrow \gamma\gamma$). The dashed blue line is a fit to the background-only hypothesis. The black curves on the bottom show the signal expectation (black solid curve) and the background subtracted data (data circles with 68% CL vertical uncertainty bars). **Right panel:** The four-lepton invariant mass spectrum from CMS (Chatrchyan, S. *et al.* 2014 [CMS Collaboration], “Measurement of the properties of a Higgs boson in the four-lepton final state”, arXiv:1312.5353.) is shown as the black data points. The prediction from backgrounds other than the Standard Model Higgs boson are shown as the blue histogram. The red curve includes the backgrounds plus the prediction of a Higgs boson with invariant mass peak of $m_h = m_{4l} = 125$ GeV.

permutations: $e^+e^-e^+e^-$, $\mu^+\mu^-\mu^+\mu^-$ or $e^+e^-\mu^+\mu^-$. This branching fraction is very small. From eqs. (6.3.29) and (11.1.43) above, we have:

$$\text{BR}(h \rightarrow ZZ^{(*)} \rightarrow 4l) = \text{BR}(h \rightarrow ZZ^{(*)})[\text{BR}(Z \rightarrow e^+e^-) + \text{BR}(Z \rightarrow \mu^+\mu^-)]^2 \quad (11.5.25)$$

$$\approx 0.0264(0.067316)^2 \approx 0.000120. \quad (11.5.26)$$

Fortunately, the backgrounds for four leptons near an invariant mass of $m_{4l} = m_h$ are also very small. This enables a signal to be discerned above the background. This is illustrated in the right panel of Fig. 11.1, which shows a plot of the invariant mass distribution of four lepton final states recorded by the CMS collaboration in the $\sqrt{s} = 7$ TeV and 8 TeV runs. Again, a similar result was obtained by ATLAS. The consistency of the diphoton and $ZZ^{(*)} \rightarrow 4\ell$ invariant mass peaks in the ATLAS and CMS experiments then allowed a definitive discovery.

The announced discovery of the Higgs boson in July 2012 has given rise to a new era in particle physics phenomenology. The present and future research efforts of the LHC will be centered around careful measurements of the Higgs boson, as well as the search for any new particles that might be associated with it.

Further Reading

Particle Data Group *The Review of Particle Physics*. Phys. Rev. D98, 030001 (2018).
<http://pdg.lbl.gov/>.

Quantum Field Theory

Peskin, M., Schroeder, D.V. *Introduction to Quantum Field Theory*. Perseus Books (1995).
Ryder, L.H. *Quantum Field Theory* (2nd ed.) Cambridge Univ. Press (1996)
Schwartz, M.D. *Quantum Field Theory and the Standard Model*. Cambridge Univ. Press (2014).
Srednicki, M. *Quantum Field Theory*. Cambridge Univ. Press (2007).

The Standard Model

Burgess, C., Moore, G. *The Standard Model: A Primer*. Cambridge Univ. Press (2007).
Donoghue, J.F., Golowich, E., Holstein, B.R. *Dynamics of the Standard Model*. Cambridge Univ. Press (1992).
Georgi, H. *Weak Interactions and Modern Particle Theory*. Dover Publications (2009).
Thomson, M. *Modern Particle Physics*. Cambridge Univ. Press (2013).

Collider Physics

Barger, V.D., Phillips, R.J.N. *Collider Physics*. Addison-Wesley (1987).
Campbell, J., Huston, J., Krauss, F. *The Black Book of Quantum Chromodynamics: A Primer for the LHC Era*. Oxford Univ. Press (2018).
Krämer, M., Soler, F.J.P (editors) *Large Hadron Collider Phenomenology*. Bristol: Institute of Physics. (2004)
Plehn, T. *Lectures on LHC Physics* arXiv:0910.4182 [hep-ph]

Group Theory

Cornwell, J.F. *Group Theory in Physics* (vols. 1 and 2). Academic Press (1984).
Georgi, H. *Lie algebras in Particle Physics*. Westview Press (1999).
Hall, B.R. *Lie groups, Lie algebras, and representations*. Springer (2003).
Ramond, P. *Group Theory: A Physicist's Survey*. Cambridge (2010).
Wybourne, B.G. *Classical Groups for Physicists*. Wiley (1974).

Supersymmetry

Martin, S.P. *A Supersymmetry Primer* arXiv:hep-ph/9709356

Appendices

A.1 Natural units and conversions

The speed of light and \hbar are:

$$c = 2.99792458 \times 10^{10} \text{ cm/sec} = 2.99792458 \times 10^8 \text{ m/sec}, \quad (\text{A.1.1})$$

$$\hbar = 1.05457148 \times 10^{-34} \text{ J sec} = 6.58211814 \times 10^{-25} \text{ GeV sec}. \quad (\text{A.1.2})$$

The value of c is exact, by definition. (Since October 1983, the official definition of 1 meter is the distance traveled by light in a vacuum in exactly 1/299792458 of a second.)

In units with $c = \hbar = 1$, some other conversion factors are:

$$1 \text{ GeV} = 1.60217646 \times 10^{-3} \text{ erg} = 1.60217646 \times 10^{-10} \text{ J}, \quad (\text{A.1.3})$$

$$1 \text{ GeV} = 1.78266173 \times 10^{-24} \text{ g} = 1.78266173 \times 10^{-27} \text{ kg}, \quad (\text{A.1.4})$$

$$1 \text{ GeV}^{-1} = 1.97326937 \times 10^{-14} \text{ cm} = 1.97326937 \times 10^{-16} \text{ m}. \quad (\text{A.1.5})$$

Conversions of particle decay widths to mean lifetimes and vice versa are obtained using:

$$1 \text{ GeV}^{-1} = 6.58211814 \times 10^{-25} \text{ sec}, \quad (\text{A.1.6})$$

$$1 \text{ sec} = 1.51926778 \times 10^{24} \text{ GeV}^{-1}. \quad (\text{A.1.7})$$

Conversions of cross-sections in GeV^{-2} to barn units involve:

$$1 \text{ GeV}^{-2} = 3.89379201 \times 10^{-4} \text{ barns} \quad (\text{A.1.8})$$

$$= 3.89379201 \times 10^5 \text{ nb} \quad (\text{A.1.9})$$

$$= 3.89379201 \times 10^8 \text{ pb} \quad (\text{A.1.10})$$

$$= 3.89379201 \times 10^{11} \text{ fb}, \quad (\text{A.1.11})$$

and in reverse:

$$1 \text{ nb} = 10^{-33} \text{ cm}^2 = 2.56819059 \times 10^{-6} \text{ GeV}^{-2}, \quad (\text{A.1.12})$$

$$1 \text{ pb} = 10^{-36} \text{ cm}^2 = 2.56819059 \times 10^{-9} \text{ GeV}^{-2}, \quad (\text{A.1.13})$$

$$1 \text{ fb} = 10^{-39} \text{ cm}^2 = 2.56819059 \times 10^{-12} \text{ GeV}^{-2}. \quad (\text{A.1.14})$$

A.2 Dirac Spinor Formulas

In the Weyl (or chiral) representation):

$$\gamma^\mu = \begin{pmatrix} 0 & \sigma^\mu \\ \bar{\sigma}^\mu & 0 \end{pmatrix} \quad (\text{A.2.1})$$

where

$$\begin{aligned} \sigma^0 &= \bar{\sigma}^0 = \begin{pmatrix} 1 & 0 \\ 0 & 1 \end{pmatrix}; & \sigma^1 &= -\bar{\sigma}^1 = \begin{pmatrix} 0 & 1 \\ 1 & 0 \end{pmatrix}; \\ \sigma^2 &= -\bar{\sigma}^2 = \begin{pmatrix} 0 & -i \\ i & 0 \end{pmatrix}; & \sigma^3 &= -\bar{\sigma}^3 = \begin{pmatrix} 1 & 0 \\ 0 & -1 \end{pmatrix}. \end{aligned} \quad (\text{A.2.2})$$

$$\gamma^{0\dagger} = \gamma^0; \quad (\gamma^0)^2 = 1 \quad (\text{A.2.3})$$

$$\gamma^{j\dagger} = -\gamma^j \quad (j = 1, 2, 3) \quad (\text{A.2.4})$$

$$\gamma^0 \gamma^{\mu\dagger} \gamma^0 = \gamma^\mu \quad (\text{A.2.5})$$

$$\gamma_\mu \gamma_\nu + \gamma_\nu \gamma_\mu = \{\gamma_\mu, \gamma_\nu\} = 2g_{\mu\nu} \quad (\text{A.2.6})$$

$$[\gamma_\rho, [\gamma_\mu, \gamma_\nu]] = 4(g_{\rho\mu}\gamma_\nu - g_{\rho\nu}\gamma_\mu) \quad (\text{A.2.7})$$

The trace of an odd number of γ^μ matrices is 0.

$$\text{Tr}(1) = 4 \quad (\text{A.2.8})$$

$$\text{Tr}(\gamma_\mu \gamma_\nu) = 4g_{\mu\nu} \quad (\text{A.2.9})$$

$$\text{Tr}(\gamma_\mu \gamma_\nu \gamma_\rho \gamma_\sigma) = 4(g_{\mu\nu}g_{\rho\sigma} - g_{\mu\rho}g_{\nu\sigma} + g_{\mu\sigma}g_{\nu\rho}) \quad (\text{A.2.10})$$

$$\begin{aligned} \text{Tr}(\gamma_{\mu_1} \gamma_{\mu_2} \cdots \gamma_{\mu_{2n}}) &= g_{\mu_1 \mu_2} \text{Tr}(\gamma_{\mu_3} \gamma_{\mu_4} \cdots \gamma_{\mu_{2n}}) - g_{\mu_1 \mu_3} \text{Tr}(\gamma_{\mu_2} \gamma_{\mu_4} \cdots \gamma_{\mu_{2n}}) \\ &\quad \cdots + (-1)^k g_{\mu_1 \mu_k} \text{Tr}(\gamma_{\mu_2} \gamma_{\mu_3} \cdots \gamma_{\mu_{k-1}} \gamma_{\mu_{k+1}} \cdots \gamma_{\mu_{2n}}) + \cdots \\ &\quad + g_{\mu_1 \mu_{2n}} \text{Tr}(\gamma_{\mu_2} \gamma_{\mu_3} \cdots \gamma_{\mu_{2n-1}}) \end{aligned} \quad (\text{A.2.11})$$

In the chiral (or Weyl) representation, in 2×2 block form:

$$\gamma_5 = \begin{pmatrix} -1 & 0 \\ 0 & 1 \end{pmatrix} \quad (\text{A.2.12})$$

$$P_L = \frac{1 - \gamma_5}{2} = \begin{pmatrix} 1 & 0 \\ 0 & 0 \end{pmatrix}; \quad P_R = \frac{1 + \gamma_5}{2} = \begin{pmatrix} 0 & 0 \\ 0 & 1 \end{pmatrix} \quad (\text{A.2.13})$$

The matrix γ_5 satisfies:

$$\gamma_5^\dagger = \gamma_5; \quad \gamma_5^2 = 1; \quad \{\gamma_5, \gamma^\mu\} = 0 \quad (\text{A.2.14})$$

$$\text{Tr}(\gamma_5) = 0 \quad (\text{A.2.15})$$

$$\text{Tr}(\gamma_\mu \gamma_5) = 0 \quad (\text{A.2.16})$$

$$\text{Tr}(\gamma_\mu \gamma_\nu \gamma_5) = 0 \quad (\text{A.2.17})$$

$$\text{Tr}(\gamma_\mu \gamma_\nu \gamma_\rho \gamma_5) = 0 \quad (\text{A.2.18})$$

$$\text{Tr}(\gamma_\mu \gamma_\nu \gamma_\rho \gamma_\sigma \gamma_5) = 4i\epsilon_{\mu\nu\rho\sigma} \quad (\text{A.2.19})$$

$$\gamma^\mu \gamma_\mu = 4 \quad (\text{A.2.20})$$

$$\gamma^\mu \gamma_\nu \gamma_\mu = -2\gamma_\nu \quad (\text{A.2.21})$$

$$\gamma^\mu \gamma_\nu \gamma_\rho \gamma_\mu = 4g_{\nu\rho} \quad (\text{A.2.22})$$

$$\gamma^\mu \gamma_\nu \gamma_\rho \gamma_\sigma \gamma_\mu = -2\gamma_\sigma \gamma_\rho \gamma_\nu \quad (\text{A.2.23})$$

$$(\not{p} - m)u(p, s) = 0; \quad (\not{p} + m)v(p, s) = 0 \quad (\text{A.2.24})$$

$$\bar{u}(p, s)(\not{p} - m) = 0; \quad \bar{v}(p, s)(\not{p} + m) = 0 \quad (\text{A.2.25})$$

$$\bar{u}(p, s)u(p, r) = 2m\delta_{sr} \quad (\text{A.2.26})$$

$$\bar{v}(p, s)v(p, r) = -2m\delta_{sr} \quad (\text{A.2.27})$$

$$\bar{v}(p, s)u(p, r) = \bar{u}(p, s)v(p, r) = 0 \quad (\text{A.2.28})$$

$$\sum_s u(p, s)\bar{u}(p, s) = \not{p} + m \quad (\text{A.2.29})$$

$$\sum_s v(p, s)\bar{v}(p, s) = \not{p} - m \quad (\text{A.2.30})$$

Index

- Abelian (commutative) group, 181
- action, 25, 47, 49
- active quarks, 211, 213
- adjoint representation, 185, 186, 188, 189, 191, 193, 194, 198
- Altarelli–Parisi (DGLAP) equations, 218, 223
- angular momentum conservation, 115–117, 147, 155
- angular momentum operator, 37
- angular resolution, 122
- annihilation operator, 54, 58, 59
- anticommutation relations, 60, 61, 97
- antineutrino, 150, 152
- antineutrino-electron scattering, 167
- antiparticle, 5, 7, 9, 41, 45–47, 59, 91, 111
- associativity property of group, 180
- asymptotic freedom, 212, 215
- ATLAS detector at LHC, 233

- BaBar experiment, 153
- bare coupling, 207, 209
- bare mass, 208, 209
- barn (unit of cross-section), 68, 279
- barred Dirac spinor, 35
- baryons, 7–9
 - ($J = 1/2$), 8
 - ($J = 3/2$), 8, 9
- Belle experiment, 153
- beta function, 210, 211, 214, 215
 - QCD, 211
 - QED, 214
- Bhabha scattering, 118
- biunitary transformation, 259
- boost, 16, 23, 33, 34

- Bose-Einstein statistics, 56
- bottomonium, 10–12, 233
- branching ratios, 13, 146
 - charged pion, 152, 171
 - Higgs boson, 146, 258
 - lepton-number violating limits, 153
 - W boson, 263
 - Z boson, 250
- Breit-Wigner lineshape, 5, 233

- Cabibbo angle, 262, 263
- Cabibbo-Kobayashi-Maskawa (CKM) mixing, 262, 263
- canonical commutation relations, 37
- canonical quantization
 - complex scalar field, 173
 - Dirac fermion fields, 61
 - real scalar fields, 53, 54
- Carbon-14 dating, 150, 151
- Casimir invariant, 184
- charge conjugation, 162
- charge conservation, 26, 27
- charge density, 26
- charge operator, 92
- charged current, 168, 169, 178
- charmonium, 10, 11, 233
- chiral (Weyl) representation of Dirac matrices, 31, 280
- chiral representations (of gauge group), 255
- chiral symmetry breaking, 8, 244, 258, 259
- closure property of group, 180, 182
- CMS detector at LHC, 233
- color, 5, 7
 - confinement, 5, 7, 107, 215

- sum over, 201
- commutation relations, 53–55
- commutative (Abelian) group, 181
- commutator of Lie algebra generators, 182
- complex conjugate of spinor expressions, 101, 119, 155–157, 169
- complex conjugate representation, 184
- complex scalar field, 172
- Compton scattering, 130–138
- confinement of color, 5, 7, 107, 215
- conservation of angular momentum, 115–117, 147, 155
- conservation of charge, 26, 27
- conservation of energy, 65, 78, 150
- conservation of helicity, 117, 172
- conservation of lepton number (or not), 153, 154, 265, 266
- conservation of momentum, 18, 71, 98, 99
- contravariant four-vector, 15, 16, 18, 24
- Coulomb potential, 122
- coupling
 - bare, 207, 209
 - electromagnetic (e), 53, 92, 248
 - electroweak (g), 178, 245, 246, 248
 - electroweak (g'), 246–248
 - Fermi (G_F), 156, 162
 - general, 88
 - QCD (g_3, α_s), 199–202, 211
 - experimental value, 213, 214
 - renormalized, 207–209, 248
 - scalar³, 77
 - scalar⁴, 62
 - scalar ^{n} , 85, 88
 - Yang-Mills gauge, 193–197, 239
 - Yukawa, 89, 143, 145, 146, 256–260
 - Yukawa, neutrino, 264
- covariant derivative
 - QED, 94, 180
 - Yang-Mills, 193
- covariant four-vector, 18
- CPT Theorem, 162
- creation operator, 54
 - fermionic, 58, 59
- cross-section, 67–69
 - differential, 72
 - two particle \rightarrow two particle, 76
- crossing, 123–128, 138, 139, 165, 167
- CTEQ parton distribution functions, 220
- current density, electromagnetic, 26, 53, 92
- cutoff, 57, 86, 99, 163, 176, 205–209, 213
- decay rate (width, Γ), 140
- defining representation, 182
- density of states, 72
- DGLAP equations, 218, 223
- differential cross-section, 72
- dimension of group (d_G), 182, 184
- dimension of representation (d_R), 182
- dimension of tensor product representation, 185
- dimensional analysis, 161, 175, 176
- dimensional regularization, 213
- dimensional transmutation, 213
- Dirac equation, 29–32
- Dirac field, 47, 50, 51, 58–61
- Dirac matrices, 31, 32, 280
- Dirac spinor, 30, 31
- direct sum representation, 184
- double-counting problem, identical particles in
 - final state, 76, 128, 139, 143
- Drell-Yan scattering, 231, 232
- electroweak Standard Model (Glashow-Weinberg-

- Salam) gauge theory, 245–249, 251–255
- electroweak vector boson interactions, 253, 254
- energy conservation, 65, 78, 150
- $\epsilon^{\mu\nu\rho\sigma}$ (Levi-Civita) tensor, 25
- equal-time commutators, 53
- equivalence of representations of group, 183
- η_b (scalar bottomonium), 10
- η_c (scalar charmonium), 10
- η meson, 233
- Euler-Lagrange equations of motion, 47–51, 61
- factorization scale, 218
- femtobarns (fb), 68
- Fermi constant (G_F), 156
 - numerical value, 161
 - relation to m_W , 178
 - relation to Higgs VEV, 253
- Fermi weak interaction theory, 156
- Fermi-Dirac statistics, 59, 97
- fermion-antifermion condensate, 244
- Feynman diagram, 66, 82–84, 86, 87
- Feynman gauge, 97, 98, 128, 195
- Feynman propagator
 - charged massive vector fields, 177
 - Dirac fields, 90, 98
 - generic fields, 89
 - gluons, 199
 - Higgs boson, 241
 - massive vector fields, 179
 - photon, 96, 97
 - scalar, complex (π^\pm), 173
 - scalar, real, 85
 - W boson, 177
 - Yang-Mills vector fields, 194
- Feynman rules, 66
 - Fermi weak interaction theory, 156, 157
 - fermion external lines, 91
 - fermions with known helicity, 111
 - general, 87–90
 - massive vector bosons, 179
 - pion decay, 173–175
 - QCD, 199, 200
 - QED, 94–99
 - scalar ϕ^n theory, 84–86, 88
 - standard electroweak gauge theory, 253–255
 - W -fermion-antifermion, 178
 - Yang-Mills, 194–197
 - Yukawa coupling, 88, 89
 - Yukawa coupling, electron, 256
- Feynman slash notation, 32
- Feynman's x , 217
- Feynman-Stückelberg interpretation, 40
- field, 46, 47
 - Dirac, 47, 50, 51, 58–61
 - electromagnetic, 25, 26, 47, 52, 53
 - Majorana, 45, 50, 265
 - scalar, 46, 47, 49, 50
 - vector, 47, 50, 52, 53
 - Weyl, 50
- field theory, 47
- fine structure constant, 92, 104
- flavors of quarks, 6, 7
- four-fermion interaction, 156, 175, 177
- four-vector, 15–17, 22
- free field theory, 61
- fundamental representation, 182
- $g_{\mu\nu}$ (metric tensor), 17
- γ (gamma) matrices, 31
 - traces, 280, 281
- γ_5 matrix, 39, 280
- gauge eigenstate fields, 247, 260–262

- gauge fixing, 96, 97
- gauge-fixing parameter (ξ), 96, 97
- gauge invariance, 27, 94, 180
 - Yang-Mills, 181, 191–196
- Gell-Mann matrices, 189
- generators
 - $SU(2)$, 186
 - $SU(3)$, 189
 - $SU(N)$, 188
 - of Lie algebra, 182, 183
- GeV, 29
- global symmetry, 188, 235
- global symmetry breaking, 236–238
- glueballs, 12
- gluon, 169, 198, 199
 - propagator, 199
- gluon collider, 228
- gluon-gluon scattering, 225–227
- gluonium, 12
- Goldstone boson, 238, 243
 - pseudo, 244
 - would-be, 241, 243, 251
- Goldstone’s theorem, 243
- Grassmann (anticommuting) numbers, 60
- gravity, 177, 209
- group, 23, 180
- hadron-hadron scattering, 215–220, 228–232
- hadronization, 216
- hadrons, 7
- half life, 150
- Hamilton’s principle, 47
- Hamiltonian
 - free Dirac field, 61
 - free scalar field, 54, 56, 57
 - general classical system, 53
 - interaction, 62, 63, 90
 - single Dirac particle, 30, 37
 - single scalar particle, 28
- hard scattering of partons, 215
- helicity, 38, 39
- helicity conservation, 117, 172
- helicity flip, 172
- helicity suppression, 172
- Higgs boson, 7, 8, 89, 145–147, 252–255, 270
 - discovery, 266
 - experimental mass, 7
 - interactions with Z, W, h , 253–255
 - mass in Standard Model, 255
- Higgs field
 - generic, 239, 241, 243, 245
 - Standard Model, 250–255
- Higgs mechanism, 239, 241, 243, 245
- hole (absence of an electron), 40
- identical final state particle overcounting problem, 76, 128, 139, 143
- identity element of group, 180
- $i\epsilon$ factor in propagators, 85
- ignorance, parameterization of, 169, 170, 207
- IN state, 63, 64
- index of representations, 183
 - $SU(2)$, 187
 - $SU(3)$, 189
 - adjoint, 185
- inertial reference frame, 15
- infinite momentum frame, 217
- infrared slavery, 212
- integrated luminosity, 67
- interaction Hamiltonian, 62, 63, 90
- interaction Lagrangian, 62
- internal line, 82

- inverse metric tensor ($g^{\mu\nu}$), 17
- inverse muon decay, 165
- inverse of group element, 180
- irreducible representation, 184
- isospin global symmetry, 188

- Jacobi identity, 183
- Jacobian, 230, 232
- jet, 107, 200, 216
- J/ψ (vector charmonium), 11, 108, 233

- Klein-Gordon equation, 29, 35, 50
- Klein-Nishina formula for Compton scattering, 137

- Lagrangian, 47, 49
- Lagrangian density, 49
- Landau gauge, 97, 98, 195
- Large Hadron Collider (LHC), 4, 145, 222, 224, 226–228, 233, 271
- lattice gauge theory, 13
- left-handed fermions
 - and weak interactions, 155, 156, 168, 188, 245, 246, 255
 - Dirac, 39
 - projection matrix (P_L), 39, 41
 - Weyl, 44, 45
- left-handed polarization of photon, 95
- lepton number (total), 154, 265, 266
- lepton numbers (individual), 153, 154
- leptons, 6
- Levi-Civita ($\epsilon^{\mu\nu\rho\sigma}$) tensor, 25
- Lie algebra, 182, 183
- Lie group, 181
- linear collider, 110
- local (gauge) symmetry, 180, 235
 - breaking, 239–241, 243
- longitudinal momentum fraction (Feynman's x), 217
- longitudinal polarization of massive vector boson, 241
- longitudinal rapidity, 21, 229
- loop corrections to muon decay, 163
- loops in Feynman diagrams, 86, 90, 99, 176, 196, 204–206, 208, 209, 258
 - fermion minus sign, 99
- Lorentz transformations, 15, 16, 23
- Lorentz-invariant phase space
 - n -body, 74, 141
 - 2-body, 74, 75, 135, 142
 - 3-body, 148, 149
- lowering operator, 54–56
- luminosity, 67

- Majorana fermion, 45, 265, 266
- Majorana field, 265
- Mandelstam variables (s, t, u), 84, 119
- Mandelstam variables, partonic ($\hat{s}, \hat{t}, \hat{u}$), 216, 223
- mass diagonalization, 259
- mass eigenstate fields, 247, 260–262
- massive vector boson, 179, 197, 240–243, 245, 247
 - propagator, 179
- matrix element, 66, 67, 71
 - reduced, 71
- Maxwell's equations, 25–27, 52
- mean lifetime, 141
- MEG, 153
- mesons, 7, 9, 10
 - ($J = 0$), 9, 10
 - ($J = 1$), 10
- metric tensor ($g_{\mu\nu}$), 17

Mexican hat potential, 236
 Møller scattering, 126
 momentum conservation, 18, 71, 98, 99
 momentum fraction (Feynman's x), 217
 $\overline{\text{MS}}$ renormalization scheme, 213, 248
 MSTW parton distribution functions, 220
 muon decay, 152, 156–161
 muon production in e^-e^+ collisions, 100–105

 Nambu-Goldstone boson, 238, 243
 pseudo, 244
 would-be, 241, 243, 251
 nanobarns (nb), 68
 natural units, 279
 neutrino, 6, 44
 anti-, 7, 150, 152
 masses, 264–266
 mixing, 265
 seesaw mechanism, 264, 265
 Yukawa coupling, 264
 neutrinoless double beta decay, 266
 neutron, 7
 neutron decay, 150
 non-Abelian gauge invariance, 181, 191–194
 non-renormalizable theories, 176, 177, 197, 209
 nuclear weak decays, 150, 151
 nucleons, 7

 ω meson, 233
 on-shell, 18
 OUT state, 63, 64
 overcounting problem for identical final state
 particles, 76, 128, 139, 143

 parity, 23, 154, 162
 parity violation, 23, 155, 156
 partial width, 13, 141

 Particle Data Group, 4
 parton, 215, 217
 parton distribution function (PDF), 217–223
 parton model, 215
 partonic subprocess, 215, 216
 Pauli exclusion principle, 40, 59
 Pauli matrices ($\sigma^{1,2,3}$), 30, 280
 ϕ meson, 233
 photon field (A^μ), 47, 92, 94–97
 photon polarization, 95, 96
 photon propagator, 96–98
 picobarns (pb), 68
 pion (π^\pm) decay, 169–175
 pion decay constant (f_π), 170
 polarization vector, 95
 and gauge transformations, 129
 massive vector boson, 179
 polarized beams, 110
 Pontecorvo-Maki-Nakagawa-Sakata (PMNS) ma-
 trix, 265
 positron, 30, 40
 potential energy, 47, 48, 235
 projection matrices for helicity (P_L, P_R), 39,
 280
 propagator
 charged massive vector boson, 177, 179
 Dirac fermion, 90, 98
 generic, 89
 gluon, 199
 Higgs boson, 241
 massive vector boson, 177, 179
 photon, 96, 97
 scalar, complex (π^\pm), 173
 scalar, real, 85
 W boson, 177

- Yang-Mills vector fields, 194
- proper interval, 17
- proper Lorentz transformations, 23
- proton, 7
- pseudo-Nambu-Goldstone boson, 244
- pseudo-rapidity, 21
- pseudo-scalar fermion bilinear, 154
- QCD coupling, 199–202, 211
 - experimental value, 213, 214
- QCD scale (Λ_{QCD}), 211, 212
- quadratic Casimir invariant, 184
- Quantum Chromo-Dynamics (QCD), 107, 188, 198–200
- Quantum Electro-Dynamics (QED), 92–94
 - Feynman rules, 94–99
- quark, 6
 - flavors, 6, 7
 - masses, 6, 7, 258, 259
- quark-antiquark condensate, 244
- quark-quark scattering, 200–202
- quarkonium, 11, 12
- raising operator, 54–56
- rapidity, 16, 34, 36
 - longitudinal, 21, 229
 - pseudo-, 21
- reduced matrix element, 71
- reducible representation, 183
- regularization, 57, 86, 176, 205, 213
- renormalizable theories, 176, 177
- renormalization, 57, 86, 163, 164
- renormalization group, 210
- renormalization scale, 207–210, 218
- renormalized (running) coupling, 207–209
 - electroweak, 248
- renormalized (running) mass, 208, 209
- representation of group, 181
- representations
 - of $SU(2)$, 186–188
 - of $SU(3)$, 188–190
 - of $SU(N)$, 191
 - of $U(1)$, 181
 - of non-Abelian group, 181–186
- Review of Particle Properties (Particle Data Group), 4, 108
- R_{hadrons} , 108, 110
- ρ meson, 233
- right-handed antifermions and weak interactions, 155, 166
- right-handed fermions
 - Dirac, 39
 - Weyl, 44
- right-handed polarization of photon, 95
- right-handed projection matrix (P_R), 41
- rotations, 23
- Rutherford scattering, 122
- scalar field, 46, 47, 49, 50
 - complex, 172
- scalar function, 24
- s -channel, 82, 84
- Schrodinger equation, 28
- Schrodinger picture of quantum mechanics, 62, 63
- sea partons, 217, 219, 221
- sea quarks, 8, 219
- seesaw mechanism for neutrino masses, 264, 265
- singlet representation, 181, 184
- slash notation, 32
- speed of light (c), 15, 279
- spin operator, 37
- spin-sum identities, 42, 281

- spinor, 30
 - Dirac, 31
 - Majorana, 45
 - Weyl, 44
- spontaneous symmetry breaking, 235
 - global, 235–238
 - local (gauge), 239–241
- Standard Model, 245–249, 251–255
- structure constants of non-Abelian group, 182
- $SU(2)$ Lie algebra, 186–188
- $SU(2)_L$ (weak isospin), 188, 245, 246
- $SU(3)$ Lie algebra, 188–190
- $SU(N)$ Lie algebra, 188, 191
- subprocess, partonic, 215, 216
- supersymmetry, 45, 222, 228
- symmetry factor (of Feynman diagram), 86, 87, 99
- tau decays, 13
- t -channel, 83, 84, 118
- technicolor, 244
- tensor, 24
- tensor product of representations, 185
- Tevatron, 68, 69, 222, 224, 228
- Thomson scattering, 137
- three-body phase space, 147–149
- time reversal (T), 22, 23, 162
- top quark, 6, 7
 - decay, 263
 - LHC production cross-section, 69, 226–228
 - Tevatron production cross-section, 69, 224–226, 228
- trace trick, 102, 103
- traces of γ matrices, 32, 102, 280, 281
- transverse momentum (p_T), 229
- transverse polarization, 95, 240
- tree-level diagrams, 85
- triangle function (λ), 142
- two-body phase space, 135
- $U(1)$ as a Lie group, 181
- $U(1)$ for electromagnetism, 181, 198
- $U(1)_Y$ (weak hypercharge), 245, 246, 249–251
- u -channel, 83, 84
- unitarity of CKM matrix, 263
- unitarity of quantum mechanical time evolution, 175, 177, 197
- unitary gauge, 241, 242
 - Standard Model, 251–254
- units, 29, 279
- Υ (vector bottomonium), 11, 233
- vacuum expectation value (VEV), 236
 - antiquark-quark, 244
 - Standard Model, 251
 - Standard Model numerical, 252
- vacuum state, 46, 55, 59
- valence quarks, 8, 169, 217, 219, 221, 226
- volume element, 25
- W boson, 5
 - branching ratios, 263
 - couplings to fermions, 261, 262
 - interactions with Z, W, h , 253, 254
 - mass, measured, 5
 - mass, prediction, 252
 - width, measured, 5
 - width, predicted, 6
- Ward identity, 129, 130
- weak hypercharge [$U(1)_Y$], 245, 246, 249–251
- weak isospin [$SU(2)_L$], 188, 245, 246
- weak mixing angle θ_W , 247

- weak mixing angle (Weinberg angle) θ_W , 248,
249, 252, 253
- weak-interaction charged current, 168, 169, 178
- Weyl (chiral) representation of Dirac matrices,
31, 280
- Weyl equation, 44
- Weyl fermion, 44
- Weyl spinor, 44
- would-be Nambu-Goldstone boson, 241, 243,
251
- Standard Model, 251
- x , Feynman (momentum fraction), 217
- ξ (gauge-fixing parameter), 96, 97
- Yang-Mills theories, 179, 191–196
- Yukawa coupling, 89, 143, 145, 146, 256–260
 - neutrino, 264
- Z boson, 5, 232
 - branching ratios, 250
 - couplings to fermions, 249, 250
 - interactions with Z, W, h , 253, 254
 - mass, measured, 5
 - mass, prediction, 252
 - resonance at LHC, 233
 - width, 5